sustainability

Topical Collection Reprint

Air Pollution Control and Sustainable Development

Urban Air Quality Assessment and Pollution Control Technologies

Edited by
Weixin Yang, Guanghui Yuan and Yunpeng Yang

mdpi.com/journal/sustainability

MDPI

Air Pollution Control and Sustainable Development: Urban Air Quality Assessment and Pollution Control Technologies

Air Pollution Control and Sustainable Development: Urban Air Quality Assessment and Pollution Control Technologies

Collection Editors

Weixin Yang
Guanghui Yuan
Yunpeng Yang

MDPI

Basel • Beijing • Wuhan • Barcelona • Belgrade • Novi Sad • Cluj • Manchester

Collection Editors

Weixin Yang
Business School
University of Shanghai for Science and Technology
Shanghai
China

Guanghui Yuan
School of Economics and Management
Shanghai University of Political Science and Law
Shanghai
China

Yunpeng Yang
Antai College of Economics and Management
Shanghai Jiao Tong University
Shanghai
China

Editorial Office
MDPI AG
Grosspeteranlage 5
4052 Basel, Switzerland

This is a reprint of the Topical Collection, published open access by the journal *Sustainability* (ISSN 2071-1050), freely accessible at: https://www.mdpi.com/journal/sustainability/topical_collections/APCSD.

For citation purposes, cite each article independently as indicated on the article page online and as indicated below:

Lastname, A.A.; Lastname, B.B. Article Title. *Journal Name* **Year**, *Volume Number*, Page Range.

ISBN 978-3-7258-5895-8 (Hbk)
ISBN 978-3-7258-5896-5 (PDF)
https://doi.org/10.3390/books978-3-7258-5896-5

Contents

About the Editors

Weixin Yang

Weixin Yang received his Ph.D. in Economics from Shanghai Academy of Social Sciences. He is currently teaching at University of Shanghai for Science and Technology. He has published over 100 papers, book chapters, and conference proceedings. He is also invited as a reviewer and academic editor of well-known journals. His main research interests are digital economy and sustainable development.

Guanghui Yuan

Guanghui Yuan received his Ph.D. degree from Shanghai University of Finance and Economics. He is currently teaching at Shanghai University of Political Science and Law. He has published more than 50 research papers. His main research interests include system modeling, information economy, data mining, and algorithm design.

Yunpeng Yang

Yunpeng Yang received his Ph.D. degree from University of Shanghai for Science and Technology. He is currently teaching at Antai College of Economics and Management, Shanghai Jiao Tong University. He has published more than 30 research papers. His main research interests include resource and environmental management, economic policy analysis, and game theory.

Preface

We are pleased to present "Air Pollution Control and Sustainable Development: Urban Air Quality Assessment and Pollution Control Technologies." This collection addresses the critical challenge of urban air pollution through a dual focus on comprehensive assessment methodologies and practical technological solutions. As urbanization accelerates globally, understanding and controlling air pollution in urban environments has become increasingly urgent for both public health and environmental sustainability. The contributions span diverse geographical contexts and technological domains, reflecting the multifaceted nature of urban air quality management and its implications for sustainable development.

The scope encompasses studies on spatial–temporal dynamics of air pollution in urban agglomerations, advanced monitoring and assessment frameworks, and innovative emission control technologies. It includes research on $PM_{2.5}$ evolution patterns, population mobility impacts on air quality, and the complex relationships between economic growth, urbanization, and environmental quality. The technological contributions cover selective catalytic reduction systems for nitrogen oxide removal, biological treatment methods for volatile organic compounds, and cyclone separator technologies for particulate matter control. Additionally, bibliometric analyses provide comprehensive reviews of research trends and future directions in pollution control technologies. Through these multidisciplinary perspectives, we aim to bridge the gap between theoretical assessment and practical implementation, providing valuable insights for researchers, engineers, policymakers, and urban planners.

The research presented here is particularly addressed to those working at the intersection of urban environmental management, pollution control engineering, and sustainable development policy. It serves as a resource for understanding how monitoring systems, analytical methodologies, and control technologies can work synergistically to improve urban air quality while supporting broader sustainability objectives.

The publication of this Reprint is the outcome of collaborative efforts by contributing authors from multiple countries and disciplines. We would like to express our deepest gratitude to all researchers who submitted their work, as well as to the reviewers who provided invaluable feedback. Special thanks are also due to the *Sustainability* editorial team, whose support and guidance have been instrumental in bringing this publication to fruition.

We hope it serves as a valuable resource for advancing both the science and practice of urban air quality management, and that it inspires further research, technological innovation, and policy development in this critical area of environmental sustainability.

Weixin Yang, Guanghui Yuan, and Yunpeng Yang
Collection Editors

sustainability

MDPI

Article

Comprehensive Evaluation and Comparative Analysis of the Green Development Level of Provinces in Eastern and Western China

Weixin Yang [1], Yue Hu [1], Qinyi Ding [1], Hao Gao [1,*] and Lingguang Li [2]

[1] Business School, University of Shanghai for Science and Technology, Shanghai 200093, China
[2] School of Mathematical Sciences, Tongji University, Shanghai 200092, China
* Correspondence: gaohao0302@outlook.com; Tel.: +86-21-5596-0082

Abstract: Considering the green development initiatives vigorously promoted by China, this paper constructs an evaluation index system that covers six areas, including resource utilization, pollution control, living environment, ecological protection, circular economy, and quality of economic growth. This paper also establishes an improved comprehensive evaluation model by using the method of Vertical Projection Distance-Set Pair Analysis in order to optimize the traditional method of Technique for Order of Preference by Similarity to Ideal Solution. Based on the official data released by China, this paper quantitatively analyzes the green development level of 21 provinces in eastern and western China in the aforementioned six areas from 2005 to 2020, and makes a regional comparison between eastern and western China. The results show that the level of green development in eastern China is significantly higher than that in western China. In 2020, when the research period ends, the comprehensive evaluation values of green development in all the eastern provinces, except Hebei, are higher than 4.0; meanwhile, no province in the western region has a comprehensive evaluation value exceeding 4.0 in 2020, and there is a large gap between the eastern region and the western region in areas such as economic growth quality and pollution control. On this basis, this paper puts forward relevant suggestions in terms of the coordinated green development of the eastern and western regions of China in the future.

Keywords: green development; evaluation index system; comprehensive evaluation model; V-SPA; TOPSIS

1. Introduction

Since the reform and opening up, China has made great achievements in economic development. However, due to the inefficient use of resources, the relationship between economic development and ecological protection has not been well balanced, which has led to a series of ecological and environmental problems [1–3]. In order to fundamentally solve the ecological and environmental problems it faces and realize sustainable development, China urgently needs to achieve green transformation and implement green development policies that suit its own economic and social development needs, as well as local conditions, and explore a green development path with its own characteristics [4].

The Chinese leaders have attached great importance to green development. The report of the 20th National Congress of the Communist Party of China has clearly pointed out that it is necessary to promote green development and the harmonious coexistence between man and nature. [5]. In recent years, China has deepened reform in various fields, has vigorously promoted the construction of ecological civilization, and has emphasized the green development of various areas such as resource utilization, pollution control, the living environment, ecological protection, the circular economy, and economic growth quality; this is with the goal of achieving a harmonious coexistence between man and nature, as well as comprehensive and coordinated sustainable development [6].

However, green development is a complex systematic project that involves various fields, including the economy [7,8], society and environment [9,10], and there are close links between each field [11]. In addition, China has a vast territory, and there are large differences in the level of development between the regions [12,13]. Compared with the eastern region, the overall development level of the central and western regions is relatively low [14,15]. Therefore, it is necessary to construct a green development index system with scientifically selected indicators, and to comprehensively and accurately evaluate the green development level of various regions in China in order to realize sustainable development. This topic has also attracted the attention of the academic community [16,17].

Therefore, the motivation of this paper is to construct a comprehensive evaluation index system that fully reflects China's green development level, covering six areas: resource utilization, pollution control, living environment, ecological protection, circular economy, and the quality of economic growth. In addition, this paper has improved the traditional model of Technique for Order of Preference by Similarity to Ideal Solution (TOPSIS) by using the Vertical Projection Distance-Set Pair Analysis (V-SPA) method. By substituting the vertical distance for the connection vector distance in the set pair analysis, this paper has constructed an optimized evaluation model in order to comprehensively evaluate and compare the green development levels of 21 provinces in eastern and western China from 2005 to 2020.

According to the official classification of the National Bureau of Statistics of China [18], this paper has selected 10 provinces in eastern China (Beijing, Tianjin, Hebei, Shanghai, Jiangsu, Zhejiang, Fujian, Shandong, Guangdong and Hainan), and 11 provinces in western China (Inner Mongolia, Guangxi, Chongqing, Sichuan, Guizhou, Yunnan, Shaanxi, Gansu, Qinghai, Ningxia and Xinjiang). The above-mentioned analysis scope has covered more than 80% of China's territory, so it has good representativeness.

This paper attempts to contribute to existing research in the following areas:

(1) By constructing an index system covering six major fields, this paper attempts to enrich the existing literature on the green development index system, and further explore improvements to the sustainable development evaluation index system.

(2) To make a contribution to the development of a research methodology, we have constructed an improved comprehensive evaluation model and adopted the set pair analysis method to improve the TOPSIS method, and further improved the model for the green development level evaluation by substituting the vertical distance for the connection vector distance in the set pair analysis.

(3) Through the comprehensive evaluation of the green development level of different regions of China and the comparative analysis of the east region and the west region, this paper attempts to provide quantitative analysis tools and research ideas for the study of green development levels of other regions and other countries, thus making contributions to academic research in the field of sustainable development.

The deficiencies in this paper are mainly as follows:

(1) Due to the availability of data, there are many gaps in China's official data released after 2020. This paper does not use simple interpolation or moving average methods to make up for missing values, but chooses to limit the research period to ensure the integrity of the data and the scientific nature of this research. Thus, there is the drawback that the data is not up to date to some extent.

(2) In order to illustrate the differences in the level of green development in China, this paper selects 21 provinces in eastern and western China, but does not include 9 provinces in central and northeastern China. Although this is more convincing from a comparative perspective, the above-mentioned 9 provinces still remain to be included in a comprehensive study in the future.

The structure of this paper is as follows: Part 2 introduces the comprehensive evaluation index system of green development, including detailed indicators in six fields, and constructs a comprehensive evaluation model for the green development level; by using the aforementioned index system and evaluation model, Part 3 calculates the evaluation results

of the eastern and western provinces of China based on the official statistical data; Part 4 discusses the evaluation results in depth, based on the development and implementation of green policies in eastern and western China during the research period; and Part 5 summarizes the paper, and provides relevant policy suggestions for China's future green development.

2. Literature Review

The academic community has conducted much research on China's green development [19–21]. The key themes that have been involved in these papers include the following:

(1) Challenges and successes. Studies have evaluated the challenges and successes of China's green development efforts. For example, a number of papers have noted the progress made in reducing carbon emissions [22,23] and promoting renewable energy [24], while others have pointed out the ongoing challenges in areas such as air quality [25,26] and balancing economic development with environmental protection [27,28].

(2) Public and private sector involvement. Many papers have focused on the role of the public and private sectors in China's green development [29,30], including the awareness and implementation of green practices by companies [31], as well as the influence of public opinion on the government's efforts [32–34].

(3) Government initiatives and measures. Many academic papers have analyzed the various policies and initiatives introduced by the Chinese government to promote environmentally friendly development. This includes the "Ecological Civilization" plan [35,36], restrictions on industrial production and coal use [37], and the promotion of renewable energy and electric vehicles [38].

(4) Evaluation of green development level. Researches on the evaluation of green development level have used comprehensive and multi-dimensional approaches to assess the progress and challenges of sustainable development, especially the Multi-criteria decision-making (MCDM) methods [39–42]. These studies emphasize the importance of considering various factors such as economic, social, and environmental impacts, as well as the availability and quality of data, in order to arrive at a more accurate evaluation of the green development level [43]. Moreover, the existing research highlights the role of government policies [44], investment [45], and public participation [46] in promoting and sustaining green development.

(5) International cooperation. A number of academic papers have explored China's role in international cooperation and its impact on green development [47], including its collaborations with other countries and organizations [48], as well as its participation in global climate agreements [49].

Overall, academic papers on China's green development have provided an understanding of the country's efforts to achieve sustainable growth, as well as the challenges and opportunities facing these efforts. The research has demonstrated the importance of continued efforts to address environmental issues and promote environmentally friendly development in China and beyond.

However, most of the studies focus on the green development level of certain cities or provinces in China. There are very few studies that comprehensively analyze the green development level of various regions in China with regional comparative analysis. Moreover, the index systems constructed are often concentrated in a specific field and fail to cover the multiple fields involved in green development such as economy, society and environment. Hence, we hope to further enrich the existing literature of green development via the research in this paper.

3. Materials and Methods

3.1. The Green Development Evaluation Index System

The evaluation of the regional green development level is a multi-dimensional and multi-faceted complex task [50]. Therefore, building an indicator system in order to evaluate the green development level is also a complex systematic project [51,52]. Different

indicators reflect different aspects of regional green development, but they are not completely independent of each other. The indicator system, formed by indicators with certain correlations, can meet the requirements of a comprehensive evaluation and analysis of the regional green development level. By referring to relevant research [53,54], and in consideration of scientificity and operability, this section has constructed an evaluation index system covering 6 Level-1 indicators (resource utilization, pollution control, living environment, ecological protection, circular economy, and quality of economic growth) and 28 Level-2 indicators (see Table 1).

Table 1. The Green Development Evaluation Index System.

Level 1 Indicator	Level 2 Indicator	Unit of Measurement	Positive/Negative
Resource Utilization	Energy Consumption per 100 Million RMB of GDP	10 Thousand Tons of Standard Coal/100 Million RMB	Negative
	Natural Gas as a Percentage of Energy Consumption	%	Positive
	Water Consumption per 100 Million RMB of Agricultural Output	10 Thousand Cubic Meters/100 Million RMB	Negative
	Water Consumption per 100 Million RMB of Industrial Output	10 Thousand Cubic Meters/100 Million RMB	Negative
	Land Occupied per 100 Million RMB of Agricultural Output	Hectare/100 Million RMB	Negative
	Land Occupied per 100 Million RMB of Industrial Output	Hectare/100 Million RMB	Negative
Pollution Control	Chemical Oxygen Demand (COD) Emissions	10 Thousand Tons	Negative
	Ammonia Nitrogen Emissions	10 Thousand Tons	Negative
	Carbon Dioxide Emissions	10 Thousand Tons	Negative
	Sulfur Dioxide Emissions	10 Thousand Tons	Negative
	Smoke (Dust) Emissions	10 Thousand Tons	Negative
Living Environment	Green Coverage Rate of Urban Areas	%	Positive
	The Rate of Garden Green Space in Urban Areas	%	Positive
	Implementation Rate of Sanitary Toilet in Rural Areas	%	Positive
	The Ratio of Number of Days Per Year in which the Air Quality of the Provincial Capital City Reaches Grade 2 or Above	%	Positive
Ecological Protection	The Proportion of Protected Areas	%	Positive
	The Proportion of Wetland	%	Positive
	Total Afforestation Area	Hectare	Positive
	Forest Coverage Rate	%	Positive
	Forest Stock	10 Thousand Cubic Meters	Positive
Circular Economy	Urban Water Recycle Rate	%	Positive
	Comprehensive Utilization Rate of Industrial Solid Waste	%	Positive
	Comprehensive Utilization Rate of Hazardous Waste	%	Positive
	Harmless Treatment Capacity of Domestic Waste	Tons per day	Positive
	Harmless Treatment Rate of Domestic Waste	%	Positive
Quality of Economic Growth	GDP per capita	RMB	Positive
	Per capita Disposable Income of Urban Residents	RMB	Positive
	Per capita Disposable Income of Rural Residents	RMB	Positive
	The Proportion of Added Values of the Tertiary Industry in GDP	%	Positive
	Main Operation Incomes of the High-Tech Industry	100 Million RMB	Positive

3.2. Index Calculation Method and Data Source

1. Resource Utilization. The resource utilization indicators reflect the use of energy, water resources and land, and focus on the utilization efficiency of these resources in economic development, with the purpose of promoting a resource-saving economy [55–57]. The level-2 indicators of resource utilization cannot be obtained directly, and need to be calculated from existing data.

2. Pollution Control. The pollution control indicators reflect the main pollutants in wastewater, the main pollutants in exhaust gas and greenhouse gas emissions, with the purpose of stimulating different regions to control the discharge of pollutants by various methods.

3. Living Environment. The living environment indicators include the green coverage rate and the rate of garden green space in urban areas, the air quality of provincial capital cities, and the implementation rate of sanitary toilets in rural areas. These indicators reflect the quality of the living environment of urban and rural residents.

4. Ecological Protection. The ecological protection indicators include the basic conditions of protected areas, wetlands, afforestation and forests in each region, with the purpose of encouraging different regions to actively protect the local ecology and make full use of the local ecological advantages.

5. Circular Economy. The circular economy indicators include the recycle rate of water resources and industrial solid waste, reflecting the ability to reuse and convert waste into renewable resources. The harmless treatment capacity and rate of domestic waste are also included in order to measure the level of recycling waste [58].

6. Quality of Economic Growth. The indicators of economic growth quality include the GDP per capita, per capita Disposable Income, the Proportion of Added Values of the Tertiary Industry in GDP, and the Main Operation Incomes of the High-Tech Industry. These indicators not only reflect the economic development level of each region, but also reflect the economic structure and high-tech industries of each region, with the purpose of encouraging different regions to improve their economic structure and focus on the development of high-tech industries.

The data of the above indicators come from various yearbooks officially released by China and statistical data recognized by academic circles [59–63], thus ensuring the reliability of the calculation results

3.3. Comprehensive Evaluation Model

Based on the above-mentioned green development index system, this section has improved the traditional TOPSIS method with the V-SPA method. This paper has established a comprehensive evaluation model in order to analyze the green development level of different regions from 2005 to 2020 by substituting the vertical distance for the connection vector distance in the set pair analysis and combing it with the approaching ideal point sorting method. TOPSIS is a multi-feature-based sample evaluation method. The basic idea is to select an optimal value and a worst value in the sample for each index, and construct a positive ideal solution and a negative ideal solution that do not actually exist. Taking these two solutions as the reference system, for each sample, the TOPSIS method respectively calculates its distances to the positive ideal solution and the negative ideal solution, and obtains the evaluation score based on the degree of proximity [64,65]. However, the traditional TOPSIS method uses the Euclidean distance when calculating the degree of proximity of the sample to the positive and negative ideal solutions. In some cases, it might happen that the sample is close to both the positive ideal solution and the negative ideal solution, thereby leading to the problem of rank reversal [66]. In order to solve this problem, this section has adopted the set pair analysis method to improve the TOPSIS method, and further improved the model for green development level evaluation by substituting the vertical distance for the connection vector distance in the set pair analysis.

The set pair analysis method is a systematic analysis method raised by Keqin Zhao [67]. This method can analyze uncertain problems based on the degree of connection. It can

analyze certainty, uncertainty, and the interaction between the two using a system of similarities and differences. In order to apply the set pair analysis method to comprehensive evaluation, first, two samples should be selected as pairs for analysis; this is the basic unit of a set-pair analysis. Next, the identity, opposition and difference between the two samples should be analyzed, in which identity and opposition are mainly used to analyze the deterministic connection between the samples, while difference is used to study the uncertainty connection between the samples. Through an analysis of the identity, opposition and difference in the samples, the degree of connection in the set pair can be obtained [68]. For example, we can analyze the set pair $H = (A, B)$, which is made up of sample A and sample B, and obtain the degree of connection between sample A and sample B, as shown in below Equation (1):

$$\mu_{AB} = a + bk + cl \tag{1}$$

In the above equation, a represents the coefficient of identity between sample A and sample B; b represents the coefficient of difference between sample A and sample B; and c is the coefficient of opposition between sample A and sample B. The vector composed of these three coefficients (a, b, c) is the connection vector between sample A and sample B. In particular, when we analyze the set pair $H = (A, A)$, which is made up of sample A and itself, the connection vector obtained will be $(1, 0, 0)$, that is, sample A is identical to itself, and there is no difference or opposition. The approaching ideal point sorting method analyzes the set pair made up of each sample and its positive and negative ideal solutions respectively, obtains the connection vector between each sample and its positive and negative ideal solutions, and then obtains the degree of connection of each sample with its positive ideal solution by calculating the connection vector distance between each sample and its positive and negative ideal solutions.

The traditional set pair analysis method calculates the distance between samples based on the connection vector distance. This method basically considers two connection vectors as two points in space, and then calculates the Euclidean distance between them. In this way, in the case that the sample is both far away from the positive ideal solution and the negative ideal solution, this method cannot correctly reflect the strength and weakness of the sample [69]. Therefore, this section has optimized the set pair analysis method by substituting the vertical distance for the connection vector distance, which has been proven effective by existing research [70,71].

By combining the vertical distance-set pair analysis method with the approaching ideal point sorting method, this paper has established a comprehensive evaluation model for the green development level of different regions. The specific steps are as follows:

Step 1: determine the positive ideal solution $S^+ = \left\{s_1^+, s_2^+, \ldots, s_n^+\right\}$ and the negative ideal solution $S^- = \left\{s_1^-, s_2^-, \ldots, s_n^-\right\}$ based on the data x_{ij}, as shown in Equations (2) and (3):

$$s_j^+ = \begin{cases} \max\limits_i x_{ij}\ j \in J_1 \\ \min\limits_i x_{ij}\ j \in J_2 \end{cases} \tag{2}$$

$$s_j^- = \begin{cases} \min\limits_i x_{ij}\ j \in J_1 \\ \max\limits_i x_{ij}\ j \in J_2 \end{cases} \tag{3}$$

Here, J_1 represents the set of positive indicators, and J_2 represents the set of negative indicators. The positive ideal solution is constructed based on the maximum value of the positive indicator and the minimum value of the negative indicator. The negative ideal solution is constructed based on the minimum value of the positive indicator and the maximum value of the negative indicator. According to the idea of set pair analysis, it can be considered that the positive ideal solution S^+ and the negative ideal solution S^- are in opposition to each other in the system.

Step 2: calculate the degree of connection μ_i^+ between sample A_i and its positive ideal solution S^+. Based on the set pair $H^+ = (A_i, S^+)$ made up of sample A_i and its positive ideal solution S^+, calculate μ_i^+ and μ_{ij}^+ according to the following Equations (4) and (5):

$$\mu_i^+ = a_i^+ + b_i^+ k + c_i^+ l = w_1\mu_{i1}^+ + w_2\mu_{i2}^+ + \ldots + w_n\mu_{in}^+ = \sum_{j=1}^{n} w_j\mu_{ij}^+, i = 1, 2, \ldots, m \quad (4)$$

$$\mu_{ij}^+ = a_{ij}^+ + b_{ij}^+ k + c_{ij}^+ l, i = 1, 2, \ldots, m, j = 1, 2, \ldots, n \quad (5)$$

in which a_i^+ represents the degree of identity between sample A_i and its positive ideal solution S^+; b_i^+ represents the degree of difference between sample A_i and its positive ideal solution S^+; and c_i^+ represents the degree of opposition between sample A_i and its positive ideal solution S^+. The vector composed of these three coefficients $\left(a_i^+, b_i^+, c_i^+\right)$ is the connection vector between sample A_i and its positive ideal solution S^+, written as $\mu_i^+ = \left(a_i^+, b_i^+, c_i^+\right)$; w_j is the weight of indicator j. When $j \in J_1$, if $x_{ij} = s_j^-$, then $a_{ij}^+ = b_{ij}^+ = 0$, and $c_{ij}^+ = 1$; otherwise, if $x_{ij} \in \left(s_j^-, s_j^+\right]$, then $a_{ij}^+ = \frac{x_{ij}}{s_j^+}$, $b_{ij}^+ = 1 - a_{ij}^+$, $c_{ij}^+ = 0$. When $j \in J_2$, if $x_{ij} = s_j^-$, then $a_{ij}^+ = b_{ij}^+ = 0$, $c_{ij}^+ = 1$; otherwise, if $x_{ij} \in \left[s_j^+, s_j^-\right)$, then $a_{ij}^+ = \frac{s_j^+}{x_{ij}}$, $b_{ij}^+ = 1 - a_{ij}^+$, $c_{ij}^+ = 0$.

Step 3: calculate the degree of connection μ_i^- between sample A_i and its negative ideal solution S^-. Based on the set pair $H^- = (A_i, S^-)$ made up of sample A_i and its negative ideal solution S^-, calculate μ_i^- and μ_{ij}^- according to the following Equations (6) and (7):

$$\mu_i^- = a_i^- + b_i^- k + c_i^- l = w_1\mu_{i1}^- + w_2\mu_{i2}^- + \ldots + w_n\mu_{in}^- = \sum_{j=1}^{n} w_j\mu_{ij}^-, i = 1, 2, \ldots, m \quad (6)$$

$$\mu_{ij}^- = a_{ij}^- + b_{ij}^- k + c_{ij}^- l, i = 1, 2, \ldots, m, j = 1, 2, \ldots, n \quad (7)$$

in which a_i^- represents the degree of identity between sample A_i and its negative ideal solution S^-; b_i^- represents the degree of difference between sample A_i and its negative ideal solution S^-; and c_i^- represents the degree of opposition between sample A_i and its negative ideal solution S^-. The vector composed of these three coefficients $\left(a_i^-, b_i^-, c_i^-\right)$ is the connection vector between sample A_i and its negative ideal solution S^-, written as $\mu_i^- = \left(a_i^-, b_i^-, c_i^-\right)$; w_j is the weight of indicator j. When $j \in J_1$, if $x_{ij} = s_j^+$, then $a_{ij}^+ = b_{ij}^+ = 0$, and $c_{ij}^+ = 1$; otherwise, if $x_{ij} \in \left(s_j^-, s_j^+\right]$, then $a_{ij}^+ = \frac{s_j^-}{x_{ij}}$, $b_{ij}^+ = 1 - a_{ij}^+$, $c_{ij}^+ = 0$. When $j \in J_2$, if $x_{ij} = s_j^+$, then $a_{ij}^+ = b_{ij}^+ = 0$, $c_{ij}^+ = 1$; otherwise, if $x_{ij} \in \left[s_j^+, s_j^-\right)$, then $a_{ij}^+ = \frac{x_{ij}}{s_j^-}$, $b_{ij}^+ = 1 - a_{ij}^+$, $c_{ij}^+ = 0$.

Step 4: calculate the connection vector distance between sample A_i and its positive ideal solution S^+. The connection vector of the positive ideal solution S^+ is $\mu^+ = (1, 0, 0)$, and the connection vector of sample A_i is $\mu_i^+ = \left(a_i^+, b_i^+, c_i^+\right)$. The connection vector distance between sample A_i and its positive ideal solution S^+ can be calculated according to Equation (8) below:

$$D_i^+ = \sqrt{\left(1 - a_i^+\right)^2 + \left(b_i^+\right)^2 + \left(c_i^+\right)^2} \quad (8)$$

Step 5: calculate the connection vector distance between sample A_i and its negative ideal solution S^-. The connection vector of the negative ideal solution S^- is $\mu^- = (1, 0, 0)$, and the connection vector of sample A_i is $\mu_i^- = \left(a_i^-, b_i^-, c_i^-\right)$. The connection vector distance between sample A_i and its negative ideal solution S^- can be calculated according to Equation (9) below:

$$D_i^- = \sqrt{\left(1 - a_i^-\right)^2 + \left(b_i^-\right)^2 + \left(c_i^-\right)^2} \quad (9)$$

Step 6: calculate the connection vector distance D between the positive ideal solution S^+ and the negative ideal solution S^-, as shown in Equation (10) below:

$$D = \sqrt{1 + \left(\sum_{j=1}^{n} w_j\right)^2} \tag{10}$$

Step 7: calculate the vertical distance VD_i^+ between sample A_i and its positive ideal solution S^+, as shown in Equation (11) below:

$$VD_i^+ = \frac{D^2 + \left(D_i^+\right)^2 - \left(D_i^-\right)^2}{2D} \tag{11}$$

Step 8: calculate the vertical distance VD_i^- between sample A_i and its negative ideal solution S^-, as shown in Equation (12) below:

$$VD_i^- = \frac{D^2 + \left(D_i^-\right)^2 - \left(D_i^+\right)^2}{2D} \tag{12}$$

Step 9: calculate the degree of relative connection C_i^+ between sample A_i and its positive ideal solution S^+, as shown in Equation (13) below:

$$C_i^+ = \frac{VD_i^-}{\left(VD_i^+ + VD_i^-\right)}, i = 1, 2, \ldots, n \tag{13}$$

where C_i^+ is the evaluation score of the sample, and $0 \leq C_i^+ \leq 1$. The closer C_i^+ is to 1, the closer sample A_i is to the ideal solution, and the higher the evaluation score of sample A_i is. In reality, the case of $C_i^+ = 1$ is very rare.

4. Results and Discussion

Based on the methods and data sources described in Section 2, this paper has obtained the calculation results of the level-1 indicators for green development, as shown in Figures 1–6 below (for specific calculated values, please refer to Tables S1–S26 in the complementary PDF file as Supplementary Materials).

4.1. Resource Utilization

In terms of resource utilization (refer to Figure 1), the evaluation values of the eastern region are significantly higher than that of the western region. As far as the situation of 2005 is concerned, the evaluation values of most provinces in the eastern region are above 0.45, while in the western region, only Chongqing, Sichuan and Shaanxi have evaluation values higher than 0.4. At the end of the research period in 2020, the evaluation values of the eastern region are still generally higher than that of the western region; the average value of the eastern region reached 0.8095, which is much higher than the 0.6201 of the western region.

However, it is worth noting that during this period, the rate of increase in the evaluation value of resource utilization in the western region exceeded that in the eastern region. Among them, the evaluation values of Qinghai, Guizhou, Gansu and Guangxi all increased by more than 100%. This is of course directly related to the low starting point of the resource utilization evaluation values in the western region; however, more importantly, the western region attaches great importance to improving resource utilization efficiency, so that the evaluation value of resource utilization has been significantly improved.

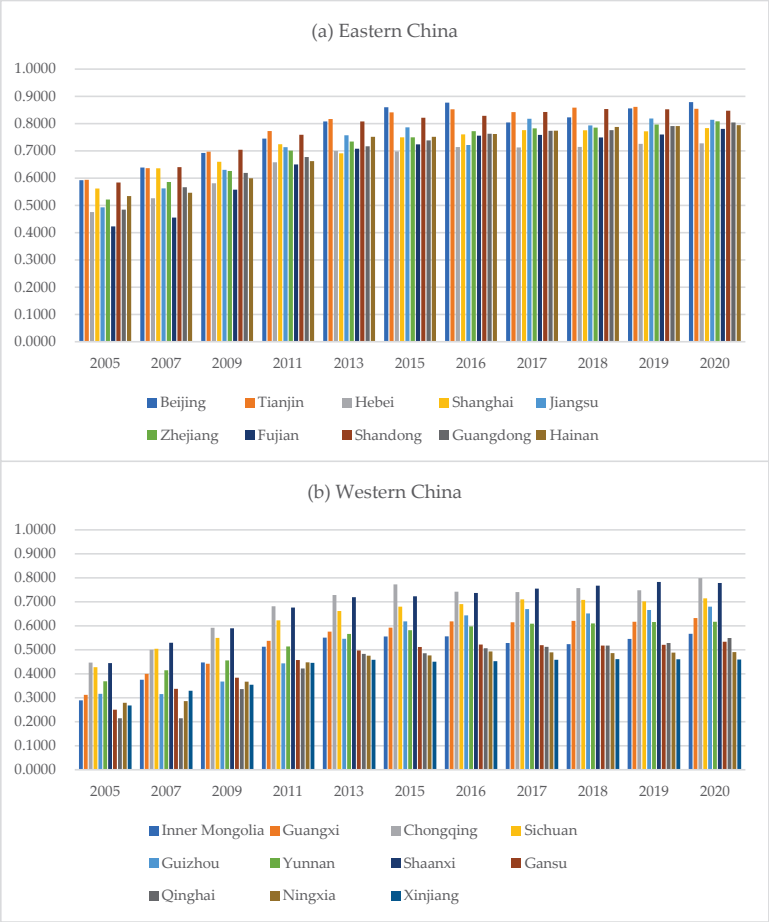

Figure 1. Calculation Results of Resource Utilization Indicators of Provinces in China, 2005–2020: (**a**) Eastern China; (**b**) Western China.

During the research period, the western provinces of China have strived to improve resource utilization efficiency, of which the major policies are as follows:

(1) Development of Clean Energy Sources: The western provinces have encouraged the development of clean energy sources such as wind, solar, hydro, and geothermal energy to reduce their dependence on fossil fuels and improve resource utilization efficiency [72].

(2) Implementation of Energy Efficiency Programs: The western provinces have implemented energy efficiency programs that are aimed at reducing energy consumption in various sectors, including the industrial, residential, and commercial sectors. These programs have helped to improve resource utilization efficiency [73].

(3) Encouragement of Water Conservation: The western provinces have taken measures to conserve water resources, such as promoting water-saving technologies, improving water management systems, and building water-saving infrastructure [74].

(4) Protection of Natural Resources: The western provinces have adopted policies to protect their natural resources, such as forests, grasslands, and wetlands [75].

These policy measures have helped to improve resource utilization performance in western China and have contributed to the increase in the evaluation value of resource utilization during the research period.

4.2. Pollution Control

In terms of pollution control (refer to Figure 2), the eastern provinces also showed a higher overall level than the western provinces. During 2005–2020, the urban agglomerations represented by the Beijing–Tianjin–Hebei region in the eastern region experienced relatively serious air pollution, resulting in fluctuations in the environmental pollution

evaluation value. However, due to the Chinese government's vigorous governance since 2013, the Beijing–Tianjin–Hebei region and other regions' environmental pollution has been well controlled.

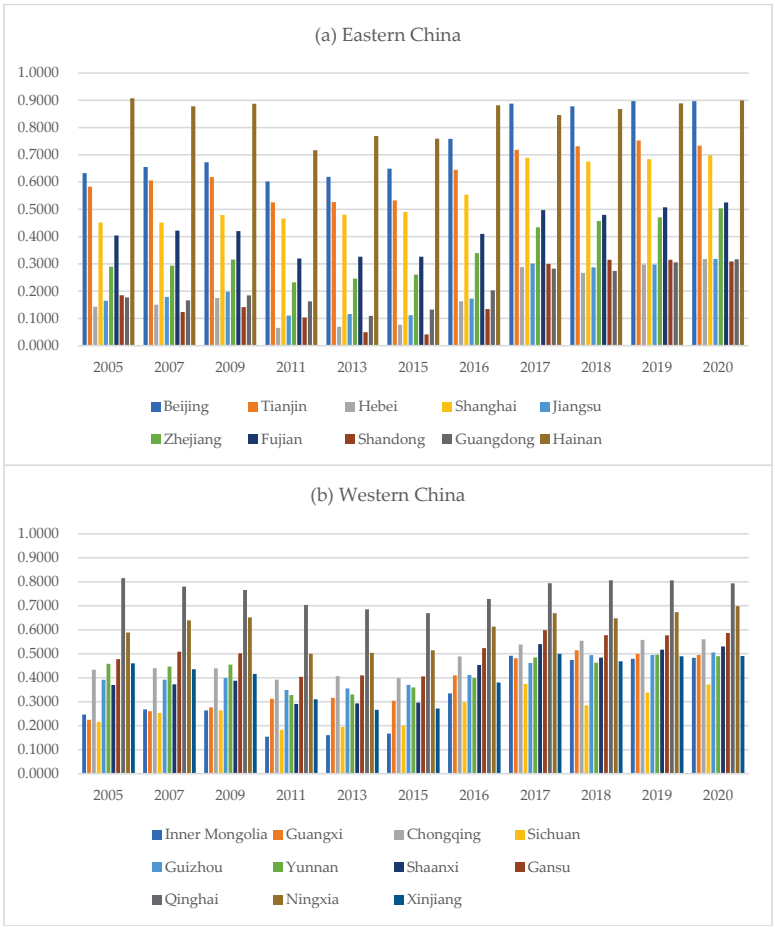

Figure 2. Calculation Results of Pollution Control Indicators of Provinces in China, 2005–2020: (**a**) Eastern China; (**b**) Western China.

In the eastern region, the pollution control policies adopted by the Chinese government mainly include the following:

(1) The Air Pollution Prevention and Control Action Plan. This was launched in 2013 and aims to reduce the concentration of fine particles in the Beijing–Tianjin–Hebei region, the Yangtze River Delta, and the Pearl River Delta by about 25%, 20%, and 15% respectively, by 2017. It also required that the annual average concentration of fine particles in Beijing be controlled at about 60 micrograms per cubic meter by 2017 [76].

(2) The Action Plan for Water Pollution Prevention and Control. It was launched in 2015 and aims to improve water quality in rivers and lakes in eastern China by 2020. It includes measures to regulate the discharge of pollutants, reduce water usage in agriculture and industry, and improve wastewater treatment facilities [77].

(3) The Action Plan for the Prevention and Control of Soil Pollution. It was launched in 2016 and aims to address soil contamination caused by industrial activities, agriculture, and waste disposal. It includes measures to assess soil pollution, clean up contaminated sites, and improve the management of hazardous waste [78].

As far as western region is concerned, overall speaking, the evaluation scores of Guangxi Province and Inner Mongolia showed the largest increase in western China from 2005 to 2020, which increased by 0.2702 and 0.2367, respectively. For Guangxi Province, its overall evaluation score in the field of pollution control showed a steady upward trend during the research period. Although the evaluation score showed a slight decline in

certain years, its growth rate is quite significant during the "Twelfth Five-Year Plan" period. This paper thinks that the underlying reasons for these findings are as follows: among the provinces and cities in the western region, Guangxi has rich non-ferrous metal mineral resources, and is one of the main producing areas of non-ferrous metals in China [79]. In its early development stage, Guangxi faced the problem of the over-exploitation of non-ferrous metal resources and old-fashioned production technologies. Compared to other types of pollution, heavy metal pollution is more prominent in certain parts of the province. In order to facilitate soil pollution control in the region, since 2011, Guangxi Province has issued the Decision on Promoting Industrial Transformation and Upgrading through Environmental Protection Initiatives. By shutting down heavy metal companies, eliminating outdated production capacity, and setting strict emission targets for heavy metal pollutant emissions in key prevention and control areas, Guangxi Province has promoted the transformation and upgrading of local traditional industries. In addition, according to the data on the portal website of the government of Guangxi Zhuang Autonomous Region, from 2011 to 2015, the compliance rate in terms of heavy metal pollutant discharge by key enterprises increased from 75.4% to 97% [80], and the heavy metal pollution has been improved to a certain extent, which is consistent with our calculation results.

For Inner Mongolia, the acceleration in industrial development is represented by the energy and heavy chemical industry during the "Eleventh Five-Year Plan" period (2006–2010). In just five years, the industrial economy of this region has achieved rapid growth. However, in some areas, the focus of development has gradually shifted to GDP growth, while the importance of pollution control has been ignored; GDP achieved rapid growth at the expense of regional ecology. At the same time, the local governments did not make sufficient investments in environmental protection. In cities such as Baotou and Chifeng, the pace of pollutant treatment cannot catch up with the speed of pollutant growth, which increased the difficulty of regional pollution control as a whole. In addition, in the early stage of the "Twelfth Five-Year Plan" period (2011–2015), the rapid increase in the number of motor vehicles and the growth in local industrial production activities led to increasingly prominent air pollution issues in Inner Mongolia, which have attracted the attention of the local government [81,82]. In the early stage of the "Thirteenth Five-Year Plan" period (2016–2020), the State Council made "strengthening environmental governance" one of the key components of ecological civilization construction, and carried out environmental protection inspections in Inner Mongolia, Guangxi and other regions. In order to actively respond to the national policies and initiatives, Inner Mongolia has strengthened the pollution prevention and control measures in key industries, such as electric power, steel, nonferrous metals, petrochemicals, metal smelting, and chemicals; they have also implemented pollutant discharge permits for industries with high energy consumption and heavy pollution, and comprehensively taken measures such as installing central heating, reducing the burning of raw coal, and using natural gas and other clean energy, which has effectively alleviated the problem of local environmental pollution [83].

4.3. Living Environment

In terms of the living environment (refer to Figure 3), the eastern region not only has a superior development foundation compared with the western region, but also continuously optimizes key elements of the living environment, such as urban greening, garden construction, and public health facilities during the research period. For example, Shanghai initiated the 13th Five-Year Plan (2016–2020) for the Greening and City Appearance of Shanghai, which aimed to increase the city's green coverage to 40% by 2020 [84]. The plan included the planting of more trees and the creation of green belts along major roads and waterways. Moreover, in Hangzhou, the capital of Zhejiang Province, Xixi Wetland has become the first and only national wetland park in China that integrates urban wetland, farming wetland and cultural wetland [85]. The park features a variety of landscapes, including reed marshes, lakes, and forests, and is home to a diverse range of flora and fauna, which provides residents with a place to enjoy nature and take part in outdoor activities.

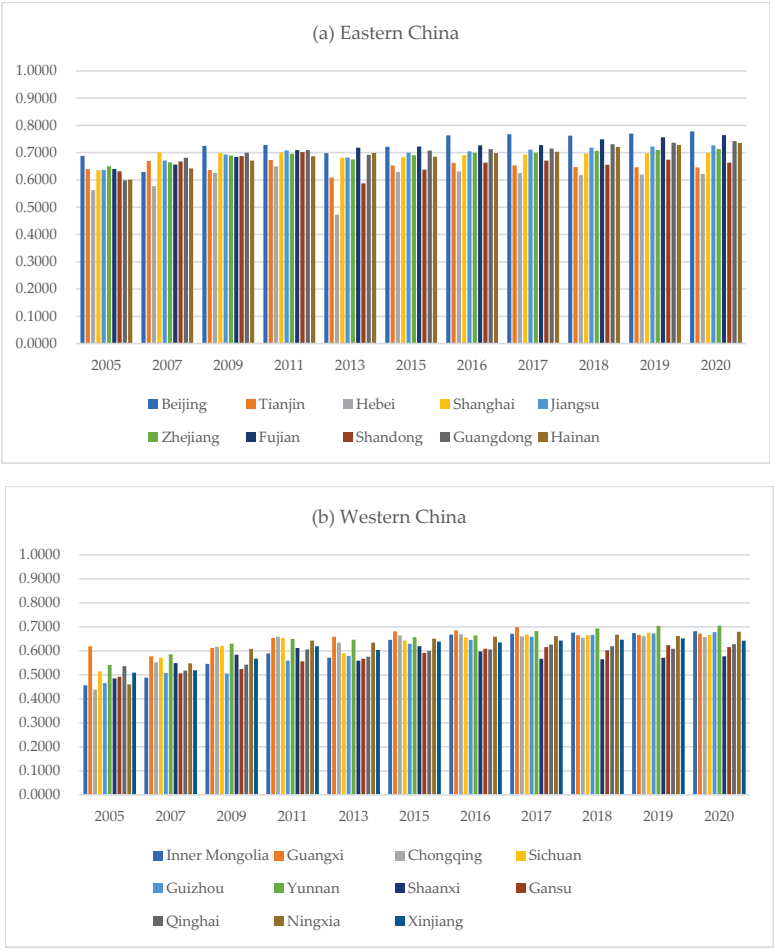

Figure 3. Calculation Results of Living Environment Indicators of Provinces in China, 2005–2020: (**a**) Eastern China; (**b**) Western China.

As far as the western region is concerned, the growth in the evaluation scores in this field is relatively low compared to the other fields. The absolute growth values of the evaluation score of Inner Mongolia, Chongqing, Guizhou, and Ningxia are around 0.2, while the evaluation scores of the other provinces and cities did not show obvious improvements. In general, it is true that the Western Development Strategy has helped various provinces and cities in the western region to achieve remarkable progress in terms of economic and social development. The urbanization process has been accelerated. As the cities continue to expand, their interior space structure and functions have been improved and updated. However, in the process of rapid economic growth, especially for cities with extremely fragile environmental conditions, more emphasis is placed on the development of commercial centers; meanwhile, the development of urban greening is ignored to some extent, resulting in a relatively low level of greening in some cities. In addition, infrastructure and the supporting infrastructure close to residential areas are still relatively simple [86]. Therefore, although the living environment of the western region has been improved slightly in the past 20 years, it is still unsatisfactory on the whole, which is also the key aspect that the western region should strive to improve during the current "14th Five-Year Plan" period.

4.4. Ecological Protection

In terms of ecological protection (refer to Figure 4), there is not much difference between the evaluation values of the eastern region and the western region, and in terms of the evaluation values in 2020, a number of provinces in the western region have surpassed the eastern region. The main reason is that the indicator of ecological protection focuses on

the proportion of protected areas, wetlands and afforestation areas in the total area of the jurisdiction, while the eastern region has a relatively small proportion of protected areas, wetlands and forests due to the high degree of urbanization. Hence, the evaluation values of a few provinces in the eastern region are lower. However, during the research period, the provinces in the eastern region have also adopted a series of measures to improve its own level of ecological protection. For example, the "Green Great Wall" program is introduced in eastern China, aiming to combat desertification and improve soil and water conservation. The Hebei province planned to afforest 4.2 million mu in 2015 as part of the program [87]. Shanghai also implemented the "Ecological Red Line" policy in 2017, designating certain areas as protected zones in which development is limited [88].

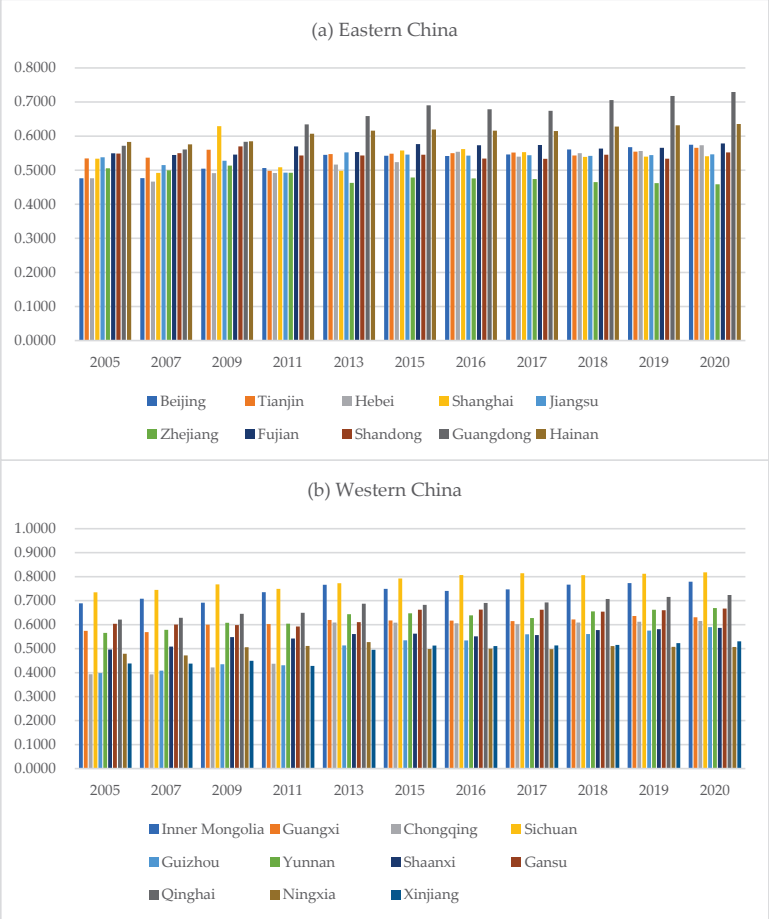

Figure 4. Calculation Results of Ecological Protection Indicators of Provinces in China, 2005–2020: (**a**) Eastern China; (**b**) Western China.

In the western region, Chongqing and Guizhou Province have shown remarkable improvements in these two fields, and their evaluation scores have ranked quite high among the provinces and cities in the western region. As an important driver of the high-quality economic development in western China, Chongqing plays a critical role in promoting the Western Development Strategy of China. In its early stage of development, Chongqing vigorously stimulated the growth of the local economy with its rich natural resources and superior natural conditions. With the growing development intensity, the conflict between economic growth and environmental protection has become increasingly prominent [89]. In recent years, in order to improve the ecological environment and achieve sustainable development, Chongqing has issued multiple policies including the Opinions on Further Promoting the Development of the Yangtze River Economic Belt and Accelerating the Construction of a Land with Beautiful Mountains and Clear Waters, Chongqing City's

Action Plan for Implementing a Green Development Strategy that Prioritizes Ecology Protection (2018–2020), and Chongqing City Pollution Prevention and Control Implementation Plan (2018–2020). With the support of a large number of local policies, the ecological environment of Chongqing has been improved to a certain extent. According to the data released by the Chongqing Municipal Bureau of Ecology and Environment, as of August 2021, Chongqing is committed to rectifying outstanding problems such as environmental pollution and ecological environment protection. In terms of environmental pollution, taking air pollution as an example, the number of days with good air quality has increased to 333 days, and the atmospheric concentrations of air pollutants such as $PM_{2.5}$, NO_2, and SO_2 have all reached the national standard for level-2 air quality. In terms of ecological environment protection, Chongqing has maintained the stability of the regional ecosystem by launching various initiatives, including ecological punch cards and experience sharing in natural ecological environment management cases. According to the data of Chongqing [90], in 2020, the forest coverage rate in Chongqing reached 52.5%, and the number of natural reserves reached 58, accounting for about 9.76% of the city's land area. However, for Guizhou, compared with other provinces and cities, although the province has a great competitive advantage in the reserves of natural resources, with high vegetation coverage and a wide variety of biological species, the local ecological environment is still highly fragile [91]. Therefore, Guizhou became the only ecological civilization pilot site in western China in 2016. Through continuous investment in ecological environment protection in recent years, Guizhou Province has made considerable achievements in this field. Since 2016, Guizhou Province has been committed to the implementation of key ecological projects, such as returning farmland to forests and the comprehensive treatment of stony desertification. A total of 4.77 million mu of farmland has been converted to forests, and 1000 square kilometers of land with stony desertification have been treated [92]. In addition, Guizhou Province has launched the compilation work of a list of provincial important wetlands while conducting the fourth general investigation into forest resources in the province, thus attaching great importance to the local ecological protection. At the same time, in the utilization of natural resources, Guizhou Province has made full use of its own forest resources. With the development of its characteristic forestry industry being the core, Guizhou Province has invested a lot of money in the construction of pilot forest health care centers, which not only improves the ecological environment, but also drives the rapid growth of the local economy.

In addition, it is worth noticing that most of the provinces and cities in western China did not perform well in ecological environment protection. This shows that, currently, the ecological environment protection work in western China is not effective enough. Problems such as soil erosion and desertification are still effectively controlled with difficulty, and it is not uncommon to see that the ecological environment is being damaged while being treated at the same time [93].

4.5. Circular Economy

In terms of the circular economy (refer to Figure 5), the development level of the eastern region is generally higher than that of the western region. Taking 2020 as an example, five provinces in the eastern region, Shanghai, Jiangsu, Zhejiang, Shandong, and Guangdong, have evaluation values exceeding 0.9, while those of the western provinces are generally lower. In addition to the relatively weak foundation and technical level of the circular economy in the western region, the provinces in the eastern region made full use of their own developed urbanization level and technological advantages in order to recycle urban water, comprehensively utilize industrial wastewater and solid waste. They also made relatively large progress in the harmless treatment capacity of domestic waste. For example, Shanghai has established a comprehensive water circulation system and built several large-scale water recycling plants, which effectively recycle and reuse treated wastewater [94]. Jiangsu has implemented a series of measures to comprehensively utilize industrial wastewater, including improving the treatment capacity of wastewater and

promoting the reuse of treated wastewater in the industrial sector [95]. Zhejiang province has actively promoted the utilization of solid waste, including the construction of several large-scale waste-to-energy plants, which effectively utilize and reduce the amount of solid waste [96]. Guangdong province has made efforts to improve the treatment capacity of domestic waste, including building several large-scale domestic waste incineration plants and promoting waste separation and recycling [97].

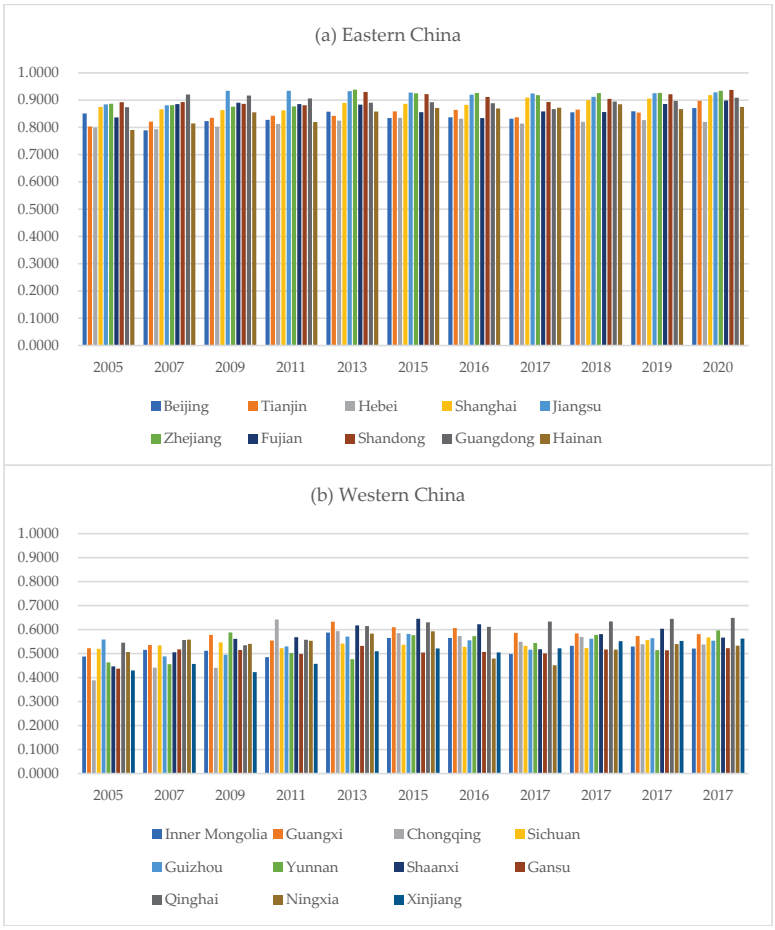

Figure 5. Calculation Results of Circular Economy Indicators of Provinces in China, 2005–2020: (**a**) Eastern China; (**b**) Western China.

In addition, it can be seen from the calculation results that although Guangxi and Inner Mongolia perform relatively well in the field of pollution control, their evaluations scores in terms of the circular economy are at an average level. In comparison, although the evaluation score of Qinghai Province in terms of pollution control has dropped instead of increased, its evaluation score in the field of the circular economy has increased significantly. The reason is that, at this stage, Qinghai Province listed 15 cities and counties, including Xining City and Haixi Prefecture, as pilot areas for Qinghai's circular economy program. Among these cities and counties, the Qaidam Circular Economy Pilot Zone was approved by the National Development and Reform Commission (NDRC) in 2005 as one of the first 13 circular economy pilot zones in China. Therefore, Qinghai Province has accumulated rich practical experience in the field of circular economy, and its evaluation score has performed well in the past fifteen years [98].

4.6. Economic Growth Quality

In terms of the quality of economic growth (refer to Figure 6), overall speaking, the evaluation scores of various provinces and cities in the western region are relatively

low compared to their counterparts in the eastern region, especially in the early stage of development. The evaluation scores of most of the provinces and cities are in the range of 0.2 to 0.3.

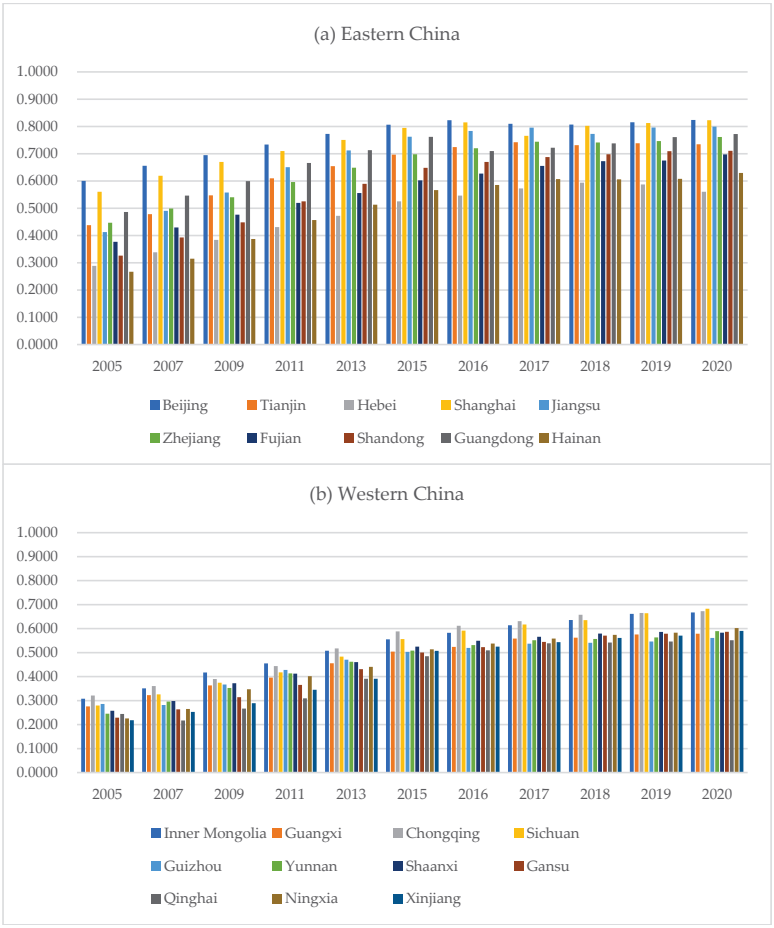

Figure 6. Calculation Results of Economic Growth Quality Indicators of Provinces in China, 2005–2020: (**a**) Eastern China; (**b**) Western China.

However, although the starting point is not high, in terms of the growth rate, the quality of economic growth in the provinces and cities of western China has seen dramatic improvements. Among these provinces and cities, the evaluation score growth of Sichuan and Inner Mongolia in the field of economic growth quality has ranked top; they have reached 0.4032 and 0.3592, respectively.

The main reason that the western region has a larger growth in the evaluation score of this field than the eastern region is that in the early stage of development, although the western region is rich in natural resources and energy reserves, the economic development of most provinces and cities is quite old-fashioned and the western region faces the risk of further widening the gap with other parts of the country [99]. In order to promote the improvement in the economic development quality of various provinces and cities in the western region while balancing it with the development of the local ecological environment, China implemented the Western Development Strategy in 2000, which greatly accelerated the overall economic development of the western region [100].

In addition, it is worth noticing that the absolute growth value of Sichuan Province's evaluation score in the field of economic growth quality is No. 1 among all the provinces and cities in the western and eastern region. This is mainly because, on the one hand, in the past 20 years, Sichuan Province has made the electronic information, equipment manufacturing, advanced materials, energy and chemical industries the pillar industries of the province. Through continuous trial and exploration, Sichuan Province has gradually

upgraded its industrial structure towards the direction of high efficiency and high end products, which has effectively promoted the rapid growth of the local economy. On the other hand, with the continuous growth in the regional economy, the economic ties between different cities have become more and more close. During the "Twelfth Five-Year Plan" period, Sichuan Province proposed to focus on the development of four major urban agglomerations in Chengdu Plain, South Sichuan, Northeast Sichuan and Panxi; they the province also defined their scope and city level, building a multi-point and multi-level support system for the development of Sichuan Province, and made full use of their unique location advantages in order to drive the development of the overall economy.

4.7. Overall Evaluation and Comparison with Other Studies

Based on the above calculation results, this paper finds that there are large differences in the level of green development among provinces and cities in the western region, and compared with the eastern region, the overall development level of the western region is relatively low. It is undeniable that in the early stage of development, the western region has lower comprehensive evaluation scores due to its location, reflected by the slow progress of economic and social development and by serious environmental pollution in the region. With the acceleration of urbanization and the attention paid by local governments to the ecological environment, most provinces and cities in the region have made great progress in terms of green development. Despite this, there are still a few provinces and cities with a small increase in the comprehensive evaluation score. The growth of their comprehensive evaluation score is not as significant as other provinces and cities in the western region, and as of 2020, their comprehensive evaluation scores are much lower than provinces and cities in the eastern region. In comparison, the comprehensive evaluation scores of provinces and cities in the eastern region were already quite high in 2005. Benefiting from their geographical advantages and the strong support of local governments' policies, the comprehensive evaluation scores of most regions in eastern China exceeded 4.0 in 2020. At the same time, compared with the western region, the eastern region has a better foundation for economic development. Therefore, although the growth of the comprehensive evaluation score of the eastern region has been slightly slower than that of the western region in the past 20 years, the comprehensive evaluation score of the eastern region is still ahead of that of the western region in general.

Through the discussions of the above research results, this paper provides detailed evaluation results for the comparison of the level of green development in the eastern and western regions of China. It can help the eastern region better apply its own advanced green development advantages in order to assist the western region to effectively improve the level of green development. On the basis of these research results and discussions, the western region can learn and gain advanced experience from its eastern counterpart in terms of developing a green economy, effectively improving its own level of green development, and making contributions to China's overall sustainable development.

The above research results are consistent with the regional differences in China's green development level in the existing research. For example, Tan et al. [101] constructed an evaluation index system for green innovation in Chinese cities, and conducted research on the level of green innovation in major cities in China during 2006–2017. The results show that the average green innovation level of China's major cities has increased significantly during the research period, but the regional imbalance is obvious: the eastern region is much higher than the average level, while the western region is lower than the average level. Yang et al. [102] used a three-stage DEA model to study the efficiency of urban green development in the Yangtze River Delta region of China. The results of the study show that the green development efficiency of the third stage in the Yangtze River Delta region is better than that of the first stage, but there are significant differences among cities in different geographical locations. Feng et al. [103] used the Super-SBM model to study the green innovation efficiency of 19 urban agglomerations in China from 2006 to 2018. The results show that the green innovation efficiency of these urban agglomerations in China

mostly had an upward trend during the research period, and that the efficiency values of the Eastern region are significantly higher than those of the Central and Western regions.

By constructing the improved evaluation index system and evaluation method, we have further confirmed the differences in green development between the eastern and western regions of China, and enriched the existing literature on green development. Since green development is an important and growing area of research that focuses on the interplay between environmental and social sustainability, our study topic in the future will further consider the impact of economic and social development on the environment, such as the impact of green development on the local economy and job creation, the relationship between green development and poverty reduction in China, and the impact of green development on the health and well-being of communities, etc.

5. Conclusions

This paper has constructed a comprehensive evaluation index system for green development, and improved the traditional TOPSIS method with the use of the V-SPA method. By substituting the vertical distance for the connection vector distance in the set pair analysis, and combining it with the approaching ideal point sorting method, this paper has conducted a comprehensive evaluation and comparative analysis of the green development levels of 21 provinces in eastern and western China from 2005 to 2020.

We find that the level of green development in eastern China is significantly higher than that in the western region, and there are large differences in the level of green development among the provinces and cities of western China; the following conclusions can be especially made:

(1) In 2020, when the research period ends, the comprehensive evaluation values of green development in all eastern provinces, except Hebei, are higher than 4.0. Among them, the evaluation values of Beijing and Hainan exceed 4.5, and the evaluation value of Shanghai is also close to 4.5. However, no province in the western region has a comprehensive evaluation value exceeding 4.0 in 2020, and there is a big gap between the eastern region and the western region in areas such as economic growth quality and pollution control.

(2) Thanks to the Western Development Strategy, the provinces and cities in the western region have greatly improved their evaluation scores in the field of economic growth quality, but the improvements in the fields of pollution control and circular economy are still lower, reflected by a low urban green coverage and insufficient infrastructure.

(3) Overall, the evaluation scores of most provinces and cities in the western region have shown an improvement trend over the years, and some provinces and cities have seen large increases in their evaluation scores. As of the end of the research period, some provinces and cities even reached the same level of evaluation scores as the eastern region. However, in terms of the overall development level, there is still a large gap between the western region and the eastern region in various fields.

In view of this, we have listed the following policy recommendations to help the eastern and western regions of China learn from each other's strengths and jointly improve their level of green development, leading to a more sustainable and environmentally friendly future for China as a whole:

(1) Establishing green development partnerships. The two regions can establish cross-regional partnerships to jointly plan, implement, and monitor green development projects. This will allow both regions to learn from each other's experiences and work together to achieve shared goals.

(2) Promoting green innovation. Both regions can encourage green innovation by providing incentives and support for entrepreneurs and businesses that are developing green technologies and products. This can include funding, mentorship, and technical assistance.

(3) Transferring green technology. The eastern region can share its advanced green technology and best practices with the western region, while the western region can provide valuable insights into the practical implementation of these technologies in local

conditions. This can be achieved through joint research and development programs, technical exchanges, and the sharing of resources.

(4) Jointly investing in green infrastructure. Both regions can invest in shared green infrastructure, such as renewable energy projects, environmental protection programs, and green transportation systems, to improve their overall green development levels. The eastern region can bring its advanced technology and experience in project management, while the western region can offer its abundant natural resources and untapped potential for green development.

(5) Promoting green consumption patterns. Both regions can work together to promote sustainable consumption patterns by encouraging the use of green products and services, and promoting environmentally friendly lifestyles. This can be achieved through education and awareness campaigns, spiritual and material rewards, and incentives for businesses and individuals to adopt green practices.

Supplementary Materials: The following supporting information can be downloaded at: https://www.mdpi.com/article/10.3390/su15053965/s1.

Author Contributions: Conceptualization, W.Y. and Q.D.; methodology, H.G.; software, Y.H.; validation, W.Y., H.G. and Y.H.; formal analysis, H.G.; resources, W.Y.; data curation, W.Y. and L.L.; writing—original draft preparation, Q.D., H.G. and Y.H.; writing—review and editing, W.Y. and Y.H.; visualization, Q.D.; supervision, W.Y.; project administration, L.L.; funding acquisition, W.Y. All authors contributed equally to this work. All authors have read and agreed to the published version of the manuscript.

Funding: Weixin Yang was financially supported by the General Project of Shanghai Philosophy and Social Science Planning (2021BGL014) and the Shangli Chenxi Social Science Special Project of University of Shanghai for Science and Technology [22SLCX-ZD-010].

Institutional Review Board Statement: Not applicable.

Informed Consent Statement: Not applicable.

Data Availability Statement: The data used in this paper are all from the statistical data officially released by China and have been explained in Section 3.2.

Conflicts of Interest: The authors declare no conflict of interest.

References

1. Jiang, B.; Li, Y.; Yang, W. Evaluation and Treatment Analysis of Air Quality Including Particulate Pollutants: A Case Study of Shandong Province, China. *Int. J. Environ. Res. Public Health* **2020**, *17*, 9476. [CrossRef]
2. Gao, H.; Yang, W.; Wang, J.; Zheng, X. Analysis of the Effectiveness of Air Pollution Control Policies Based on Historical Evaluation and Deep Learning Forecast: A Case Study of Chengdu-Chongqing Region in China. *Sustainability* **2021**, *13*, 206. [CrossRef]
3. Lan, K.; Chen, Y. Air Quality and Thermal Environment of Primary School Classrooms with Sustainable Structures in Northern Shaanxi, China: A Numerical Study. *Sustainability* **2022**, *14*, 12039. [CrossRef]
4. Altenburg, T.; Corrocher, N.; Malerba, F. China's Leapfrogging in Electromobility. A Story of Green Transformation Driving Catch-up and Competitive Advantage. *Technol. Forecast. Change* **2022**, *183*, 121914. [CrossRef]
5. Xi, J. Report at the 20th National Congress of the Communist Party of China. Available online: http://www.gov.cn/xinwen/2022-10/25/content_5721685.htm (accessed on 1 February 2022).
6. Udemba, E.N.; Tosun, M. Moderating Effect of Institutional Policies on Energy and Technology towards a Better Environment Quality: A Two Dimensional Approach to China's Sustainable Development. *Technol. Forecast. Soc. Change* **2022**, *183*, 121964. [CrossRef]
7. Yang, W.; Gao, H.; Yang, Y. Analysis of Influencing Factors of Embodied Carbon in China's Export Trade in the Background of "Carbon Peak" and "Carbon Neutrality". *Sustainability* **2022**, *14*, 3308. [CrossRef]
8. Kshitij, G.; Khanna, N.; Yıldırım, Ç.V.; Dağlı, S.; Sarıkaya, M. Resource Conservation and Sustainable Development in the Metal Cutting Industry within the Framework of the Green Economy Concept: An Overview and Case Study. *Sustain. Mater. Technol.* **2022**, *34*, e00507. [CrossRef]
9. Płotka Wasylka, J.; Mohamed, H.M.; Kurowska-Susdorf, A.; Dewani, R.; Fares, M.Y.; Andruch, V. Green Analytical Chemistry as an Integral Part of Sustainable Education Development. *Curr. Opin. Green Sustain. Chem.* **2021**, *31*, 100508. [CrossRef]

10. Zikargae, M.H.; Woldearegay, A.G.; Skjerdal, T. Empowering Rural Society through Non-Formal Environmental Education: An Empirical Study of Environment and Forest Development Community Projects in Ethiopia. *Heliyon* **2022**, *8*, e09127. [CrossRef]
11. Yang, W.; Gao, H.; Yang, Y.; Liao, J. Embodied Carbon in China's Export Trade: A Multi Region Input-Output Analysis. *Int. J. Environ. Res. Public Health* **2022**, *19*, 3894. [CrossRef]
12. Magazzino, C.; Mele, M. On the Relationship between Transportation Infrastructure and Economic Development in China. *Res. Transp. Econ.* **2021**, *88*, 100947. [CrossRef]
13. Zheng, J.; Mi, Z.; Coffman, D.; Milcheva, S.; Shan, Y.; Guan, D.; Wang, S. Regional Development and Carbon Emissions in China. *Energy Econ.* **2019**, *81*, 25–36. [CrossRef]
14. Lv, C.; Bian, B.; Lee, C.-C.; He, Z. Regional Gap and the Trend of Green Finance Development in China. *Energy Econ.* **2021**, *102*, 105476. [CrossRef]
15. Azam, M.; Younes, B.Z.; Hunjra, A.I.; Hussain, N. Integrated Spatial-Temporal Decomposition Analysis for Life Cycle Assessment of Carbon Emission Intensity Change in Various Regions of China. *Resour. Policy* **2022**, *79*, 103062. [CrossRef]
16. Lu, S.; Zhao, Y.; Chen, Z.; Dou, M.; Zhang, Q.; Yang, W. Association between Atrial Fibrillation Incidence and Temperatures, Wind Scale and Air Quality: An Exploratory Study for Shanghai and Kunming. *Sustainability* **2021**, *13*, 5247. [CrossRef]
17. Hasan, M.M.; Du, F. Nexus between Green Financial Development, Green Technological Innovation and Environmental Regulation in China. *Renew. Energy* **2023**, *204*, 218–228. [CrossRef]
18. National Bureau of Statistics of China. Method of Dividing China's East, West, Central and Northeastern Regions. Available online: http://www.stats.gov.cn/ztjc/zthd/sjtjr/dejtjkfr/tjkp/201106/t20110613_71947.htm (accessed on 26 December 2022).
19. Zhu, J.; Lu, C.; Wei, Z. Perception of Air Pollution and the Evaluation of Local Governments' Environmental Governance: An Empirical Study on China. *Atmosphere* **2023**, *14*, 212. [CrossRef]
20. Shen, X.; Yang, W.; Sun, S. Analysis of the Impact of China's Hierarchical Medical System and Online Appointment Diagnosis System on the Sustainable Development of Public Health: A Case Study of Shanghai. *Sustainability* **2019**, *11*, 6564. [CrossRef]
21. Li, Y.; Yang, W.; Shen, X.; Yuan, G.; Wang, J. Water Environment Management and Performance Evaluation in Central China: A Research Based on Comprehensive Evaluation System. *Water* **2019**, *11*, 2472. [CrossRef]
22. Andersson, F.N.G. International Trade and Carbon Emissions: The Role of Chinese Institutional and Policy Reforms. *J. Environ. Manag.* **2018**, *205*, 29–39. [CrossRef]
23. Udara Willhelm Abeydeera, L.H.; Wadu Mesthrige, J.; Samarasinghalage, T.I. Global Research on Carbon Emissions: A Scientometric Review. *Sustainability* **2019**, *11*, 3972. [CrossRef]
24. Abbasi, K.R.; Shahbaz, M.; Zhang, J.; Irfan, M.; Alvarado, R. Analyze the Environmental Sustainability Factors of China: The Role of Fossil Fuel Energy and Renewable Energy. *Renew. Energy* **2022**, *187*, 390–402. [CrossRef]
25. Bhatti, U.A.; Zeeshan, Z.; Nizamani, M.M.; Bazai, S.; Yu, Z.; Yuan, L. Assessing the Change of Ambient Air Quality Patterns in Jiangsu Province of China Pre-to Post-COVID-19. *Chemosphere* **2022**, *288*, 132569. [CrossRef]
26. Filonchyk, M.; Peterson, M. Air Quality Changes in Shanghai, China, and the Surrounding Urban Agglomeration During the COVID-19 Lockdown. *J. Geovis, Spat. Anal.* **2020**, *4*, 22. [CrossRef]
27. Stavropoulos, S.; Wall, R.; Xu, Y. Environmental Regulations and Industrial Competitiveness: Evidence from China. *Appl. Econ.* **2018**, *50*, 1378–1394. [CrossRef]
28. Wang, D.; Ding, R.; Gong, Y.; Wang, R.; Wang, J.; Huang, X. Feasibility of the Northern Sea Route for Oil Shipping from the Economic and Environmental Perspective and Its Influence on China's Oil Imports. *Mar. Policy* **2020**, *118*, 104006. [CrossRef]
29. Yang, W.; Li, L. Energy Efficiency, Ownership Structure, and Sustainable Development: Evidence from China. *Sustainability* **2017**, *9*, 912. [CrossRef]
30. Shahbaz, M.; Raghutla, C.; Song, M.; Zameer, H.; Jiao, Z. Public-Private Partnerships Investment in Energy as New Determinant of CO2 Emissions: The Role of Technological Innovations in China. *Energy Econ.* **2020**, *86*, 104664. [CrossRef]
31. Zameer, H.; Wang, Y.; Yasmeen, H. Reinforcing Green Competitive Advantage through Green Production, Creativity and Green Brand Image: Implications for Cleaner Production in China. *J. Clean. Prod.* **2020**, *247*, 119119. [CrossRef]
32. Yang, W.; Yang, Y. Research on Air Pollution Control in China: From the Perspective of Quadrilateral Evolutionary Games. *Sustainability* **2020**, *12*, 1756. [CrossRef]
33. Qazi, A.; Hussain, F.; Rahim, N.A.B.D.; Hardaker, G.; Alghazzawi, D.; Shaban, K.; Haruna, K. Towards Sustainable Energy: A Systematic Review of Renewable Energy Sources, Technologies, and Public Opinions. *IEEE Access* **2019**, *7*, 63837–63851. [CrossRef]
34. Yang, Y.; Yang, W.; Chen, H.; Li, Y. China's Energy Whistleblowing and Energy Supervision Policy: An Evolutionary Game Perspective. *Energy* **2020**, *213*, 118774. [CrossRef]
35. Geall, S.; Ely, A. Narratives and Pathways towards an Ecological Civilization in Contemporary China. *China Q.* **2018**, *236*, 1175–1196. [CrossRef]
36. Liu, Q.; Zhu, Y.; Yang, W.; Wang, X. Research on the Impact of Environmental Regulation on Green Technology Innovation from the Perspective of Regional Differences: A Quasi-Natural Experiment Based on China's New Environmental Protection Law. *Sustainability* **2022**, *14*, 1714. [CrossRef]
37. Eguchi, S.; Takayabu, H.; Lin, C. Sources of Inefficient Power Generation by Coal-Fired Thermal Power Plants in China: A Metafrontier DEA Decomposition Approach. *Renew. Sustain. Energy Rev.* **2021**, *138*, 110562. [CrossRef]

38. Bresser, D.; Hosoi, K.; Howell, D.; Li, H.; Zeisel, H.; Amine, K.; Passerini, S. Perspectives of Automotive Battery R&D in China, Germany, Japan, and the USA. *J. Power Sources* **2018**, *382*, 176–178. [CrossRef]
39. Zhou, F.; Wang, X.; Lim, M.K.; He, Y.; Li, L. Sustainable Recycling Partner Selection Using Fuzzy DEMATEL-AEW-FVIKOR: A Case Study in Small-and-Medium Enterprises (SMEs). *J. Clean. Prod.* **2018**, *196*, 489–504. [CrossRef]
40. Abdul, D.; Wenqi, J. Evaluating Appropriate Communication Technology for Smart Grid by Using a Comprehensive Decision-Making Approach Fuzzy TOPSIS. *Soft Comput.* **2022**, *26*, 8521–8536. [CrossRef]
41. Irfan, M.; Elavarasan, R.M.; Ahmad, M.; Mohsin, M.; Dagar, V.; Hao, Y. Prioritizing and Overcoming Biomass Energy Barriers: Application of AHP and G-TOPSIS Approaches. *Technol. Forecast. Soc. Change* **2022**, *177*, 121524. [CrossRef]
42. Zhou, F.; Lim, M.K.; He, Y.; Pratap, S. What Attracts Vehicle Consumers' Buying: A Saaty Scale-Based VIKOR (SSC-VIKOR) Approach from after-Sales Textual Perspective? *Ind. Manag. Data Syst.* **2019**, *120*, 57–78. [CrossRef]
43. Harlan, T. Conservation or Decarbonization? Small Hydropower and State Logics of Green Development in China. *Ann. Am. Assoc. Geogr.* **2020**, *110*, 1464–1482. [CrossRef]
44. Sahu, B.K. Wind Energy Developments and Policies in China: A Short Review. *Renew. Sustain. Energy Rev.* **2018**, *81*, 1393–1405. [CrossRef]
45. Zhang, S.; Wu, Z.; Wang, Y.; Hao, Y. Fostering Green Development with Green Finance: An Empirical Study on the Environmental Effect of Green Credit Policy in China. *J. Environ. Manag.* **2021**, *296*, 113159. [CrossRef]
46. Yang, W.; Yang, Y.; Chen, H. How to Stimulate Chinese Energy Companies to Comply with Emission Regulations? Evidence from Four-Party Evolutionary Game Analysis. *Energy* **2022**, *258*, 124867. [CrossRef]
47. Liu, M.; Lo, K. Governing Eco-Cities in China: Urban Climate Experimentation, International Cooperation, and Multilevel Governance. *Geoforum* **2021**, *121*, 12–22. [CrossRef]
48. Wu, H.; Ren, S.; Yan, G.; Hao, Y. Does China's Outward Direct Investment Improve Green Total Factor Productivity in the "Belt and Road" Countries? Evidence from Dynamic Threshold Panel Model Analysis. *J. Environ. Manag.* **2020**, *275*, 111295. [CrossRef]
49. Gallagher, K.S.; Zhang, F.; Orvis, R.; Rissman, J.; Liu, Q. Assessing the Policy Gaps for Achieving China's Climate Targets in the Paris Agreement. *Nat. Commun.* **2019**, *10*, 1256. [CrossRef]
50. Ullah, A.; Pinglu, C.; Ullah, S.; Qaisar, Z.H.; Qian, N. The Dynamic Nexus of E-Government, and Sustainable Development: Moderating Role of Multi-Dimensional Regional Integration Index in Belt and Road Partner Countries. *Technol. Soc.* **2022**, *68*, 101903. [CrossRef]
51. Kumari, R.; Verma, R.; Debata, B.R.; Ting, H. A Systematic Literature Review on the Enablers of Green Marketing Adoption: Consumer Perspective. *J. Clean. Prod.* **2022**, *366*, 132852. [CrossRef]
52. Liu, H.; Liu, J.; Yang, W.; Chen, J.; Zhu, M. Analysis and Prediction of Land Use in Beijing-Tianjin-Hebei Region: A Study Based on the Improved Convolutional Neural Network Model. *Sustainability* **2020**, *12*, 3002. [CrossRef]
53. Hickel, J. The Sustainable Development Index: Measuring the Ecological Efficiency of Human Development in the Anthropocene. *Ecol. Econ.* **2020**, *167*, 106331. [CrossRef]
54. Kwatra, S.; Kumar, A.; Sharma, P. A Critical Review of Studies Related to Construction and Computation of Sustainable Development Indices. *Ecol. Indic.* **2020**, *112*, 106061. [CrossRef]
55. Wang, M.; Feng, C. Regional total-factor productivity and environmental governance efficiency of China's industrial sectors: A two-stage network-based super DEA approach. *J. Clean. Prod.* **2020**, *273*, 123110. [CrossRef]
56. Li, L.; Yang, W. Total Factor Efficiency Study on China's Industrial Coal Input and Wastewater Control with Dual Target Variables. *Sustainability* **2018**, *10*, 2121. [CrossRef]
57. Cheng, X.; Long, R.; Yang, J. Interactive effects of two-way information and perceived convenience on waste separation behavior: Evidence from residents in eastern China. *J. Clean. Prod.* **2022**, *374*, 134032. [CrossRef]
58. National Bureau of Statistics of China. China's Circular Economy Development Index Was 137.6 in 2013. Available online: http://www.stats.gov.cn/tjsj/zxfb/201503/t20150318_696673.html (accessed on 1 February 2023).
59. National Bureau of Statistics of China. *China Statistical Yearbook, 2005–2020*; China Statistics Press: Beijing, China, 2021.
60. National Bureau of Statistics of China; Ministry of Environmental Protection. *China Statistical Yearbook on Environment, 2005–2020*; China Statistics Press: Beijing, China, 2021.
61. National Bureau of Statistics of China; National Development and Reform Commission; Ministry of Science and Technology. *China Statistics Yearbook on High Technology Industry, 2005–2020*; China Statistics Press: Beijing, China, 2021.
62. Department of Energy Statistics, National Bureau of Statistics. *China Energy Statistical Yearbook, 2005–2020*; China Statistics Press: Beijing, China, 2021.
63. CEADs. Carbon Emission Accounts & Datasets. Available online: https://www.ceads.net/ (accessed on 1 February 2022).
64. Marchetti, D.; Wanke, P. Efficiency of the Rail Sections in Brazilian Railway System, Using TOPSIS and a Genetic Algorithm to Analyse Optimized Scenarios. *Transp. Res. Part E Logist. Transp. Rev.* **2020**, *135*, 101858. [CrossRef]
65. Więckowski', J.; Sałabun, W. How to Handling with Uncertain Data in the TOPSIS Technique? *Procedia Comput. Sci.* **2020**, *176*, 2232–2242. [CrossRef]
66. García Cascales, M.S.; Lamata, M.T. On Rank Reversal and TOPSIS Method. *Math. Comput. Model.* **2012**, *56*, 123–132. [CrossRef]
67. Zhao, K. Set Pair and Set Pair Analysis—A New Concept and Systematic Analysis Method. In Proceedings of the National Conference on System Theory and Regional Planning, Baotou, China; 1989; pp. 87–91.

68. Kumar, K.; Chen, S. Multiattribute Decision Making Based on Interval-Valued Intuitionistic Fuzzy Values, Score Function of Connection Numbers, and the Set Pair Analysis Theory. *Inf. Sci.* **2021**, *551*, 100–112. [CrossRef]
69. Xiang, W.; Yang, X.; Babuna, P.; Bian, D. Development, Application and Challenges of Set Pair Analysis in Environmental Science from 1989 to 2020: A Bibliometric Review. *Sustainability* **2022**, *14*, 153. [CrossRef]
70. Meng, F.; Zou, Y. The Optimization Degree Evaluation of Energy Structure Based on the SPA-TOPSIS. *Oper. Res. Manag. Sci.* **2018**, *27*, 122–130.
71. Huang, L.; Liu, C.; Wu, F.; Yang, Z.; Li, X. An Improved TOPSIS Method Based on Vertical Projection Distance of Connection Vector. *Syst. Eng.* **2019**, *37*, 119–129.
72. Li, L.; Fan, F.; Liu, X. Determinants of Rural Household Clean Energy Adoption Intention: Evidence from 72 Typical Villages in Ecologically Fragile Regions of Western China. *J. Clean. Prod.* **2022**, *347*, 131296. [CrossRef]
73. Zheng, C.; Deng, F.; Li, C.; Yang, Z. The Impact of China's Western Development Strategy on Energy Conservation and Emission Reduction. *Environ. Impact Assess. Rev.* **2022**, *94*, 106743. [CrossRef]
74. Xue, J.; Li, Z.; Feng, Q.; Gui, J.; Zhang, B. Spatiotemporal Variations of Water Conservation and Its Influencing Factors in Ecological Barrier Region, Qinghai-Tibet Plateau. *J. Hydrol. Reg. Stud.* **2022**, *42*, 101164. [CrossRef]
75. Zameer, H.; Yasmeen, H.; Wang, R.; Tao, J.; Malik, M.N. An Empirical Investigation of the Coordinated Development of Natural Resources, Financial Development and Ecological Efficiency in China. *Resour. Policy* **2020**, *65*, 101580. [CrossRef]
76. The State Council of People's Republic of China. Notice of the State Council on Issuing the Air Pollution Prevention and Control Action Plan. Available online: http://www.gov.cn/zwgk/2013-09/12/content_2486773.htm (accessed on 1 February 2023).
77. The State Council of People's Republic of China. Notice of the State Council on Printing and Distributing the Action Plan for Water Pollution Prevention and Control. Available online: http://www.gov.cn/zhengce/content/2015-04/16/content_9613.htm (accessed on 1 February 2023).
78. The State Council of People's Republic of China. Notice of the State Council on Printing and Distributing the Action Plan for the Prevention and Control of Soil Pollution. Available online: http://www.gov.cn/zhengce/content/2016-05/31/content_5078377.htm (accessed on 1 February 2023).
79. Chen, X.; Li, H.; Mu, Y.; Wei, X. Difficulties and Suggestions for Guangxi's "Carbon Peak" and "Carbon Neutralization". *Pop. Sci. Technol.* **2022**, *24*, 155–158.
80. Yu, F.; Chang, M. Guangxi Strengthens the Prevention and Control of Heavy Metal Pollution and Ranks Well in the "Twelfth Five-Year Plan" Assessment. Available online: https://v.gxnews.com.cn/a/15773911 (accessed on 26 December 2022).
81. Lu, Y.; Yan, B.; Song, Z. Research on Present Ambient Air Quality of the Key Environmental Protection Cities in Inner Mongolia in Recent 5 Years. *Environ. Dev.* **2010**, *22*, 37–39.
82. Liu, K.; Wang, X.; Sun, H. Analysis on the Main City Air Quality of Inner Mongolia. *Meteorol. J. Inn. Mong.* **2012**, *6*, 18–20.
83. Wen, S. A Brief Discussion on the Effects of Inner Mongolia's Ecological Environment Governance Construction. *Inn. Mong. Sci. Technol. Econ.* **2015**, *22*, 54–56.
84. General Office of Shanghai Municipal People's Government. Notice of the General Office of the Shanghai Municipal People's Government on Forwarding the "13th Five-Year Plan for Greening and City Appearance of Shanghai" Formulated by the Municipal Bureau of Greening and City Appearance. Available online: https://www.shanghai.gov.cn/shssswzxgh/20200820/0001-22403_50466.html (accessed on 1 February 2023).
85. Hangzhou Municipal Bureau of Culture, Radio, Television and Tourism. Xixi National Wetland Park. Available online: https://wgly.hangzhou.gov.cn/art/2021/10/22/art_1229578164_58938616.html (accessed on 1 February 2023).
86. Wang, W.; Deng, X.; Wang, Y.; Peng, L.; Yu, Z. Impacts of Infrastructure Construction on Ecosystem Services in New-Type Urbanization Area of North China Plain. *Resour. Conserv. Recycl.* **2022**, *185*, 106376. [CrossRef]
87. Xinhua News Agency. Hebei Plans to Afforest 4.2 Million Mu This Year to Expand the Beijing-Tianjin-Hebei "Green Great Wall". Available online: http://www.gov.cn/xinwen/2015-01/09/content_2802513.htm (accessed on 1 February 2023).
88. Shanghai Municipal Bureau of Ecology and Environment. Information on the Release of the "Shanghai Ecological Protection Red Line". Available online: https://sthj.sh.gov.cn/hbzhywpt1272/hbzhywpt5406/20180627/0024-114011.html (accessed on 1 February 2023).
89. Wu, X.; Zhang, H. Evaluation of Ecological Environmental Quality and Factor Explanatory Power Analysis in Western Chongqing, China. *Ecol. Indic.* **2021**, *132*, 108311. [CrossRef]
90. Chongqing Municipal Bureau of Statistics; Chongqing Survey Team of National Bureau of Statistics. *Chongqing Statistical Yearbook 2021*; China Statistics Press: Beijing, China, 2021.
91. Sun, M.; Li, X.; Yang, R.; Zhang, Y.; Zhang, L.; Song, Z.; Liu, Q.; Zhao, D. Comprehensive Partitions and Different Strategies Based on Ecological Security and Economic Development in Guizhou Province, China. *J. Clean. Prod.* **2020**, *274*, 122794. [CrossRef]
92. Guizhou Provincial Bureau of Statistics; Guizhou Survey Team of National Bureau of Statistics. *Guizhou Statistical Yearbook 2018*; China Statistics Press: Beijing, China, 2018; ISBN 978-7-5037-8540-5.
93. National Development and Reform Commission, People's Republic of China Catalog of Encouraged Industries in the Western Region (2020 Edition). Available online: https://www.ndrc.gov.cn/xxgk/zcfb/fzggwl/202101/P020210806381700640950.pdf (accessed on 11 October 2022).

94. Shanghai Municipal Bureau of Ecology and Environment. Statistical Data on Water Environment Protection in Shanghai in 2018. Available online: https://sthj.sh.gov.cn/hbzhywpt1133/hbzhywpt1135/20191120/0024-139854.html (accessed on 1 February 2023).
95. Jiangsu Provincial Government. Notice of the Jiangsu Provincial Government on Printing and Distributing the Work Plan for Water Pollution Prevention and Control in Jiangsu Province. Available online: http://www.jiangsu.gov.cn/art/2016/2/2/art_46642_2556174.html (accessed on 1 February 2023).
96. Zhejiang Daily. Implementation Plan of Urban Domestic Waste Classification in Zhejiang Province. Available online: http://www.gov.cn/xinwen/2018-03/01/content_5269698.htm (accessed on 1 February 2023).
97. Department of Housing and Urban-Rural Development of Guangdong Province. "Guangdong Province's 13th Five-Year Plan for Urban and Rural Domestic Waste Treatment" Was Officially Released, and Rural Domestic Waste Should Be Classified and Reduced by 50%. Available online: http://zfcxjst.gd.gov.cn/zcjd/wzjd/content/post_1392572.html (accessed on 1 February 2023).
98. People's Daily Exploring the Circular Economy in Qinghai Province: Both Green and Rich. Available online: http://www.gov.cn/jrzg/2011-11/27/content_2004242.htm (accessed on 26 December 2022).
99. Zhuo, C.; Deng, F. How Does China's Western Development Strategy Affect Regional Green Economic Efficiency? *Sci. Total Environ.* **2020**, *707*, 135939. [CrossRef]
100. Jia, J.; Ma, G.; Qin, C.; Wang, L. Place-Based Policies, State-Led Industrialisation, and Regional Development: Evidence from China's Great Western Development Programme. *Eur. Econ. Rev.* **2020**, *123*, 103398. [CrossRef]
101. Tan, F.; Gong, C.; Niu, Z. How Does Regional Integration Development Affect Green Innovation? Evidence from China's Major Urban Agglomerations. *J. Clean. Prod.* **2022**, *379*, 134613. [CrossRef]
102. Yang, Q.; Sun, Z.; Zhang, H. Assessment of Urban Green Development Efficiency Based on Three-Stage DEA: A Case Study from China's Yangtze River Delta. *Sustainability* **2022**, *14*, 12076. [CrossRef]
103. Feng, S.; Kong, Y.; Liu, S.; Zhou, H. Study on the Spatio-Temporal Evolution and Influential Factors of Green Innovation Efficiency in Urban Agglomerations of China. *Sustainability* **2023**, *15*, 676. [CrossRef]

sustainability

MDPI

Article

Urban Air Quality Monitoring in Decarbonization Context; Case Study—Traditional Coal Mining Area, Petroșani, Romania

Evelina Rezmerița [1], Sorin Mihai Radu [2], Angelica-Nicoleta Călămar [3], Csaba Lorinț [4], Adrian Florea [4,*] and Aurelian Nicola [2]

[1] Mining Research, Technological Engineering and Design Institute—CEPROMIN, 330166 Deva, Romania; rezmeritaevelin@gmail.com
[2] Electrical and Mechanical Engineering Faculty, University of Petroșani, 332006 Petroșani, Romania; sorinradu@upet.ro (S.M.R.); aureliannicola@upet.ro (A.N.)
[3] Environmental Protection Laboratory, National Institute for Research and Development in Mine Safety and Protection to Explosion—INSEMEX, 332047 Petroșani, Romania; angela.calamar@insemex.ro
[4] Mining Faculty, University of Petroșani, 332006 Petroșani, Romania; csabalorint@upet.ro
* Correspondence: adrianflorea@upet.ro

Abstract: Humanity is a fossil-fueled civilization with a large influence on the environment. The World Health Organization (WHO) has pointed out that air pollution is now the single biggest environmental threat to human health. The air quality in Petroșani, a traditional mining region from the Jiu Valley bituminous coal basin, Romania, is rarely debated; however, it is not often investigated. In this paper, the main air pollution sources of Petroșani are identified and the performed measurements emphasize the air quality in the area of its transit road. The monitoring program set out the objectives, parameters, and points of the monitoring system, as well as the frequency and duration of the program and other monitoring parameters. The equipment used was provided by the National Institute for Research and Development in Mine Safety and Protection to Explosion from Petroșani, within an institutional partnership with the University of Petroșani. The monitoring of the air quality parameters was conducted from March to July 2020, at six points located on the road that crosses the city. It was thus possible to capture a variety of concentrations of the monitored parameters in different weather conditions to determine the air quality in this area. Based on the variation of the measured values in one of the most important historical Romanian bituminous coal mining basins, the preliminary results suggest a worsening of local air quality parameters in relation to the decarbonization process.

Keywords: decarbonization; bituminous coal; air quality; pollution source; monitoring; road traffic

1. Introduction

The current geo-politic and economic context, with special reference to the military conflicts located at the national border of Romania, as well as around the world, brings to the attention of specialists the need to re-evaluate the strategies of the energetic and the non-energetic mining sector. The reopening of mines can mean tens of thousands of direct jobs and hundreds of thousands of jobs in related industries [1].

Regarding the energetic mining sector, the main challenge comes from the perspective of compliance with environmental requirements, which means that the use of bituminous coal is preferable in terms of lower environmental loads compared to the use of lignite [2].

The fastest solution and a first option, especially in a time of crisis, must be to rely on the existing infrastructure. From this perspective, in Romania there are only two power plants which use bituminous coal for energy production, the Mintia and Paroșeni thermal power plants (TPP), respectively, and both are located in Hunedoara County. Of these, Paroșeni TPP is currently in use and its future operation can be based either on the resources

obtained by continuing the exploitation of bituminous coal locally in the mines from the Jiu Valley mining basin or on imported coal.

2. General and Local Context

Generally, the environmental analysis has the following objectives: to assess the current state of the environmental components; to establish the local and temporal trends; to evaluate the sources of pollution; and, last but not least, to make measurements to estimate the potential risks and environmental impact. Urban air pollution under certain weather conditions (temperature inversion) often causes smoke fog (smog). According to the Cambridge dictionary [3], this is a mixture of smoke, gases, and chemicals that makes the atmosphere difficult to breathe and harmful for health, especially in cities

The World Health Organization (WHO) has reported that the global burden of disease associated with air pollution exposure exacts a massive toll on human health worldwide: exposure to air pollution is estimated to cause millions of deaths and lost years of healthy life annually; there were 3.315 million deaths from air pollution only in first five months of this year [4]. The burden of disease attributable to air pollution is now estimated to be on a par with other major global health risks such as unhealthy diet and tobacco smoking, and air pollution is now recognized as the single biggest environmental threat to human health. Despite some notable improvements in air quality, the global toll in terms of deaths and lost years of healthy life has barely declined since the 1990s [5,6].

Increasing the air quality and dealing with unfolding climate change entail a massive decarbonization of society. Humanity has experienced three major energy transitions and is now struggling to kick off a fourth. First was the mastery of fire, which allowed us to liberate energy from the sun by burning plants. Second came farming, which converted and concentrated solar energy into food, freeing people for pursuits other than sustenance. During that second era, which ended just a few centuries ago, farm animals and larger human populations also supplied energy, in the form of muscle power. Third came industrialization and, with it, the rise of fossil fuels. Coal, oil, and natural gas each, in turn, rose to prominence, and energy production became the domain of machines, such as coal-fired power plants [7,8].

We are a fossil-fueled civilization whose technical and scientific advances, quality of life, and prosperity rest on the combustion of huge quantities of fossil carbon, and we cannot simply walk away from this critical determinant of our fortunes in a few decades, never mind years.

Complete decarbonization of the global economy by 2050 is now conceivable only at the cost of unthinkable global economic retreat or as a result of extraordinarily rapid transformations relying on near-miraculous technical advances [9].

Worldwide fossil fuel production has grown steadily in recent decades from 9.572 billion metric tons in 1990 to 15.503 billion metric tons in 2019 (up nearly 62 percent), followed by a slight decline, probably as a result of the SARS-CoV-2 pandemic in 2020, to 14,756 billion metric tons [10].

The European Union still relies heavily on fossil fuels to meet its energy needs, as illustrated by the ratio of fossil fuels to gross energy available (the total energy demand of a country or region). In 2020, fossil fuels accounted for 70% of the gross energy available in the EU, down from 71% in 2019. In the last three decades, this percentage has fallen significantly (by 13 percent compared to 1990) [11].

Other statistics show an interesting outlook for resources extracted or mined from the earth: over 33 billion tons of resources were extracted and over 22 billion tons of resources were mined from the earth only in the first five months of this year alone, of which almost 3 billion tons is coal [4].

In Romania, known bituminous coal deposits are only in the Middle Carpathians, in the Carpathian orogen, in both the Danubian and the Getic domains, but also in the post-tectonic intra-mountainous basins [12]. From all of these deposits, the active mines actually exist only in the Jiu Valley Mining Basin [13,14].

Petroșani is the most important city in the Jiu Valley bituminous coal mining basin (Figure 1). According to the statistics of the last decade, the reserves of bituminous coal in the Lonea, Livezeni, Vulcan, and Lupeni mining perimeters total about 361 million of tons. Of the total reserves, only the recoverable (proven) reserves are available for valorization, and that means about 154 million tons in these four perimeters [13,14].

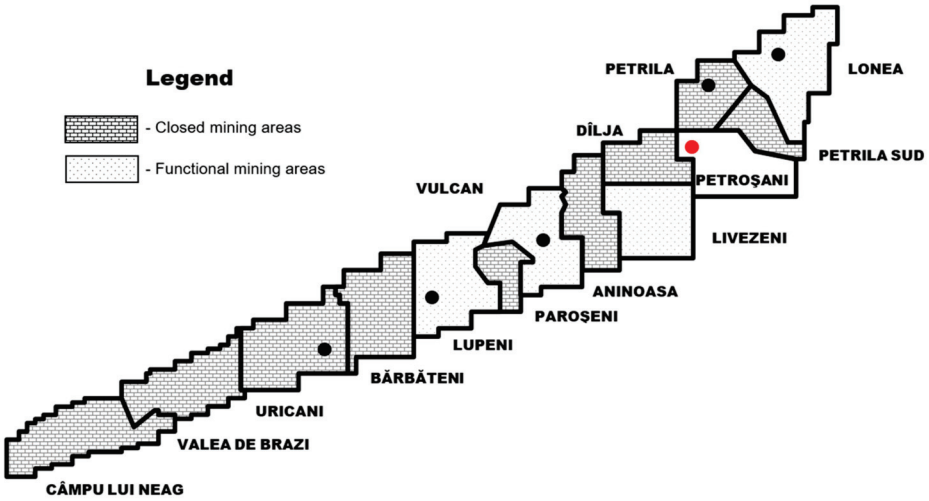

Figure 1. Location and status of mining perimeters in the Jiu Valley bituminous coal basin. (Petroșani is highlighted with a red dot, the other cities in the Jiu Valley are marked with black dots.).

Since the times of intensive mining activities, the inhabitants from Petroșani have been heating their homes mainly by using individual coal stoves, often through several pre-existing installations in each building, with all the released gases from the burning of fossil fuels being eliminated directly into the atmosphere without special filters installed in the chimneys of the houses. This practice is still encountered today, but now, in addition to coal, people also burn other materials (textile waste from secondhand stores and warehouses); thereby, the gases released into the atmosphere have a worsening effect on the air quality parameters.

With the simultaneous growth of urban scales and vehicle ownerships, on-road vehicles have the potential to overtake industrial and residential sectors as the dominant emission source [15–19]. The means of transport also contribute to the global pollution of the environment (air, soil, water) with a number of primary pollutants (carbon monoxide, nitrogen oxides, hydrocarbons, and particulate matter—PM), and they contribute to the genesis of secondary pollutants (tropospheric ozone, photochemical smoky fog, acid particles, and rain). Carbon dioxide emissions also contribute to the greenhouse effect, with well-known consequences which lead to climate change. The noise and vibration generated by road traffic come on top of the chemical emissions effects. [20]. On the other hand, transport infrastructure requires the occupation of large areas and contributes to habitat fragmentation and surface waterproofing [21,22]. Overall, transport is therefore a major source of environmental pressure and contributes to climate change, air pollution, and rising noise levels.

On these premises, the designed monitoring program was based on measurements in six monitoring points located along the transit road of Petroșani (Figure 2).

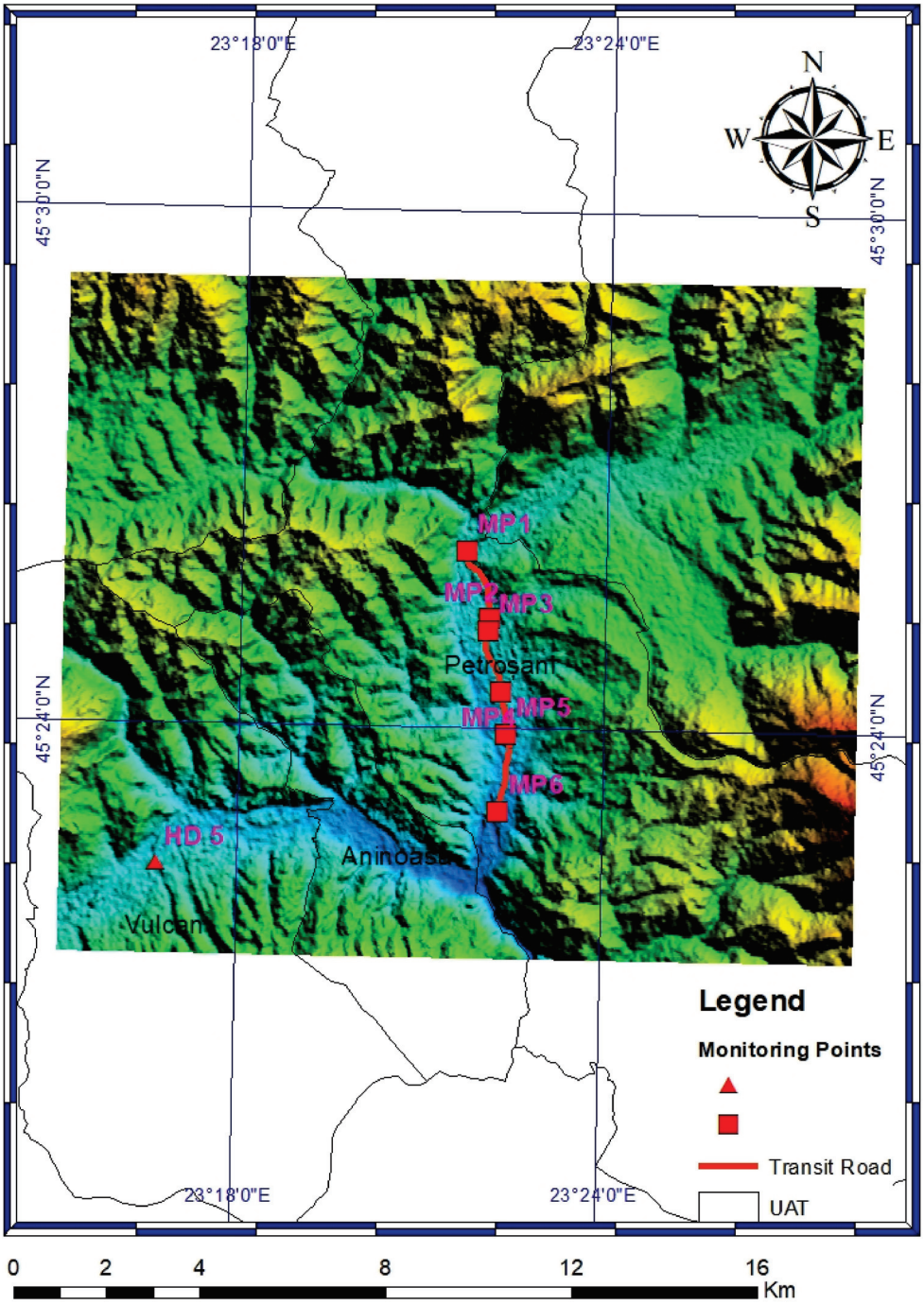

Figure 2. The DTM model of Petroșani area with transit road (red line), location of the monitoring points MP (red squares), and monitoring station HD 5 (red triangle) [23].

The duration of the designed monitoring program was three months, and the estimated outcome, as a result of weekly measurements, was twelve datasets. Due to the restrictions on every activity, as imposed by the authorities to combat the spread of the new COVID-19 virus, the initial program was disrupted, resulting in a total of five datasets of measurements, as follows: 7 March; 13 March; 18 May; 24 May (night); and 2 July 2020.

The equipment used for the air quality monitoring was provided by the National Institute for Research and Development in Mine Safety and Protection to Explosion Petroșani, through the existing institutional agreements between the research unit and the University of Petroșani. The results of all the measurements were processed, and the minimum, maximum, and average concentrations of all the monitored pollutants were determined.

3. Materials and Methods

3.1. Working Methodology

Environmental monitoring comprises a surveillance system, prognosis, and warning and intervention, which take into account the systematic assessment of the dynamics of the qualitative characteristics of the environmental factors, in order to know their quality status and ecological significance and the evolution and social implications of the changes produced. This is followed by the necessary measures [24]. The pollutant monitoring procedures are relatively well established and are based on a comparison with the acceptable limits of concentrations, based on the established knowledge at the time. This monitoring approach facilitates quantification that can be useful in environmental decision making [25]. In order to be able to use the data obtained from a monitoring system, the sampling and measurements were performed on the basis of the procedures, in accordance with the recognized and validated methods; these are the "Standard methods", which ensure the acquisition of the data of equivalent scientific quality. A number of factors must be also considered: the source and area of pollution, the type of pollutant, and the experiment purposes, such as the pollution spreading area, the level of pollution, or the short-term concentrations.

The monitoring points were located along the transit road that demarcates the historical areas/neighborhoods/peripheries (Colonie, Livezeni, etc.) from the other areas of the city. These points are the places of interference by the main sources of air pollution in Petroșani. These pollution sources are represented by the coal burning stoves used for home heating in the historical areas of the city (Colonie, Livezeni outskirts, etc.) and by the road traffic from the transit road (Figure 3).

(**a**) (**b**)

Figure 3. The two main sources of air pollution: (**a**) heating stoves and (**b**) road traffic.

Most of the pollutants emitted into the atmosphere from these two main sources have harmful influences on human health and the environment. In this respect, the monitoring points (MPs) were fixed at the main crossroads of the transit road; this resulted in five roundabouts and an intermediate point where the measurements were performed (Figure 4), as follows:

- MP_1 at the intersection of E79 with the entrance to the city of Petrila, at the roundabout from Dărănești;
- MP_2 at the intersection of E79 with the road to the Parâng Mountain Resort, at the roundabout from Victoriei Square;
- MP_3 at the intersection of E79 with Mihai Viteazul Street, at the roundabout next to the prosecutor's office attached to Petroșani Court;
- MP_4 at the intersection of E79 with December 1, 1918 Street, at the roundabout known as At the plane (La Avion);
- MP_5 on the E79 road, near the Livezeni Mining Exploitation;

– MP_6 at the intersection of E79 with the entrance to the Kaufland Supermarket, at the roundabout.

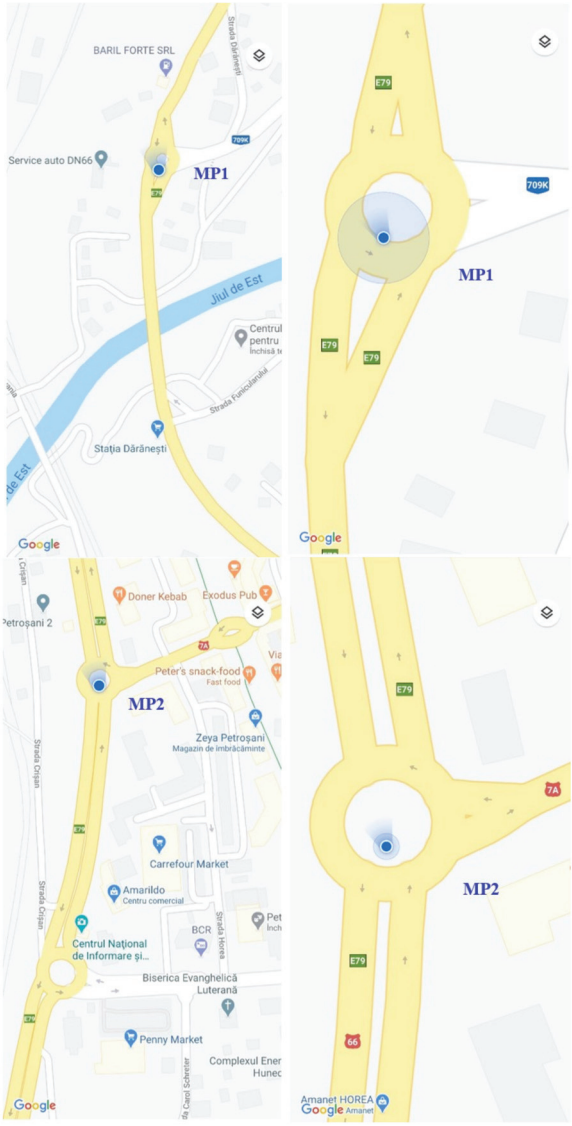

Figure 4. *Cont.*

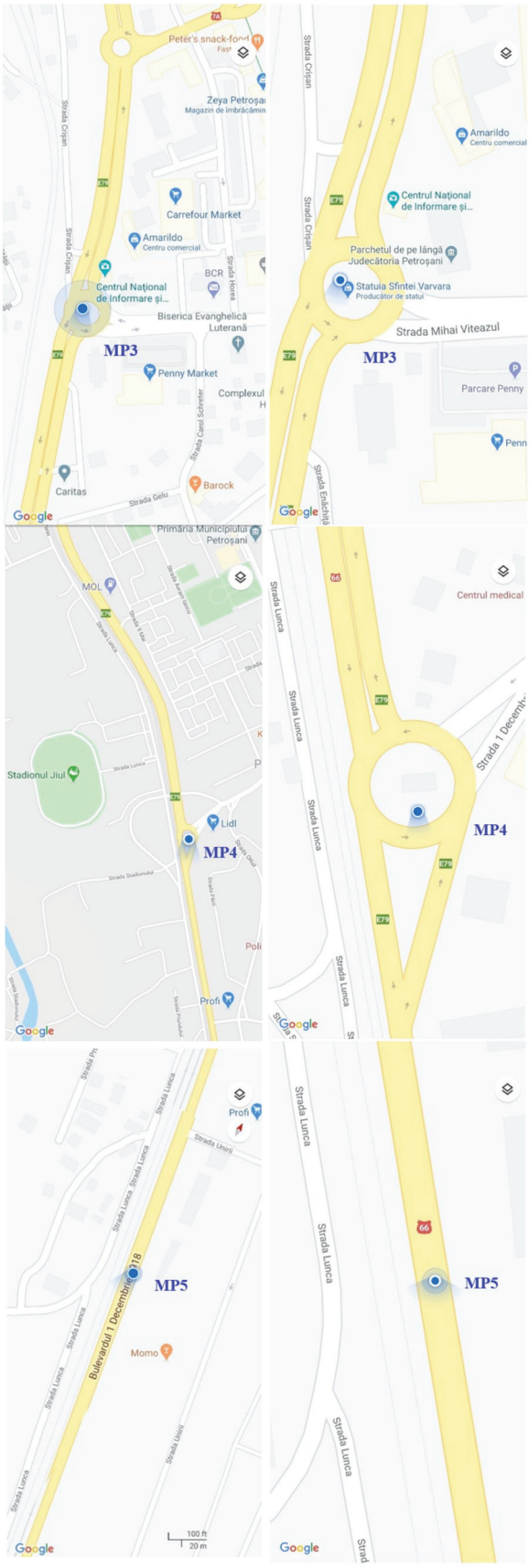

Figure 4. *Cont*.

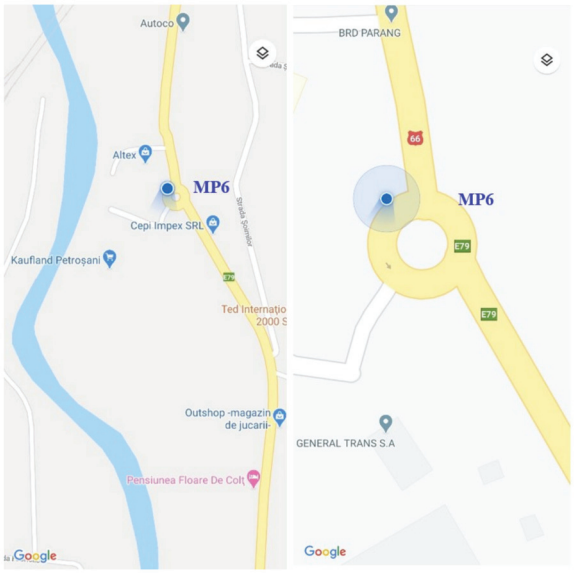

(**a**) (**b**)

Figure 4. Monitoring points on the E79 transit road: (**a**) general views and (**b**) details.

According to the No. 104/2011 law on ambient air quality, the sampling points were placed in such a manner as to avoid the microenvironment measurement effects, so that the obtained values resulted in being of proven relevance for the air quality. The sampling port was placed a few meters away from buildings, trees, or other obstacles, so that an area of 270° was clear from any interfering object; thereby, the air flow in the proximity of the sampler behaved normally.

It should be noted that the equipment used in this sampling study has small measuring ranges (0–30 ppm), being recommended (also by the manufacturer) for use in environmental measurements. Moreover, before the measurement, in order to ensure the accuracy of the results, each probe was calibrated with reference gas cylinders (the data are recorded in the laboratory documents). Moreover, the equipment has valid calibration certificates, and transient laboratory inspections are periodically performed with other similar equipment. Therefore, all the procedures regarding the accuracy of the data recorded are in table no. 1, as well as those regarding the microclimate parameters (table no. 2); they are held by the laboratory and are observed, validated, and accredited by the Romanian Accreditation Association (RENAR). After calibration of the instruments in the laboratory, the gas and the particulate matter sampling were placed at a height between 1.5–2 m from the ground (breathing height) [26]. The measurements were performed for 30 min at each monitoring point, both for the five monitored gases and for the particulate matter [27].

3.2. Monitoring Equipment

More devices from the GrayWolf Sensing Solutions, Shelton, CT, USA [28] and Kimo AMI 300 series [29] from the KIMO—A KGF Group company, Montpon, France were used in the monitoring activity, each of them having a certain measuring range. The measuring range represents the difference between the maximum and the minimum value which can be measured using each device.

The GrayWolf PC-4000 Particle/Mass Monitor Plus (Figure 5) measures particle sized/particulate matter (PM) from 0.3 µm to 25 µm, with a flow rate of 2.83 LPM (Litres Per Minute), which is the equivalent of 0.1 CFM (Cubic Feet Per Minute). It displays 6 size ranges simultaneously. The sizes 0.3 µm, 0.5 µm, 1.0 µm, 2.5 µm, 5 µm, and 10.0 µm are standard. Particulate matter PM 2.5, PM 10, and TSP (total suspended particulate) may also be concurrently displayed and logged. As a "stand-alone" instrument, it can be used as a portable device, or it can be integrated into a building's automation system [28].

Figure 5. Gray Wolf PC-4000 Particle/Mass Monitor Plus.

When using Direct Sense II smart probes, the air monitoring probes accommodate from two up to eight smart sensors into a single hand-held device. It is possible to select 25 different aspects of indoor air quality, TVOCs (Total Volatile Organic Compounds), carbon dioxide (Nondispersive Infrared—NDIR—CO_2 Sensors), carbon monoxide, ozone, nitrogen dioxide, ammonia, sulfur dioxide, chlorine, hydrogen sulfide, humidity (%RH), temperature (°C), and many others. The Direct Sense II probes (Figure 6) connect to Gray Wolf's Advanced Sense® meters, which enable additional parameters, such as particulates, differential pressure, air velocity, and formaldehyde [28].

Figure 6. The Direct Sense II probes and Gray Wolf's Advanced Sense® meters.

The Kimo AMI 300 is a multifunction device which is used to measure pressure, temperature, humidity, air velocity and air quality. This kit (Figure 7) is the ideal tool for any maintenance and commissioning engineer [29].

Figure 7. The multifunction device KIMO AMI 300.

Features:

- Manometer—used for pressure and airflow measurement;
- Thermo-hygrometer—used for testing dew point, wet temperature, enthalpy and absolute temperature;
- Air quality probe—used for measuring the level of CO in a space;
- Current/voltage module;
- Thermometer—thermocouple and thermocouple temperature probes.

4. Results

Particular attention is paid to the activity of monitoring, maintaining, and improving air quality as it is the fastest way to understand the transport of pollutants in the environment. At the European and international level, air pollution has become a permanent concern. The monitoring process was carried out along the transit road of the municipality with the aim of capturing the two identified sources of air pollution—released gases from burning stoves and exhaust gases from car traffic. Air sampling aims at the analysis of either the gaseous compounds or the pollutant compounds present in the atmosphere in the form of solid particles [25]. The following parameters were measured: CO, CO_2, NO, NO_2, SO_2, PM_1, $PM_{2,5}$, PM_{10}, and TSP. The monitoring points were located at five roundabouts and at an intermediate point on the transit road of Petroșani because this transit road is the line that delimits the historical areas/neighborhoods/outskirts (Colonie, Livezeni, etc.) from the rest of the city. Following the performance of the measurements, sets of 30 values were obtained for each monitored parameter at each of the six measurement points. All these sets of values were centralized; the most representative in assessing the air quality are the maximum values measured during the entire monitoring project. The exceedances of the values in the regulations [27] are marked with bold font in Table 1.

Table 1. Maximum of measured values.

Parameter	Monitoring Point / Date	7 March 2020	13 March 2020	18 May 2020	24 May 2020 * (Night)	2 July 2020	M.A.C.
CO [mg/m^3]	MP1	1.00	4.50	2.40	-	5.30	6.0 mg/m^3
	MP2	1.20	3.00	3.40	-	2.30	
	MP3	1.40	1.20	2.30	0.40	2.00	
	MP4	1.80	1.20	0.00	0.90	0.00	
	MP5	1.30	0.50	4.10	-	3.80	
	MP6	1.10	1.80	2.60	-	1.30	
CO_2 [mg/m^3]	MP1	565.00	1081.00	682.66	-	948.00	**
	MP2	505.00	824.00	748.55	-	1046.00	
	MP3	458.00	828.00	774.17	549.06	1015.0	
	MP4	492.00	1002.00	724.76	580.17	1061.0	
	MP5	475.00	964.00	770.51	-	966.00	
	MP6	1624.0	766.00	768.68	-	1025.0	
NO [mg/m^3]	MP1	0.30	0.30	0.00	-	0.09	**
	MP2	0.30	0.30	0.00	-	0.08	
	MP3	0.30	0.30	0.00	0.00	0.10	
	MP4	0.31	0.30	0.00	0.00	0.02	
	MP5	0.30	0.30	0.00	-	0.04	
	MP6	0.30	0.30	0.00	-	0.04	
NO_2 [mg/m^3]	MP1	0.12	0.12	0.07	-	0.20	0.3 mg/m^3
	MP2	0.11	0.11	0.13	-	0.20	
	MP3	0.10	0.11	0.11	0.12	**6.00**	
	MP4	0.15	0.10	0.12	0.14	**4.20**	
	MP5	0.11	0.10	0.17	-	**11.40**	
	MP6	0.13	0.11	0.13	-	**4.90**	
SO_2 [mg/m^3]	MP1	0.12	0.11	0.18	-	0.02	0.75 mg/m^3
	MP2	0.08	0.00	0.53	-	0.00	
	MP3	0.04	0.00	0.40	0.20	0.00	
	MP4	0.06	0.00	0.30	0.06	0.00	
	MP5	0.03	0.00	0.26	-	0.00	
	MP6	0.04	0.00	0.23	-	0.00	
PM_1 [mg/m^3]	MP1	0.02	0.04	0.01	-	0.01	**
	MP2	0.06	0.01	0.01	-	0.01	
	MP3	0.02	0.02	0.01	0.00	0.01	
	MP4	0.01	0.01	0.03	0.01	0.01	
	MP5	0.02	0.01	0.01	-	0.01	
	MP6	0.02	0.02	0.00	-	0.01	
$PM_{2.5}$ [mg/m^3]	MP1	0.03	0.17	0.03	-	0.03	**
	MP2	0.06	0.10	0.03	-	0.10	
	MP3	0.02	0.12	0.07	0.01	0.08	
	MP4	0.03	0.06	0.03	0.01	0.03	
	MP5	0.03	0.06	0.02	-	0.03	
	MP6	0.04	0.10	0.02	-	0.04	
PM_{10} [mg/m^3]	MP1	0.04	1.54	0.26	-	0.29	**
	MP2	0.06	1.11	0.19	-	0.54	
	MP3	0.03	0.51	0.43	0.03	0.64	
	MP4	0.20	0.26	0.17	0.02	0.09	
	MP5	0.04	0.40	0.09	-	0.17	
	MP6	0.08	0.83	0.10	-	0.09	
TSP [mg/m^3]	MP1	0.04	**1.55**	0.26	-	**0.54**	0.5 mg/m^3
	MP2	0.06	**1.12**	0.19	-	**0.97**	
	MP3	0.04	**0.52**	0.43	0.04	**1.10**	
	MP4	0.20	0.27	0.18	0.04	0.34	
	MP5	0.04	0.41	0.11	-	0.47	
	MP6	0.08	**0.83**	0.11	-	0.43	

* Determinations performed at night to capture air quality at a lower level of road traffic values; ** parameters without normative.

Moreover, in the present monitoring project the meteorological conditions were taken into account (Table 2); these were, respectively, wind speed and direction and pressure; humidity and temperature; the geographical conditions in the area where the sources and receivers were located; and the landforms and the land use.

Table 2. Measured average values of atmospheric conditions.

Parameter	Monitoring Point / Date	7 March 2020	13 March 2020	18 May 2020	24 May 2020 * (Night)	2 July 2020
V [m/s]	MP1	0.311	0.363	0.576	-	1.012
	MP2	0.161	0.398	0.728	-	1.455
	MP3	0.496	1.354	0.415	0.272	1.386
	MP4	0.331	1.508	0.840	0.237	0.828
	MP5	0.156	1.380	1.180	-	0.909
	MP6	0.194	0.408	0.455	-	2.962
P [hPa]	MP1	936.9	937.9	944.4	-	940.3
	MP2	936.8	937.2	944.6	-	941.2
	MP3	935.7	937.1	945.6	947.0	941.2
	MP4	937.2	939.0	949.0	950.0	943.4
	MP5	939.0	940.1	949.0	-	944.5
	MP6	940.4	941.2	952.1	-	945.6
W [%RH]	MP1	59.95	38.53	43.14	-	42.89
	MP2	68.28	40.02	31.13	-	41.99
	MP3	76.43	36.55	25.72	64.01	37.43
	MP4	82.19	34.00	31.36	70.69	42.57
	MP5	77.66	34.76	25.31	-	36.58
	MP6	75.63	38.45	27.42	-	38.40
T [°C]	MP1	8.8	19.0	8.0	-	28.0
	MP2	8.4	20.2	11.0	-	29.0
	MP3	9.3	22.1	12.0	11.0	29.6
	MP4	6.8	23.2	13.0	11.0	29.6
	MP5	9.0	22.6	14.0	-	30.3
	MP6	8.0	20.9	14.0	-	31.1

* Determinations performed at night to capture air quality at a lower level of road traffic values.

The total suspended particulate (TSP) concentrations recorded on 13 March exceeded the maximum allowed concentrations (MAC), as related to the norms taken into account, with an average recorded atmospheric humidity of 37% and an average temperature of 21 °C. The maximum allowed concentrations of the TSP were also exceeded on 2 July, with an average value of atmospheric humidity of 40% and an average temperature of 29.6 °C, which was most likely due to heavy traffic (road trains) on the transit road of Petroșani. In this context, it seems that the only source of the increase in nitrogen dioxide concentrations are the internal combustion engines using fossil fuels as a result of car traffic. The maximum values of 24 May, during the night measurements performed at the two monitoring points, MP3 and MP4, respectively, show significant decreases compared to the values determined during the day monitoring, which suggests that a lower level of traffic values at the time of the measurements has a positive effect on air quality. In order to measure the ecological impact generated by road traffic, several case studies were carried out in Petroșani (Romania) on the impact of road traffic on the population by using an improved ecological footprint calculation method [30]. The measurements performed in 2017 revealed a relatively high value of ecological footprint generated by road traffic for Petroșani. As a consequence, Petroșani town hall recommended annual monitoring of the road traffic ecological footprint. The synergy of the road traffic with the new environmental objectives for sustainable development requires new correlations between the inputs of the instruments measuring road traffic pressures on ecosystems and the environmental targets [30].

For comparison, presented below are the results of the closest station of the National Air Quality Monitoring Network (RNMCA). This network is dedicated to public information in real time regarding the air quality parameters, monitored in over 100 stations all

over Romania [31]. The single monitoring station of RNMCA in the Jiu Valley bituminous coal basins, named HD-5, is located about 2 km from Paroșeni TPP, in Vulcan city. We chose to bring into the discussion the values provided by the HD-5 automated station, not necessarily for comparison with the measured values, but to especially highlight the reduced influence of the Paroșeni TPP on local air quality parameters in the context of the recent activity decline due to the decarbonization process. In this automated station, not all the parameters monitored in the current study performed in Petroșani can be found. Therefore, the CO_2, PM_1, $PM_{2.5}$, and TSP values are missing, but even so, the comparison is conclusive for all the other values (Table 3).

Table 3. Values provided by automated HD-5 station.

Parameter \ Date	7 March 2020	13 March 2020 *	18 May 2020	24 May 2020 (Night)	2 July 2020 *	M.A.C.
CO [mg/m^3]	0.82–1.07	0.94–1.25	1.47–1.59	1.43–1.47	0.15–0.44	6.0 mg/m^3
CO_2 [mg/m^3]	-	-	-	-	-	**
NO [mg/m^3]	0.01–0.02	0.01–0.03	0.01–0.03	0.01–0.02	0.01–0.02	**
NO_2 [mg/m^3]	0.01–0.02	0.01–0.02	0.01–0.02	0.02	0.01–0.02	0.3 mg/m^3
SO_2 [mg/m^3]	0.01	0.01–0.04	0.01	0.01	0.00	0.75 mg/m^3
PM_1 [mg/m^3]	-	-	-	-	-	**
$PM_{2.5}$ [mg/m^3]	-	-	-	-	-	**
PM_{10} [mg/m^3]	0.02	0.01–0.04	0.01–0.03	0–0.01	0.02	**
TSP [mg/m^3]	-	-	-	-	-	0.5 mg/m^3

* In these days, the Paroșeni TPP was in working order, generating about 3000 MWh electricity daily out of the approximately 107,000 MWh produced in 2020 [32]; ** Parameters without normative.

As can be seen in Figure 8, the maximum allowed concentrations—the red line on the charts, was exceeded in the case of NO_2 and TSP at certain monitoring points under specific weather circumstances.

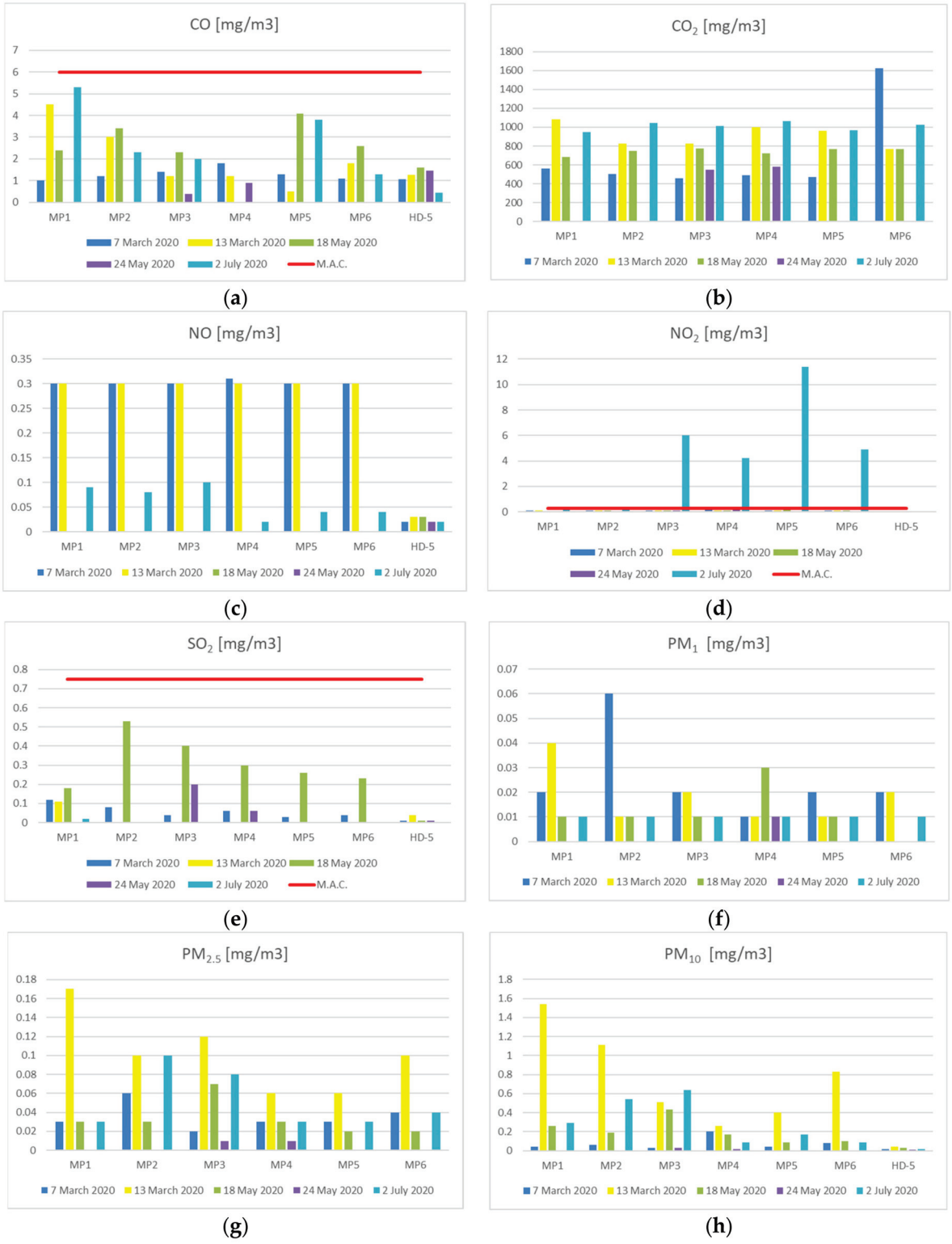

Figure 8. *Cont.*

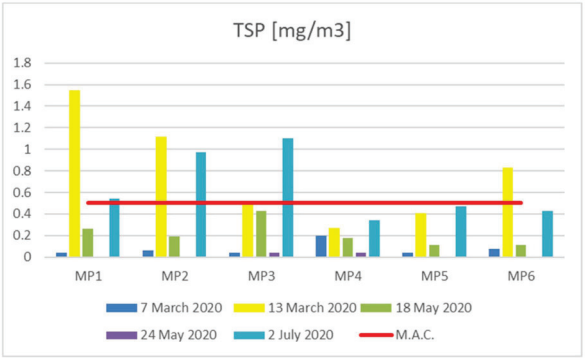

(i)

Figure 8. Maximum of measured values of CO (**a**), CO_2 (**b**), NO (**c**), NO_2 (**d**), SO_2 (**e**), PM_1 (**f**), $PM_{2.5}$ (**g**), PM_{10} (**h**) and TSP (**i**) at the monitoring points on the E79 transit road and at the automated station HD-5.

The values of the atmospheric conditions provided by the HD-5 automated station are pretty similar to the values provided by the measurements performed on the transit road of Petroșani city (Table 4).

Table 4. Values of atmospheric conditions provided by the HD-5 automated station.

Parameter \ Date	7 March 2020	13 March 2020	18 May 2020	24 May 2020 (Night)	2 July 2020
V [m/s]	0–3.8	0.2–5.7	0.4–3.6	0.1–3.1	0.3–3.0
P [hPa]	933.4–935.1	936.1–941.1	948.6–949.6	944.2–946.3	939.9–941.7
W [%RH]	62–99	52–99	79–99	93–99	58–99
T [°C]	5.1–12.3	3.6–20.7	14.1–22.2	10.7–14.4	17.1–28.6

For total compliance, all the values were taken from the daily statistics generated by the HD-5 automatic station for the same time slots as the measurements performed on the transit road of Petroșani city. We can note that, for the most part, the values measured by the HD-5 automated station are lower than those measured in the current study on the transit road of Petroșani, which suggests a reduced influence of the Paroșeni TPP on the local air quality parameters.

5. Discussion

The mining industry in the Jiu Valley had and still has a significant influence on the environmental pollution factors, both by the discharge of noxious substances into the atmosphere and the large quantities of waste produced, as well as by their variety. Air pollution is a complex phenomenon involving a multitude of pollutants that can cause alterations in the health of the population and in the quality of the environment, causing serious effects, depending on the concentration or duration, acting either through high concentrations for a short period or through reduced concentrations for a long period [25,33].

Currently, the technology that Paroșeni TPP benefits from allows it to operate within the environmental standards in force, both in the production phase and in terms of waste storage (ashes).

Caprișoara tailing pond is located near the city of Vulcan in the western Jiu Valley, in the Meridional Carpathian Mountains, and stores the ashes from the Paroșeni TPP. Previous research has developed various climate scenarios to model the PM dispersion generated by the Caprișoara tailings pond and the effect on the city of Vulcan in the Jiu Valley.

According to that research, the contribution of the Caprișoara tailings pond to PM generation in Vulcan is limited to periods when the wind blows from the south and south-southwest, with an above-average intensity in the conditions of a turbulent atmosphere, which happens during the summer storms [33].

The national energy picture shows variable shares of the use of different resources, with nocturnal/diurnal and seasonal oscillations and percentages exceeding 30% for coal in the winter months and decreasing to below 15% in the summer months (Figure 9) [34].

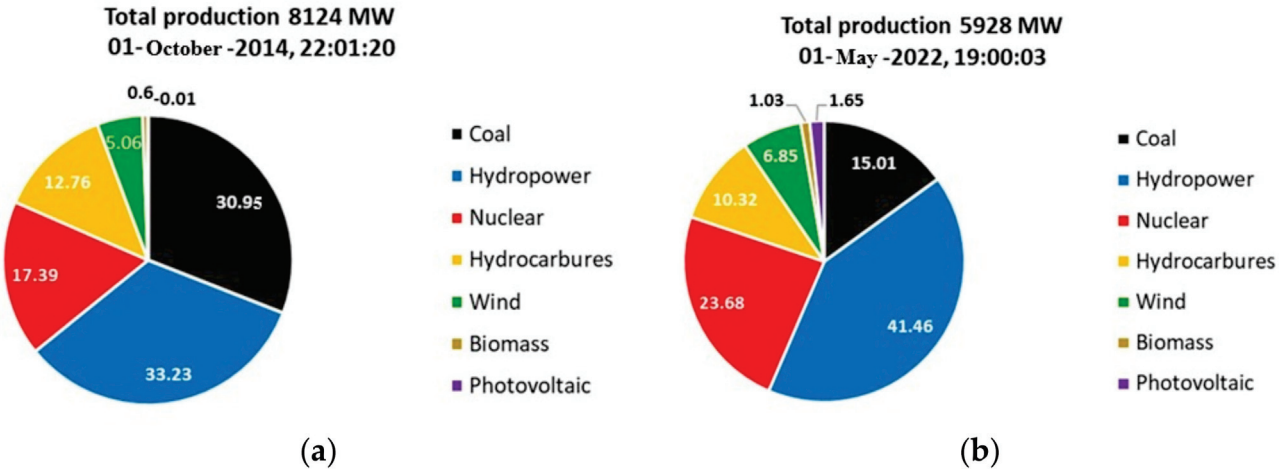

Figure 9. The share of energy sources in Romania on (**a**) 1 October 2014 and (**b**) 1 May 2022.

In 2020, the Romanian energy industry produced 53.74 TWh of various resources, of which fossil fuels accounted for almost 35% (gas 18.17%, coal 16.55%, fuel oil 0.11%). The Paroșeni TPP produced in 2020 about 107,000 MWh, which means 0.2% of the total electricity production in Romania [35].

Over the last decade, bituminous coal has contributed about 5 to 7 percent to the electricity sector [13,14], but in the current context of Romanian energy resources the bituminous coal represents 1–2% and sometimes under one percent. From an ecological perspective, the share of bituminous coal participation must be increased at the expense of lignite usage.

6. Conclusions

Based on the performed measurements, we found that at humidity above 50% and low temperatures (6–9 °C) there were no exceedances of the values of the monitored parameters related to the norms taken into account. In the case of average humidity and temperatures (between 30–40% and 19–23 °C), there were in some places exceedances of total particulate matter, while at medium humidity (36–43%) and high temperatures (28–31 °C) there were sometimes exceedances of both NO_2 and total particulate matter. This suggests that the dispersion of pollutants is influenced by the weather. Due to the exceeding of the limit values for NO_2 only in the warm season, its origin from the burning in stoves of different types of fuels can be excluded. Thus, it turns out that the internal combustion engines (ICE) are responsible for the high values of this parameter, as a result of road traffic. In order to improve the air quality control and management in Petroșani, considering all that was presented in this case study, to obtain a clearer picture of the share of the two main sources of air pollution, it is recommended that the monitoring activities during all the seasons in different weather conditions be intensified and that there should even be continuous monitoring, corroborated with the modeling of the pollutant dispersion and with more road traffic studies.

The comparison between the values provided by the HD-5 automated station and the measured values in the current study on the transit road of Petroșani suggested a reduced influence of the Paroșeni TPP on local air quality parameters.

Based on the variation of the measured values in one of the most important historical Romanian bituminous coal mining basins, the preliminary result suggests a decrease in local air quality parameters related to the decarbonization process. The Paroșeni TPP's activity diminished but the combustion of non-compliant materials (textile waste from secondhand stores and warehouses) in individual stoves has increased and the gases released by the combustion process are eliminated directly (without special filters installed in the chimneys of the houses) into the atmosphere with a negative effect on local air quality.

The current geo-politic and economic context has brought to the attention of specialists the need to also re-evaluate the strategies of the energetic and non-energetic mining sector.

In energetic mining sector, even if it is expected that the decarbonization process will slow down, diminish, or even stop, fossil fuel burning still remains a necessity. Until the regaining of energy independence, the finding of an energetic alternative at the expense of the simple shutting down of the thermal power plants is preferred. This is an opportunity for those regions rich in fossil fuels and especially coal. Moreover, it is more important to renounce the use of stoves for home heating even if they burn coal or non-compliant materials, but first of all, the local, regional, or central authorities must find optimal solutions before the decommissioning the fossil fuel industry, in order to not compel the population affected by poverty to improvise heating solutions, which can have much higher environmental costs for all of us.

Regarding the energetic mining sector, the main challenge comes from the perspective of compliance with environmental requirements, which means that the use of bituminous coal is preferable in terms of lower environmental loads compared to the use of lignite. In Romanian energetical resource usage, from an ecological perspective, the share of bituminous coal participation must be increased at the expense of lignite usage.

Author Contributions: Conceptualization, C.L. and A.F.; methodology, C.L. and A.F.; validation, E.R., S.M.R., A.-N.C., A.F. and A.N.; formal analysis, E.R., C.L. and A.F.; investigation, E.R., C.L., A.F. and A.-N.C.; resources, S.M.R. and A.-N.C.; data curation, E.R., C.L. and A.F.; writing—original draft preparation, E.R. and C.L.; writing—review and editing, A.F., S.M.R., E.R. and C.L.; visualization, E.R., C.L. and A.F.; supervision, C.L., A.F. and S.M.R.; project administration, C.L., A.F. and A.N. All authors have read and agreed to the published version of the manuscript.

Funding: This research received no external funding.

Institutional Review Board Statement: Not applicable.

Informed Consent Statement: Not applicable.

Data Availability Statement: Not applicable.

Conflicts of Interest: The authors declare no conflict of interest.

References

1. Lorinț, R.C.; Buia, G. Romanian mining industry, assumptions of last decade and future insights. *Qual.—Access Success* **2017**, *18* (Suppl. 1), 362–365.
2. Guo, L.; Zhai, M.; Wang, Z.; Zhang, Y.; Dong, P. Comparison of bituminous coal and lignite during combustion: Combustion performance, coking and slagging characteristics. *J. Energy Inst.* **2019**, *92*, 802–812. [CrossRef]
3. Cambridge Dictionary. Available online: https://dictionary.cambridge.org/ (accessed on 24 March 2022).
4. The World Counts Gives an Overview of Critical Global Challenges. Available online: https://www.theworldcounts.com/challenges/planet-earth (accessed on 16 May 2022).
5. World Health Organization. *WHO Global Air Quality Guidelines: Particulate Matter (PM2.5 and PM10), Ozone, Nitrogen Dioxide, Sulfur Dioxide and Carbon Monoxide*; World Health Organization: Geneva, Switzerland, 2021.
6. Chukwu, T.M.; Morse, S.; Murphy, R.J. Spatial Analysis of Air Quality Assessment in Two Cities in Nigeria: A Comparison of Perceptions with Instrument-Based Methods. *Sustainability* **2022**, *14*, 5403. [CrossRef]
7. Smil, V. *Energy Transitions. History, Requirements, Prospects*; Praeger ABC-CLIO: Santa Barbara, CA, USA, 2010.
8. Smil, V. *Energy Transitions: Global and National Perspectives (Second Expanded and Updated Edition)*; Praeger ABC-CLIO: Westport, CT, USA, 2016.
9. Smil, V. *How the World Really Works*; Viking: London, UK, 2022.

10. Reichl, C.; Schatz, M. World Mining Data, Volume 37, Minerals Production, Federal Ministry of Agriculture, Regions and Tourism, Vienna, 2022. Available online: https://www.world-mining-data.info/ (accessed on 16 May 2022).
11. Eurostat—The Statistical Office of the European Union. Available online: https://ec.europa.eu/eurostat/web/products-eurostat-news/-/ddn-20220216-1 (accessed on 16 May 2022).
12. Buia, G.; Lorinţ, C. Hard Coal Deposits in Romania/Depozite de huilă din România. *Rev. Min. Min. Rev.* **2010**, *16*, 9–14.
13. Buia, G.; Lorinţ, C.; Rădulescu, M. Considerations About Economic Outlook of Jiu Valley Hard Coal Deposit. *Rom. J. Miner. Depos.* **2014**, *87*, 41–46.
14. Buia, G.; Lorinţ, C.; Nimară, C.; Lupuleac, R. Role of Jiu Valley Hard Coal Deposits Between Eastern and Western European Energetic Constraints. *Ann. Univ. Petroşani Min. Eng.* **2014**, *15*, 21–28.
15. Wang, L.; Chen, X.; Xia, Y.; Jiang, L.; Ye, J.; Hou, T.; Wang, L.; Zhang, Y.; Li, M.; Li, Z.; et al. Operational Data-Driven Intelligent Modelling and Visualization System for Real-World, On-Road Vehicle Emissions—A Case Study in Hangzhou City, China. *Sustainability* **2022**, *14*, 5434. [CrossRef]
16. Liang, X.; Zhang, S.; Wu, Y.; Xing, J.; He, X.; Zhang, K.M.; Wang, S.; Hao, J. Air quality and health benefits from fleet electrification in China. *Nat. Sustain.* **2019**, *2*, 962–971. [CrossRef]
17. Wang, L.; Chen, X.; Zhang, Y.; Li, M.; Li, P.; Jiang, L.; Xia, Y.; Li, Z.; Li, J.; Wang, L.; et al. Switching to electric vehicles can lead to significant reductions of $PM_{2.5}$ and NO_2 across China. *One Earth* **2021**, *4*, 1037–1048. [CrossRef]
18. Zhang, Q.; Zheng, Y.; Tong, D.; Shao, M.; Wang, S.; Zhang, Y.; Xu, X.; Wang, J.; He, H.; Liu, W.; et al. Drivers of Improved $PM_{2.5}$ Air Quality in China from 2013 to 2017. *Proc. Natl. Acad. Sci. USA* **2019**, *116*, 24463–24469. [CrossRef] [PubMed]
19. Xue, Y.; Cao, X.; Ai, Y.; Xu, K.; Zhang, Y. Primary Air Pollutants Emissions Variation Characteristics and Future Control Strategies for Transportation Sector in Beijing, China. *Sustainability* **2020**, *12*, 4111. [CrossRef]
20. Nicola, A.H.; Radu, S.M. *Analysis of Polluting Emissions of Vehicles/Analiza Emisiilor Poluante ale Autovehiculelor*; Universitas: Petroşani, Romania, 2019. (In Romanian)
21. Lorinţ, C. *Protected Natural Areas and Biodiversity Conservation/Arii Naturale Protejate şi Conservarea Biodiversităţii*; Universitas: Petroşani, Romania, 2012. (In Romanian)
22. European Environmental Agency. Available online: https://www.eea.europa.eu/ (accessed on 24 March 2022).
23. Environmental Systems Research Institute. *ArcGIS Desktop, Release 10*; ESRI: Redlands, CA, USA, 2011.
24. Mihăiescu, R. *Integrated Environmental Monitoring/Monitoringul Integrat al Mediului*; Bioflux: Cluj-Napoca, Romania, 2014. (In Romanian)
25. Călămar, A.N.; Găman, G.A.; Pupăzan, D.; Toth, L.; Kovacs, I. Analysis of environmental components by monitoring gas concentrations in the environment. *Environ. Eng. Manag. J.* **2017**, *16*, 1249–1256. [CrossRef]
26. Law, No. 104/2011 on Ambient Air Quality. Available online: https://legislatie.just.ro/Public/DetaliiDocument/129642 (accessed on 24 March 2022). (In Romanian)
27. *STAS 12574-87*; Air from Protected Areas. Quality Conditions/Aer din Zonele Protejate. Condiţii de Calitate. Asociaţia de Standardizare din Romania: Bucharest, Romania, 1987. (In Romanian)
28. GrayWolf Sensing Solutions. Available online: https://graywolfsensing.com/ (accessed on 24 March 2022).
29. Kimo Instruments AMI 300 Multifunction Data Logger. Available online: https://www.inlec.com/kimo-ami-300-multifunction-data-logger (accessed on 24 March 2022).
30. Călămar, A.N.; Simion, A.; Toth, L.; Simion, S.; Nicolescu, C. Improving the method of calculating the ecological footprint generated by road traffic—Case study. *Environ. Eng. Manag. J.* **2019**, *18*, 781–788. [CrossRef]
31. National Air Quality Monitoring Network. Available online: https://www.calitateaer.ro/ (accessed on 10 April 2022).
32. Society Energetic Complex Hunedoara S.A./Societatea Complexul Energetic Hunedoara S.A. Available online: www.cenhd.ro (accessed on 16 May 2022). (In Romanian).
33. Florea, A.; Lorint, C.; Danciu, C. Particulate matters generated by Caprişoara tailing pond and their impact on air quality. *Environ. Eng. Manag. J.* **2019**, *18*, 803–810. [CrossRef]
34. National Energetic System. Available online: https://www.transelectrica.ro/web/tel/sistemul-energetic-national (accessed on 1 May 2022).
35. National Energy Regulatory Authority. Report on the Results of Monitoring the Electricity Market in December 2020/Raport Privind Rezultatele Monitorizării Pieţei de Energie Electrică în Luna Decembrie 2020. Available online: https://www.anre.ro/download.php?f=fqeCg6I%3D&t=vdeyut7dlcecrLbbvbY%3D (accessed on 18 May 2022). (In Romanian).

sustainability

MDPI

Article

Analysis of Spatial Dynamic Correlation and Influencing Factors of Atmospheric Pollution in Urban Agglomeration in China

Liangli Wei [1] and Xia Li [2,3,*]

[1] School of Economics and Management, Hefei Normal University, Hefei 230601, China
[2] School of Accounting, Anhui University of Finance and Economics, Bengbu 233030, China
[3] School of Management, University of Science and Technology of China, Hefei 230026, China
* Correspondence: 120081631@aufe.edu.cn

Abstract: The fluidity of air pollution makes a cross-regional joint effort to control pollution inevitable. Exploring the dynamic correlation and affecting factors of air pollution in urban agglomerations is conducive to improving the effectiveness of pollution control and promoting the high-quality development of the regional economy. Based on daily data on $PM_{2.5}$ concentration, the article identifies the dynamic association relationship of atmospheric pollution in urban agglomerations of Beijing–Tianjin–Hebei (BTH) air pollution transmission channel under the framework of the vector autoregressive model, building the spatial correlation network of atmospheric pollution in urban agglomerations of BTH atmospheric pollution transmission channel, investigating the structure characteristics and influencing factors. The results show that the atmospheric pollution in BTH cities has a general dynamic correlation, which shows a stable multithreaded complex network structure; the overflow direction of air pollution is highly consistent with the weight matrix of northwest wind direction; economic development level, population density, openness degree, geographical location, and the relationship of wind direction are the important factors affecting the spatial association network of atmospheric pollution. We should actively explore the construction mode of urban agglomeration under the constraint of atmospheric pollution and improve the cross-regional collaborative governance mechanism.

Keywords: urban agglomeration of atmospheric pollution transmission channel; dynamic association; QAP (quadratic assignment procedure); BTH (Beijing–Tianjin–Hebei); spatial wind weight matrix

1. Introduction

Given the early extensive economic growth model, inefficient energy use efficiency, the high proportion of coal, and, in the end, energy consumption, atmospheric pollution has wreaked havoc in many Chinese cities since 2012. The pattern of urban expansion characterized by high-density construction and high-intensity consumption of resources further leads to more frequent and wider outbreaks of urban air pollution in China. Chinese people should work together to control air pollution, and air quality in Chinese cities has improved markedly. The 2020 World Air Quality Report showed that 86 percent of Chinese cities had higher air quality than the previous year, and the $PM_{2.5}$ exposure levels of the population had dropped by 11 percent. However, China still dominates the list of the 100 most polluted cities in the world, despite continuous improvements in urban air quality. According to the 2020 China Environmental Bulletin, air quality in 135 out of 337 cities exceeded the standard, with $PM_{2.5}$ being the main culprit among pollutants.

The atmosphere is fluid, and air pollution has the characteristics of spatial agglomeration and diffusion [1–4]. Each 1% increase in the Air Quality Index of neighboring cities will lead to a 0.45% increase in the Air Quality Index of the city [5]. Spatial spillover effect and regional agglomeration features of atmospheric pollution mean "unilateral" efforts to treat

haze may become in vain because of the regional haze pollution "leakage effect" [6]. In view of the spread of air pollution, any individual industrial structure adjustment in any region is ineffective. Only by coordinating with each other and establishing a joint prevention and control mechanism can achieve the goal of coordinated air pollution control [7].

Atmospheric pollution will reduce the attractiveness of cities and thus slow down the process of urbanization [8]. First of all, atmospheric pollution has a significant effect on the healthy life of urban people. Long exposure to a bad air environment will increase respiratory infections, cardiovascular and cerebrovascular diseases, and even cause premature death, increasing health costs [9,10]. Secondly, with the expansion of cities, the weight of the ecological environment in population competitiveness is increasing, and urban air pollution may lead to a decrease in the floating population's residence intention, resulting in the "reverse urbanization" phenomenon, hindering the promotion of new urbanization strategy and having a negative impact on urban development [11]. Some scholars think that the decline of air quality in big cities is an important factor restricting labor supply, resulting in the "expelling effect" of human capital [12], and groups with high human capital are more sensitive to the air pollution [13].

The BTH region is located in eastern China, where the northwest wind prevails and in the semi-closed terrain of Taihang Mountain and Yanshan Mountain. Pollutants are easy to accumulate there, and the region has a high level of urbanization and a high population density [14]. In addition, coal is the main source of energy, and environmental governance problems have been prominent. As the air pollution transmission channel of The BTH region, the urban agglomeration is an essential part of China's core economic zone, with a high proportion of GDP. However, the contradiction between economy and environment is prominent. The Ecological and Environmental Conditions report of China in 2020 shows that 15 cities in the urban agglomeration of BTH atmospheric pollution transmission channel, including Anyang, Shijiazhuang, and Taiyuan, were ranked in the bottom 20 among 168 cities in the urban ambient air quality comprehensive index in 2020; the average number of good days in the urban agglomeration was 63.5%, much lower than the 87.0% average; the average $PM_{2.5}$ concentration in 2020 was 51 micrograms per cubic meter, much higher than the average concentration in the Yangtze River Delta, another key region (35 micrograms per cubic meter).

Air pollution control is complicated by the transport of air pollutants in neighboring areas; the BTH region is also facing the double pressure of improving regional air quality and controlling cross-regional pollution. It is urgent to explore the regional atmospheric pollution dynamic association of space and its influence factors, to search for ways to establish trans-regional coordinated prevention and control of air pollution, to win the battle of pollution prevention and governance, to promote coordinated development between regions, to boost the joint law enforcement action to improve air quality improvement effect. Spatial autocorrelation analysis originated from biometrics and has become one of the basic methods in theoretical geography [15]. Spatial data are almost all spatially dependent, so the study of regional pollution coordination and governance is no exception. Exploratory spatial data analysis has been used in several pieces of literature to analyze the spatio-temporal characteristics and interactive effects of regional air quality in China [16–19]; The existing literature on air pollution in the process of urban expansion is mostly based on static analysis and lacks dynamic excavation of the spatial-temporal evolution of internal air pollution within urban agglomerations. The spatial weight is mainly set by the spatial geographic weight matrix or spatial adjacent weight matrix [16,20,21]. However, the vector wind has a certain ability to explain the variation of $PM_{2.5}$ concentration [22]. The prevailing monsoon transported $PM_{2.5}$ from the upwind region to the downwind region; $PM_{2.5}$ concentration is generally affected by wind direction [23]. The east of China is a monsoon region, and the northwest wind prevails in autumn and winter in the "2 + 26" urban agglomeration. the northwest wind is essential in the diffusion of $PM_{2.5}$. Therefore, attention should be paid to the new characteristics of spatial spillover of urban agglomeration.

The marginal contribution of this paper lies in: First, in terms of the selection of research regions, the BTH region and its surrounding areas, which are called the BTH air pollution transmission channel urban agglomeration, are selected as the research object to highlight the air quality changes of urban agglomeration and the correlation between surrounding cities. This area is one of the typical key pollution regions and has better representativeness in China. Second, based on daily $PM_{2.5}$ data, to analyze the spatial dynamic correlation structure characteristics between urban agglomerations in typical regions and thoroughly and meticulously sort out the dynamic correlation relationship between cities, which can provide new empirical evidence for the joint prevention and control of air pollution in other key regions. Third, taking into full account the fact that the strong northwest wind in autumn and winter caused long-term air pollution in the urban agglomeration of the BTH atmospheric pollution transmission channel, the spatial weight matrix of wind direction was constructed, presenting a new feature of the spatial spillover direction of air pollution.

The remainder of the paper is arranged as follows: Section 2 is the research model and data description of the spatial dynamic correlation of air pollution in the urban agglomeration of the BTH air pollution transmission channel. Section 3 presents the empirical results and analysis. Section 4 summarizes the conclusion and offers proposals.

2. Model and Data

2.1. Model Construction

2.1.1. Spatial Correlation Analysis

In order to explore whether air pollution has the characteristics of non-randomness and spillover effect in spatial distribution, the exploratory spatial analysis method was used, and Moran's Index was adopted to investigate the overall spatial distribution characteristics of $PM_{2.5}$. The formula is as follows [24]:

$$Moran'I = \frac{n}{\sum_i (x_i - \overline{x})^2} \frac{\sum_i \sum_{j \neq i} W_{ij}(x_i - \overline{x})(x_j - \overline{x})}{\sum_i \sum_{j \neq i} W_{ij}} \quad (1)$$

where n is the total city number in the research sample; x_i and x_j, respectively, represent the observed value of $PM_{2.5}$ of city i and city j; $\overline{x}$ presents the average value of $PM_{2.5}$; and w_{ij} is the spatial weight matrix.

Three matrices are respectively selected in this paper. The first is the weight matrix of spatial wind direction (w_1), which presents the transmission effect of northwest wind on $PM_{2.5}$ diffusion in the urban agglomeration of the BTH air pollution transmission channel, measuring the spatial dynamic correlation of air pollution taking a city as a unit. If the northwest wind of the city i comes from the upwind city j, the value is 1; otherwise, the value is 0. The second is the spatial adjacent weight matrix (w_2). If the city i and city j is adjacent, the value is 1; otherwise, it is 0. The third is the geographical distance weight matrix (w_3); according to the first law of geography, the longer the distance between two places, the weaker the spatial connection effect will be; therefore, the reciprocal of geographical distance is used to construct geographical distance weight matrix [25].

The Moran's value is between -1 and 1. If the value approaches 0, there is no spatial autocorrelation of air pollution. If it is greater than 0, air pollution has a positive spatial correlation, indicating the areas with similar air pollution concentrations are clustered together. If it is less than 0, air pollution is negatively correlated in space, indicating that areas with different concentrations of air pollution are clustered together.

2.1.2. Spatial Network Correlation Measurement of Air Pollution

The social network analysis method is a kind of interdisciplinary analysis method aiming at "relational data" and taking "relationship" as the basic analysis unit. It builds the association network and carries out global analysis and structural relationship analysis. In this paper, the spatial correlation network is the relational set of air pollution of each city

in the BTH air pollution transmission channel urban agglomeration. Each city is a point in the network, and the air pollution correlation relationship between cities are lines in the network. The network composed of points and lines can clearly reflect the spatial dynamic correlation of air pollution in urban agglomeration along the air pollution transmission channel.

In this paper, the method of Granger causality test was used to identify spatial associations and correlations of the urban agglomerations. Based on the unit root stationarity test of $PM_{2.5}$ concentration series in 28 cities, the function model of $PM_{2.5}$ concentration series variables between two cities in 28 cities was established, namely the vector autoregression model (VAR) [21].

$$X_t = \alpha_1 + \sum_{i=1}^{m} \beta_{1,i} X_{t-i} + \sum_{i=1}^{n} \gamma_{1,i} Y_{t-i} + \varepsilon_{1,t} \quad (2)$$

$$Y_t = \alpha_2 + \sum_{i=1}^{p} \beta_{2,i} Y_{t-i} + \sum_{i=1}^{q} \gamma_{2,i} X_{t-i} + \varepsilon_{2,t} \quad (3)$$

where X_t and Y_t are the time series variables of the air pollution level of any two cities; m, n, p, and q are the lags; α_1, α_2, $\beta_{1,i}$, $\beta_{2,i}$, $\gamma_{1,i}$, and $\gamma_{2,i}$ are parameters to be estimated; $\varepsilon_{1,t}$ and $\varepsilon_{2,t}$ are random disturbance terms. The Granger causality test is conducted under the framework of the VAR model above-mentioned, and the significance level of 5% is taken to determine the spatial correlation. If $\gamma_{1,j}$ is significant at 5% significance level, it is considered that the atmospheric pollution concentration of city Y can be explained by the pollution concentration of city X, that is, the air pollution of city Y produces a spillover effect on city X, and the corresponding element of the spatial correlation matrix $M_{ij} = 1$ is obtained; otherwise, the value is 0, and the corresponding element of spatial correlation matrix $M_{ij} = 0$. Similarly, if $\gamma_{2,i}$ is significant at 5% significance level, it is considered that the atmospheric pollution concentration of city X can be explained by the pollution concentration of city Y, that is, the air pollution of city X has a spillover effect on city Y, and the value is assigned to 1; otherwise, the value is assigned to 0. There are four possibilities in the test results, that is, one-way correlation, two-way correlation, or no correlation between city X and city Y. Thus, the spatial correlation matrix M of air pollution between cities is constructed, which can represent the spatial correlation network system of the urban agglomeration of the BTH air pollution transmission channel.

In the network system, individual characteristics directly reflect the relative importance and status of each city. The characteristics of individual network structure can be characterized by out-degree centrality, in-degree centrality, point centrality, closeness centrality, and betweenness centrality. Out-degree centrality is the relationship number emitted by this node, which represents the spillover influence of one city on other cities in the networks. In-degree centrality is the number of relationships received by this node, which represents the influence that a city receives from other cities on it. The software can automatically calculate the out-degree centrality and in-degree centrality. Point centrality is used to measure the ability of a city to produce a linkage relationship of air pollution with other cities; it is measured by the number of cities directly connected with other cities. The high point centrality of a city shows the city is directly connected with others, and it is in the center of the network. Closeness centrality measures the extent to which a city is not controlled by other cities and reflects the independence of the city in the network; if the "distance" of a city is very short, the city has a high degree of closeness to the center, and the city has a rapid influence on the spatial linkage of air pollution. Betweenness centrality is an index representing "control ability", which mainly measures how much each city is located in the "middle" of other cities in the network. The higher the betweenness centrality of a city is, the stronger the city's ability to control the air pollution associations of other cities is.

Equations (4)–(6) are the calculation methods of point centrality, betweenness centrality, and closeness centrality [26].

$$\deg_i = \sum_j x_{ij}/(2n-2) \tag{4}$$

$\sum_j x_{ij}$ is the associated number of nodes i, and n is the network scale.

$$clo_i = [\sum_j d_{ij}/(n-1)]^{-1} \tag{5}$$

$\sum_j d_{ij}$ represents a shortcut between nodes i and j.

$$bet_i = \frac{2\sum_j \sum_k g_{ij}(i)}{n^2 - 3n + 2} \tag{6}$$

$g_{jk}(i)$ represents the total number of shortcuts that pass-through node i between nodes j and k. $j \neq k \neq i$, and $j < k$.

2.1.3. QAP Regression Analysis

Based on Environmental Kuznets Curve theory, taking into account geographical distance, meteorological and socioeconomic factors, the influencing factor model of air pollution spatial association network is constructed as follows:

$$M = f(D, W, RGDP, Density, Industrial, Open, Fiscal, Energy) \tag{7}$$

All variables in model (7) are matrices, where M presents the spatial correlation matrix of air pollution in the urban agglomeration, which is obtained from the VAR model above. The geographical distance factor D is the spatial adjacency matrix of the urban agglomeration of the BTH air pollution transmission channel; the meteorological factor W is the relationship matrix of wind direction between cities. Social and economic factors include economic development ($RGDP$), population density ($Density$), industrial structure ($Industrial$), degree of openness ($Open$), fiscal freedom ($Fiscal$), and energy consumption structure ($Energy$). $RGDP$ is the difference matrix of economic development level between cities and the per capita GDP is used to measure the economic development level of each city. $Density$ is difference matrix of population density between cities, population density is described by the population number of per unit area of each city. Industrial is the difference matrix of Industrial structure between cities; the industrial structure is measured by the secondary industry proportion of cities. $Open$ is the difference matrix of openness degree between cities, the actual amount of foreign direct investment used by each city represents the level of openness degree of a city. $Fiscal$ is the difference matrix of Fiscal freedom between cities, the ratio of budgetary Fiscal revenue and budgetary Fiscal expenditure in each city is selected to measure Fiscal freedom. $Energy$ is the difference matrix of Energy consumption structure between cities. Referring to relevant literature [16], this paper selects the proportion of the output of the high-consumption coal industry in regional GDP as an indicator to measure energy consumption structure.

Model (7) adopts QAP (Quadratic Assignment Process) analysis. The spatial correlation data of urban air pollution belong to relational data, which generally cannot be tested by traditional statistical testing methods because there may be a high degree of correlation between these relational data. QAP is a method based on matrix data replacement, which compares the similarity of each lattice value in the two square matrices, the correlation coefficient between the two matrices is obtained, and the correlation coefficient is tested non-parametrically [27]. The QAP analysis method does not need to assume that the inde-

pendent variables are independent of each other, which is more robust than the parametric method [28].

2.2. Data Sources

The research object of this paper is the Urban agglomeration of the BTH air pollution transmission channel, which specifically includes 28 cities. The geographical locations of the 28 cities are shown in Figure 1. Although these cities belong to different administrative regions, they are an inseparable whole in terms of air pollution.

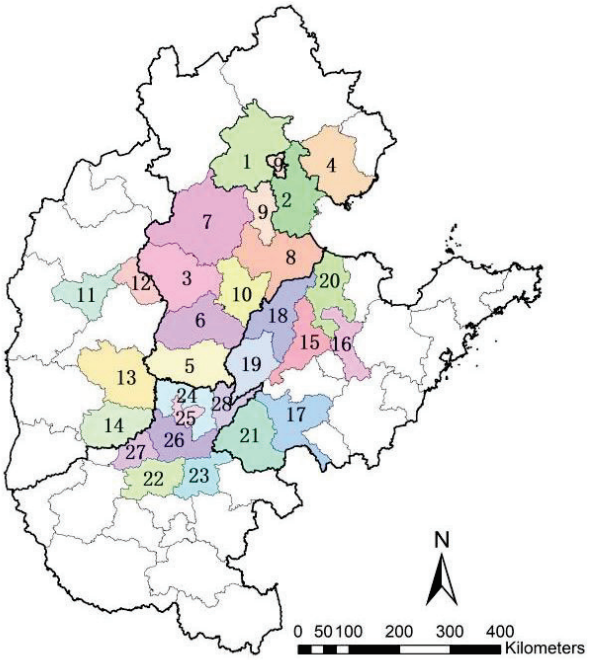

Figure 1. Geographical location of 28 cities. Note: 1. Beijing 2. Tianjin 3. Shijiazhuang 4. Tangshan 5. Handan 6. Xingtai 7. Baoding 8. Cangzhou 9. Langfang 10. Hengshui 11. Taiyuan 12. Yangquan 13. Changzhi 14. Jincheng 15. Jinan 16. Zibao 17. Jining 18. Dezhou 19. Liaocheng 20. Binzhou 21. Heze 22. Zhengzhou 23. Kaifeng 24. Anyang 25. Hebi 26. Xinxiang 27. Jianzuo 28. Puyang.

$PM_{2.5}$ concentration is selected to measure the urban air pollution level. Compared with the traditional air pollution index, $PM_{2.5}$ source and composition are more complex, and the harm degree is higher, which is the "culprit" of pollutants.

The data period in this paper is from 1 January 2020 to 31 December 2021. The daily data of $PM_{2.5}$ concentration were obtained from the website of "Weather Report" through the web crawler program, the website is www.tianqihoubao.com/aqi (accessed on 1 September 2022). The annual average processing of daily data of $PM_{2.5}$ concentration was carried out during the spatial correlation analysis. During QAP analysis, the period from 2016 to 2020 was selected as the sample observation period to calculate the average value of the corresponding index in model (7) during the investigation period, and then the absolute difference of the average value constituted the corresponding difference matrix. All data were from statistical yearbooks, statistical gazette, and China Economic Network statistical database of 28 cities over the years.

3. Empirical Results

3.1. Spatial Correlation of Air Pollution in Urban Agglomeration

According to the above Formula (1), the universe spatial correlation index of $PM_{2.5}$ was calculated, and the results are shown in Table 1. Based on the Moran's I results in Table 1, the spatial wind direction weight matrix (w_1), spatial adjacent weight matrix (w_2), and spatial inverse geographical distance weight matrix (w_3) were selected. At the significance

level of 1% or 5%, the universe Moran's was significantly positive. The results show that air pollution in the urban agglomeration of the BTH atmospheric pollution transmission channel has a significant positive correlation.

Table 1. Universe spatial correlation test in urban agglomeration.

Weight Matrix	Year	Moran's I	Expected Value of Moran's I	Standard Deviation of Moran's I	Z	*p*-Value
W_1	2020	0.187	−0.037	0.102	2.196	0.014 **
	2021	0.191	−0.037	0.103	2.222	0.013 **
W_2	2020	0.213	−0.037	0.133	1.874	0.030 **
	2021	0.246	−0.037	0.134	2.115	0.017 **
W_3	2020	0.068	−0.037	0.037	2.884	0.002 ***
	2021	0.095	−0.037	0.037	3.586	0.000 ***

Note: *** and ** represent 1% and 5% significance levels, respectively.

The spatial wind weight matrix (w_1) was further selected to draw the Moran scatter diagram, which showed that most cities lay in the first and third quadrants, and only a few lay in the second and fourth quadrants, presenting high–high aggregation mode (H–H) and low–low aggregation mode (L–L). As shown in the Figure 2, there is a positive correlation between the spatial distribution of air pollution.

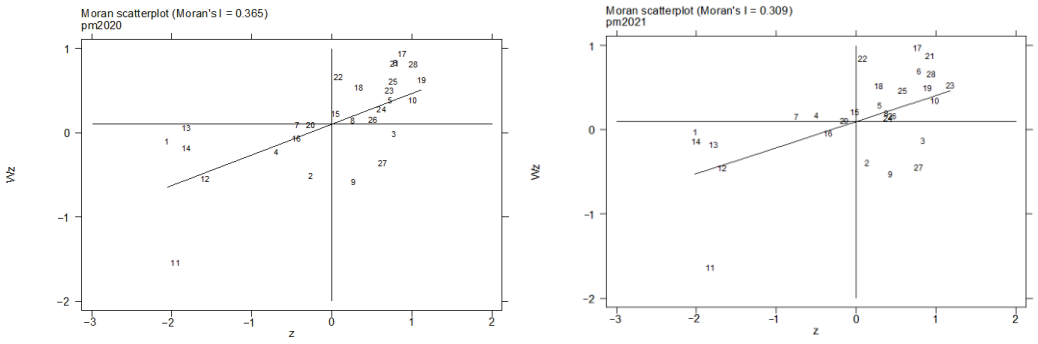

Figure 2. Moran scatter plots of urban agglomerations, 2020 and 2021.

3.2. Characteristics of Spatial Association Network of Air Pollution in Urban Agglomeration

3.2.1. Overall Network Characteristics

The net-draw tool of UCINET was used for visualizing the processing above, as shown in Figure 3. There is no independent point in the spatial correlation of the network; the $PM_{2.5}$ concentration of urban agglomeration presents a complex and multithreaded spatial correlation. The air pollution of a city is not only affected by local meteorological and socioeconomic factors but also associated with other atmospheric pollution of the city, and the relationship goes beyond mere geography in the sense of "adjacent" or "similar" effect; each city has at least one more spatial correlation.

The overall network density of the air pollution spatial correlation network is 0.872, indicating that the air pollution of each city in the network has a very close correlation, the air pollution spatial correlation breaks through the pure relationship between adjacent cities and presents a multithreaded cross network distribution; the measurement result of network correlation degree is 1, shows that the 28 cities are all correlated with each other in air pollution, and the accessibility between cities in the network is very high, there is no isolated city, and the network is very robust, and every city is directly affected by the spatial network. Overall speaking, there is a general spatial dynamic correlation between air pollution in various cities. The network has a high degree of accessibility, which belongs to a relatively uniform structure, with decentralized power and low level. Each city can

easily generate spatial correlation with other cities, which also indicates that it is difficult for any city to be "isolated" in pollution control.

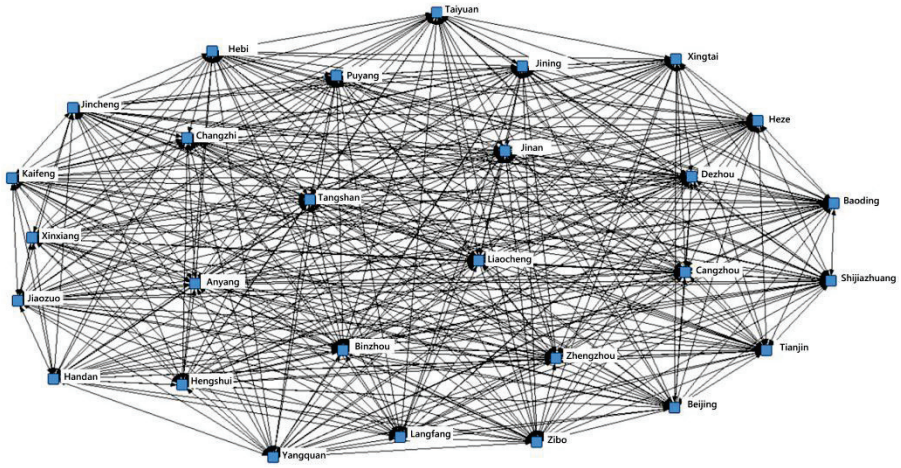

Figure 3. Spatial correlation network of urban air pollution.

3.2.2. Individual Network Characteristics

Table 2 shows the node characteristics of the spatial association network during the sample observation period.

Table 2. Centrality of spatial association network.

City	Out-Degree	In-Degree	Centrality Degree Index			City	Out-Degree	In-Degree	Centrality Degree Index		
			Degree	Closeness	Betweenness				Degree	Closeness	Betweenness
Beijing	26	14	74.074	81.965	0.896	Binzhou	24	25	90.741	91.552	3.054
Tianjin	29	25	81.482	85.123	2.058	Jining	11	27	70.371	81.396	1.216
Shijiazhuang	27	25	96.297	96.552	5.802	Heze	19	26	83.333	86.786	2.417
Tangshan	24	23	87.037	88.549	3.081	Zhengzhou	27	25	96.297	96.552	5.619
Baoding	26	16	77.778	83.741	1.655	Xinxiang	23	24	87.037	88.549	4.431
Langfang	26	17	79.630	86.786	1.763	Hebi	25	23	88.889	90.100	4.005
Cangzhou	22	27	90.741	92.188	3.974	Anyang	27	19	85.185	88.572	2.360
Hengshui	24	36	92.593	93.215	3.065	Jiaozuo	26	25	94.445	94.766	4.121
Handan	25	21	85.186	87.461	2.790	Puyang	26	24	92.593	93.215	3.367
Xingtai	26	21	87.037	89.124	2.567	Kaifeng	25	26	94.445	94.766	5.591
Jinan	14	27	75.926	83.750	1.556	Taiyuan	26	22	88.889	90.402	4.429
Zibo	18	27	83.333	87.500	3.022	Yangquan	25	23	88.889	90.100	4.194
Liaocheng	21	25	85.186	87.461	2.060	Changzhi	26	25	94.445	94.766	5.803
Dezhou	25	27	96.297	96.552	5.200	Jincheng	26	24	92.593	93.215	5.903
Mean value	23.54	23.54	87.170	89.810	3.430	-	-	-	-	-	-

As shown in Table 2, the mean values of out-degree centrality and in-degree centrality are both 23.54. Among them, there are 21 cities whose out-degree centrality is over the mean value, indicating the air pollution of these cities will spill out to others and have a great impact on others. There are 18 cities with in-degree centrality greater than the mean, indicating that these cities are more susceptible to air pollution than other cities. The cities with the highest out-degree centrality of 27 are Zhengzhou and Anyang in Henan Province and Shijiazhuang in Hebei Province, indicating that these three cities have the strongest radiation and are most likely to affect the air pollution level of others. Several cities have the highest in-degree centrality of 27, indicating they are in the middle of the air pollution networks and are most susceptible to the impact of air pollution fluctuations of other cities. They are Jinan, Jining, Zibo, Dezhou in Shandong Province, and Cangzhou in Hebei Province.

The mean point centrality of BTH air pollution transmission channel urban agglomeration was 87.170. There are 14 cities above the average, from high to low, Shijiazhuang, Zhengzhou, Dezhou, Changzhi, Kaifeng, Jiaozuo, Hengshui, Puyang, Jincheng, Binzhou, Cangzhou, Taiyuan, Yangquan, and Hebi; there are many correlations between air pollution in these cities and other cities. Among them, five cities belong to Henan Province, four

cities belong to Shanxi Province, three cities belong to Hebei Province, and two cities belong to Shandong Province. Therefore, comparatively speaking, Henan province and Shanxi Province are regions with relatively concentrated spatial correlation in air pollution. The three cities with the least number of spatial correlation relationships are Jining, Jinan in Shandong Province, and Beijing; these cities are located at the edge of the network and are less connected to other cities.

According to the closeness centrality, the mean value of the urban agglomeration was 89.810, and 14 cities were higher than the mean value, which were Shijiazhuang, Zhengzhou, Dezhou, Changzhi, Kaifeng, Jiaozuo, Hengshui, Puyang, Jincheng, Binzhou, Cangzhou, Taiyuan, Yangquan, and Hebi in turn. These cities can quickly associate with other cities in the spatial association network and are network centric actors in the network.

As to the betweenness centrality, the top six cities are Taiyuan, Jincheng, and Changzhi in Shanxi Province, Shijiazhuang in Hebei province, and Zhengzhou and Kaifeng in Henan Province. It can be seen that some cities of Shanxi Province and other provincial capitals are relatively in the central position, playing the role of "intermediary" and "bridge", and have a strong influence on air pollution in other cities.

The measurement results of individual network characteristics show that Shanxi Province and provincial capitals are the most likely to affect the air pollution of other cities, and cities in Shandong Province are the most likely to be affected by other cities, while Beijing is a relatively independent position. The reason is that Shanxi Province is China's first coal production, coal transport province, and energy-heavy chemical base; coal is its main resource, coal combustion process produces not only a large number of soot but also the formation of carbon monoxide, carbon dioxide, sulfur dioxide, nitrogen oxides, and other harmful substances, aggravating the air pollution of the city. Shandong province is located in the northwest of other cities and is affected by the northwest wind. The air pollutants of Shanxi Province and other cities will be transmitted and diffused to Shandong Province through the northwest wind, aggravating the air pollution of Shandong Province. Therefore, Shandong province is more vulnerable to air pollution from other cities. Beijing is located on the northern edge of the urban cluster. Due to its own unique geographical location and meteorological factors, it is in a relatively "independent" position in the urban agglomeration and has relatively little correlation with the air pollution of other cities.

3.3. Influencing Factors of Spatial Association Network in the Urban Agglomeration

The QAP method was used for regression of model (7), and 5000 random replacements were selected, obtaining the QAP regression results of the spatial correlation matrix and influencing factors of air pollution in the urban agglomeration, as shown in Table 3.

Table 3. QAP regression results of influencing factors of spatial network structure of air pollution.

Variable	Unstandardized Coefficients	Standardized Coefficients	Significance Level	$p \geq 0$	$p \leq 0$
D	−0.1269	−0.1342	0.000	1.000	0.000
W	−0.2596	−0.2847	0.000	1.000	0.000
RGDP	−0.0000	−0.1216	0.010	0.990	0.010
Density	0.0002	0.1508	0.002	0.002	0.999
Industrial	0.0504	0.0115	0.426	0.426	0.575
Open	−0.0010	−1.1472	0.037	0.963	0.037
Fiscal	0.0714	0.0302	0.269	0.963	0.037
Energy	−0.0258	−0.0191	0.290	0.711	0.290

Note: $p \geq 0$ and $p \leq 0$ separately mean the probability that the regression coefficient generated by random displacement is not less than and not greater than the final regression coefficient.

The results of QAP regression show that 5000 random displacement and within the range of sample volume of 756 (the total number of interrelated influences of 28 cities), the adjusted determination coefficient R^2 is 0.324, indicating that the variable explanatory power of the regression model to air pollution spatial network association was 32.4%. Among them, the regression coefficient of spatial adjacency matrix D is −0.1269, indicating

geographical proximity does have an important effect on the spatial correlation of urban agglomeration air pollution, which is consistent with the research conclusion of Lin L and Li J [29]. The regression coefficient of the wind direction relation matrix W was -0.2596, indicating the northwest wind would significantly affect the spatial correlation relationship of air pollution, which according to the view of Wang ZJ et al. [30], mentioned that meteorological factors would affect the concentration and diffusion of atmospheric particles, and there are leading, and lagging relations of atmospheric concentration between cities are similar. The coefficient of *RGDP* of the difference matrix of economic development level is negative and close to 0, indicating the difference in economic development level between cities has a significant impact on the spatial correlation of air pollution, but the effect is not obvious. The regression coefficient of the population density difference matrix *Density* is positive, indicating the greater the difference in population density between cities, the more air pollution conduction relationship is. Areas with high population density are not conducive to the diffusion of pollutants due to the influence of high residential density on wind speed. Therefore, the greater the difference in population density between cities, the more obvious the diffusion effect of pollutants is. The gap matrix of openness degree between Cities *Open* is negative, indicating that the greater the similarity of openness between cities is, the greater the conduction relationship and spatial spillover effect of air pollution between cities are. Compared with community economy factors, geographical location and meteorological factors have a greater direct impact on the spatial correlation of air pollution. While the financial freedom difference matrix *Fiscal*, industrial structure difference matrix *Industrial*, and energy consumption structure difference matrix *Energy* did not pass the significance level test, indicating under the condition that other factors remain unchanged, financial freedom, industrial structure, and energy consumption structure are not the core factors that affect the spatial correlation network of air pollution.

4. Conclusions

In this paper, the spatial dynamic correlation and influencing factors of air pollution were analyzed by using $PM_{2.5}$ data of Urban agglomeration. The results show that air pollution in urban agglomeration has a significant spatial correlation. The dynamic correlation effect of air pollution shows a complex network structure of multithreading; the air pollution goes beyond the "adjacent" or "close" effect in the pure geographical sense, the spillover effect of air pollution also exists between distant cities, and the spillover direction coincides with the northwest wind direction. The spatial association network structure of air pollution is stable, and each city occupies different positions in the spatial association network. Shijiazhuang, Zhengzhou, and Dezhou are located at the core of the network; Jining, Jinan, and Beijing are located at the edge of the network. The causes of spatial association networks of air pollution are complex. Geographical adjacency, wind direction, economic development, population density, and openness are all important factors affecting the dynamic association network of air pollution. Geographical and meteorological factors have a significant direct impact on the spatial correlation of air pollution. Differences in fiscal freedom, industrial structure, and energy consumption structure have no significant impact on the spatial correlation of air pollution.

Based on this research, the following enlightenments can be obtained. Firstly, we need to be fully aware of the difficulty of pollution control, with the goal of working together to fight pollution for a long time; we need to optimize the mechanism for coordinated trans-regional governance, implement a long-term trans-regional joint prevention and control mechanism for urban agglomerations, unify standards for atmospheric governance in urban agglomerations, and implement interest coordination mechanisms such as standards for ecological compensation, government incentives, and emission trading. Secondly, we need to clarify the functions and roles of pollution control in individual urban and make accurate decisions. The monitoring should focus on the cities that play the role of "intermediary" and "bridge" to achieve global and local coordination and breakthrough and

build a cross-regional joint prevention and control system. Thirdly, we need to formulate a reasonable population mobility policy and urban opening policy, build an appropriate industrial structure and energy consumption structure, maintain a reasonable urban population density and urban openness, and optimize urban pollution problems from multiple perspectives, as well as actively explore the construction mode of urban agglomeration under the constraint of air pollution, promote the coordinated and sustainable development of urban economy-environment system, introduce market mechanism, and improve environmental and economic policies, so as to achieve the overall improvement of economic development and environmental quality.

Author Contributions: Conceptualization, L.W. and X.L.; methodology, L.W.; software, L.W.; validation, X.L.; formal analysis, L.W.; investigation, L.W.; resources, X.L.; data curation, L.W.; writing—original draft preparation, L.W.; writing—review and editing, X.L.; visualization, L.W.; supervision, X.L.; project administration, L.W.; funding acquisition, X.L. All authors have read and agreed to the published version of the manuscript.

Funding: This research was funded by the social science foundation of China, grant number 21BGL097 and the key project of humanities and social science research in Anhui Universities, grant number SK2020A0143.

Institutional Review Board Statement: Not applicable.

Informed Consent Statement: Not applicable.

Data Availability Statement: The daily data of PM2.5 concentration were obtained from the website of "Weather Report" through the web crawler program, the website is www.tianqihoubao.com/aqi (accessed on 1 September 2022). Other data were from statistical yearbooks, statistical gazette and China Economic Network statistical database of 28 cities over the years.

Conflicts of Interest: The authors declare no conflict of interest.

References

1. Anselin, L. Spatial Effects in Econometric Practice in Environmental and Resource Economics. *Am. J. Agric. Econ.* **2001**, *83*, 705–710. [CrossRef]
2. van Donkclaar, A.; Martin, R.V.; Brauer, M.; Kahn, R.; Levy, R.; Verduzco, C.; Villeneuve, P.J. Global Estimates of Ambinet Fine Particulate Matter Concentrations from Satellite-based Aerosol Optical Depth: Development and Application. *Environ. Health Perspect.* **2010**, *118*, 847–855. [CrossRef] [PubMed]
3. Li, G.Q.; Qin, J.H.; He, R.W. Spatial-Temporal Evolution and Influencing Factors of China's $PM_{2.5}$ Pollution. *Econ. Geogr.* **2018**, *38*, 11–18.
4. Wang, Y.X.; Sun, S.; Yao, L. Temporal and Spatial Differences and Driving Forces of $PM_{2.5}$ in BTH Urban Agglomeration from the EKC Perspective. *J. Nat. Sci. Hunan Norm. Univ.* **2021**, *44*, 11–18.
5. Liu, H.; Fang, C.; Zhang, X.; Wang, Z.; Bao, C.; Li, F. The effect of natural and anthropogenic factors on haze pollution in Chinese cities: A spatial econometrics approach. *J. Clean. Prod.* **2017**, *165*, 323–333. [CrossRef]
6. Shao, S.; Li, X.; Cao, J.H.; Yang, L.L. China's Economic Policy Choices for Governing Smog Pollution Based on Spatial Spillover Effects. *Econ. Res. J.* **2016**, *51*, 73–88.
7. Hao, Y.; Liu, Y.M. The influential factors of urban $PM_{2.5}$ concentrations in China: A spatial econometric analysis. *J. Clean. Prod.* **2016**, *112*, 1443–1453. [CrossRef]
8. Hanlon, W.W. Coal Smoke, City Growth, and the Costs of the Industrial Revolution. *Econ. J.* **2020**, *130*, 462–488. [CrossRef]
9. Evans, M.F.; Smith, V.K. Do New Health Conditions Support Mortality-Air Pollution Effects? *J. Environ. Econ. Manag.* **2005**, *50*, 496–518. [CrossRef]
10. Fan, M.Y.; He, G.J.; Zhou, M.G. The Winter Choke: Coal-Fired Heating, Air Pollution, and Mortality in China. *J. Health Econ.* **2020**, *71*, 1–17. [CrossRef]
11. Sun, Z.W.; Sun, C.L. Be Alert to"Counter Urbanization"Induced by Air Pollution: Based on an Empirical Study of the Settlement Intention of Floating Population. *J. South China Norm. Univ.* **2018**, *5*, 134–141.
12. Sun, W.Z.; Zhang, X.N.; Zheng, S.Q. Air Pollution and Spatial Mobility of Labor Force: Study on the Migrants' Job Location Choice. *Econ. Res. J.* **2019**, *54*, 102–117.
13. Shao, Z.Y.; Wang, X.Z. Does Air Pollution Affect the Movement of People between Cities? *Stat. Manag.* **2021**, *36*, 11–17.
14. Han, L.; Zhou, W.; Li, W.; Li, L. Impact of urbanization level on urban air quality: A case of fine particles ($PM_{2.5}$) in Chinese cities. *Environ. Pollut.* **2014**, *194*, 163–170. [CrossRef]

15. Chen, Y.G. Reconstructing the mathematical process of spatial autocorrelation based on Moran's statistics. *Geogr. Res.* **2009**, *28*, 1449–1463.
16. Ma, L.M.; Zhang, X. The Spatial Effects of China's Haze Pollution and the Impact from Economic Change and Energy Structure. *China Ind. Econ.* **2014**, *313*, 19–31.
17. Xiang, K.; Song, D.Y. Spatial Analysis of China's $PM_{2.5}$ Pollution at the Provincial Level. *China Popul. Resour. Environ.* **2015**, *25*, 153–159.
18. Bai, L.; Jiang, L.; Jiang, L.; Zhou, H.; Chen, Z. Spatio-temporal Characteristics of Air Quality Index and Its Driving Factors in the Yangtze River Economic Belt: An Empirical Study Based on Bayesian Spatial Econometric Model. *Sci. Geogr. Sin.* **2018**, *38*, 2100–2108.
19. Zhang, X.M.; Luo, S.; Li, X.M.; Li, Z.F.; Fan, Y.; Sun, J.W. Spatio-temporal Variation Features of Air Quality in China. *Sci. Geogr. Sin.* **2020**, *40*, 190–199.
20. Liu, H.J.; Du, G.J. Spatial Pattern and Distributional Dynamics of Urban Air Pollution in China-An Empirical Study Based on Aqi and Six Sub-Pollutants of 161 Cities. *Econ. Geogr.* **2016**, *36*, 33–38.
21. Du, M.Z.; Liu, W.J.; Hao, Y.Z. Spatial Correlation of Air Pollution and Its Causes in Northeast China. *Int. J. Environ. Res. Public Health* **2021**, *18*, 10619. [CrossRef] [PubMed]
22. Tai, A.P.; Mickley, L.J.; Jacob, D.J. Correlations between fine particulate matter ($PM_{2.5}$) and meteorological variables in the United States: Implications for the sensitivity of $PM_{2.5}$ to climate change. *Atmos. Environ.* **2010**, *44*, 3976–3984. [CrossRef]
23. Sun, D.D.; Yang, S.Y.; Wang, T.J.; Chen, P.; Liu, B.; Dai, Q. Characteristics of O_3 and $PM_{2.5}$ and its impact factors in Yangtze River Delta. *J. Meteorol. Sci.* **2019**, *39*, 164–177.
24. Moran, P.A.P. The Interpretation of Statistical Maps. *J. R. Stat. Soc. Ser. B* **1948**, *10*, 243–251. [CrossRef]
25. Huang, Y.P.; Zhou, J.J.; Shang, X.T. Analysis of the Impact of China's Housing Price Rise on the Per Capita Income Gap of the Province. *Econ. Geogr.* **2018**, *38*, 29–35.
26. Freeman, L.C. Centrality in social networks:Conceptual clarification. *Soc. Netw.* **1979**, *1*, 215–239. [CrossRef]
27. Everett, M.G. *Social Network Analysis*; Textbook at Essex Summer School in SSDA: Essex, UK, 2002.
28. Liu, J. *Lectures on Whole Network Approach: A Practical Guide to UCINET*; Truth & Wisdom Press: Beijing, China, 2009.
29. Lin, L.; Li, J. The Net Work Analysis on Spatial Correlation of Environmental Pollution in the Yangtze River Economic Belt: Based on the Comprehensive Indicator of Water and Air Pollution. *Econ. Probl.* **2019**, *9*, 86–92.
30. Wang, Z.J.; Han, L.H. Characteristics and sources of $PM_{2.5}$ in typical atmospheric pollution episodes in Beijing. *J. Saf. Environ.* **2012**, *12*, 122–126. [CrossRef]

sustainability

MDPI

Review

Bibliometric Network Analysis of Trends in Cyclone Separator Research: Research Gaps and Future Direction

Frimpong J. Alex [1,2], Gangfeng Tan [1,*], Philip K. Agyeman [1,3], Prince O. Ansah [2], Isaac O. Olayode [4], Jamshid V. Fayzullayevich [1] and Shuang Liang [5]

[1] School of Automotive Engineering, Wuhan University of Technology, Wuhan 430070, China
[2] Mechanical Engineering Department, Faculty of Engineering, Kumasi Technical University, Kumasi 00233, Ghana
[3] Mechanical Engineering Department, College of Engineering, Kwame Nkrumah University of Science and Technology, Kumasi 00233, Ghana
[4] Mechanical and Industrial Engineering Technology Department, University of Johannesburg, Johannesburg P.O. Box 2028, South Africa
[5] Suizhou-Wuhan University of Technology Industry Research Institute, Suizhou 441300, China
* Correspondence: auto_nova@whut.edu.cn

Abstract: Cyclone separators are used extensively in diverse applications and research domains to collect particle-laden flows. Despite the technological advances in this field, no bibliometric reports on this topic have been documented. Understanding the state of the art in this field is crucial for future research. Using bibliometric mapping techniques, this study examined the quality, quantity, and development of research on cyclone separators. Relevant data were extracted in plain text formats through search queries refined by publication year (2000–2021) and document type (article and review articles). A sample of 487 publications, limited to the Web of Science Core Collection (WoSCC) database was used for the bibliometric analysis. Data analysis was performed using RStudio software package (R Bibliometrix tool). Of the 487 publications that appeared during this period, China had the highest number, followed by the Islamic Republic of Iran, whereas chemical engineering journals dominated the cyclone separator research publications. Collaboration among the researchers was low (MCPR < 0.5000). Furthermore, the pattern of single-author publications was found to outstrip that of the multiple-author publications. The findings suggest that researchers in various parts of the world, particularly Africa and the Middle East, should route their research efforts towards this field, in light of the lack of publications from these regions on this subject. The aim of this study was to serve as a seminal reference for potential technological research directions and collaboration among researchers in this and other related fields.

Keywords: cyclone separator; bibliometric analysis; collection efficiency; numerical simulation; pressure drop

1. Introduction

Particle separation and control of bulk solids or powder, solid-gas particles, fine particulate matter, and solid-liquid particles remain among the developed axes of investigative research in industrial processing and handling applications because of the drastic emissions and environmental threat of pollutants [1]. A plethora of professional research engineers and scientists across different engineering and industrial fields have employed particle separation technologies in their fields. These include mechanical engineers, chemists, metallurgists, pharmacists, environmental engineers, civil engineers, biologists, and plastic and cosmetic scientists in different generic forms over the past 100 years. Furthermore, statutory environmental control requirements of various countries have resulted in significant improvements in the design of equipment for large solid particles, intermediate-sized particles, solid-liquid-gas particulates, and fine particulate matter (PM), such as cyclone

separators, baghouse filter collectors, wet scrubbers, and electrostatic precipitators, to control gaseous and particulate matter emissions [2–4]. The most widely used piece of equipment for dedusting, separation, classification, and collection of particles from a gas flow is the cyclone separator [5]. A cyclone separator is an important piece of equipment employed in most air pollution control systems and other applications such as the recovery of inhalable smaller particles for lung delivery [6].

As abatement particulate emission devices, cyclone separators have experienced rapid improvements in terms of geometrical modifications using numerical and experimental investigations for efficient particle separation performance since the early days of Shepherd and Lapple (who conducted the first scientific cyclone study) in 1939. Because of their particle separation capabilities, low cost, simplicity of construction, high efficiency, low maintenance, and adaptability to high-temperature-pressure operating conditions, many researchers prefer to use cyclone separators in various settings for particle classification [5], aerosol sampling [7], pressure fluidization, flue recycling, and the heterogeneous removal of particulate matter (PM10) [8]. The geometric layout of a typical cyclone separator comprises a tangential inlet (through which the dust-gas enters the cyclone), cylinder-on-cone compartment (where the particles spiral downward), hopper (where the particles collect at the bottom into a dust collector), and vortex finder (which permits the centrifugal upward reversal of the clean gas to exit the cyclone), as illustrated in Figure 1. The performance of a cyclone separator significantly depends on its geometric design variables [9].

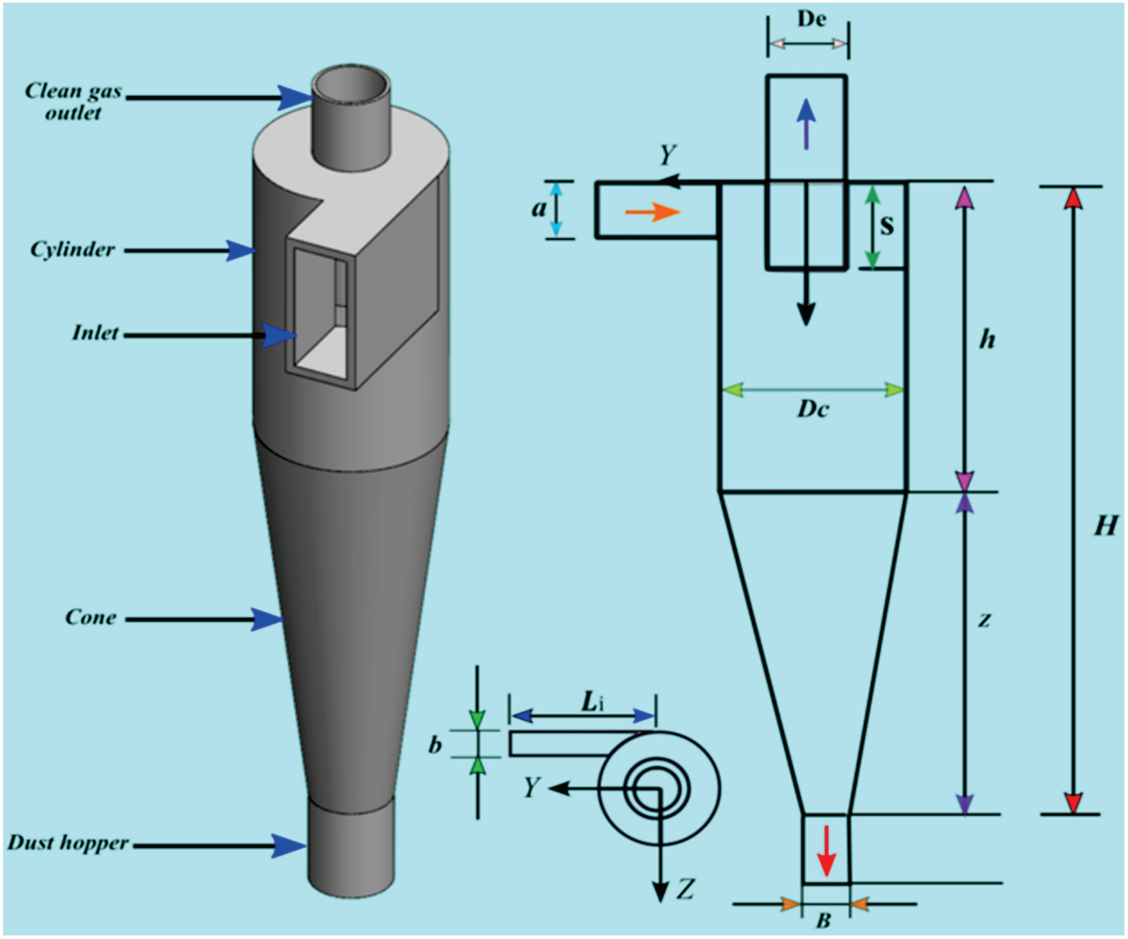

Figure 1. Schematic representation of a cyclone separator with geometric parameters: (a) height of inlet, (b) width of inlet, (De) vortex finder diameter, (Dc) cyclone diameter, (s) vortex finder height, (h) cylinder height, (z) cone height, (H) cyclone height, and (B) diameter of dust outlet.

Consequently, parametric studies on geometric variables, such as the inlet duct width/height, cyclone diameter, vortex height, cylinder height, and other parameters, and their effects on performance parameters, such as pressure drop [10], collection efficiency [11], particle concentration/distribution [10], separation efficiency, and gas flow fields/pattern [9], are usually investigated. These include experimental and numerical studies [2,5,12].

Studies conducted by other researchers have anticipated improvements in the performance of cyclone separators. These studies were conducted by investigating cyclone separators under different temperature and flow conditions [13], configurations or arrangements [14], and applications [15]. Furthermore, new cyclone separator models, coupled with geometric design variations, have been proposed to improve the performance. Modabberifar et al. [16] proposed three new cyclone separator geometries by increasing the vortex length to improve pressure drop and cyclone collection efficiency. It was concluded that cyclones 1D3Dn and 1D2Dn followed 2D2Dn with a marked collection efficiency difference of approximately 20%. Behrang et al. [17] designed and investigated a multi-helical dust cyclone separator using experimental and computational fluid dynamics (CFD) simulations. A novel cyclone separator has been reported for separating fine particles at low velocities. Jebeli et al. [8] optimized the removal efficiency of particulate matter (PM10) using a newly designed cyclone separator with adjustable vortex finder height and inlet angle.

In addition to experimental investigations, advanced numerical and analytical simulation approaches have been employed to predict and validate the performance of cyclone separators in terms of turbulence effects, gas-particle flows, particle distribution, and particle trajectory. These include the Reynolds stress turbulence model (RSM) for turbulent flow simulations [18], hybrid Euler–Lagrange [19], large-eddy simulations (LES) [20], discrete element method (DEM) [21] for particle trajectory tracking, and three-dimensional computational fluid dynamics (CFD) methods [21]. Others have combined several modeling techniques [21,22]. Izadi et al. [23] combined CFD, multi-gene genetic programming (MGGP), design of experiments (DOE), and ten different algorithms to optimize six geometrical variables of the cyclone separator. The optimized designs increased the collection efficiency and decreased the pressure drop by 5.64% and 3.3%–27.5%, respectively. Park et al. [22] modelled the critical diameter of a cyclone separator using CFD and machine learning techniques and showed a significant response in performance prediction.

The literature presents a growing body of evidence on how cyclone separators have gained attention in various engineering and industrial domains. However, on a broader scale, there remains a lack of all-inclusive research on cyclone separators from these perspectives, especially as publications in this field continue to grow. Owing to the diversity of methodologies and applications of cyclone separator research, only quantitative and qualitative data analysis can be useful for defining and evaluating the output level of publications on cyclone separator performance and applications.

Bibliometric analysis is a comprehensive statistical knowledge system that focuses on publication patterns and acknowledges the academic efforts of authors, publishers, and other related documents [24,25]. Using a bibliometric study would significantly improve trend identification and detect growing collaboration patterns, research activities [26], and the volume of publications on cyclone separators as a baseline for future studies [27]. Therefore, researchers need a more prolific literature review tool to measure, analyze, and understand previous experimental findings. Through bibliometric analysis, the new volume of information, topics researched, content information, contributions of scholars, and trends of articles over time in a particular discipline can be effectively analyzed [25,28]. Moreover, a bibliometric study is a suitable scientific mapping technique to assess empirical contributions, knowledge of research themes, conceptual developments, research hotspots, and authors' contributions [25,28] within a particular study field, as it is gradually becoming burdensome and impracticable to remain abreast with everything being published.

This science mapping technique has been employed to determine the evolution of research publications in different thematic fields, including public health and environmen-

tal sustainability-related subjects, such as malaria control [29], air pollution [30], water energy [31], urban sustainability [32], atmospheric pollution by microplastics [33], carbon emissions [34], hepatocellular carcinoma liver-related cancer [35], epidemic and pandemic studies [36], renewable energy [37], acid rain [38], airborne microorganisms [39], and process safety research [40].

Despite the significant traction in cyclone separator performance research in recent years, no bibliometric mapping analysis has been documented to summarize the existing body of literature in the field prior to this review. The distinct themes, unabridged scope, and most prominent scholars in the field, from the past to the present, have not yet been revealed. Therefore, there is a need for a bibliometric mapping overview that combines quantitative and qualitative analyses to provide a framework for understanding past, present, and future studies on the performance and applications of cyclone separators.

1.1. Research Objectives

Against this backdrop, the main objective of this study was to provide a comprehensive overview of the literature in the past two decades in the field of cyclone separator research using bibliometric mapping techniques. The specific objectives were to explicitly focus on contributing countries, sources, influential authors, and thematic evolution in the field. The results of this study serve as a reference for understanding the existing methodologies, tools, applications, and directions of cyclone separator research. Interested target groups can use them to learn about existing tools, methods, and approaches for assessing cyclone separators. Thus, the results would be useful in providing multiple stakeholders with a holistic picture, including researchers, authorities, and practitioners, in identifying key areas that require further exploration in the coming years.

This study contributes to achieving the study objectives by asking the following questions to address this research gap: (1) What are the topic clusters and main themes in cyclone separator research and their level of evolution? (2) What is the focus of the current investigations on the performance of cyclone separators and their applications? (3) Based on the analysis, what is the scope of theoretical and practical research directions towards future research in this field?

1.2. Research Organization

The overall structure of this paper can be summarized in five sections, including an introduction. The materials and methods used for data collection and the analytical tools used are discussed in Section 2. Sections 3 and 4 report the key findings and discuss the main findings to understand the research output in the field from the bibliometric analysis. In addition, the research gaps and an outlook on future research opportunities for the application of cyclone separators are presented in this section. Finally, Section 5 summarizes the findings and concludes the study.

2. Data and Methods

In Figure 2, the main steps taken to analyze the bibliometric dataset are data collection, data transformation and processing, data visualization and analysis, and interpretation using the R bibliometric software package (Biblioshiny version. 3.1) are shown (Figure 2a). Bibliometric protocols are briefly described in this section.

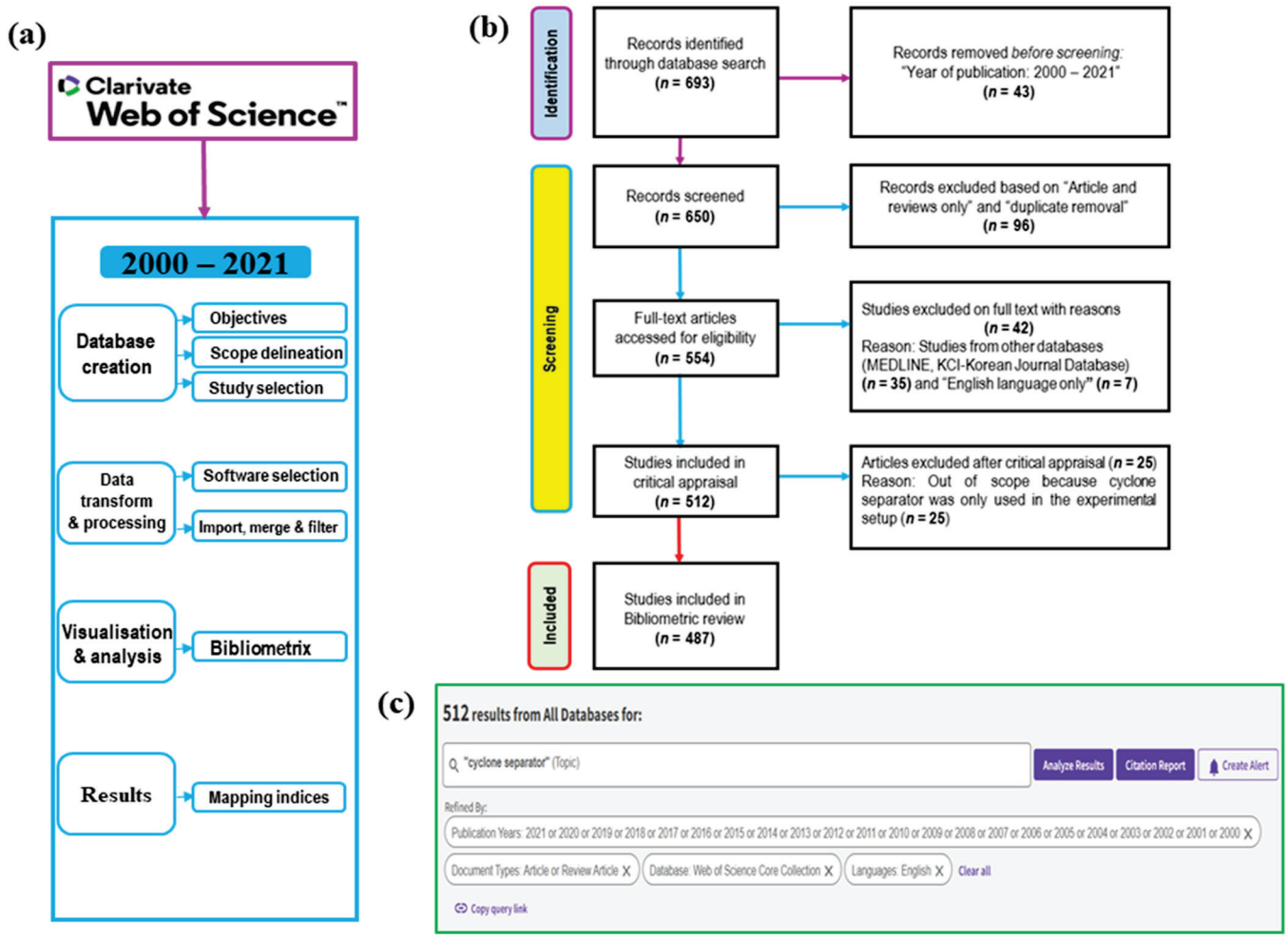

Figure 2. Schematic representation of the method used in this study: (**a**) workflow adopted; (**b**) PRISMA flow diagram showing the screening process; and (**c**) database creation steps.

2.1. Database Creation

To satisfy the study objectives, a search strategy (Table 1) was adopted to capture the terms and applications of the cyclone separator, ranging from geometric and performance variables to simulation terms. Keywords, titles, and abstracts of English-indexed documents ('articles and review articles') in the study field were accessed from the Clarivate Analytics Web of Science Core Collection database (WoSCC) on 22 August 2022. The WoSCC database provides a dynamic collection of peer-reviewed publication indices of science and engineering disciplines and other citation indexes with seamless navigation for high-quality bibliometric data and past literature from interdisciplinary or specific fields [41]. The WoSCC database was chosen because of its extensive content of academic information for bibliometric analysis, ease of exporting extensive data in batches, and record package for old citations [42].

To include data related to the cyclone separator domains, the Boolean and filtering functions were applied to the search scope for the keyword: TOPIC: ("cyclone separator"). The time period was refined to include publications from 2000 to 2021. Exclusion criteria involved the following document types: corrections, news items, editorial materials, and letters [43]. To ensure fidelity and eliminate conflicting documents from other research fields, sources belonging to other research fields such as plant sciences, respiratory systems, and government law were excluded because they may not be relevant to the performance of the cyclone separator and its applications. A preferred reporting item for systematic reviews and meta-analysis (PRISMA) flow diagram was used to gauge the quality of the

bibliometric review (Figure 2b). The search was limited to English language and review articles, resulting in a total of 512 articles (Figure 2c). Subsequently, the articles were narrowed to those related to cyclone separators. This was conducted by carefully reading the titles and abstracts of the literature. In the event that, the abstracts and titles failed to distinguish between relevant and unrelated studies on cyclone separator research, the full article was read independently, and a decision was made on whether to include the article. After reading the abstracts and removing duplicates, screening of articles based on the inclusion criteria resulted in 487 related articles that were used for bibliometric analysis.

Table 1. Database creation strategy.

Screening Criteria	Details
TS *	TS = ("cyclone separator") (*n* = 693)
Period	"2000–2021" (*n* = 650)
Document types	"Articles" and "Review Articles" (*n* = 554)
Database	"Web of Science Core Collection (WoSCC)" (*n* = 519)
Language	"English Language only" (*n* = 512)
Screened articles	cyclone separator related only (*n* = 487)

TS * = Topic field, quotation marks ("") are operators for words that appear in the title source and in combination with Boolean operators.

2.2. Visualization and Analysis of Data

RStudio software (version 4.1.2) with a biblioshiny package for tabulation, visualization, and systematic mapping analysis of the bibliometric indicators was used in this study [25]. Three plain text datasets (Wos1–Wos3) were downloaded independently into the R environment and merged into a single comma-separated values (CSV) file before uploading to the bibliometric R-package (biblioshiny) for further analysis, as outlined previously [44]. The merging of different files has the potential to duplicate the data. As a result, duplicate data were eliminated using the R codes "Combined-Database = mergedDbSources (Wos1, Wos2, Wos3, remove.duplicated = TRUE)". The combined dataset (cyclone.xlsx) was loaded into R bibliometrix (version 3.1) through biblioshiny (interface for R bibliometrix) for a systematic bibliometric workflow analysis (https://www.bibliometrix.org/Biblioshiny.html, accessed on 22 August 2022). The publication structure analysis workflow was obtained, which included annual article publications, most cited articles, top citations per country, most productive authors, most productive countries, most relevant sources, and most relevant keywords. Visualization of the country collaboration network, co-citations, keyword co-occurrence, authors' collaboration, authors' publications over time, and institutional collaboration were performed.

3. Results

3.1. Publication Trends

The number of publications in the study domain was 487 (481 articles = 98.77% and six review articles = 1.23%) from 70 journals and book sources with 518 keywords plus (ID) and 930 author keywords (DE), as shown in Table 2. This implies that the most frequently used keywords by the authors of the cyclone separator studies numbered 930 and a keyword frequency distribution of 518 was in the journal domain. Of the 965 authors, 25 were reported as authors of single-author documents and 940 as multi-author published documents with 1860 appearances.

Table 2. Characteristics of the articles on cyclone separators from 2000 to 2021.

Publication Variables	Article Records
Total number of articles	487
Publication type: articles	481
Publication type: review articles	6
Duration/timespan	2000–2021
Sources (journals, books)	70
Mean years from publication	7.78
Mean citations per publication	18.91
Mean citations per year per article	2.12
References	6252
Keywords plus (ID)	518
Authors' keywords (DE)	930
Authors	965
Author appearances	1860
Authors of single-authored publication	25
Authors of multi-authored publication	940
Single-authored publication	33
Publication per author	0.505
Authors per publication	1.98
Co-authors per publication	3.82
Collaboration index	2.07

The ratio of the total number of documents (487) to the total number of authors (965) was 0.505, and the estimated metric reciprocal ratio of the number of authors per publication (965/487) was 1.98. Additionally, the number of multiple co-authorships per publication was 3.82, whereas the total number of multi-authored publications to the number of multi-authored publications (940/454) yielded a collaborative index of 2.07. These data corroborate the productivity, robust research, and multiple collaborative engagements per publication among authors in the field. Furthermore, the mean number of citations per publication is 18.91, which implies that cyclone separator research/articles are cited in journals approximately 19 times.

The publication trend based on the number of articles provides a perspective on the level of attention paid to research on cyclone separators, as illustrated in Figure 3. A polynomial model fitted to the data generated positive correlation values ($y = (0.01)x^3 + (-55.88)x^2 + (112)x + (-749)$; $R^2 = 0.88$). This indicates that further studies and research publications on this subject will be conducted in the future. These results signify a continuing interest in the use of cyclone separators, and that this study may also have scientific potential. The trend and number of publications grew significantly, as can be seen when grouped into five research periods. The first period corresponded to 2000–2004, during which 39 articles were published.

Publications on cyclone separators attracted a great deal of attention in the second period between 2005 and 2009, while the number of articles increased significantly throughout the third period, from 2010 to 2014, especially in 2013. During the fourth period, which spanned from 2015 to 2019, a spurt in publication was witnessed as 184 articles were published compared to the immediately preceding period (2010–2014). The fifth period corresponds to 2020–2021, with 100 published articles on the apparatus, despite consisting of only two years compared with the other periods. This period provides insight into how cyclone separators will be explored in future research based on the trends and roles revealed. For each of the five research periods, 39, 75, 89, 184, and 100 articles were published, respectively (Figure 3). During these periods, the lowest reported number of published articles was in 2002 ($n = 5$) and the highest was recorded in 2019 ($n = 59$). During this period, the number of publications increased at a rate of 9.49%, but the number of publications gradually increased from 2.8 to 4.5 between 2016 and 2017.

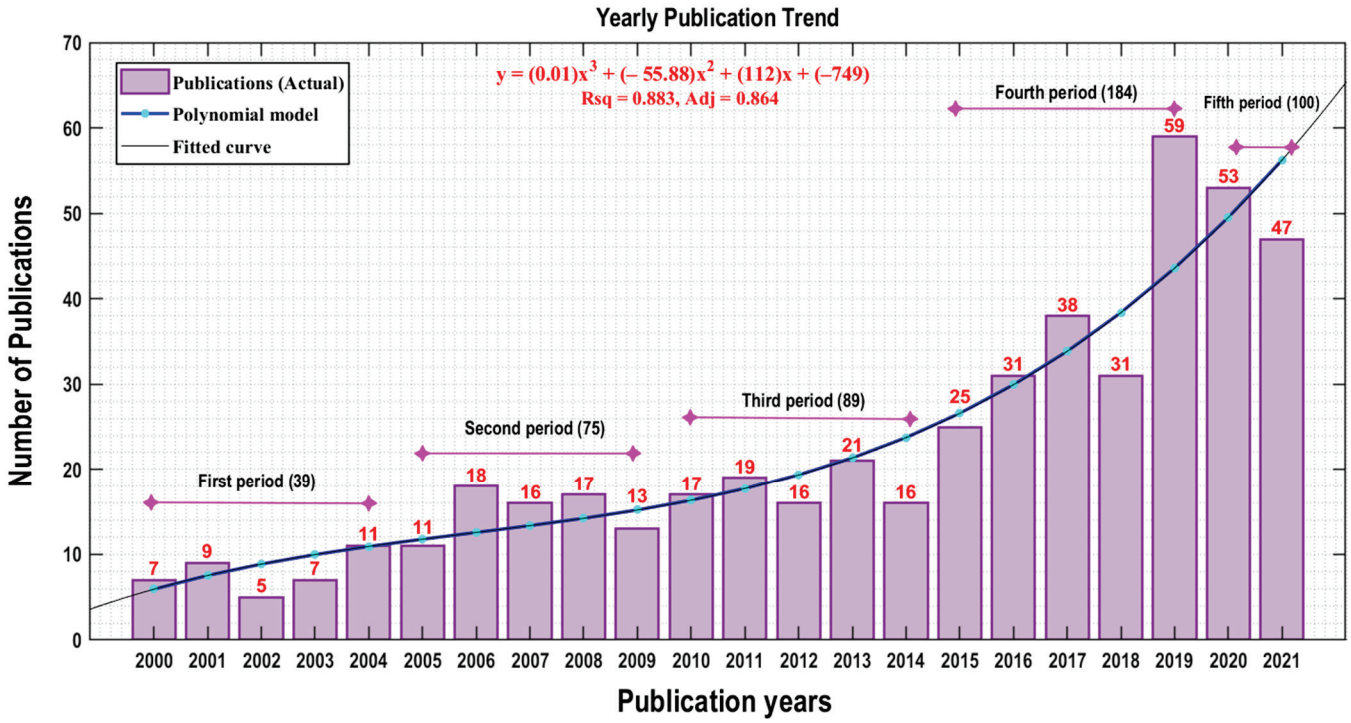

Figure 3. Publication trends on cyclone separators from the present study.

3.2. Contributing Countries

A country-by-country analysis was conducted to elucidate the contributions of the most productive countries in the cyclone separator research domain. It is imperative to recognize the countries that have contributed to the development in the field of research on this type of apparatus. Table 3 shows the 20 leading countries in terms of publications during the study period (2000–2021). During the study period, more than 44 countries contributed articles to this research niche. The People's Republic of China, Iran, India, Brazil, Japan, Republic of Korea, Poland, the USA, Canada, and Turkey emerged as the top 10 countries to have contributed the most articles on the topic, accounting for 79.88% of the overall production. China topped the list with 196 publications, corresponding to 40.25% of the overall records, followed by Iran (n = 42, 8.62%), India (n = 30, 6.16%), Brazil (n = 20, 4.11%), and Japan (n = 19, 3.90%). The People's Republic of Korea (n = 19, 3.90%), Poland (n = 18, 3.70%), the USA (n = 16, 3.29%), Canada (n = 15, 3.08%), and Turkey (n = 14, 2.87%) were added chronologically to make the top 10 most productive countries. Among the top 20 countries in cyclone separator research, only Iran is from the Arabian Peninsula. In addition, none of the African countries were among the top 20 countries. Furthermore, by comparing the number of single- and multi-authored publications, single-authored publications were more prevalent in cyclone separator research, as shown in Table 3. Among the five countries cited as having the highest international publication collaboration on this subject, Australia, Belgium, Norway, Belarus, and Sweden have multiple-country publication ratios (MCPR) of 0.556, 0.500, 0.667, 0.800, and 0.750 (MCPR > 0.5000), respectively.

Regarding rank, the overall number of citations per country has changed slightly. China (n = 2975) and Iran (n = 817) are the two countries that generated the most citations. The total number of publications and citations a nation produces explains its influence in a particular field. Thus, it can be assumed that these countries have significantly affected this niche area. This also reflects the impact of articles on creating changes in practice, discussion, recognition by the scientific community, controversies, and directions for future research on cyclone separators, as the number of citations offers a measure of research quality [45].

Table 3. The top 20 countries in cyclone separator research by citations and records.

Most Productive Countries								Overall Number of Citations per Country			
Rank	**Country**	**Publications**	**Frequency**	**%**	**SCP**	**MCP**	**MCPR**	**Rank**	**Country**	**Total Citations**	**Average Citations**
1	China	196	0.40246	40.25	168	28	0.143	1	China	2975	15.18
2	Iran	42	0.08624	8.62	32	10	0.238	2	Iran	817	19.45
3	India	30	0.0616	6.16	23	7	0.233	3	India	583	19.43
4	Brazil	20	0.04107	4.11	19	1	0.05	4	Brazil	537	26.85
5	Japan	19	0.03901	3.90	16	3	0.158	5	Republic of Korea	412	21.68
6	Republic of Korea	19	0.03901	3.90	17	2	0.105	6	Belgium	407	67.83
7	Poland	18	0.03696	3.70	14	4	0.222	7	Australia	357	39.67
8	USA	16	0.03285	3.29	12	4	0.25	8	Spain	330	66.00
9	Canada	15	0.0308	3.08	9	6	0.4	9	Japan	327	17.21
10	Turkey	14	0.02875	2.87	14	0	0	10	United Kingdom	321	29.18
11	United Kingdom	11	0.02259	2.26	11	0	0	11	Turkey	288	20.57
12	Australia	9	0.01848	1.85	4	5	0.556	12	Poland	251	13.94
13	Belgium	6	0.01232	1.23	3	3	0.5	13	Canada	248	16.53
14	Norway	6	0.01232	1.23	2	4	0.667	14	Norway	221	36.83
15	Singapore	6	0.01232	1.23	4	2	0.333	15	Malaysia	134	134.00
16	Austria	5	0.01027	1.03	3	2	0.4	16	USA	124	7.75
17	Belarus	5	0.01027	1.03	1	4	0.8	17	Sweden	122	30.50
18	France	5	0.01027	1.03	4	1	0.2	18	Singapore	119	19.83
19	Spain	5	0.01027	1.03	5	0	0	19	Netherlands	107	53.50
20	Sweden	4	0.00821	0.82	1	3	0.75	20	France	106	21.20

MCPR: Multiple-country publications ratio; MCP: Multiple-country publications; SCP: Single-country publications.

African countries were not among the top 20 nations with the highest number of article citations, which is noteworthy. This could be due to the low interest in environmental issues and health implications of pollution on the continent. Research interest in this field has been negatively impacted by this. Furthermore, the lack of technological capability in terms of industrial space on the continent could have impacted research on improving cyclone efficiency. Iran was the only country from the Arabian Peninsula to make the list of the top 10 countries with respect to the number of citations per country. These findings are of great concern, as the application of cyclone separators has shown significant mitigation benefits [7,46] for particulate matter removal, and can be adopted to control the colossal level of industrial emissions and resuspended road dust emissions observed in these countries [47,48].

A stark disparity was observed, with approximately 92.61% of research on cyclone separators emerging from developed countries. By contrast, the number of publications in this field is minimal in low-income countries [49]. This reason may not be distant from the reality that most advanced industries, institutions, research laboratories, and leading research centers in the world are found in developed countries [50,51]. Other contributing factors may include research grant opportunities, research and development (R&D) policies, technical progress factors, exchange program opportunities, and availability of state-of-the-art research facilities and environments in developed countries [50,51]

3.3. Research Collaboration and Institutions

Collaborative research involves the coordination and integration of highly interdisciplinary researchers and academic scientists, which forms an essential part of advancing scientific knowledge and increasing efficiency and quality [28]. With the increasing complexities associated with scientific research, collaborative research is gradually gaining incremental significance because of the immense advantages of this research initiative. These advantages may include improved quality research output, research breakthroughs, high-profile journal publications, acquisition of bespoke funding opportunities, and problem-solving techniques [52]. Furthermore, this initiative permits the transfer of technology, promotion of creative thinking, development of young scientists, etc. Collaborative research among scholars increases the number of citations, particularly if an international networking scheme is used to develop research proposals for joint publications [53].

Collaboration between researchers in this niche area spanning different countries is evident in this study. Of the 487 publications extracted from the database of cyclone separators, 451 were contributed by the top 20 leading countries. Single-country publications

numbered 362 (74.33%), while 89 (18.27%) were inter-country publications (Table 3). For example, China generated 168 single-country documents and 28 inter-country publications. Iran recorded 32 publications as single-country research articles with ten multiple-country published articles, and India reported 23 single-country publications and seven inter-country articles. Turkey, the United Kingdom, and Spain made the top 20 leading countries with 14, 11, and 5 publications, respectively. However, they did not produce inter-country publications. Collaboration between leading and African countries is relatively scarce, and most collaboration occurs between developed countries.

A collaborative network map of the cyclone separator research is shown in Figure 4. Line routes connect countries and represent knowledge on a visualization map. The line connections show the collaboration relationships that exist among countries, whereas the line thickness shows the link strength/frequency of the collaboration. There are 60 collaborations among various countries worldwide, with a maximum of 24 collaborations. Four countries stand out as the top collaborating countries: China, the USA, India, and Iran. Among the 12 lines, China had the highest collaborative strength with the other countries. Intense collaboration occurred with Australia, Japan, and the United States (Figure 4). The USA (with eight connection lines) had the second highest collaborative strength, followed by India and Iran, with seven connection lines each. Canada is the fifth largest country with four connection lines of collaboration. The inset shows the collaboration network between the top 10 countries (Figure 4). China and Australia had the highest collaboration network with 15 collaborations, followed by Iran and the United States with 9 collaborations, China and Japan with 6 collaborations, Sweden and Belarus with 6 collaborations, and the United States and Egypt with 6 collaborations.

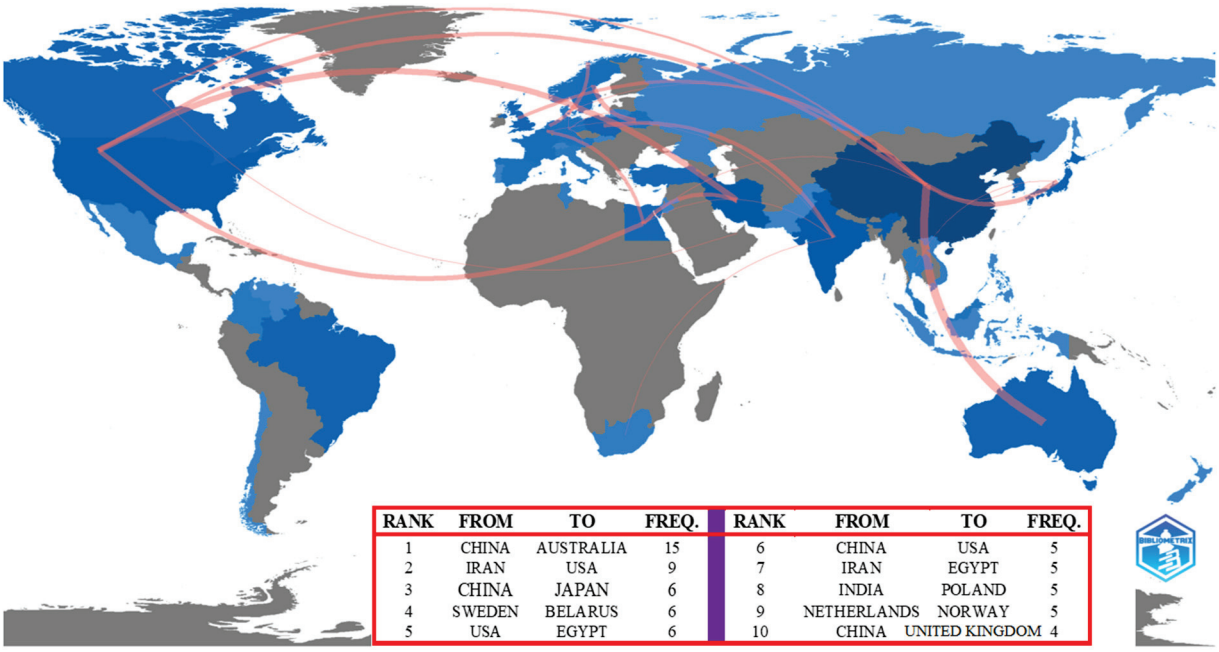

RANK	FROM	TO	FREQ.	RANK	FROM	TO	FREQ.
1	CHINA	AUSTRALIA	15	6	CHINA	USA	5
2	IRAN	USA	9	7	IRAN	EGYPT	5
3	CHINA	JAPAN	6	8	INDIA	POLAND	5
4	SWEDEN	BELARUS	6	9	NETHERLANDS	NORWAY	5
5	USA	EGYPT	6	10	CHINA	UNITED KINGDOM	4

Figure 4. Country collaboration network map on cyclone separator literature around the world (blue color indicates whether a country has publications in the field; dark blue indicates more prolific publishing countries; gray indicates no publication; the red line routes connecting countries indicate the frequency of collaboration and the line thickness represents the strength of collaboration among the countries).

Figure 5 presents the top 20 institutions affiliated with authors who publish articles in the field of cyclone separators (in terms of total publications) from a list of 350 entries. Research institutions play a significant role in the dissemination and support of scientific knowledge. Therefore, it is vital to acknowledge the institutions that make intensive

contributions to cyclone separator research. The authors affiliated with the China University of Petroleum published the most articles in this field (n = 59). This was followed by East China University of Science and Technology (n = 18), Hiroshima University (n = 18), Lanzhou University (n = 14), and Beijing Key Laboratory for Processes, fluid filtration, and separation (n = 13), ranking as the top five. Together, they represent 45.86% of the top 20 institutions in cyclone separator research. At the institutional level, it was observed that no African institution made it into the list of the top 20 institutions. Furthermore, the authors observed a significant dominance of Chinese institutions, corroborating the findings with respect to the bibliometric indices reported in Table 3 and Figure 4, respectively.

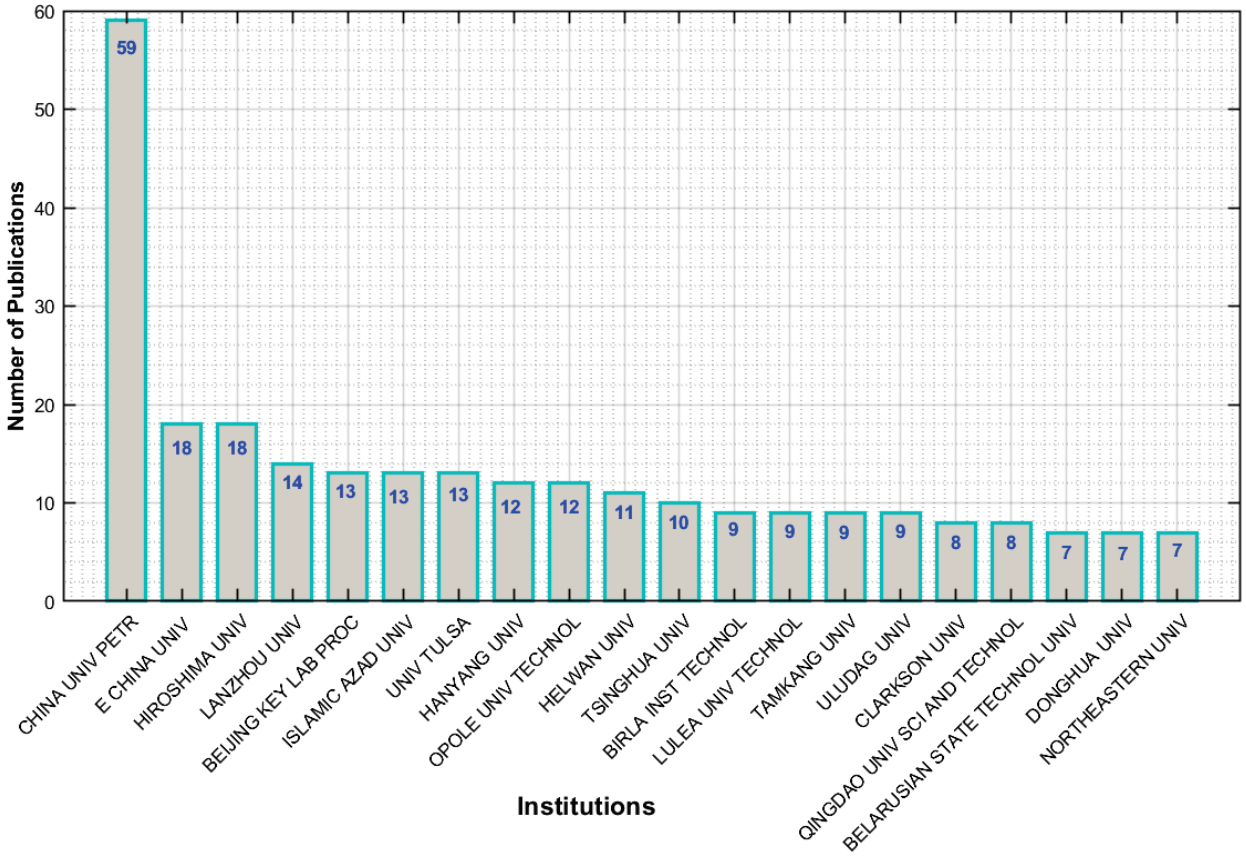

Figure 5. Most contributing institutions.

3.4. Keywords Analysis

The frequency of words in a research domain serves as a source of information on the patterns and development of knowledge structures in a particular research niche [54]. Additionally, keyword analysis is important in scientific publications as a tool for bibliographic indexing, identifying hot topics, and enabling authors to expand their publication outlook to other related concepts [55]. This is one of the main reasons editors of journals require authors to submit five to seven keywords per manuscript for peer review purposes.

A semantic analysis of keywords related to the most relevant themes of cyclone separator research was conducted. A total of 930 author keywords (DE) and 518 keywords plus (ID) were identified in 487 articles (Supplementary Table S1). Authentic indicators of the subject areas were assumed to be the authors' keywords. From the table, 'cyclone separator' was the most frequently used keyword, with 95 occurrences (10%), which indicates that this word alone is used as a termed concept in the literature. The three most frequently used keywords were 'pressure drop' (92 occurrences), 'cyclone' (84 occurrences), and 'separation efficiency' (67 occurrences). Furthermore, 'CFD' (n = 64), 'collection efficiency' (n = 60), 'computational fluid dynamics' (n = 57), 'flow-field' (n = 33), 'numerical-

simulation' (n = 27 and 'collection' (n = 23) followed chronologically in the top 10 keywords. In contrast to the most relevant author keywords, performance, efficiency, computational fluid dynamics (CFD), pressure drop, flow, simulation, collection efficiency, design, gas, and numerical simulations were used. An important finding from the analysis is that there was no unanimity in the conceptualization of cyclone separators, and that a lack of standardized meaning compels authors to use the terms cyclone separator (n = 95), cyclone (n = 84), cyclone separators (n = 16), and cyclones (n = 14) interchangeably.

Furthermore, through a timeline view analysis, the authors explored trends in cyclone separator research to understand their evolution over time. Different timeline intervals were evaluated in the ranges 2000–2007, 2008–2013, 2014–2020, and 2021–2021 (Figure 6). Between 2000 and 2007, keywords such as particle separation, CFD, cyclone, cyclone separator, efficiency, pressure drop, and separation efficiency were the most frequently used for cyclone separator articles. 'Pressure drop' appeared most frequently, 185 times in total; 'separation efficiency' appeared 70 times, ranking second; 'cyclone separator' appeared 68 times, ranking third; and 'cyclone' also appeared more frequently. From 2008 to 2013, terms such as collection efficiency and numerical simulation emerged in succession. A pressure drop was recorded 112 times during this period. In subsequent years, the discrete phase model, computational fluid dynamics, and RSM were mentioned more frequently during 2014–2020. However, the word cyclone became a hot topic in 2018. Cyclone separators became a hot research topic in 2020, with 258 appearances. In recent years (2021), through the analysis of hot issue keywords and the time evolution process, it has been found that numerical simulation, cyclone, and pressure drop have become a hot research issue, and there is a greater inclination to optimize the performance of cyclone separators through numerical simulation. Significantly, increasing attention has been paid to studying the cyclone separator performance criteria through variations in geometric parameters during this period.

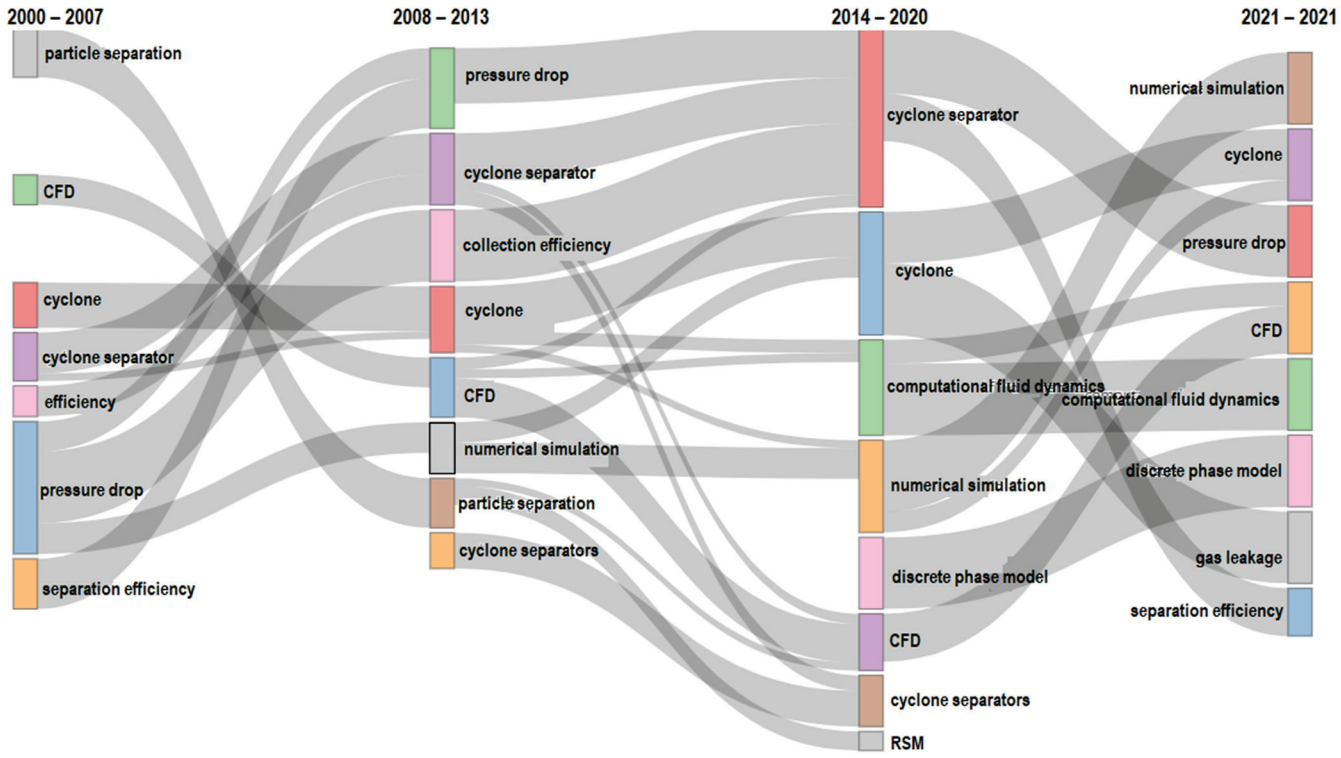

Figure 6. Thematic evolution of cyclone separator research at different time intervals.

Furthermore, this period saw the development of different methods for evaluating cyclone separators by researchers in the field, such as introducing different models, numerical simulations, and many more, depending on the application of cyclone separators [7,56,57]. The detection of fluid flow patterns and characteristics inside the cyclone separator serves as the focal point of research, as keywords such as numerical simulation, computational fluid dynamics (CFD), and discrete phase models are frequently mentioned as techniques for evaluating cyclone separator performance. This could be why the flow pattern and performance of cyclone separators have become hot research topics and have appeared in most publications. Consequently, increasing attention has been paid to numerical simulations and other computational fluid dynamics (CFD) techniques to the study flow behavior and performance using different geometric design models. The outcome of future research on this topic will revolve around a combination of computational fluid dynamics and numerical simulation algorithms to evaluate the performance of cyclone separators.

3.5. Contribution of Journals

The 487 publications analyzed were dispersed across 70 journals. Figure 7 presents a list of the top journals that publish cyclone separator research. The top 20 journals published 410 articles, representing 84.19% of the total publications. The publications on cyclone separators are dominated by chemical engineering journals (150 publications). The Thermal Science journal is the only non-chemical journal on this list. Powder Technology, with a Clarivate Analytics 2021 impact factor (IF) of 5.64, tops the list as the most productive platform with the highest number of articles on cyclone separators (n = 123), followed by separation and purification technology (n = 71) with a 2021 journal impact factor of 9.136, Chemical Engineering & Technology (n = 28, 2021IF = 2.215), Advanced Powder Technology (n = 26, 2021IF = 4.969), and Chemical Engineering Research and Design (n = 26, 2021IF = 4.119) ranked fifth.

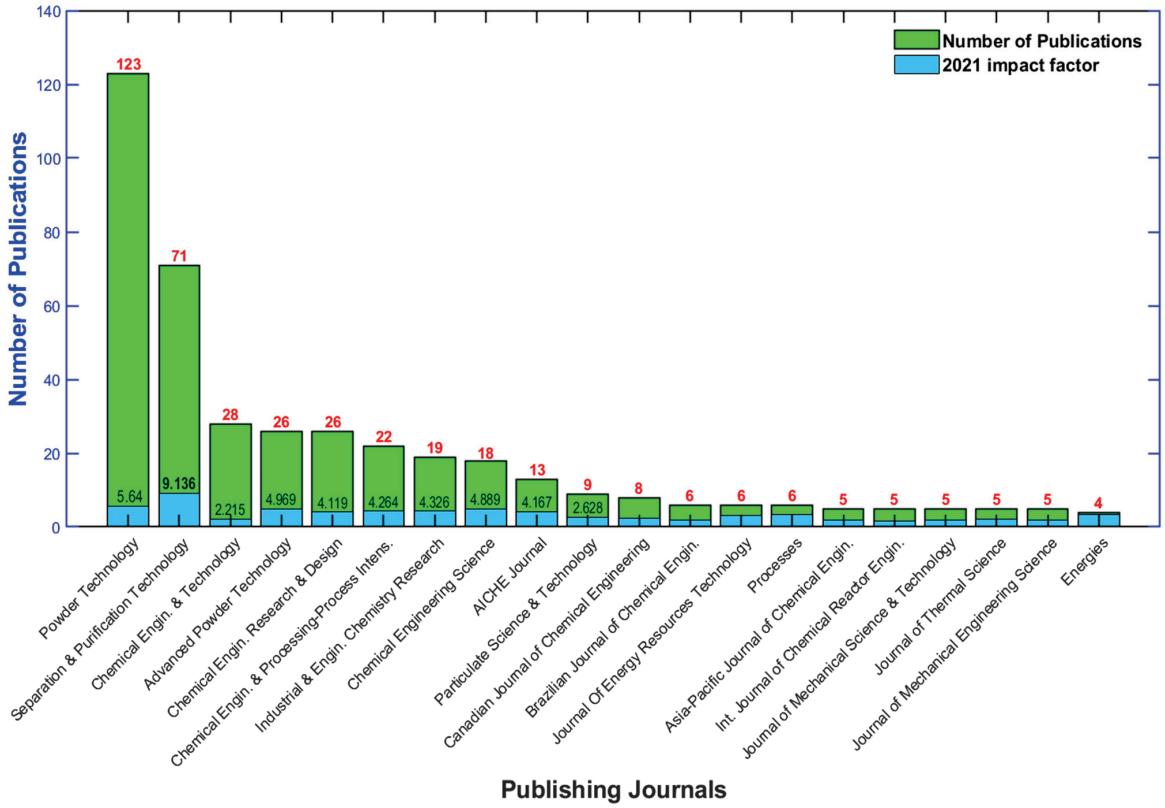

Figure 7. The top-cited journals and their 2021 impact factor (IF) according to Clarivate Analytics' journal citation report.

As shown in Figure 7, the Separation and Purification Technology journal recorded the highest impact factor in 2021 among the 20 top journals listed (9.136). Seven other journals had an impact factor between 4.00 and 5.70, namely, Powder Technology (5.64), Advanced Powder Technology (4.969), Chemical Engineering Science (4.889), Industrial & Engineering Chemistry Research (4.326), Chemical Engineering and Processing-Process Intensification (4.264), AICHE Journal (4.167), and Chemical Engineering Research and design (4.119). It is worth noting that seven Elsevier journals with considerably high impact factors dominated the top 20 journals that reported studies on cyclone separators. The top ten most-cited publications citing cyclone separator research were powder technology (n = 1943), separation and purification technology (n = 851), Chemical Engineering Science (n = 578), Journal of Aerosol Science (n = 519), Minerals Engineering (n = 509), Chemical Engineering Research and Design (n = 406), AIChE Journal (n = 390), and Chemical Engineering and Processing (n = 343). Further scrutiny of the publishers of the journals among the 20 top journals reveals that Elsevier and Wiley Online Library publishers generated 59.75% and 8.42% of the articles on this topic, respectively. Eight other publishers published the following documents: AIChE Journal, ACS publications, Sage, Taylor and Francis, De Gruyter, ASME Digital Collection, MDPI, and Springer, amounting to 16.02% of the total articles from the top journals in the field.

3.6. Most Influential Authors

In total, 965 authors contributed to the total number of publications during the study period. This section analyzes the most prolific authors in terms of the number of publications, output, citations, and production over time. Research achieves its purpose only when it is comprehensively shared and when an author's ideas fall within the scope of the audience/stakeholder's interest based on its findings and well-defined production results. However, in recent years, the reader's interest has been aroused by the number of views or downloads, and the number of citations an article receives. The 20 most distinguished authors are listed in Table 4. Wang J led the list with 16 publications since 2005, followed by Elsayed K and Sun G with 14 articles. Yoshida H and Fukui K authored 12 and 11 articles in the fourth and fifth positions, respectively. Furthermore, among the top 20 authors, seven authors published ten or more articles. This was followed by Wang J (n = 16), Elsayed K (n = 14), and Wei Y (n = 10) (Table 4). It is worth noting that out of the 20 top authors, 16 had 100 or more citations.

Table 4. The most prolific authors in terms of number of publications and the total number of citations.

Rank	Author(s)	NP	h_Index	g_Index	m_Index	TC	PY_Start
1	Elsayed K.	14	12	14	0.923	654	2010
2	Sun G.	14	7	14	0.412	203	2006
3	Wang J.	16	7	13	0.389	191	2005
4	Yoshida H.	12	8	12	0.364	242	2001
5	Fukui K.	11	8	11	0.364	213	2001
6	Zhao B.	11	9	11	0.474	465	2004
7	Wei Y.	10	5	8	0.714	69	2016
8	Wang B.	9	6	9	0.5	306	2011
9	Brar L.	8	7	8	0.875	249	2015
10	Misiulia D.	8	7	8	0.875	178	2015
11	Wasilewski M.	8	6	8	0.857	166	2016
12	Ahmadi G.	7	4	7	0.667	102	2017
13	Andersson A.	7	7	7	0.875	171	2015
14	Avci A.	7	6	7	0.5	90	2011
15	Chen J.	7	5	7	0.313	174	2007
16	Karagoz I.	7	6	7	0.4	142	2008
17	Liu Z.	7	5	7	0.294	71	2006
18	Safikhani H.	7	6	7	0.5	257	2011
19	Wang D.	7	2	4	0.5	25	2019
20	Zhang M.	7	5	7	0.278	128	2005

TC—total citations; NP—number of publications; PY_Start—first publication year of author's.

Author citation analysis is another important parameter. The citation index of the authors shows that Elsayed K has the most citations, with 654 citations, followed by Zhao B with 465 citations, and Wang B in the third position with 306 citations. In terms of the number of citations and publications offered, Elsayed K was the most influential author in the field of cyclone separator research (h-index: 12, g-index: 14), despite being published only in 2010. To understand the research frontiers in a field, the authors delineated another significant index that measures the number of citations and productivity over time. The authors' productivity over time was based on the total number of articles and yearly citations generated (see Supplementary Figure S1 for details). The blue nodes (legend) reflect the number of articles published in a calendar year, whereas the thread connectors (shown in red) linking the nodes signify the consistency of an author's research output on a topic over a specific time span. The node size indicates the number of papers published in relation to a particular year. The depth of the node color reflects the number of citations; the darker the node color, the more citations there are per year.

From the results, in the past 11 years between 2010 and 2021, Elsayed K, Sun G, and Zhao B have been consistent. The authors also deduced that the 16 leading authors from the list were published in 2020. In combination, the h-index, total number of citations, and total number of publications showed that Chinese authors dominated the list. On the other hand, authors from other parts of the world, such as Africa and the Arabian Peninsula, did not make the list of the top 20 most productive authors.

3.7. Most Cited Documents

Research citations are progressively utilized as indicators to monitor research performance and within many aspects of the research structure [58]. They are often regarded as potential indicators that reflect a combination of high-quality and impactful research results [58]. Furthermore, a scientific publication's impact on a topic indicates the number of citations generated by that publication [59]. For example, the higher the number of citations, the more significant is the impact of research output on the subject, which can provide constructive feedback for a long time. Therefore, it takes time for publications to attract more citations.

This section analyzes the most cited global publications on cyclone separators. The top 20 most-cited studies on cyclone separators are presented in Table 5. The total number of citations is related to the total number of citations received within the same collection, or from another document in the same collection. By contrast, the total number of citations per year refers to the total number of publication citations divided by the number of years in which the document was cited. The degree to which others cite a document in a particular field reflects its impact on research terrain. Research articles may serve as a source of significant methodology, great foundation, and valuable discussion for empirically driven research by other researchers in the future [60]. The most cited publication or article was placed first and the least cited was placed last.

An experimental study by Cortés et al. (2007) obtained the highest number of citations, with 236 and 15 citations per year, respectively. The research publications of Slack et al. (2000) and Chu et al. (2011) had 192 and 167 citations, respectively, and were ranked second and third, respectively. Elsayed K had three articles in the top 20 lists of the most-cited documents. Chemical engineering journals were found to have reported 50% of the top 20 most cited publications, while powder technology had 35% of publications that made the list of the top 20 in this field. This reflects the plethora of journal types for authors publishing research on this subject. Although articles in the past decade have accrued citations, those in the last two decades have dominated the top 20 most-cited publications.

Table 5. Publications with the most citations on cyclone separator literature (Top 20).

First Author	Pub. Year	Journal Name	DOI	Total Citations	TC per Year	Normalized TC
Cortes C.	2007	Prog. Energ. Combust.	10.1016/j.pecs.2007.02.001	236	14.75	6.2457
Slack M.D.	2000	Chem. Eng. Res. Des.	10.1205/026387600528373	192	8.3478	3.0078
Chu K.W.	2011	Chem. Eng. Sci.	10.1016/j.ces.2010.11.026	167	13.9167	4.4415
Elsayed K.	2010	Chem. Eng. Sci.	10.1016/j.ces.2010.08.042	150	11.5385	4.6763
Chuah T.G.	2006	Powder Technol.	10.1016/j.powtec.2005.12.010	135	7.9412	3.7565
Gimbun J.	2005	Chem. Eng. Process.	10.1016/j.cep.2004.03.005	134	7.4444	2.8646
Bernado S.	2006	Powder Technol.	10.1016/j.powtec.2005.11.007	134	7.8824	3.7287
Zhao B.	2006	Chem. Eng. Res. Des.	10.1205/cherd06040	131	7.7059	3.6452
Raoufi A.	2008	Chem. Eng. Process.	10.1016/j.cep.2007.08.004	121	8.0667	4.1987
Hu L.Y.	2005	AIChE J.	10.1002/aic.10354	100	5.5556	2.1378
Derksen J.J.	2003	AIChE J.	10.1002/aic.690490603	92	4.6	2.1801
Elsayed K.	2012	Powder Technol.	10.1016/j.powtec.2011.10.015	90	8.1818	4.2857
Chen J.Y.	2007	Powder Technol.	10.1016/j.powtec.2006.09.014	86	5.375	2.276
Xiang R.B.	2005	Chem. Eng. Process.	10.1016/j.cep.2004.09.006	82	4.5556	1.753
Kaya F.	2008	Curr. Sci. India	http:www.jstor.org/stable/24100235	79	5.2667	2.7413
Peng W.	2002	Powder Technol.	10.1016/S0032-5910(02)00148-1	78	3.7143	2.766
Elsayed K.	2011	Sol. Energy	10.1016/j.powtec.2011.05.002	77	6.4167	2.0479
Zhao B.T.	2004	Powder Technol.	10.1016/j.powtec.2004.06.001	76	4	3.4545
Brar L.S.	2015	Powder Technol.	10.1016/j.powtec.2015.09.003	74	9.25	3.0515
Hoffmann A.C.	2001	AIChE J.	10.1002/aic.690471109	69	3.1364	3.4888

TC—total citations.

4. Discussion

4.1. Summary of the Findings

Bibliometric analysis is increasingly used to review themes, trends, and progress in several fields and areas of research. This study contributes to the literature by presenting valuable findings that can enhance collaboration among researchers from diverse areas of interest in researching cyclone separators. This study reveals that cyclone separators have received significant attention because they are widely employed in different separation process domains. Publication trends have evolved and have continuously increased since the early 2000s, and publications and citations have shown a spurt in productivity. Furthermore, the pattern of single-author publications outstripped that of multiple author publications.

In most cases, the keyword analysis results revealed the research interests of cyclone separators. An analysis of the keywords indicated that research on cyclone separators has sprung up within the milieu of experimental and numerical investigations to improve its performance by targeting reduced pressure drop, collection, and separation efficiencies. Furthermore, investigations by varying the geometric dimensions and operational parameters, such as the vortex finder length, inlet velocity, inlet height, cylinder height, and body diameter (Figure 1), have provided researchers with an unlimited number of options to improve the separation efficiency, collection efficiency, and particle classification or performance of cyclone separators. Research on cyclone separators has been enhanced by the introduction of multiple numerical simulation models, semi-empirical models, computational fluid dynamics techniques, and other optimization methods [23], including the Reynolds stress model, RNG-k-ε model, standard k-ε model, large eddy simulation (LES) [61], discrete phase model (DPM), and discrete random walk (DRW), to predict and improve turbulence flow patterns, velocity fluctuations, and particle trajectories. This is due to the complex vortex flow regimes, inherent inner flow characteristics, and other performance parameter optimization failures under specific eddy-viscosity turbulence approaches and varying experimental conditions [62].

The country distribution of authors of cyclone separator-based research shows that China contributed markedly and dominated all bibliometric records on cyclone separators, which may be an indication of the level of understanding of Chinese researchers in the design and implementation of cyclone separators in process safety [40], particulate matter control [63], heavy metal collection owing to the wide variety of China's landscape and

climate, large-scale industries [64], and engineering research concerns. For example, Du et al. [63] developed a test system to evaluate the flow, separation, and load characteristic performance of three commonly used cyclone separators in China. This could also be attributed to the country's experienced and young researchers, overwhelming government support, regional collaborative networks, concern for commercial enterprises, and other institutional sponsored support [26,40].

Analysis of the country collaboration map revealed a significant number of publications resulting from collaborative research between other regions of the world, which agrees with the findings of Ojemaye et al. [50]. Furthermore, it is encouraging that most publications from countries and journal sources receive more attention regarding the number of citations and referrals. However, less international collaboration (MCPR > 0.5000) has been observed among researchers in this field. This shows that the knowledge exchange across geographic boundaries is limited. Countries specializing in cyclone separators and their applications can exchange ideas and/or collaborate.

Bibliometric data regarding the most productive journal publishing cyclone separator research revealed some exciting results. Powder Technology and Chemical Engineering journals remain the top journals publishing cyclone separator research. The differing quality of journal publications on cyclone separator research indicates its level of scrutiny and physical significance. This shows that the research niche has matured across different research horizons. Data analysis in terms of productivity showed that Elsayed K was the most influential author to have contributed to this field.

The number of citations generated by Cortés et al. (2007) can be attributed to the critical development of an algebraic model for predicting the tangential velocity and pressure drop inside an inverse-flow cyclone separator. Furthermore, the fact that their review presented a classical approach in determining the cyclone separator 'natural' length, which led to secondary flows and instability discovery, may account for the significant number of citations this publication accrued. This multifaceted bibliometric review of the literature presents some gaps as substantial space for the development of cyclone separator research, which should receive additional attention from researchers in the future.

It is vital to mention that cyclone separator research has received massive attention in multi-disciplinary, high-impact factor, chemical, and environmental engineering journals dedicated to publishing and disseminating high-quality and novel methodological research. The large number of articles on cyclone separator research in high-impact journals confirms the attention given to this field. This indicates that premier journals are receptive to publishing research in cyclone separators. Furthermore, these premier journals provide a forum for researchers to retrieve, read, and cite a significant amount of global information. This is also important for cyclone separator researchers as a reliable reference source for future research.

4.2. Limitations

This study has a few methodological limitations. First, the results of this study stem from the information retrieved from the WoSCC database, and only documents in the English language were selected. The omission of documents from the study written in other languages might have led to bias in the analysis of the results. Therefore, future studies should consider the adding non-English publications, meeting proceedings, media, and other bibliometric databases to make room for articles that might significantly impact the bibliometric outcomes of this subject matter. A blend of different bibliometric analysis software is also recommended to examine citation correlations and calculate TCLS, total global citation score (TGCS) and other bibliometric metrics. Second, this study considered datasets from 2000 to 2021 (early published papers of relevance), and backdated datasets should be considered in future studies on this subject matter. Despite these limitations, this study's distinct value and significance is that no bibliometric analysis has been conducted in the literature. The authors hope that this study will provide directions for researchers

in the field to identify hotspots and other application avenues to enhance collaboration in cyclone separator research and solve the challenges that confront us.

4.3. Suggestions for Future Research

The following section presents several potential scientific directions for future research on cyclone separators. The present study shows that, in addition to particle recovery, cyclone separator performance can be improved and used for other applications, including road dust particle recovery.

4.3.1. Evaluation of the Performance of the Cyclone Separator Using Road Dust Samples

Research evaluating the cyclone separator performance in relation to road dust particles remains in its infancy. Few studies related to the sampling of road dust in cyclone separator research include the performance evaluation of the cyclone separator for a high-volume sampling of aerosols using the guiding vane angle at 1000 L/min sampling flow rate of road dust [7], or the direct sampling and characterization of resuspended road dust to determine the composition of urban PM10 [46] collected at 0.5, above the road surface. In recent times, road dust particles due to vehicular-induced resuspension and other traffic-related emissions [65] have become an urgent concern, as an estimated 90% of the global population is reported to be exposed to PM2.5 (less than 2.5 μm) in 2019 [66], and this was found to exceed the World Health Organization's (WHO) recommended air quality guidelines (AQG) of 10 μg m^{-3}.

In addition, road dust is a potential habitat and reservoir for viral particles from roads, pathogenic microbes, and other infectious diseases [33], the roles of which in the spread of epidemiology and viral particles have been scarcely explored. Yilbas et al. [67] reported on human saliva cloaking faster (0.05 s) and infusion with environmental dust particles, which has a high propensity for the spread of viruses such as SARS-CoV-2 in dusty environmental settings. On the other hand, Magnano et al. [68] also demonstrated that percutaneous metals in road dust powder could penetrate damaged human skin at an accelerated rate and diffuse further into the bloodstream. An appropriate application of cyclone separator models to sample and collect worrisome fractions of road dust is worth exhaustive investigation in light of the colossal human risk exposures of resuspended road dust. Road dust trapping technologies must address the shortcomings of the existing particulate matter trapping technologies, including the low separation efficiency of fine particles. The authors proposed that novel gas cyclone separators should be developed to refine and match different sizes of road dust particle trapping. The removal efficiency and flow characteristics of road dust can first be investigated using numerical simulation methods, and the separation efficiency of different road dust particles can then be experimentally and numerically studied. A recent study by Wang et al. [57] demonstrated excellent applicability for the separation of fine particles using a gas cyclone–liquid jet separator. This is currently being investigated by our research group by using cyclone separators. Collaborative research on cyclone separators that consider the harmful emitted particles is essential. From an environmental perspective, human activities using new technologies create hazardous gases, toxic chemicals, and dangerous particles [69]. Unfortunately, these emitted particles penetrate the deepest regions of the human lung and have adverse consequences [70]. Therefore, these observations are why improving the efficiency of cyclone separator collection and other performance parameters have been the main objectives among researchers in the field to separate particles with diameters of 0.1 μm or more [71].

4.3.2. The Performance of Cyclone Separators under Varying Particle Properties

Most researchers in this field have focused on improving the separation performance of cyclone separators by evaluating the effects of particle agglomeration and dust concentration on their overall separation efficiency. Paiva et al. [72] developed a more realistic model to improve the collection efficiency of the sub-micro particles. The model numerically optimized the particles and achieved higher collection efficiency. They concluded that

particle agglomeration inside a turbulent cyclone flow seems to justify the higher than predicted collection efficiencies observed for smaller particles in a cyclone separator.

The influence of the attrition and agglomeration of dust particles on the separation efficiency of a Stairmand cyclone was experimentally investigated in ref. [73], and the agglomeration of fine particles was observed at the initial stages. Ahuja et al. [74] and Kim et al. [75] reported that the collection efficiency of fine particles increases substantially with humidity. However, few studies have investigated the effects of dust particle properties, such as particle humidity, particle temperature, and classification, through experimental and numerical simulations.

Cyclone separators have been used in various methods and applications for dust and particle recoveries. However, none of these methods completely solve the problem of road dust sampling. Road dust and its PM10 particles (with diameters less than 10 μm) are difficult to distinguish, and their classification and dust loading concentrations are complex [76]. Furthermore, road dust resuspension is influenced by relative humidity, wind, and vehicle speed [76,77]. The advantages of cyclone separators include the development of adjustable models and improved performance to allow total suspended particle sampling. However, it has been established that as the dust concentration increases, the overall separation efficiency of the cyclone separators increases [78]. The improvement in performance with increased dust loading varies with cyclone separator geometry and inlet velocity [79]. As such, in recovering road dust using cyclone separators, it is important to thoroughly investigate the impact of increased particle humidity on particle size distribution, collection efficiency, and grade efficiency.

5. Conclusions

In this study, 487 publications indexed in the WoSCC database from 2000 to 2021 were retrieved. A bibliometric analysis was conducted to track the publication progress path and research hotspots and provide research directions for cyclone separator research. The most productive authors, influential publications, institutional affiliations, journals, and keywords were identified and discussed. In addition, the most-cited documents over time and keyword dynamics were analyzed to understand the historical evolution of the most recent development. Since 2000, articles on cyclone separator research have seen a spurt at a significant rate, and it is envisaged that the number of publications will increase in the coming years. Visualizations of publication trends, collaboration networks of publications, journal networks, country and institution networks, and keywords of focus topics were provided. Thus, bibliometric analysis can be used to gain insight into the development of cyclone separators. The results can contribute to the understanding of the overall structure and progression of cyclone separators and help prospective researchers identify impactful scholars and institutions for international collaboration. Countries in Africa and the Arabian Peninsula have contributed only a small amount to this field. The authors hope that this study will serve as a driving force to encourage researchers in these regions to contribute to cyclone separator research and collaborate with those in developed regions to expand methods of controlling dust particle emissions.

Supplementary Materials: The following supporting information can be downloaded at: https://www.mdpi.com/article/10.3390/su142214753/s1, Table S1: Most Frequent words, Figure S1: Top-Authors' Production over Time.

Author Contributions: Conceptualization, F.J.A. and P.K.A.; methodology, F.J.A., G.T. and P.K.A.; validation, G.T. and P.O.A.; formal analysis, F.J.A., P.K.A., J.V.F. and I.O.O.; investigation, G.T., and I.O.O.; resources, G.T. and I.O.O.; data curation, F.J.A. and P.K.A.; writing—original draft preparation, F.J.A., P.K.A., J.V.F. and P.O.A.; writing—review and editing, F.J.A., J.V.F., I.O.O., S.L. and P.O.A.; supervision, G.T. All authors have read and agreed to the published version of the manuscript.

Funding: This study was funded by the Ministry of Science of Technology (MOST) Power Economy 2020 Project (SQ2020YFF0418394).

Institutional Review Board Statement: Not applicable.

Informed Consent Statement: Not applicable.

Data Availability Statement: Not applicable.

Acknowledgments: The authors acknowledge the Suizhou-WUT Industry Research Institute, Hubei Key Laboratory of Advanced Technology for Automotive Components, Hubei Collaborative Innovation Center for Automotive Components Technology, Wuhan University of Technology, Wuhan 430070, China.

Conflicts of Interest: The authors declare no conflict of interest.

References

1. Kanojiya, M.T.; Mandavgade, N.; Kalbande, V.; Padole, C. Design and fabrication of cyclone dust collector for industrial Application. *Mater. Today Proc.* **2022**, *49*, 378–382. [CrossRef]
2. Sonawane, C.R.; Dhanorkar, M.; Mishra, I.; Kirdat, A.; Bhatwadekar, S.; Sawant, R.; Pandey, A. Numerical simulation of hydro-cyclone separator used for separation of highly dense suspended particulate matter. *Mater. Today Proc.* **2022**, *59*, 85–92. [CrossRef]
3. Bächler, P.; Szabadi, J.; Meyer, J.; Dittler, A. Simultaneous measurement of spatially resolved particle emissions in a pilot plant scale baghouse filter applying distributed low-cost particulate matter sensors. *J. Aerosol Sci.* **2020**, *150*, 105644. [CrossRef]
4. Yang, J.; Tang, T.; Jiang, Y.; Karavalakis, G.; Durbin, T.D.; Wayne Miller, J.; Cocker, D.R.; Johnson, K.C. Controlling emissions from an ocean-going container vessel with a wet scrubber system. *Fuel* **2021**, *304*, 121323. [CrossRef]
5. Erman Caliskan, M.; Karagoz, I.; Avci, A.; Surmen, A. An experimental investigation into the particle classification capability of a novel cyclone separator. *Sep. Purif. Technol.* **2019**, *209*, 908–913. [CrossRef]
6. Singh, A.; Rana, V. Exploration of modified cyclone separator for the enhanced recovery of inhalable spray dried cubosomal powder intended to be used for lung delivery. *J. Drug Deliv. Sci. Technol.* **2021**, *66*, 102848. [CrossRef]
7. Lim, J.-H.; Yook, S.-J. Development of a high-volume ambient aerosol sampling inlet with an adjustable cutoff size and its performance evaluation using road dust. *Environ. Res.* **2022**, *204*, 112302. [CrossRef]
8. Borhani Jebeli, M.; Moridi, P.; Beheshti, M.H.; Yarahmadi, R. A new cyclone design with adjustable inlet angle and external geometry for optimal PM10 removal. *Int. J. Environ. Sci. Technol.* **2020**, *17*, 1075–1086. [CrossRef]
9. Yohana, E.; Tauviqirrahman, M.; Yusuf, B.; Choi, K.-H.; Paramita, V. Effect of vortex limiter position and metal rod insertion on the flow field, heat rate, and performance of cyclone separator. *Powder Technol.* **2021**, *377*, 464–475. [CrossRef]
10. Haake, J.; Oggian, T.; Utzig, J.; Rosa, L.M.; Meier, H.F. Investigation of the pressure drop increase in a square free-vortex cyclonic separator operating at low particle concentration. *Powder Technol.* **2020**, *374*, 95–105. [CrossRef]
11. Wójtowicz, R.W.P.W.-W.A. Numerical and Experimental Analysis of Flow Pattern, Pressure Drop Collection Efficiency in a Cyclone with a Square, Inlet Different Dimensions of a Vortex, Finder. *Energies* **2021**, *14*, 111. [CrossRef]
12. Karagoz, I.; Avci, A.; Surmen, A.; Sendogan, O. Design and performance evaluation of a new cyclone separator. *J. Aerosol Sci.* **2013**, *59*, 57–64. [CrossRef]
13. Jafarnezhad, A.; Salarian, H.; Kheradmand, S.; Khaleghinia, J. Performance improvement of a cyclone separator using different shapes of vortex finder under high-temperature operating condition. *J. Braz. Soc. Mech. Sci. Eng.* **2021**, *43*, 81. [CrossRef]
14. Venkatesh, S.; Sakthivel, M.; Saranav, H.; Saravanan, N.; Rathnakumar, M.; Santhosh, K.K. Performance investigation of the combined series and parallel arrangement cyclone separator using experimental and CFD approach. *Powder Technol.* **2020**, *361*, 1070–1080. [CrossRef]
15. Yamasaki, H.; Kizilkan, Ö.; Yamaguchi, H.; Kamimura, T.; Hattori, K.; Nekså, P. Experimental investigation of dry ice cyclone separator for ultra-low temperature energy storage using carbon dioxide. *Energy Storage* **2020**, *2*, e149. [CrossRef]
16. Modabberifar, M.; Nazaripoor, H.; Safikhani, H. Modeling and numerical simulation of flow field in three types of standard new design cyclone separators. *Adv. Powder Technol.* **2021**, *32*, 4295–4302. [CrossRef]
17. Behrang, M.; Shirvani, M.; Hashemabadi, S.H. Multi-Helical-Channel dust separator: CFD simulation and experiment. *Chem. Eng. Res. Des.* **2019**, *146*, 1–10. [CrossRef]
18. Chen, L.; Ma, H.; Sun, Z.; Ma, G.; Li, P.; Li, C.; Cong, X. Effect of inlet periodic velocity on the performance of standard cyclone separators. *Powder Technol.* **2022**, *402*, 117347. [CrossRef]
19. Kozołub, P.; Klimanek, A.; Białecki, R.A.; Adamczyk, W.P. Numerical simulation of a dense solid particle flow inside a cyclone separator using the hybrid Euler–Lagrange approach. *Particuology* **2017**, *31*, 170–180. [CrossRef]
20. Gao, Z.-W.; Liu, Z.-X.; Wei, Y.-D.; Li, C.-X.; Wang, S.-H.; Qi, X.-Y.; Huang, W. Numerical analysis on the influence of vortex motion in a reverse Stairmand cyclone separator by using LES model. *Pet. Sci.* **2022**, *19*, 848–860. [CrossRef]
21. El-Emam, M.A.; Zhou, L.; Shi, W.; Han, C. Performance evaluation of standard cyclone separators by using CFD–DEM simulation with realistic bio-particulate matter. *Powder Technol.* **2021**, *385*, 357–374. [CrossRef]
22. Park, D.; Go, J.S. Design of Cyclone Separator Critical Diameter Model Based on Machine Learning and CFD. *Processes* **2020**, *8*, 1521. [CrossRef]
23. Izadi, A.; Kashani, E.; Mohebbi, A. Combining 10 meta-heuristic algorithms, CFD, DOE, MGGP and PROMETHEE II for optimizing Stairmand cyclone separator. *Powder Technol.* **2021**, *382*, 70–84. [CrossRef]

24. Donthu, N.; Kumar, S.; Mukherjee, D.; Pandey, N.; Lim, W.M. How to conduct a bibliometric analysis: An overview and guidelines. *J. Bus. Res.* **2021**, *133*, 285–296. [CrossRef]
25. Aria, M.; Cuccurullo, C. bibliometrix: An R-tool for comprehensive science mapping analysis. *J. Informetr.* **2017**, *11*, 959–975. [CrossRef]
26. Semerjian, L.; Okaiyeto, K.; Ojemaye, M.O.; Ekundayo, T.C.; Igwaran, A.; Okoh, A.I. Global Systematic Mapping of Road Dust Research from to Research Gaps Future, Direction. *Sustainability* **2021**, *13*, 11516. [CrossRef]
27. Youngblood, M.; Lahti, D. A bibliometric analysis of the interdisciplinary field of cultural evolution. *Palgrave Commun.* **2018**, *4*, 120. [CrossRef]
28. Zhang, Y.; Zhang, T.; Liu, X.; Zhang, L.; Hong, F.; Lu, M. Research trends of pregnancy with scarred uterus after cesarean: A bibliometric analysis from 1999 to 2018. *J. Matern. -Fetal Neonatal Med.* **2022**, *35*, 3555–3564. [CrossRef]
29. Du, Y.-Q.; Zhu, G.-D.; Cao, J.; Huang, J.-Y. Research supporting malaria control and elimination in China over four decades: A bibliometric analysis of academic articles published in Chinese from 1980 to 2019. *Malar. J.* **2021**, *20*, 158. [CrossRef]
30. Sun, J.; Zhou, Z.; Huang, J.; Li, G. A Bibliometric Analysis of the Impacts of Air Pollution on Children. *Int. J. Environ. Res. Public Health* **2020**, *17*, 1277. [CrossRef]
31. Sarkodie, S.A.; Owusu, P.A. Bibliometric analysis of water–energy–food nexus: Sustainability assessment of renewable energy. *Curr. Opin. Environ. Sci. Health* **2020**, *13*, 29–34. [CrossRef]
32. Sharifi, A. Urban sustainability assessment: An overview and bibliometric analysis. *Ecol. Indic.* **2021**, *121*, 107102. [CrossRef]
33. Can-Güven, E. Microplastics as emerging atmospheric pollutants: A review and bibliometric analysis. *Air Qual. Atmos. Health* **2021**, *14*, 203–215. [CrossRef]
34. Su, Y.; Yu, Y.; Zhang, N. Carbon emissions and environmental management based on Big Data and Streaming Data: A bibliometric analysis. *Sci. Total Environ.* **2020**, *733*, 138984. [CrossRef]
35. Miao, Y.; Zhang, Y.; Yin, L. Trends in hepatocellular carcinoma research from 2008 to 2017: A bibliometric analysis. *PeerJ* **2018**, *6*, e5477. [CrossRef]
36. Mahi, M.; Mobin, M.A.; Habib, M.; Akter, S. A bibliometric analysis of pandemic and epidemic studies in economics: Future agenda for COVID-19 research. *Soc. Sci. Humanit. Open* **2021**, *4*, 100165. [CrossRef]
37. Gan, L.; Jiang, P.; Lev, B.; Zhou, X. Balancing of supply and demand of renewable energy power system: A review and bibliometric analysis. *Sustain. Futures* **2020**, *2*, 100013. [CrossRef]
38. Liu, Z.; Yang, J.; Zhang, J.; Xiang, H.; Wei, H. A Bibliometric Analysis of Research on Acid Rain. *Sustainability* **2019**, *11*, 3077. [CrossRef]
39. Jia, Y.; Chen, Y.; Yan, P.; Huang, Q. Bibliometric Analysis on Global Research Trends of Airborne Microorganisms in Recent Ten Years (2011–2020). *Aerosol Air Qual. Res.* **2021**, *21*, 200497. [CrossRef]
40. Yang, Y.; Chen, G.; Reniers, G.; Goerlandt, F. A bibliometric analysis of process safety research in China: Understanding safety research progress as a basis for making China's chemical industry more sustainable. *J. Clean. Prod.* **2020**, *263*, 121433. [CrossRef]
41. Liu, W. Caveats for the use of Web of Science Core Collection in old literature retrieval and historical bibliometric analysis. *Technol. Forecast. Soc. Chang.* **2021**, *172*, 121023. [CrossRef]
42. Mascarenhas, C.; Ferreira, J.J.; Marques, C. University–industry cooperation: A systematic literature review and research agenda. *Sci. Public Policy* **2018**, *45*, 708–718. [CrossRef]
43. Dhital, S.; Rupakheti, D. Bibliometric analysis of global research on air pollution and human health: 1998–2017. *Environ. Sci. Pollut. Res.* **2019**, *26*, 13103–13114. [CrossRef] [PubMed]
44. Agbo, F.J.; Sanusi, I.T.; Oyelere, S.S.; Suhonen, J. Application of Virtual Reality in Computer Science Education: A Systemic Review Based on Bibliometric and Content Analysis Methods. *Educ. Sci.* **2021**, *11*, 142. [CrossRef]
45. Fardi, A.; Kodonas, K.; Gogos, C.; Economides, N. Top-cited Articles in Endodontic Journals. *J. Endod.* **2011**, *37*, 1183–1190. [CrossRef]
46. Jancsek-Turóczi, B.; Hoffer, A.; Nyírő-Kósa, I.; Gelencsér, A. Sampling and characterization of resuspended and respirable road dust. *J. Aerosol Sci.* **2013**, *65*, 69–76. [CrossRef]
47. Aslam, J.; Khan, S.A.; Khan, S.H. Heavy metals contamination in roadside soil near different traffic signals in Dubai, United Arab Emirates. *J. Saudi Chem. Soc.* **2013**, *17*, 315–319. [CrossRef]
48. Altuwayjiri, A.; Pirhadi, M.; Kalafy, M.; Alharbi, B.; Sioutas, C. Impact of different sources on the oxidative potential of ambient particulate matter PM10 in Riyadh, Saudi Arabia: A focus on dust emissions. *Sci. Total Environ.* **2022**, *806*, 150590. [CrossRef]
49. Lv, T.; Wang, L.; Xie, H.; Zhang, X.; Zhang, Y. Evolutionary overview of water resource management (1990–2019) based on a bibliometric analysis in Web of Science. *Ecol. Inform.* **2021**, *61*, 101218. [CrossRef]
50. Ojemaye, M.O.; Okoh, A.I. Global research direction on Pt and Pt based electro-catalysts for fuel cells application between 1990 and 2019: A bibliometric analysis. *Int. J. Energy Res.* **2021**, *45*, 15783–15796. [CrossRef]
51. Zhou, P.; Tijssen, R.; Leydesdorff, L. University-Industry Collaboration in China and the USA: A Bibliometric Comparison. *PLoS ONE* **2016**, *11*, e0165277. [CrossRef] [PubMed]
52. Loving, V.A. Collaborative interdepartmental teams: Benefits, challenges, alternatives, and the ingredients for team success. *Clin. Imaging* **2021**, *69*, 301–304. [CrossRef] [PubMed]
53. Puljak, L.; Vari, S.G. Significance of research networking for enhancing collaboration and research productivity. *Croat. Med. J.* **2014**, *55*, 181–183. [CrossRef] [PubMed]

54. Cheng, Q.; Wang, J.; Lu, W.; Huang, Y.; Bu, Y. Keyword-citation-keyword network: A new perspective of discipline knowledge structure analysis. *Scientometrics* **2020**, *124*, 1923–1943. [CrossRef]
55. Polat, Z.A.; Alkan, M.; Paulsson, J.; Paasch, J.M.; Kalogianni, E. Global scientific production on LADM-based research: A bibliometric analysis from 2012 to 2020. *Land Use Policy* **2022**, *112*, 105847. [CrossRef]
56. Karagoz, I.; Kaya, F. CFD investigation of the flow and heat transfer characteristics in a tangential inlet cyclone. *Int. Commun. Heat Mass Transf.* **2007**, *34*, 1119–1126. [CrossRef]
57. Wang, L.; Chen, E.; Ma, L.; Yang, Z.; Li, Z.; Yang, W.; Wang, H.; Chang, Y. Numerical simulation and experimental study of gas cyclone–liquid jet separator for fine particle separation. *Chin. J. Chem. Eng.* **2021**, *51*, 43–52. [CrossRef]
58. Aksnes, D.W.; Langfeldt, L.; Wouters, P. Citations, Citation Indicators, and Research Quality: An Overview of Basic Concepts and Theories. *SAGE Open* **2019**, *9*, 2158244019829575. [CrossRef]
59. Van Noorden, R.; Maher, B.; Nuzzo, R. The top 100 papers. *Nat. News* **2014**, *514*, 550. [CrossRef]
60. Cooper, I.D. Bibliometrics basics. *J. Med. Libr. Assoc.* **2015**, *103*, 217–218. [CrossRef]
61. Misiulia, D.; Andersson, A.G.; Lundström, T.S. Large Eddy Simulation Investigation of an Industrial Cyclone Separator Fitted with a Pressure Recovery Deswirler. *Chem. Eng. Technol.* **2017**, *40*, 709–718. [CrossRef]
62. Hamdy, O.; Bassily, M.A.; El-Batsh, H.M.; Mekhail, T.A. Numerical study of the effect of changing the cyclone cone length on the gas flow field. *Appl. Math. Model.* **2017**, *46*, 81–97. [CrossRef]
63. Du, P.; Liu, J.; Gui, H.; Zhang, J.; Yu, T.; Wang, J.; Cheng, Y.; Lu, Y.; Yao, Y.; Fu, Q.; et al. Development of a static test apparatus for evaluating the performance of three PM2.5 separators commonly used in China. *J. Environ. Sci.* **2020**, *87*, 238–249. [CrossRef]
64. Fu, S.; Zhou, F.; Sun, G.; Yuan, H.; Zhu, J. Performance evaluation of industrial large-scale cyclone separator with novel vortex finder. *Adv. Powder Technol.* **2021**, *32*, 931–939. [CrossRef]
65. Casotti Rienda, I.; Alves, C.A. Road dust resuspension: A review. *Atmos. Res.* **2021**, *261*, 105740. [CrossRef]
66. Health Effects Institute. State of Global Air 2020. Data source: Global Burden of Disease Study 2019. IHME. 2020. Available online: https://www.stateofglobalair.org/sites/default/files/documents/2020-10/soga-2020-report-10-26_0.pdf (accessed on 16 June 2022).
67. Yilbas, B.S.; Hassan, G.; Yilbas, A.E.; Abubakar, A.A.; Al-Qahtani, H. On the Mechanism of Human Saliva Interaction with Environmental Dust in Relation to Spreading of Viruses. *Langmuir* **2021**, *37*, 4714–4726. [CrossRef]
68. Magnano, G.C.; Marussi, G.; Pavoni, E.; Adami, G.; Larese Filon, F.; Crosera, M. Percutaneous metals absorption following exposure to road dust powder. *Environ. Pollut.* **2022**, *292*, 118353. [CrossRef]
69. Shrimpton, J.S.; Crane, R.I. Small Electrocyclone Performance. *Chem. Eng. Technol.* **2001**, *24*, 951–955. [CrossRef]
70. Carotenuto, C.; Di Natale, F.; Lancia, A. Wet electrostatic scrubbers for the abatement of submicronic particulate. *Chem. Eng. J.* **2010**, *165*, 35–45. [CrossRef]
71. Brouwers, J.J.H. Particle collection efficiency of the rotational particle separator. *Powder Technol.* **1997**, *92*, 89–99. [CrossRef]
72. Paiva, J.; Salcedo, R.; Araujo, P. Impact of particle agglomeration in cyclones. *Chem. Eng. J.* **2010**, *162*, 861–876. [CrossRef]
73. Haig, C.W.; Hursthouse, A.; McIlwain, S.; Sykes, D. The effect of particle agglomeration and attrition on the separation efficiency of a Stairmand cyclone. *Powder Technol.* **2014**, *258*, 110–124. [CrossRef]
74. Ahuja, S.M. Wetted wall cyclone—A novel concept. *Powder Technol.* **2010**, *204*, 48–53. [CrossRef]
75. Kim, G.-N.; Choi, W.-K.; Jung, C.-H. The development and performance evaluation of a cyclone train for the removal of contaminated hot particulate in a hot cell. *Sep. Purif. Technol.* **2007**, *55*, 313–320. [CrossRef]
76. Matthaios, V.N.; Lawrence, J.; Martins, M.A.G.; Ferguson, S.T.; Wolfson, J.M.; Harrison, R.M.; Koutrakis, P. Quantifying factors affecting contributions of roadway exhaust and non-exhaust emissions to ambient PM10–2.5 and PM2.5–0.2 particles. *Sci. Total Environ.* **2022**, *835*, 155368. [CrossRef]
77. Alshetty, D.; Nagendra, S.M.S. Impact of vehicular movement on road dust resuspension and spatiotemporal distribution of particulate matter during construction activities. *Atmos. Pollut. Res.* **2022**, *13*, 101256. [CrossRef]
78. Kumar, V.; Jha, K. Effects of Mass-Loading on Performance of the Cyclone Separators. In *Applications of Computational Fluid Dynamics Simulation and Modeling*; IntechOpen: London, UK, 2022. [CrossRef]
79. Li, Y.; Qin, G.; Xiong, Z.; Ji, Y.; Fan, L. The effect of particle humidity on separation efficiency for an axial cyclone separator. *Adv. Powder Technol.* **2019**, *30*, 724–731. [CrossRef]

sustainability

MDPI

Article

Study on Spatio-Temporal Evolution Law and Driving Mechanism of $PM_{2.5}$ Concentration in Changsha–Zhuzhou–Xiangtan Urban Agglomeration

Wenhao Chen [1], Chang Zeng [1], Chuheng Ding [2], Yingfang Zhu [3] and Yurong Sun [3,*]

[1] School of Business, Central South University of Forestry and Technology, Changsha 410004, China
[2] Bangor College China, Central South University of Forestry and Technology, Changsha 410004, China
[3] College of Science, Central South University of Forestry and Technology, Changsha 410004, China
* Correspondence: yurongsun@csuft.edu.cn; Tel.: +86-130-3733-9678

Abstract: Since the 21st century, China has made many explorations to alleviate the increasingly serious air pollution problem. This study analyses the spatio-temporal evolution characteristics and future development of $PM_{2.5}$ concentration in the Changsha–Zhuzhou–Xiangtan urban agglomeration from 2008 to 2019. In addition, the driving mechanism of spatial differentiation of $PM_{2.5}$ concentration in this urban agglomeration was also investigated. The results were as follows. Firstly, the $PM_{2.5}$ concentration showed a trend of gradual decline between 2008 and 2019. Secondly, the $PM_{2.5}$ concentration distribution was high in the northwest and low in the southeast. Thirdly, $PM_{2.5}$ concentration showed a strong spatial agglomeration. Fourth, except for some rural areas of Chaling County and Yanling County, the concentration of $PM_{2.5}$ in other areas was very likely to continue the past trend of gradual decline. Finally, natural and meteorological conditions played a leading role in the evolution of $PM_{2.5}$ concentration. The influence of socioeconomic factors is small now, but the trend is increasing. To improve air quality deeply, policymakers need to promote comprehensive control of regional air pollution by simultaneously reducing emissions and taking comprehensive treatment. They also need to strengthen supervision to prevent excessive pollution in some rural areas from worsening air quality in the surrounding areas.

Keywords: resource-saving and environment-friendly society; air pollution; Hurst index

1. Introduction

In recent years, haze weather has occurred frequently in China, and high-intensity air pollution has disturbed most cities, which has brought a serious threat to the sustainable economic and social development and the health of the people [1]. A high concentration of $PM_{2.5}$ is an important factor affecting the formation of haze. $PM_{2.5}$ in the air comes from socioeconomic factors such as urbanization dust, coal combustion, and automobile exhaust emissions. The concentration of $PM_{2.5}$ is also closely related to natural and meteorological conditions such as topography, vegetation coverage, air pressure, humidity, and precipitation [2,3]. Therefore, it is important to promote the comprehensive management of the regional atmospheric environment, to ensure sustainable socioeconomic development, and to safeguard the health of people by exploring the evolution law and drive mechanism of $PM_{2.5}$.

Since 2008, there have been more and more researchers showing their concern with the theme of $PM_{2.5}$. On the spatial scale, they are mainly focused on single cities [4,5], urban agglomeration [6–8], basins [9–11], and countries [12,13]. For example, Zhou et al. [14] analysed the characteristics and driving factors of the spatio-temporal evolution of $PM_{2.5}$ concentration in China from 2000 to 2011. Luna et al. [15] performed a spatial and temporal assessment of $PM_{2.5}$ in the ambient air of Colombia. In the research content, the analyses are mainly regarding the physical and chemical properties, spatio-temporal evolution

trend, spatial heterogeneity, spatial agglomeration, influencing factors, and governance measures of $PM_{2.5}$ [16–22]. For example, Li et al. [23] analysed the spatiotemporal evolution trend of $PM_{2.5}$ concentration on the global scale. Jin et al. [24] analysed the relationship between the satellite-retrieved aerosol optical depth (AOD) and the $PM_{2.5}$ concentration, as well as their spatio-temporal heterogeneity in the eastern United States from 2003 to 2017. Carmona et al. [25] analysed the influence of meteorological factors on $PM_{2.5}$ concentration in northeastern Mexico. Casallas et al. [26] assessed the impact of policy implementation on PM2.5 in northwestern South America at different scales. In terms of research methods, the Moran index [27], geographical detector [28], spatial econometric model [29], land use regression (LUR) [30], geographically weighted regression (GWR) [31], data envelopment analysis (DEA) [32], generalized additive model (GAM) [33], STIRPAT [34] and LOESS [35], etc., were mainly used. For example, Xia et al. [36] used geographically weighted regression and a geographical detector to analyse the changing trend and determinants of $PM_{2.5}$ concentration in the Yangtze River Economic Belt from 2000 to 2017. Londoño Ciro and Cañón Barriga [37] used geographically weighted regression and spatial econometric models to characterize the temporal and spatial distribution of the urban area of the city of Medellín-Colombia's $PM_{2.5}$ concentration from 2013 to 2014. Kim et al. [38] evaluated the effect of the Particulate Matter Comprehensive Plan introduced by the Korean government to improve air quality, and proposed improvement measures. Generally speaking, the current studies mainly pay attention to the temporal and spatial distribution, evolution trend, influencing factors, and comprehensive governance of $PM_{2.5}$ on the city, specific topography, or national scales, but there is little literature studying the effectiveness of comprehensive reform experimental areas in atmospheric environmental governance with $PM_{2.5}$.

Changsha–Zhuzhou–Xiangtan urban agglomeration is taken as the study area by this paper, which is one of the first comprehensive reform pilot areas for the construction of a resource-saving and environment-friendly society (also called a Two Oriented Society) in China. On the basis of the raster data of $PM_{2.5}$ concentration from 2008 to 2019, retrieved from NASA atmospheric remote sensing images, we were concerned with problems of the construction of Two Oriented Society in this urban agglomeration from the grid scale, such as the temporal and spatial evolution characteristics, future development trends and driving factors of $PM_{2.5}$ concentration. We used the gravity model, Moran index, Hurst index, and geographical detector in this study. It provides decision-making reference for the prevention and control of air pollution and the sustainable development of the economy and society.

2. Materials and Methods

2.1. Description of Changsha–Zhuzhou–Xiangtan Urban Agglomeration

Changsha–Zhuzhou–Xiangtan urban agglomeration is situated in the central and eastern parts of Hunan Province, including Changsha, Zhuzhou, and Xiangtan. The total area is about 2.8×10^4 km^2, which is a part of the region in the middle reaches of the Yangtze River (Figure 1). In 2018, the GDP of this region accounted for 41.98% of Hunan's GDP. It is the core growth pole of Hunan's economic development. With the rapid development of the economy, this region is also the most intense area of resource consumption and ecological destruction in Hunan Province. It is the key area for air pollution prevention and control in China. Changsha–Zhuzhou–Xiangtan urban agglomeration has a high topography to the east, south, and west, and a low topography to the north. It is a typical humid subtropical monsoon climate with distinct rains and heat in the same period, four seasons, rich precipitation, and uneven seasonal distribution. It is controlled by tropical depression in the summer, and has abundant precipitation. The wind direction is mostly southeast, which is conducive to the diffusion of $PM_{2.5}$. Winter is controlled by Mongolian high pressure, with less precipitation and mostly northwest wind, which easily leads to $PM_{2.5}$ accumulation. In addition, it is an important heavy industrial base in China, involving many high-energy and high-pollution industries, such as iron and steel, non-ferrous metals,

construction machinery, automotive and parts, petrochemical, rail transit, and equipment manufacturing. Moreover, the main urban areas of Changsha, Zhuzhou, and Xiangtan are not more than 40 km apart, which also leads to the accumulation of $PM_{2.5}$ in the region. The government's analysis of $PM_{2.5}$ sources shows that the contribution rate of motor vehicle exhaust to $PM_{2.5}$ concentration is close to 25%, and that of industrial emissions is about 20%. The contribution rates of coal fume, dining fume, and fume are 11.6–12.9%, 10.2–14.3%, and 13.3–16.3%, respectively [39]. In 2009, the average annual $PM_{2.5}$ concentration was 62.26 $\mu g/m^3$, which was much higher than the 10 $\mu g/m^3$ standard set in the air quality guidelines issued by the World Health Organization (WHO) in 2005. The construction of the pilot area for the comprehensive reform of a Two Oriented Society provides not only a major opportunity but also an arduous challenge for the environmental protection work.

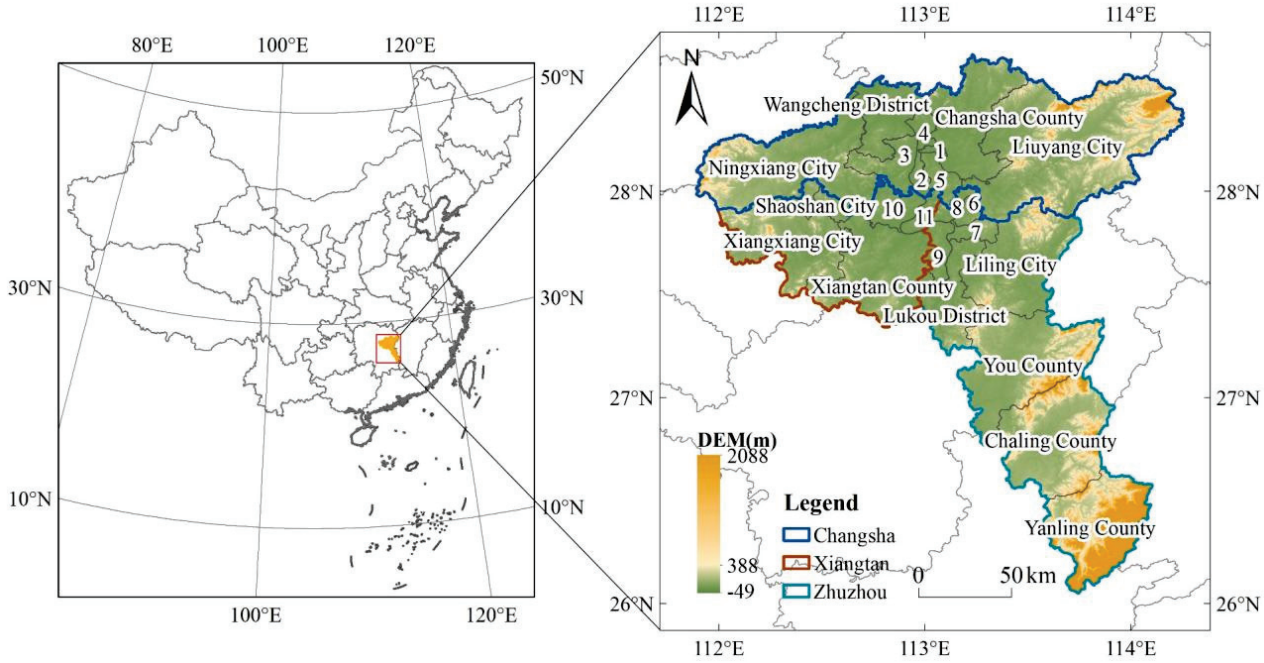

Figure 1. Geographic location of Changsha–Zhuzhou–Xiangtan urban agglomeration (1–11 stands for Furong District, Tianxin District, Yuelu District, Kaifu District, Yuhua District, Hetang District, Lousong District, Shifeng District, Tianyuan District, Yuhu District, and Yuetang district, respectively.).

2.2. Data

The data used in this study includes $PM_{2.5}$ concentration raster data, Changsha–Zhuzhou–Xiangtan urban agglomeration administrative boundary vector data, and driving factor data. (1) The annual $PM_{2.5}$ concentration raster data are retrieved from NASA Socioeconomic Data and Applications Centre (https://sedac.ciesin.columbia.edu/, accessed on 2 March 2022), from 2008 to 2019. Hammer et al. [40] verified their high accuracy (a resolution of $0.01° \times 0.01°$, $R^2 = 0.81$). Then, the raster data were smoothed for three years to ensure their stationarity and reliability. Hourly and monthly $PM_{2.5}$ concentration data were collected by reconstructing 6-hourly $PM_{2.5}$ datasets from 1960 to 2020 in China from Zenodo (https://zenodo.org/, accessed on 2 March 2022.). (2) The administrative boundary vector data were taken from the Resource and Environmental Science and Data Centre of the Chinese Academy of Sciences (https://www.resdc.cn/, accessed on 2 March 2022). On the basis of the administrative boundary vector data, this study uses the fishing net tool of ArcGIS software to create a 3 km × 3 km grid (a total of 3392 grids), calculates the average $PM_{2.5}$ concentration of each grid in each year, and establishes the spatial and temporal database of $PM_{2.5}$ concentration. (3) Driving factor data: eco-environmental quality data from China's historical 1 km resolution eco-environmental quality data (EEQ) from Zenodo;

night-time light index data from an extended time-series (2000–2018) of global NPP-VIIRS-like night-time light data from the Harvard Dataverse platform [41]; population density raster data from Scientific Data World Pop dataset (https://hub.worldpop.org/, accessed on 2 March 2022); altitude; leaf area index (LAI); normalized difference vegetation index (NDVI); and net primary productivity (NPP) data from the Resource and Environmental Science and Data Centre of the Chinese Academy of Sciences. The meteorological data of wind speed, pressure, precipitation rate, specific humidity, and temperature from China's meteorological forcing dataset (1979–2018) of the National Tibetan Plateau Data Centre were also used [42].

2.3. Methods

2.3.1. Gravity Model

The centre of gravity in geography refers to a point in regional space. The forces acting on the point in all directions remain relatively balanced. The movement of the centre of gravity can be used to reflect the changes in the spatial distribution of geographical objects and phenomena. Zhou et al. [14] studied spatial cluster characteristics of $PM_{2.5}$ in China using a gravity model. In our study, the centre of gravity is calculated in order to reveal the $PM_{2.5}$ pollution spatial migration process. Weight $PM_{2.5}$ concentration centre of gravity in the study area is calculated by Equation (1):

$$\overline{X} = \frac{\sum_{i=1}^{n}(W_i \times S_i \times X_i)}{\sum_{i=1}^{n}(W_i \times S_i)}, \ \overline{Y} = \frac{\sum_{i=1}^{n}(W_i \times S_i \times Y_i)}{\sum_{i=1}^{n}(W_i \times S_i)} \quad (1)$$

In this equation, $\overline{X}$ is the longitude of the $PM_{2.5}$ pollution centre of gravity. $\overline{Y}$ is the latitude of the $PM_{2.5}$ pollution centre of gravity. n is the total number of grids in the study area, and i is the grid serial number. X_i and Y_i are the longitude and latitude of the geometric centre of grid i, respectively. W_i represents the $PM_{2.5}$ concentration of grid i, and S_i represents the area of grid i.

2.3.2. Spatial Autocorrelation

We used the global Moran's I index to test the average similarity of the spatial correlation of $PM_{2.5}$ concentration in adjacent areas based on the size of the index. The calculation is performed using Equations (2) and (3):

$$S_0 = \sum_{i=1}^{n}\sum_{j=1}^{n} w_{ij} \quad (2)$$

$$I = \frac{n}{S_0} \times \frac{\sum_{i=1}^{n}\sum_{j=1}^{n} w_{ij}(C_i - \overline{C})(C_j - \overline{C})}{\sum_{i=1}^{n}(C_i - \overline{C})^2} \quad (3)$$

where I is the global Moran index and $I \in [-1, 1]$. When $I \in (0, 1]$, it shows that the research unit has a positive spatial autocorrelation; the higher the value is, the stronger the spatial aggregation of $PM_{2.5}$ concentration is. When $I \in [-1, 0)$, it shows that the research unit has a negative spatial autocorrelation; the smaller the value is, the stronger the spatial discreteness of $PM_{2.5}$ concentration is. When $I = 0$, there is no correlation between study units. n is the number of study units. C_i and C_j denote the $PM_{2.5}$ concentration values of the i and j study units, respectively. $\overline{C}$ is the average $PM_{2.5}$ concentration of all study units. w_{ij} is the spatial weight value (when unit i is next to j, $w_{ij} = 1$; when not adjacent, $w_{ij} = 0$,).

Local Moran's I is used to reveal the local spatial autocorrelation of $PM_{2.5}$ concentration, that is, the degree of correlation between the $PM_{2.5}$ concentration of a study unit and the adjacent unit. The calculation equation is shown in Equation (4).

$$I_i = \frac{n(C_i - \overline{C})}{\sum_{i=1}^{n}(C_i - \overline{C})^2} \sum_{j=1}^{m} w_{ij}(C_j - \overline{C}), (i \neq j) \quad (4)$$

where I_i is the local Moran index; n is the total number of spatial units; m is the number of cities geographically adjacent to the spatial unit i; C_i and C_j represent the $PM_{2.5}$ concentration of the spatial unit i and spatial unit j, respectively; $\overline{C}$ is the average $PM_{2.5}$ concentration of all spatial units; and w_{ij} is the spatial weight value. At the same time, the standardized counter Z is often used to test the significance of the Moran index. The standardized counter of the Moran index is defined as Equation (5):

$$Z(I) = \frac{[I - E(I)]}{\sqrt{Var(I)}} \tag{5}$$

where $Z\ (I)$ is the significance level of global Moran's I, $Var\ (I)$ is the variance of global Moran's I, and $E\ (I)$ is the mathematical expectation of global Moran's I. Taking 99% confidence as an example, when $Z\ (I) < -2.58$, it shows that $PM_{2.5}$ concentration has the characteristics of negative correlation in spatial distribution, including "low–high" correlation and "high–low" correlation; when $-2.58 \leq Z\ (I) \leq 2.58$, it shows that $PM_{2.5}$ concentration has no spatial autocorrelation and an independent random distribution. When $Z\ (I) > 2.58$, it shows that $PM_{2.5}$ concentration presents the characteristics of positive correlation in spatial distribution, including "high–high" aggregation and "low–low" aggregation, which is also called hot spot and cold spot distribution.

2.3.3. Hurst Index

In this study, the Hurst index (H) is used to predict the future evolution trend of $PM_{2.5}$ concentration in various portions of the study area. The Hurst index is proposed by the British scholar Hurst to quantitatively describe the long-range similarity or persistence of the time series. Generally, it is calculated by the method of R/S. The time series for obtaining the response at times $t_1, t_1, \ldots, t_n$ are $T_1, T_1, \ldots, T_n$. For any positive integer $\tau \geq 1$, the average of the time series is calculated by Equation (6):

$$\langle T \rangle_\tau = \frac{1}{\tau} \sum_{t=1}^{\tau} T(t), \tau = 1, 2, 3, \ldots, n \tag{6}$$

The cumulative deviation expressed by *X(t)* is calculated by Equation (7):

$$X(t, \tau) = \sum_{\mu=1}^{t} (T(\mu) - \langle T \rangle_\tau) \quad 1 \leq t \leq \tau \tag{7}$$

The difference between the maximum $X(t)$ value and the minimum *X(t)* value corresponding to the same τ value is turned into a range, which is recorded as Equation (8):

$$R(\tau) = \underset{1 \leq t \leq \tau}{max}\ X(t, \tau) - \min_{1 \leq t \leq \tau} X(t, \tau), \tau = 1, 2, 3, \ldots, n \tag{8}$$

The standard deviation $S(\tau)$ is calculated by Equation (9):

$$S(\tau) = \left[\frac{1}{\tau} \sum_{t=1}^{\tau} (T(t) - \langle T \rangle_\tau)^2 \right]^2 \quad \tau = 1, 2, 3, \ldots, n \tag{9}$$

The final R/S is calculated by Equation (10):

$$R/S = (\tau/2)^H \tag{10}$$

where H is the Hurst index. When $0.5 < H < 1$, it means that the long-term correlation feature of the sequence is positive persistence, and the future change trend is the same as the current change trend. The closer to 1 the H value is, the stronger the positive persistence is. When $0 < H < 0.5$, it means that the long-term correlation of the time series is characterized by anti-persistence. The future change trend is opposite to the current

change trend. The closer to 0 the H value is, the stronger the anti-persistence is. When $H = 0.5$, it means that the future change trend of the time series is random and independent of the present.

2.3.4. Geographical Detector

Spatial differentiation is one of the basic characteristics of geographical phenomena and the spatial expression of natural and socio-economic processes. As a powerful tool to detect spatial differentiation and reveal the driving factors of spatial differentiation, the geographical detector has the characteristics of a nonlinear hypothesis, elegant form, and clear physical meaning. At present, it has been widely used in the fields of ecology, meteorology, hydrology, social economy, and so on [43]. The geographical detector covers four aspects: interactive detection, ecological detection, factor detection, and risk detection. The principle is to analyse the spatial stratification heterogeneity of each factor by comparing the interlayer variance and total variance of each factor, in order to explore the driving force of each factor on the dependent variable. This paper mainly uses factor detection and interactive detection to calculate the explanation degree of factors to the spatial differentiation of $PM_{2.5}$ concentration in the study area. It also reveals its spatial differentiation mechanism.

Factor detection uses q statistics to characterize the explanatory power of each factor for the dependent variable. The value of q means that the independent variable X explains $100 \times$ q% of the spatial differentiation of $PM_{2.5}$ concentration. The expression is shown in Equations (11) and (12):

$$q = 1 - \frac{\sum_{h=1}^{L} N_h \sigma_h^2}{N\sigma^2} = 1 - \frac{SSW}{SST} \tag{11}$$

$$SSW = \sum_{h=1}^{L} N_h \sigma_h^2, SST = N\sigma^2 \tag{12}$$

where h is the stratification of independent variable X or $PM_{2.5}$ concentration Y; N_h and N are the number of units in layer h and the whole area, respectively; and σ_h^2 and σ^2 are the variance of the layer h and Y values of the whole region. SSW and SST are the sum of intra-layer variance and total variance of the whole region, respectively. The value range of q is between 0–1. The larger its value is, the higher the explanatory degree of the independent variable to the dependent variable is.

Interaction detection is used to identify the interaction between different factors, that is, to evaluate whether the joint action of the two factors will enhance or weaken the explanatory power of dependent variables. When $q(x_1 \cap x_2) < min(q(x_1), q(x_2))$, it indicates that the type of the two-factor interaction is nonlinear weakening. When $min(q(x_1), q(x_2)) < q(x_1 \cap x_2) < max(q(x_1), q(x_2))$, it indicates that the type of the two-factor interaction is unidirectional weakening. When $q(x_1 \cap x_2) > max(q(x_1), q(x_2))$, it indicates that the type of the two-factor interaction is a bidirectional enhancement. When $q(x_1 \cap x_2) > q(x_1) + q(x_2)$, it indicates that the type of the two-factor interaction is a nonlinear enhancement. When $q(x_1 \cap x_2) = q(x_1) + q(x_2)$, it indicates that the two factors are independent of each other.

3. Results

3.1. Spatio-Temporal Evolution Characteristics of $PM_{2.5}$ Concentration

3.1.1. Characteristics of Time Evolution

The concentration of $PM_{2.5}$ showed an inverted U-shaped trend from 2009 to 2018 (Figure 2). Before 2011, the average annual $PM_{2.5}$ concentration showed an upward trend, from 62.26 $\mu g/m^3$ in 2009 to 63.6 $\mu g/m^3$ in 2011, with an average annual growth rate of 1.08%. In 2011, the State Council successively issued the Circular on the Planning of National Main Functional Areas and the Circular on the 12th Five-year Plan of National Environmental Protection. Since then, documents on the prevention and control of air pollution in key areas have been issued, such as the 12th Five-year Plan and the Environmental Air Quality Standard, and the average annual $PM_{2.5}$ concentration has shown a

steady downward trend. It dropped from 63.6 $\mu g/m^3$ in 2011 to 41.4 $\mu g/m^3$ in 2018, with an average annual decrease of 4.99%, indicating that the decline in $PM_{2.5}$ concentration is closely related to the national environmental functional zoning for air pollution prevention and control, environmental quality monitoring and assessment system, pollution reduction statistics, monitoring and assessment system, and comprehensive control of a variety of air pollutants. In particular, after the State Council approved the implementation of the Action Plan for the Prevention and Control of Air Pollution in 2014 and the notice of the 13th Five-Year Plan issued in 2016, the concentration of $PM_{2.5}$ decreased significantly by 7.98% and 10.95%, respectively, in 2013 and 2016. According to the air quality guidelines issued by the World Health Organization (WHO) in 2009 and the $PM_{2.5}$ concentration standard classified by China's Environmental Air Quality Standard (GB3095–2012), and combined with the actual situation of this urban agglomeration, the $PM_{2.5}$ concentration grade of this area is divided into six grades. The area ratio of each $PM_{2.5}$ concentration grade from 2009 to 2018 (Figure 2) is calculated. Meanwhile, a linear fitting model ($y = -2.6734x + 69.305$) is constructed in years.

The results show the following. (1) The proportion of areas with $PM_{2.5}$ concentration which is lower than 35 $\mu g/m^3$ (the average annual limit of China Environmental Air Quality Standard) increased from 0% in 2009 to 10.38% in 2018. The proportion of areas where it is higher than 75 $\mu g/m^3$ increased from 0% in 2009 to 2.36% in 2011, and then decreased rapidly to 0% in 2013. (2) The proportion of areas with a $PM_{2.5}$ concentration which is lower than 50 $\mu g/m^3$ increased from 11% in 2013 to 99.73% in 2018, showing an increase of more than eight times, which was the most obvious increase in 2017–2018. (3) The proportion of areas with $PM_{2.5}$ concentrations between 50–75 $\mu g/m^3$ decreased from 88.74% in 2009 to 0.27% in 2018, with the most obvious decrease in 2013–2017. (4) Compared with 2009, the $PM_{2.5}$ concentration in all areas decreased by various degrees in 2018. The biggest areas, where the $PM_{2.5}$ concentration decreased by two grades, accounts for 90.63%. The following areas where the $PM_{2.5}$ concentration decreased by three grades account for 7.84%, and the last areas, where the $PM_{2.5}$ concentration decreased by one grade, account for 1.53%. (5) According to the linear fitting model ($\mu g/m^3$), the $PM_{2.5}$ concentration shows a significant decline (negative) trend ranging from -3.32 to -2.03 $\mu g/m^3$ per year. (6) The $PM_{2.5}$ concentration is low in the daytime and higher at night. The highest concentration occurs at 8:00 in the morning. Because there is an obvious temperature inversion in the lower atmosphere at night, it is easy for $PM_{2.5}$ to accumulate [44]. In addition, the morning is the peak time for people to travel, and there is a significant amount of vehicle exhaust emissions, leading to the highest $PM_{2.5}$ concentration. (7) The $PM_{2.5}$ concentration is highest in the winter and lowest in the summer. We believe that this is related to terrain conditions and wind patterns. The study area is typically located in the inland, with a horseshoe-shaped structure with the opening facing north. The dominant wind direction of the city throughout the year is northwest. The urban wind speed is relatively small in autumn and winter, which is not conducive to the diffusion of air pollutants. However, affected by the southeast monsoon in the summer, it is conducive to $PM_{2.5}$ diffusion [45].

3.1.2. Spatial Evolution Characteristics of the $PM_{2.5}$

On the basis of the $PM_{2.5}$ concentration data of Changsha–Zhuzhou–Xiangtan urban agglomeration from 2009 to 2018, 3 km × 3 km fishing nets (a total of 3392 grids) were created by using ArcGIS software, the average annual $PM_{2.5}$ concentration of each grid was calculated, and the spatial distribution maps of $PM_{2.5}$ concentration in 2009, 2011, and 2018 of this study area (Figure 3) were drawn. From 2009 to 2018, the spatial distribution of $PM_{2.5}$ concentration was quite different, showing a spatial distribution pattern which was high in the west and low in the east, high in the north and low in the south, and decreasing from northwest to southeast. Regional differences showed the characteristics of expanding at first, and then shrinking. Taking 50 $\mu g/m^3$ (the third grade $PM_{2.5}$ concentration limit) as the dividing point, the $PM_{2.5}$ concentration is divided into a high-value area and a low-value area.

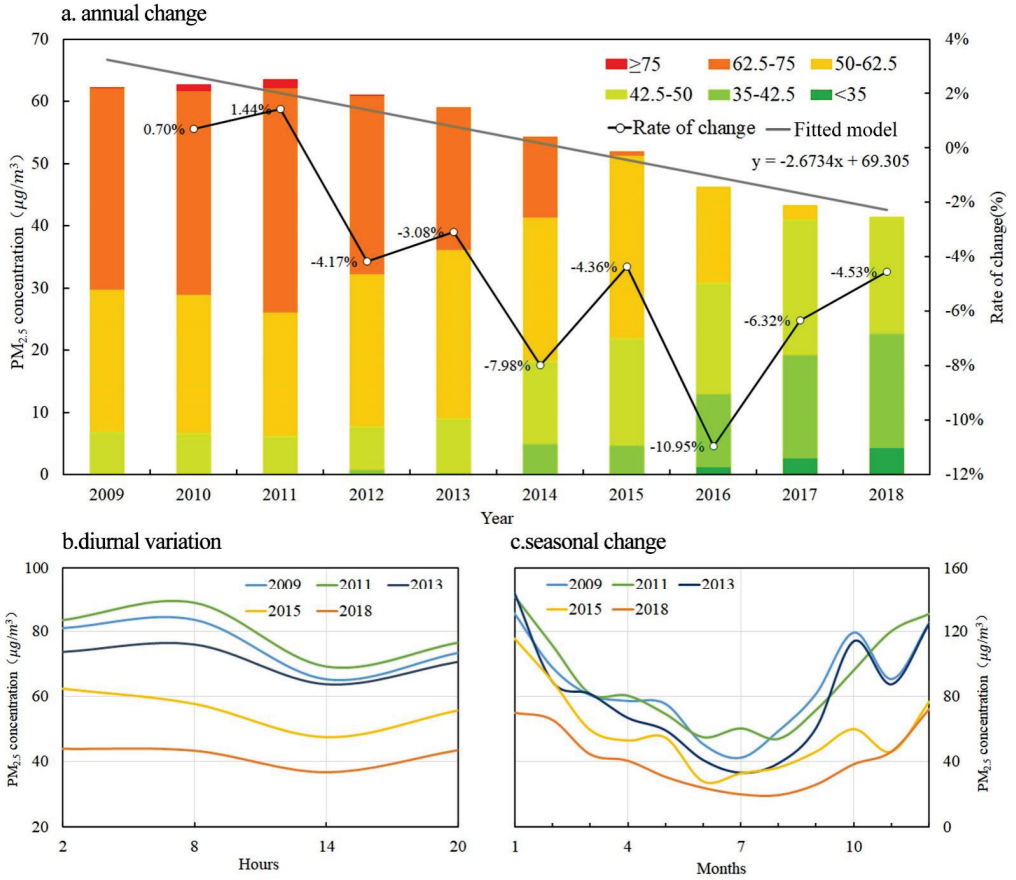

Figure 2. Spatial Evolution of $PM_{2.5}$ concentration in Changsha–Zhuzhou–Xiangtan urban agglomeration from 2009 to 2018. (**a**) Annual change; (**b**) diurnal variation; (**c**) seasonal change. Remarks: (**a**) The left coordinate describes the annual change of $PM_{2.5}$ concentration, which is represented by a histogram (the height of different colours represents the annual area proportion of different $PM_{2.5}$ concentration grades). The right coordinate describes the annual growth rate, which is represented by black lines.

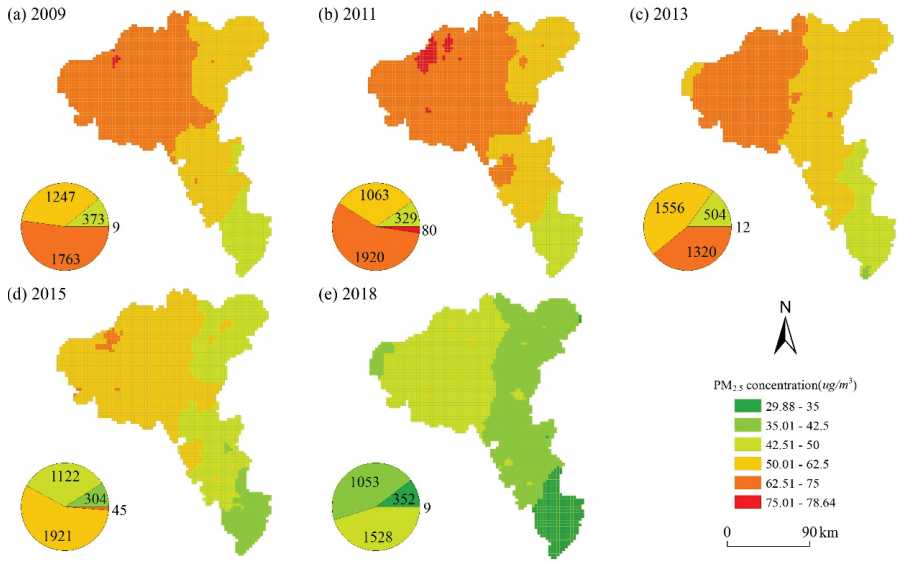

Figure 3. Spatial variation of annual average $PM_{2.5}$ concentration. (**a**) 2009, (**b**) 2011, (**c**) 2013, (**d**) 2015, (**e**) 2018. The pie chart at the lower left corner shows the annual area proportion of concentrations.

The spatial distribution difference of $PM_{2.5}$ concentration is mainly reflected as follows. (1) The $PM_{2.5}$ concentration has obvious agglomeration and distribution characteristics. The high-value areas are primarily scattered in the low-lying and economically developed areas such as Xiangtan City, Changsha City, and Zhuzhou City in the northwest, and the low-value areas are primarily scattered in the high-lying areas of Liuyang, You County, Chaling County, and Yanling County in the east and south, indicating that $PM_{2.5}$ concentration is closely related to topography and economic development. (2) In 2009, 89% of this urban agglomeration was in the area with a high $PM_{2.5}$ concentration, and 0.27% of the areas had a $PM_{2.5}$ concentration over 75 $\mu g/m^3$, which is distributed in the main urban area of Ningxiang City. The whole territory of Yanling County is a low-value area, and some low-value areas are also distributed in some high-lying areas of Chaling County and You County. (3) The high-value area of $PM_{2.5}$ concentration showed a trend of diffusion from 2009 to 2011. In 2011, 90.3% of the areas were high-value areas, and 2.36% were higher than 75 $\mu g/m^3$, primarily distributed in the main urban areas and agricultural areas of Ningxiang City and Wangcheng District. (4) In 2018, 99.73% of areas had low $PM_{2.5}$ concentration, indicating that the air pollution control actions taken by the government achieved practical results in key areas after the introduction of a series of policies including the 12th Five-Year Plan for the Prevention and Control of Air Pollution. With the development of the social economy, the concentration of $PM_{2.5}$ increased at first, and then decreased. It is worth noting that 0.27% of the areas still had a $PM_{2.5}$ concentration over 50 $\mu g/m^3$, scattered in the heavily populated areas of districts and counties in the northwest of this urban agglomeration in 2018.

3.2. Spatio-Temporal Migration Characteristics of $PM_{2.5}$ Concentration

In geography, the geographical centre of gravity is the vector resultant point that describes the geographical attributes or the distribution of things [46]. In this study, on the basis of the annual $PM_{2.5}$ concentration grid data of Changsha—Zhuzhou–Xiangtan urban agglomeration, the longitude and latitude coordinates of the annual $PM_{2.5}$ concentration centre of gravity are calculated by Equation (1), and the result is shown in Figure 4. The results show that the centre of gravity of $PM_{2.5}$ concentration from 2009 to 2018 was situated in Lukou District of Zhuzhou City, and the interannual change is obvious. From 2009 to 2011, the centre of gravity moved about 0.58 km to the east-north of 24.8°, with an average annual moving distance of about 0.57 km. According to "Hunan Province 13th Five-Year Plan for Environmental Protection," compiled by the Ecology and Environment Department of Hunan (EEDH), the economy of Changsha–Zhuzhou–Xiangtan urban agglomeration was in a stage of rapid development, with an average annual gross domestic product growth rate of 22.09%. There were too many enterprises with high pollution and energy consumption during this stage. They further increased the concentration of $PM_{2.5}$ in this region [47]. From 2011 to 2014, the centre of gravity moved about 1.25 km to the southwest, with an average annual shift of 0.61 km. During this period, Changsha–Zhuzhou–Xiangtan urban agglomeration issued and implemented "Environmental Co-governance Planning for Changsha–Zhuzhou–Xiangtan urban agglomeration (2010–2020)." It advocated for the vigorous development of clean energy sources such as natural gas, wind energy, and solar energy, and, meanwhile, reduced the proportion of coal used in primary energy, and carried out comprehensive control actions for pollutants such as sulphur dioxide as well as smoke and dust produced by the iron and steel, non-ferrous, chemical, building materials, and other industries [48]. From 2014 to 2018, the centre of gravity moved 2.36 km to the southeast by 34.37°, with an average annual shift of 0.78 km. During the implementation of "the 13th Five-Year Plan for Eco-environmental Protection," Hunan Province successively issued a series of policies and regulations, such as the "Regulations on Responsibility for Eco-environmental Protection in Hunan Province" and the "Measures for Responsibility for Major Eco-environmental Problems (Events) in Hunan Province," which improved the system for the prevention and control of atmospheric pollution. They closed more than 1000 highly polluting enterprises and further optimized the industrial

structure. Emissions of sulphur dioxide and nitrogen oxides decreased by 28.7% and 18.8%, respectively, compared with 2015. Significant achievements have been made in the prevention and control of air pollution [49].

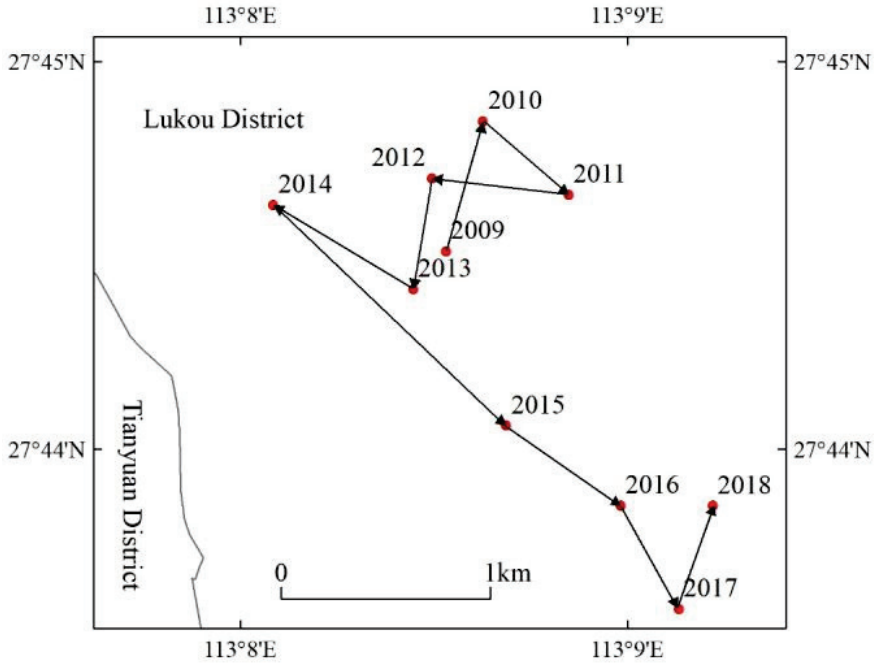

Figure 4. Change trend of $PM_{2.5}$ concentration centre of gravity in Changsha—Zhuzhou–Xiangtan urban agglomeration from 2009 to 2018.

3.3. Spatial Agglomeration Characteristics of $PM_{2.5}$ Concentration

3.3.1. Global Spatial Autocorrelation Feature

According to the global Moran's I calculation equations and using ArcGIS's Spatial statistics tools, it was calculated that the statistical values of Moran's I of $PM_{2.5}$ concentration of Changsha–Zhuzhou–Xiangtan urban agglomeration in 2009, 2011, 2013, 2015, and 2018 were 0.986 (Z = 79.80), 0.984 (Z = 79.66), 0.988 (Z = 79.97), 0.984 (Z = 79.69), and 0.983 (Z = 79.58), respectively. The results show that the statistical values of Moran's I are all positive and greater than 0.98, and that it has passed the significance test threshold level of 1%. They also show that the $PM_{2.5}$ concentration has a strong spatial correlation, and that areas with high $PM_{2.5}$ concentrations are often distributed together.

3.3.2. Local Spatial Autocorrelation Analysis

Using ArcGIS clustering and outlier analysis tools, we calculated the local Moran's I (Figure 5) of 3392 grids of the study area in 2009, 2011, 2013, 2015, and 2018. The grid cells showing significant local spatial autocorrelation were divided into four types: High–High Cluster, High–Low Outlier, Low–High Outlier, and Low–Low Cluster. The results show that the concentration of $PM_{2.5}$ in more and more areas of the region from 2009 to 2018 showed strong spatial aggregation. The types of spatial aggregation are "High–High Cluster" and "Low–Low Cluster," showing a strong positive autocorrelation. The proportion of hot spots increased from 28.57% in 2009 to 29.39% in 2018, with an average annual increase of 0.29%. The proportion of cold spot areas increased from 19.13% in 2009 to 23.29% in 2018, with an average annual increase of 2.17%. The proportion of cold spot areas and hot spot areas showed an upward trend, and the rising speed of cold spot areas was faster. From a spatial point of view, the hot spot areas were concentrated in the areas with heavy industrial pollution and vehicle exhaust emissions, such as the whole of Xiangtan City and the west of Changsha City. The cold spot areas were concentrated in the high-lying and underdeveloped areas, such as the south of Zhuzhou City and the east of

Liuyang City. The southwest of Chaling County was a cold spot distribution area in 2009 and 2011, but it had no characteristic point distribution in 2018. Agricultural non-point source pollution and straw burning may be the reasons for the deterioration of air quality in this area [50]. The southeast of Liuyang City had no characteristic point distribution in 2009 and 2011, but in 2018, it was a cold spot distribution area. The air quality has been significantly improved, indicating that the prevention and control of air pollution in this area has achieved remarkable results [51].

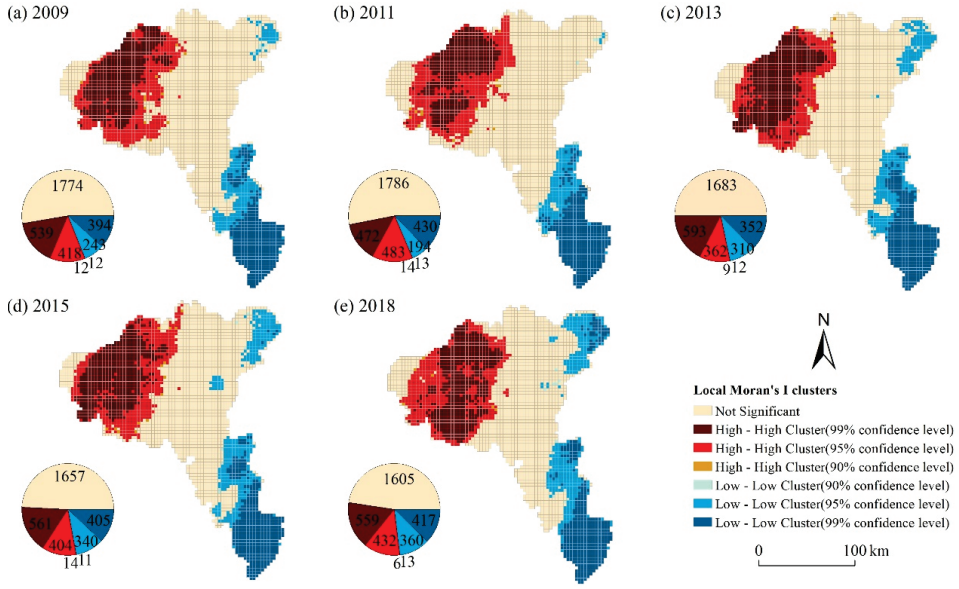

Figure 5. Local autocorrelation of $PM_{2.5}$ concentration in (**a**) 2009, (**b**) 2011, (**c**) 2013, (**d**) 2015, and (**e**) 2018. The pie chart at the lower left corner shows the annual area proportion of clusters.

3.4. Future Development Trend of $PM_{2.5}$ Concentration

On the basis of the $PM_{2.5}$ concentration data of the study area from 2009 to 2018, each grid Hurst index is calculated with the aid of Equation (6–10). Combined with the characteristics of the Hurst index and natural breakpoint method, the results are classified in Figure 6. It can be noted that the Hurst index of each area of this region ranges from 0.46 to 0.97. The regional difference is obvious. The high-value areas are mainly distributed in Xiangtan City and Changsha City. The low value areas are mainly distributed in Zhuzhou City, as well as in the central and eastern parts of Changsha City. The areas with a Hurst index greater than 0.5 account for 99.76%, indicating that the $PM_{2.5}$ concentration in most areas is positively persistent. There is an obvious Hurst phenomenon, that is, the future $PM_{2.5}$ concentration in most areas of this region is very likely to continue the trend of a gradual decline in $PM_{2.5}$ concentration which has been observed in the past [52]. It should be noted that the Hurst index of 0.24% of the areas is less than 0.5. These are mainly distributed in some rural areas of Chaling County and Yanling County, indicating that the non-point source pollution caused by agricultural development will lead to the future evolution of $PM_{2.5}$ concentration in these areas. The future trend is contrary to the continuous decline in $PM_{2.5}$ concentration in the past.

3.5. Spatial Differentiation Mechanism of $PM_{2.5}$ Concentration

The spatial difference of $PM_{2.5}$ concentration in Changsha–Zhuzhou–Xiangtan urban agglomeration is significant. The reasons are difficult to discern, and the driving factors may be various. Past research has found that the driving factors are related to natural factors, such as topography, vegetation, and forest fires. They are also related to human factors, such as industrial soot emissions, coal burning, and motor vehicle exhaust. At the same time, they are also closely related to meteorological factors like rainfall, temperature, and air pressure. In this study, we formulated the rules for screening driving factors for

spatial differentiation of $PM_{2.5}$ concentration in this urban agglomeration based on the relevant research results [53,54], and considering the actual situation of the study area and the availability of data. We selected the following 13 driving factors which contributed greatly to the spatial differentiation of $PM_{2.5}$ concentration from three aspects: natural conditions, socio-economic conditions, and meteorology. These are altitude (X_1), slope (X_2), eco-environmental quality (EEQ) (X_3), normalized difference vegetation index (NDVI) (X_4), leaf area index (LAI) (X_5), net primary productivity (NPP) (X_6), population density (X_7), night-time light index (X_8), wind speed (X_9), pressure (X_{10}), precipitation rate (X_{11}), specific humidity (X_{12}), and temperature (X_{13}).

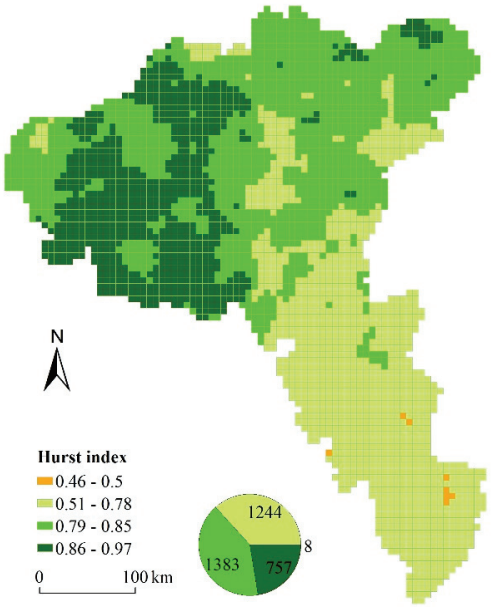

Figure 6. Hurst index of Changsha–Zhuzhou–Xiangtan Urban agglomeration in 2009–2018.

3.5.1. Factor Detection

In order to more accurately analyse the driving factors of spatial differentiation of $PM_{2.5}$ concentration in Changsha–Zhuzhou–Xiangtan urban agglomeration, this study used ArcGIS software to create a 3 km × 3 km fishing net (with a total of 3392 grids), and calculated the observations of the 13 driving factors in each grid. Then, we used the Jenks natural breakpoint method to divide the observations of the driving factors in each grid into six categories. In the end, we imported the discrete data into the geographic detector for factor detection and interactive detection. The factor detection results can be seen in Table 1.

Table 1. Factor detection result analysis over 5 years.

Driving Factor		2009		2011		2013		2015		2018		Average Value
		q	*p*	*q*	*p*	*q*	*p*	*q*	*p*	*q*	*p*	
Natural condition	Altitude (X_1)	0.55	0.00	0.55	0.00	0.50	0.00	0.50	0.00	0.58	0.00	0.40
	Slope (X_2)	0.42	0.00	0.41	0.00	0.39	0.00	0.40	0.00	0.45	0.00	
	Eco-environmental quality (X_3)	0.49	0.00	0.44	0.00	0.45	0.00	0.47	0.00	0.53	0.00	
	NDVI (X_4)	0.20	0.00	0.27	0.00	0.36	0.00	0.34	0.00	0.31	0.00	
	LAI (X_5)	0.55	0.00	0.54	0.00	0.53	0.00	0.54	0.00	0.60	0.00	
	NPP (X_6)	0.11	0.00	0.09	0.00	0.12	0.00	0.12	0.00	0.13	0.00	
Socioeconomic status	Population density (X_7)	0.09	0.01	0.09	0.00	0.08	0.03	0.08	0.20	0.10	0.15	0.08
	Night-time light index (X_8)	0.03	1.00	0.05	0.99	0.07	0.36	0.07	0.67	0.14	0.00	
Meteorology	Wind speed (X_9)	0.39	0.00	0.09	0.00	0.11	0.00	0.18	0.00	0.07	0.00	0.32
	Pressure (X_{10})	0.54	0.00	0.55	0.00	0.50	0.00	0.49	0.00	0.58	0.00	
	Precipitation rate (X_{11})	0.14	0.00	0.57	0.00	0.53	0.00	0.52	0.00	0.42	0.00	
	Specific humidity (X_{12})	0.24	0.00	0.11	0.00	0.09	0.00	0.26	0.00	0.21	0.00	
	Temperature (X_{13})	0.28	0.00	0.32	0.00	0.30	0.00	0.29	0.00	0.30	0.00	

Note: *q* represents the driving force of each driving factor, and *p* represents the significant level of each driving factor.

The driving effect of night-time light index (X_8) in 2009, 2011, 2013, and 2015 and that of population density (X_7) in 2015 and 2018 were not significant, while the other driving factors had a significant impact on the spatial differentiation of $PM_{2.5}$. The driving forces for each factor are quite different. According to the five-year average *Q* value, the explanatory power of each driving factor to the spatial differentiation of $PM_{2.5}$ concentration was as follows: LAI (0.564) > altitude (0.559) > pressure (0.556) > eco-environmental quality (0.487) > slope (0.426) > precipitation rate (0.377) > temperature (0.299) > NDVI (0.260) > specific humidity (0.188) > wind speed (0.185) > NPP (0.108) > population density (0.093) > night-time light index (0.072).

The average Q value of the natural condition driving factor was 0.40, which shows an upward trend, indicating that it plays a dominant role in the spatial differentiation of $PM_{2.5}$ concentration. The average Q value of meteorological driving factors was 0.32. Its annual change is small, which indicates that it plays a key role in the spatial differentiation of $PM_{2.5}$ concentration. The average Q value of the driving factors for the socio-economic status was only 0.08, which is relatively low. However, in 2009–2018, the average Q value increased by 95.04%, which meant that it was a rapid driving force for the spatial difference of $PM_{2.5}$.

From the point of view of natural conditions, the western and northern parts of this urban agglomeration have low topography and gentle slope. $PM_{2.5}$ gathers easily here, and does not easily spread due to the surrounding mountains, which leads to the increase in $PM_{2.5}$ concentration in the area. Low vegetation coverage and vegetation quality are also important reasons for the high $PM_{2.5}$ concentration in this region. Vegetation can directly reduce the concentration of $PM_{2.5}$ in the air by adsorption and blocking, or it can indirectly reduce the concentration of $PM_{2.5}$ by leaf transpiration, increasing atmospheric humidity, and absorbing and transforming sulphur, lead, and other metals and nonmetals in the air. Increasing vegetation coverage and improving vegetation quality are important ways to reduce $PM_{2.5}$ concentration.

In terms of social and economic conditions, population density and night-time light index are the driving factors for regional population and economic vitality. Their driving force for the $PM_{2.5}$ spatial differentiation is weak, but they are on the rise. The reasons are as follows: The secondary industry accounted for a high proportion in Xiangxiang City, Xiangtan County, Ningxiang City, and other areas at the initial stage of the establishment of the Two Oriented Society. Industrial soot emissions are significant, and contribute greatly to the $PM_{2.5}$ concentration. In contrast, the population density in these areas is relatively low. Its influence on $PM_{2.5}$ concentration is also relatively small. With the gradual progress of the construction of the Two Oriented Society, the industrial structure of this urban agglomeration is gradually upgraded and rationalized. Polluting enterprises are optimized and eliminated, and industrial pollution decreases year by year. Its driving force on $PM_{2.5}$ concentration gradually decreases. Meanwhile, the driving force of population and economic vitality increases rapidly.

From a meteorological point of view, pressure has the strongest driving force on the spatial differentiation of $PM_{2.5}$ concentration (Q > 0.5). Air pressure is the atmospheric pressure acting on a unit area, which is closely associated with the situation of atmospheric circulation. The surrounding high-pressure air masses flow to the centre when the local surface is controlled by low pressure, resulting in an updraft in the centre. The increasing wind force is advantageous to the upward evacuation of pollutants, and the $PM_{2.5}$ concentration is lower. On the contrary, there is a downdraft in the centre if the ground is controlled by high pressure, which inhibits the upward diffusion of pollutants. Under the control of stable high pressure, pollutants accumulate and $PM_{2.5}$ concentration increases [55]. The average driving forces of precipitation rate and temperature are 0.377 and 0.299, respectively, which are also at a high level. Precipitation can effectively reduce the concentration of $PM_{2.5}$, but the process is slow. The driving forces of wind speed and specific humidity are relatively low. Previous studies have pointed out that wind direction affects the long-distance transport of $PM_{2.5}$ [56]; the government's analysis of the source of $PM_{2.5}$ concentration also indicates that about 10% of the fine particles in the Changsha–Zhuzhou–Xiangtan urban agglomeration come from the surrounding areas [39].

3.5.2. Interactive Detection

The interactive detection results of spatial differentiation of $PM_{2.5}$ concentration in Changsha–Zhuzhou–Xiangtan urban agglomeration (Figure 7) show that the driving force of the interaction of any two driving factors on the spatial differentiation of $PM_{2.5}$ concentration is greater than that of a single driving factor. The main types of pairwise interaction are two-factor enhancement and nonlinear enhancement, indicating that the spatial differentiation of $PM_{2.5}$ concentration is not caused by a single influence factor; it is the result of the joint action of different factors [57]. Among them, the driving force of pressure ∩ specific humidity was the strongest, and the q value of this factor interaction was the highest at 0.75 in 2009. The q value of wind speed ∩ precipitation rate reached 0.89 in 2011 and 2015, which was the strongest driving force for the spatial differentiation of $PM_{2.5}$ concentration. The driving force of LAI ∩ precipitation rate was the strongest in 2018, and the q value of this factor interaction was at its highest at 0.76. The driving forces of the following two-factor interactions on the spatial differentiation of $PM_{2.5}$ concentration are greater than 0.8: altitude ∩ precipitation rate, LAI ∩ precipitation rate, and pressure ∩ precipitation rate in 2011 and 2013, and specific humidity ∩ precipitation rate in 2015. It also can be seen that the driving force of two factors is stronger than that of a single factor in the spatial differentiation of $PM_{2.5}$ concentration, although other driving factors all have forces less than 0.8.

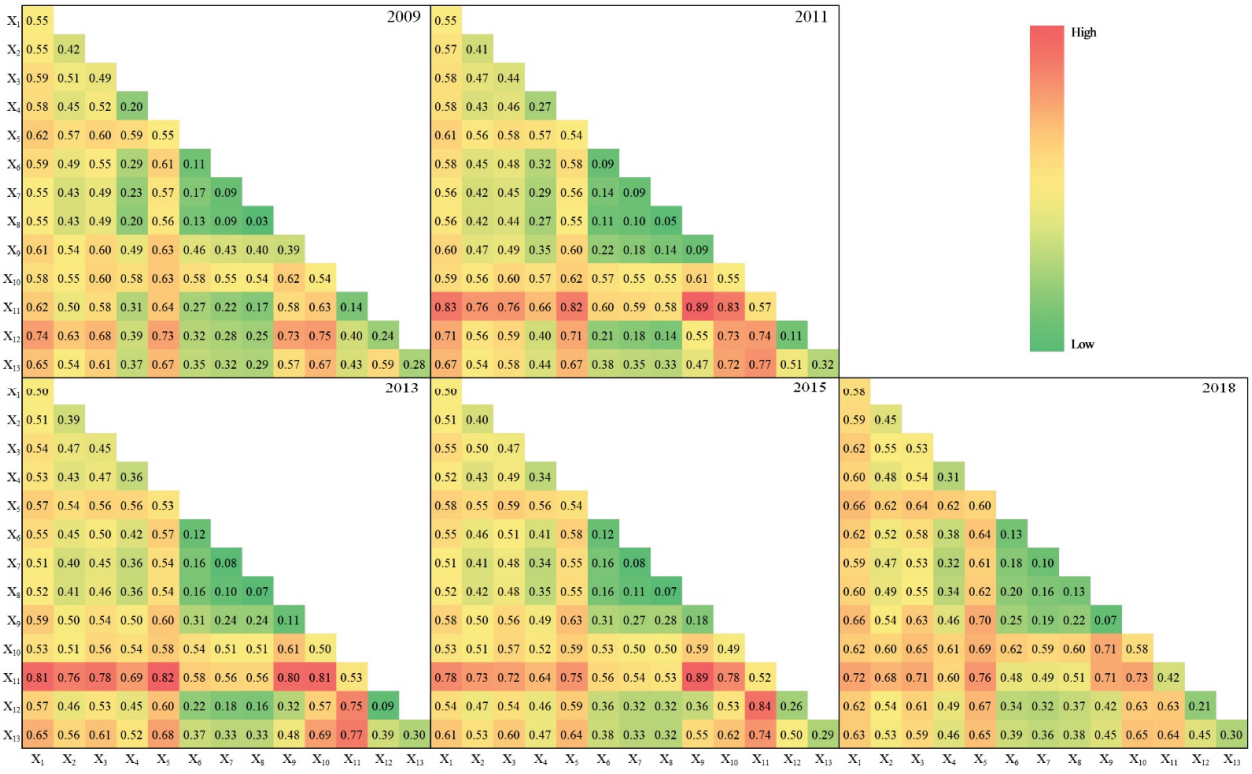

Figure 7. Interactive detection results between factors in 2009, 2011, 2013, 2015. and 2018.

4. Discussion

The Environmental Kuznets Curve (EKC) theory shows that environmental pollution presents an inverted U-shaped development trend with the development of social economy [58]. Our study confirms this point of view.

Past research has suggested that population density is positively associated with $PM_{2.5}$ concentration [59]. In this study, we noted that there is a prominent positive correlation between population density and $PM_{2.5}$ concentration. That is, the higher the population density, the higher the $PM_{2.5}$ concentration [60]. Taking Changsha–Zhuzhou–Xiangtan urban agglomeration as the study area, we found that the correlation between night-time light index and $PM_{2.5}$ is not high (only 0.034 in 2009), but this correlation showed an upward

trend, reaching 0.135 in 2018. It can be seen from the results that the effect of different indexes on $PM_{2.5}$ concentration changed with the change in time and region. The dominant factors in spatial differentiation of $PM_{2.5}$ concentration are meteorological factors, natural conditions, and socio-economic status [61]. Our study shows that natural conditions are the dominant factor affecting $PM_{2.5}$ concentration, followed by meteorological factors, and, finally, social and economic conditions, in which leaf area index (LAI) has the strongest driving force on the spatial differentiation of $PM_{2.5}$ concentration [62]. As for the source of $PM_{2.5}$, previous studies have pointed out that the high concentration of $PM_{2.5}$ in the northwest of this urban agglomeration mainly comes from industrial emissions from thermal power, iron and steel, non-ferrous smelting, and cement industries. Sudden air pollution incidents are often related to straw burning [63]. Therefore, this urban agglomeration needs to speed up the pace of industrial transformation and upgrading, reduce the share of enterprises with high energy consumption and high pollution, and strengthen the management and control of straw burning and non-point source pollution in agricultural production [64]. Population density and the night light index reflect the degree of traffic exhaust to a certain extent. Under the condition of data limitation, based on the strong correlation among them, we used population density and night light index instead of traffic exhaust to study its impact on $PM_{2.5}$ concentration. In fact, traffic exhaust is an important source of $PM_{2.5}$ concentration. We will further study the mechanism by which traffic exhaust affects the change in $PM_{2.5}$ concentration and its centre of gravity in the future, with the help of these sources such as Waze, Google, or NOx.

Poor air quality not only seriously restricts the sustainable development of the social economy, but also threatens the health of people. Changsha–Zhuzhou–Xiangtan urban agglomeration is a key area for the prevention and control of air pollution in China. Since 2011, the joint prevention and control of air pollution in this region has achieved remarkable results, and the quality of air has been dramatically improved. Its achievements in building a resource-saving and environment-friendly society are undeniable [65]. However, it is worth noting that the decline rate of $PM_{2.5}$ concentration in the region has slowed significantly since 2016, possibly due to coal combustion, industrial pollution emissions, and motor vehicle exhaust emissions [39]. Furthermore, our study showed that the abnormal development trend of $PM_{2.5}$ concentration in some agricultural areas of this urban agglomeration is becoming more and more significant. The government needs to make more efforts to reach the goal of an annual average $PM_{2.5}$ concentration of less than 35 $\mu g/m^3$ by 2025, which was set in the "Fourteenth Five-Year Plan for Ecological Environment Protection."

5. Conclusions

This paper systematically analyses the spatial and temporal evolution characteristics and the future development trend of $PM_{2.5}$ concentration in Changsha–Zhuzhou–Xiangtan urban agglomeration from 2009 to 2018 by using the gravity model, spatial autocorrelation, Hurst index, and GIS spatial analysis methods. It also reveals the driving mechanism of the spatial differentiation of $PM_{2.5}$ concentration from the aspects of natural conditions, meteorological factors, and social and economic conditions.

The results of our study indicate that the concentration of $PM_{2.5}$ showed an inverted U-shaped trend from 2009 to 2018, rising from 62.26 $\mu g/m^3$ in 2009 to 63.6 $\mu g/m^3$ in 2011, and then decreasing to 41.4 $\mu g/m^3$ in 2018. The spatial distribution of $PM_{2.5}$ concentration shows significant differences and aggregation. The high-value area is primarily scattered in the northwest region, with low elevation and a developed economy, while the low-value area is primarily scattered in the southeast region, with high altitude and an underdeveloped economy. From 2009 to 2018, the spatial centre of gravity of $PM_{2.5}$ concentration showed an overall trend of moving to the southeast. In addition, the concentration of $PM_{2.5}$ in most areas will continue the trend of gradual decline which has been seen the past, except in some rural areas of Chaling and Yanling counties. This may be due to the increase of $PM_{2.5}$ concentration caused by straw burning, waste incineration, mining, and large-scale project construction.

The geographical detection results regarding the spatial differentiation of $PM_{2.5}$ concentration show that natural condition driving factors, as well as meteorological driving factors, have a significant influence on the spatial differentiation of $PM_{2.5}$ concentration in this urban agglomeration, while the influence of socio-economic factors is small, but rapidly increasing.

Author Contributions: Conceptualization, Y.S. and Y.Z.; methodology, W.C. and Y.S.; software, W.C.; validation, C.D.; formal analysis, C.Z.; data curation, W.C.; writing—original draft preparation, W.C.; writing—review and editing, Y.S. and C.Z.; visualization, C.D.; supervision, Y.S.; funding acquisition, Y.S. and Y.Z. All authors have read and agreed to the published version of the manuscript.

Funding: This research was funded by Hunan Provincial Forest Quality and Efficiency Improvement Demonstration Project (OT-S-KTA6) under the Loan of the European Investment Bank; Forestry Department of Hunan Province: XLK202103-2; Central South University of Forestry and Technology: none.

Institutional Review Board Statement: Not applicable.

Conflicts of Interest: The authors declare no conflict of interest.

References

1. Ding, Y.; Wu, P.; Liu, Y.; Song, Y. Environmental and Dynamic Conditions for the Occurrence of Persistent Haze Events in North China. *Engineering* **2017**, *3*, 266–271. [CrossRef]
2. Yang, D.; Wang, X.; Xu, J.; Xu, C.; Lu, D.; Ye, C.; Wang, Z.; Bai, L. Quantifying the influence of natural and socioeconomic factors and their interactive impact on $PM_{2.5}$ pollution in China. *Environ. Pollut.* **2018**, *241*, 475–483. [CrossRef]
3. Zhang, N.; Huang, H.; Duan, X.; Zhao, J.; Su, B. Quantitative association analysis between $PM_{2.5}$ concentration and factors on industry, energy, agriculture, and transportation. *Sci. Rep.* **2018**, *8*, 9461. [CrossRef] [PubMed]
4. Hu, C.-G.; Lee, K.-H. Chemical Composition of Fine Particulate Matter in the Downtown Area of Jeju City. *J. Environ. Sci. Int.* **2018**, *27*, 597–610. [CrossRef]
5. Park, S. COVID-19 (Coronavirus Disease 2019) Outbreaks and Their Relationship with Atmospheric Concentrations of PM_{10} and $PM_{2.5}$: A Case Study for Daegu Metropolitan City. *J. Korean Geogr. Soc.* **2020**, *55*, 453465.
6. Huang, Q.; Chen, G.; Xu, C.; Jiang, W.; Su, M. Spatial Variation of the Effect of Multidimensional Urbanization on $PM_{2.5}$ Concentration in the Beijing-Tianjin-Hebei (BTH) Urban Agglomeration. *Int. J. Environ. Res. Public Health* **2021**, *18*, 12077. [CrossRef]
7. Mi, Y.; Sun, K.; Li, L.; Lei, Y.; Wu, S.; Tang, W.; Wang, Y.; Yang, J. Spatiotemporal pattern analysis of $PM_{2.5}$ and the driving factors in the middle Yellow River urban agglomerations. *J. Clean. Prod.* **2021**, *299*, 126904. [CrossRef]
8. Yan, J.-W.; Tao, F.; Zhang, S.-Q.; Lin, S.; Zhou, T. Spatiotemporal Distribution Characteristics and Driving Forces of $PM_{2.5}$ in Three Urban Agglomerations of the Yangtze River Economic Belt. *Int. J. Environ. Res. Public Health* **2021**, *18*, 2222. [CrossRef]
9. Hu, W.; Zhao, T.; Bai, Y.; Kong, S.; Xiong, J.; Sun, X.; Yang, Q.; Gu, Y.; Lu, H. Importance of regional $PM_{2.5}$ transport and precipitation washout in heavy air pollution in the Twain-Hu Basin over Central China: Observational analysis and WRF-Chem simulation. *Sci. Total Environ.* **2021**, *758*, 143710. [CrossRef]
10. Liu, Y.; Shi, G.; Zhan, Y.; Zhou, L.; Yang, F. Characteristics of $PM_{2.5}$ spatial distribution and influencing meteorological conditions in Sichuan Basin, southwestern China. *Atmos. Environ.* **2021**, *253*, 118364. [CrossRef]
11. Thunis, P.; Clappier, A.; Beekmann, M.; Putaud, J.P.; Cuvelier, C.; Madrazo, J.; de Meij, A. Non-linear response of $PM_{2.5}$ to changes in NO_x and NH_3 emissions in the Po basin (Italy): Consequences for air quality plans. *Atmos. Chem. Phys.* **2021**, *21*, 9309–9327. [CrossRef]
12. Bai, K.; Ma, M.; Chang, N.-B.; Gao, W. Spatiotemporal trend analysis for fine particulate matter concentrations in China using high-resolution satellite-derived and ground-measured $PM_{2.5}$ data. *J. Environ. Manag.* **2019**, *233*, 530–542. [CrossRef] [PubMed]
13. Liu, X.; Hadiatullah, H.; Tai, P.; Xu, Y.; Zhang, X.; Schnelle-Kreis, J.; Schloter-Hai, B.; Zimmermann, R. Air pollution in Germany: Spatio-temporal variations and their driving factors based on continuous data from 2008 to 2018. *Environ. Pollut.* **2021**, *276*, 116732. [CrossRef] [PubMed]
14. Zhou, L.; Zhou, C.; Yang, F.; Che, L.; Wang, B.; Sun, D. Spatio-temporal evolution and the influencing factors of $PM_{2.5}$ in China between 2000 and 2015. *J. Geogr. Sci.* **2019**, *29*, 253–270. [CrossRef]
15. Luna, M.A.G.; Luna, F.A.G.; Espinosa, J.F.M.; Cerón, L.C.B. Spatial and temporal assessment of particulate matter using AOD data from MODIS and surface measurements in the ambient air of Colombia. *Asian J. Atmos. Environ.* **2018**, *12*, 165–177. [CrossRef]
16. Tiwari, S.; Chate, D.M.; Pragya, P.; Ali, K.; Bisht, D.S. Variations in Mass of the PM_{10}, $PM_{2.5}$ and PM1 during the Monsoon and the Winter at New Delhi. *Aerosol Air Qual. Res.* **2012**, *12*, 20–29.
17. Wang, Y.; Duan, X.; Wang, L. Spatial-Temporal Evolution of $PM_{2.5}$ Concentration and its Socioeconomic Influence Factors in Chinese Cities in 2014–2017. *Int. J. Environ. Res. Public Health* **2019**, *16*, 985. [CrossRef]

18. Wu, Q.; Guo, R.; Luo, J.; Chen, C. Spatiotemporal evolution and the driving factors of $PM_{2.5}$ in Chinese urban agglomerations between 2000 and 2017. *Ecol. Indic.* **2021**, *125*, 107491. [CrossRef]
19. Xia, X.-S.; Wang, J.-H.; Song, W.-D.; Cheng, X.-F. Spatio-temporal Evolution of $PM_{2.5}$ Concentration During 2000–2019 in China. *Huan Jing Ke Xue* **2020**, *41*, 4832–4843.
20. Yang, D.; Chen, Y.; Miao, C.; Liu, D. Spatiotemporal variation of $PM_{2.5}$ concentrations and its relationship to urbanization in the Yangtze River delta region, China. *Atmos. Pollut. Res.* **2020**, *11*, 491–498. [CrossRef]
21. Ye, C.; Chen, R.; Chen, M.; Ye, X. A new framework of regional collaborative governance for $PM_{2.5}$. *Stoch. Environ. Res. Risk Assess.* **2019**, *33*, 1109–1116. [CrossRef]
22. Zou, Y.; Jin, C.; Su, Y.; Li, J.; Zhu, B. Water soluble and insoluble components of urban $PM_{2.5}$ and their cytotoxic effects on epithelial cells (A549) in vitro. *Environ. Pollut.* **2016**, *212*, 627–635. [CrossRef] [PubMed]
23. Li, J.; Wang, N.; Wang, J.; Li, H. Spatiotemporal evolution of the remotely sensed global continental $PM_{2.5}$ concentration from 2000–2014 based on Bayesian statistics. *Environ. Pollut.* **2018**, *238*, 471–481. [CrossRef] [PubMed]
24. Jin, Q.; Crippa, P.; Pryor, S. Spatial characteristics and temporal evolution of the relationship between $PM_{2.5}$ and aerosol optical depth over the eastern USA during 2003–2017. *Atmos. Environ.* **2020**, *239*, 117718. [CrossRef]
25. Carmona, J.M.; Gupta, P.; Lozano-Garcia, D.F.; Vanoye, A.Y.; Yepez, F.D.; Mendoza, A. Spatial and Temporal Distribution of $PM_{2.5}$ Pollution over Northeastern Mexico: Application of MERRA-2 Reanalysis Datasets. *Remote Sens.* **2020**, *12*, 2286. [CrossRef]
26. Casallas, A.; Castillo-Camacho, M.P.; Guevara-Luna, M.A.; González, Y.; Sanchez, E.; Belalcazar, L.C. Spatio-temporal analysis of $PM_{2.5}$ and policies in Northwestern South America. *Sci. Total Environ.* **2022**, *852*, 158504. [CrossRef]
27. Lim, C.-H.; Park, D.-H. Spatial clustering of $PM_{2.5}$ concentration and their characteristics in the Seoul Metropolitan Area for regional environmental planning. *J. Korean Soc. Environ. Restor. Technol.* **2022**, *25*, 41–55.
28. Yang, J.; Liu, P.; Song, H.; Miao, C.; Wang, F.; Xing, Y.; Wang, W.; Liu, X.; Zhao, M. Effects of Anthropogenic Emissions from Different Sectors on $PM_{2.5}$ Concentrations in Chinese Cities. *Int. J. Environ. Res. Public Health* **2021**, *18*, 10869. [CrossRef]
29. Hao, Y.; Liu, Y.-M. The influential factors of urban $PM_{2.5}$ concentrations in China: A spatial econometric analysis. *J. Clean. Prod.* **2016**, *112*, 1443–1453. [CrossRef]
30. Knibbs, L.D.; Van Donkelaar, A.; Martin, R.V.; Bechle, M.J.; Brauer, M.; Cohen, D.D.; Cowie, C.T.; Dirgawati, M.; Guo, Y.; Hanigan, I.C.; et al. Satellite-Based Land-Use Regression for Continental-Scale Long-Term Ambient $PM_{2.5}$ Exposure Assessment in Australia. *Environ. Sci. Technol.* **2018**, *52*, 12445–12455. [CrossRef]
31. Zhai, L.; Li, S.; Zou, B.; Sang, H.; Fang, X.; Xu, S. An improved geographically weighted regression model for $PM_{2.5}$ concentration estimation in large areas. *Atmos. Environ.* **2018**, *181*, 145–154. [CrossRef]
32. Zhou, Y.; Li, L.; Sun, R.; Gong, Z.; Bai, M.; Wei, G. Haze Influencing Factors: A Data Envelopment Analysis Approach. *Int. J. Environ. Res. Public Health* **2019**, *16*, 914. [CrossRef] [PubMed]
33. Li, S.; Zhai, L.; Zou, B.; Sang, H.; Fang, X. A Generalized Additive Model Combining Principal Component Analysis for $PM_{2.5}$ Concentration Estimation. *ISPRS Int. J. Geo-Inf.* **2017**, *6*, 248. [CrossRef]
34. Huang, W.; Wang, H.; Zhao, H.; Wei, Y. Temporal–spatial characteristics and key influencing factors of $PM_{2.5}$ concentrations in China based on Stirpat model and Kuznets curve. *Environ. Eng. Manag. J.* **2019**, *18*, 2587–2604. [CrossRef]
35. Singh, V.; Singh, S.; Biswal, A. Exceedances and trends of particulate matter ($PM_{2.5}$) in five Indian megacities. *Sci. Total Environ.* **2021**, *750*, 141461. [CrossRef]
36. Xia, S.; Liu, X.; Liu, Q.; Zhou, Y.; Yang, Y. Heterogeneity and the determinants of $PM_{2.5}$ in the Yangtze River Economic Belt. *Sci. Rep.* **2022**, *12*, 4189. [CrossRef]
37. Londoño-Ciro, L.A.; Cañón-Barriga, J.E. Metodología para la caracterización espacio-temporal de $PM_{2.5}$ en el área urbana de la ciudad de Medellín-Colombia. *Rev. EIA* **2018**, *15*, 113–132. [CrossRef]
38. Kim, E.; Bae, C.; Kim, B.-U.; Kim, H.C.; Kim, S. Evaluation of the Effectiveness of Emission Control Measures to Improve $PM_{2.5}$ Concentration in South Korea. *J. Korean Soc. Atmos. Environ.* **2018**, *34*, 469–485. [CrossRef]
39. EEDH. Phased Achievements Have Been Made in the Analysis of PM2.5 Sources of Urban Ambient Air in Changsha, Zhuzhou and Xiangtan. 2014. Available online: https://sthjt.hunan.gov.cn/sthjt/xxgk/xwdt/zxdt/201402/t20140207_4638787.html (accessed on 29 October 2022).
40. Hammer, M.S.; Van Donkelaar, A.; Li, C.; Lyapustin, A.; Sayer, A.M.; Hsu, N.C.; Levy, R.C.; Garay, M.J.; Kalashnikova, O.V.; Kahn, R.A.; et al. Global Estimates and Long-Term Trends of Fine Particulate Matter Concentrations (1998–2018). *Environ. Sci. Technol.* **2020**, *54*, 7879–7890. [CrossRef]
41. Chen, Z.; Yu, B.; Yang, C.; Zhou, Y.; Yao, S.; Qian, X.; Wang, C.; Wu, B.; Wu, J. An extended time series (2000–2018) of global NPP-VIIRS-like nighttime light data from a cross-sensor calibration. *Earth Syst. Sci. Data* **2021**, *13*, 889–906. [CrossRef]
42. Yang, K.; He, J.; Tang, W.; Qin, J.; Cheng, C.C. On downward shortwave and longwave radiations over high altitude regions: Observation and modeling in the Tibetan Plateau. *Agric. For. Meteorol.* **2010**, *150*, 38–46. [CrossRef]
43. Wang, J.-F.; Zhang, T.-L.; Fu, B.-J. A measure of spatial stratified heterogeneity. *Ecol. Indic.* **2016**, *67*, 250–256. [CrossRef]
44. Zhang, N.-N.; Guan, Y.; Yu, L.; Ma, F.; Li, Y.-F. Spatio-temporal distribution and chemical composition of $PM_{2.5}$ in Changsha, China. *J. Atmos. Chem.* **2020**, *77*, 1–16. [CrossRef]
45. Zhang, Y.; Jiang, W. Pollution characteristics and influencing factors of atmospheric particulate matter ($PM_{2.5}$) in Chang-Zhu-Tan area. *IOP Conf. Ser. Earth Environ. Sci.* **2018**, *108*, 042047. [CrossRef]

46. Zhu, M.; Yan, J.; Cheng, X.; Li, F. Investigating the spatiotemporal $PM_{2.5}$ dynamic and socioeconomic driving forces in Beijing based on geographical weighted regression. *J. Nonlinear Convex Anal.* **2021**, *22*, 2331–2345.
47. EEDH. Notice of Hunan Provincial Environmental Protection Department on Printing and Distributing the 13th Five Year Environmental Protection Plan of Hunan Province. 2016. Available online: https://sthjt.hunan.gov.cn/sthjt/xxgk/ghcw/ghjh/zhgh/201609/t20160919_4662756.html (accessed on 29 August 2022).
48. EEDH. Letter on the Implementation of the Environmental Co Governance Plan for the Changsha Zhuzhou Xiangtan Urban Agglomeration (2010–2020). 2012. Available online: https://sthjt.hunan.gov.cn/sthjt/xxgk/ghcw/ghjh/zxgh/201206/t20120605_4662567.html (accessed on 29 October 2020).
49. EEDH. Notice on Printing and Distributing the "Fourteenth Five Year" Ecological Environment Protection Plan of Hunan Province. 2022. Available online: https://sthjt.hunan.gov.cn/sthjt/xxgk/ghcw/ghjh/zhgh/202207/t20220728_27569082.html (accessed on 29 October 2022).
50. CCPG. Jujube Town: Straw Burning is Prohibited, Publicizing "Volunteer Red", Guarding "Ecological Green". 2022. Available online: https://www.chaling.gov.cn/c12925/20220516/i1859783.html (accessed on 29 October 2022).
51. LMPG. Liuyang Has the Highest Air Quality Excellence Rate in Changsha. 2018. Available online: https://www.liuyang.gov.cn/lyszf/zfgzdt/zwdt/201801/t20180108_5109544.html (accessed on 29 October 2022).
52. Wang, X.; Li, T.; Ikhumhen, H.O.; Sá, R.M. Spatio-temporal variability and persistence of $PM_{2.5}$ concentrations in China using trend analysis methods and Hurst exponent. *Atmos. Pollut. Res.* **2022**, *13*, 101274. [CrossRef]
53. Huang, C.; Liu, K.; Zhou, L. Spatio-temporal trends and influencing factors of $PM_{2.5}$ concentrations in urban agglomerations in China between 2000 and 2016. *Environ. Sci. Pollut. Res.* **2021**, *28*, 10988–11000. [CrossRef] [PubMed]
54. Wang, T.; Song, H.; Wang, F.; Zhai, S.; Han, Z.; Wang, D.; Li, X.; Zhao, H.; Ma, R.; Zhang, G. Hysteretic effects of meteorological conditions and their interactions on particulate matter in Chinese cities. *J. Clean. Prod.* **2020**, *274*, 122926. [CrossRef]
55. Chen, P. Study on coordinated development of urban environment and economy based on cluster computing. *Clust. Comput.* **2019**, *22*, 6335–6343. [CrossRef]
56. Wang, J.; Ogawa, S. Effects of Meteorological Conditions on $PM_{2.5}$ Concentrations in Nagasaki, Japan. *Int. J. Environ. Res. Public Health* **2015**, *12*, 9089–9101. [CrossRef]
57. Zhang, F.; Peng, H.; Sun, X.; Song, T. Influence of Tourism Economy on Air Quality—An Empirical Analysis Based on Panel Data of 102 Cities in China. *Int. J. Environ. Res. Public Health* **2022**, *19*, 4393. [CrossRef] [PubMed]
58. Tenaw, D.; Beyene, A.D. Environmental sustainability and economic development in sub-Saharan Africa: A modified EKC hypothesis. *Renew. Sustain. Energy Rev.* **2021**, *143*, 110897. [CrossRef]
59. Han, S.; Sun, B. Impact of Population Density on $PM_{2.5}$ Concentrations: A Case Study in Shanghai, China. *Sustainability* **2019**, *11*, 1968. [CrossRef]
60. Zhao, X.; Zhou, W.; Han, L.; Locke, D. Spatiotemporal variation in $PM_{2.5}$ concentrations and their relationship with socioeconomic factors in China's major cities. *Environ. Int.* **2019**, *133*, 105145. [CrossRef] [PubMed]
61. Yun, G.; He, Y.; Jiang, Y.; Dou, P.; Dai, S. $PM_{2.5}$ Spatiotemporal Evolution and Drivers in the Yangtze River Delta between 2005 and 2015. *Atmosphere* **2019**, *10*, 55. [CrossRef]
62. Liang, D.; Ma, C.; Wang, Y.-Q.; Wang, Y.-J.; Chen-Xi, Z. Quantifying $PM_{2.5}$ capture capability of greening trees based on leaf factors analyzing. *Environ. Sci. Pollut. Res.* **2016**, *23*, 21176–21186. [CrossRef]
63. Xu, B.; You, X.; Zhou, Y.; Dai, C.; Liu, Z.; Huang, S.; Luo, D.; Peng, H. The study of emission inventory on anthropogenic air pollutants and source apportionment of $PM_{2.5}$ in the Changzhutan Urban Agglomeration, China. *Atmosphere* **2020**, *11*, 739. [CrossRef]
64. Pei, T.; Gao, L.; Yang, C.; Xu, C.; Tian, Y.; Song, W. The Impact of FDI on Urban $PM_{2.5}$ Pollution in China: The Mediating Effect of Industrial Structure Transformation. *Int. J. Environ. Res. Public Health* **2021**, *18*, 9107. [CrossRef]
65. EEDH. Environmental Quality in Hunan Province in the First Half of 2016. 2016. Available online: https://sthjt.hunan.gov.cn/sthjt/xxgk/zdly/hjjc/hjtj/201607/t20160722_4663842.html (accessed on 30 October 2022).

sustainability

MDPI

Article

Research on Consumer Trust Mechanism in China's B2C E-Commerce Platform for Second-Hand Cars

Xueqian Li *, Jiaqi Ma, Xinyu Zhou and Ruixia Yuan

Business School, University of Shanghai for Science and Technology, Shanghai 200093, China
* Correspondence: xqli81@usst.edu.cn

Abstract: The rapid development of China's e-commerce industry has led to the rise of China's second-hand car e-commerce. With the increasingly rich trust theory and the rapid development of e-commerce platforms, the issue of online consumer trust has attracted more and more scholars' attention. This paper takes China's B2C second-hand car e-commerce platforms as an example, combines the second-hand car research conclusions and consumer trust theory, and conducts a systematic study on the formation of consumer trust in second-hand car e-commerce platforms. Based on the trust of individual consumers, system environment, website/APP and platform companies, this paper explores the influencing factors of consumer trust and constructs the influencing factors model of trust formation. The empirical study was conducted by using the structural equation model and multiple regression to verify the degree of fitting of the theoretical hypothesis and the model. The research results have a certain reference value for the development of second-hand car e-commerce platforms.

Keywords: second-hand car; e-commerce platforms; consumer trust; structural equations; multiple regression

1. Introduction

Second-hand car e-commerce is a new business model of China's second-hand car industry. In recent years, the development of second-hand car e-commerce in China has been particularly rapid. From the perspective of car ownership, Chinese automobiles are changing from incremental to stock, and the upgrade and replacement rate will increase year by year.

The trade volume has increased due to the trend of replacing second-hand cars. In 2021, China's second-hand car transaction volume exceeded CNY 1.1 trillion, with a year-on-year growth of 27.3%, becoming a veritable trillion-yuan market. Around 2013, China's second-hand car trading market began to see an investment boom, and investment institutions believed that e-commerce would become the main channel of second-hand car trading. Therefore, there was an emergence of a number of second-hand car e-commerce companies. Under the influence of the booming second-hand car market and the popularity of e-commerce, the number of second-hand cars traded on e-commerce platforms showed a rapid growth trend. In 2021, the transaction scale of second-hand e-commerce in China reached CNY 400.17 billion, with a year-on-year growth of 29.27%. However, compared with most other e-commerce platforms (comprehensive and vertical), the development speed of second-hand e-commerce is relatively stable and slow. Over the past three years, market penetration growth has fallen far short of expectations, as shown in Figure 1. What factors restrict its development in the end? Through the survey, the researchers found that the key obstacle to the development of China's second-hand car e-commerce platforms is still the low level of consumer trust. Compared with general commodities, second-hand cars have a high unit price, complex quality information, life safety and low consumption frequency, so there may be some unique mechanism in the process of consumer trust

formation. When the traditional trading mode of the market has not yet cultivated enough consumer trust, will people have high trust in the natural place? This is doubtful. Therefore, this is a research work with both theoretical and practical value to deeply understand the formation mechanism of consumer trust in the second-hand car trading scenario and propose measures to enhance consumer trust based on this.

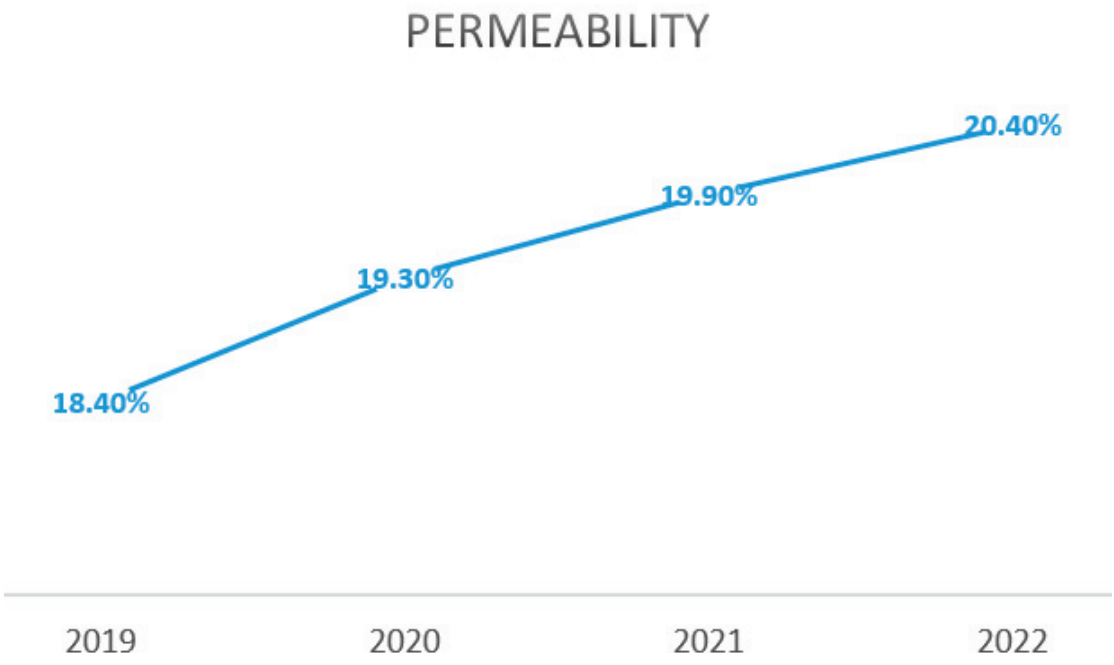

Figure 1. China's second-hand car e-commerce permeability from 2019–2022.

The business model of a second-hand car e-commerce platform is divided into four types. The C2B mode starts from the C-end seller users, who sell the car to the B-end car dealers; such platforms include Che Zhibao, Da Souche, etc. The B2C mode leads the source of B-end vehicles to the demand of the C-end. Such platforms include Youxin Second-hand Car, 99 Good car, etc. B2B and C2C businesses directly face two car dealers or two major trading user groups. Platforms focusing on a B2B model include Youxin Pai, Cheyipai, etc., while those focusing on C2C model include person-to-person car, Guazi second-hand car, etc. In general, after years of exploration and operation, brand value, operation experience and business channels are the core barriers of competition for each e-commerce platform.

In these four types of businesses, the highest degree of marketization is in the B2C and C2C modes, that is, the end-user-oriented businesses. We want to explore the transaction process facing end users and the trust formation mechanism of end consumers in the transaction process. Since the B2C model is a transaction between enterprises and individuals, while the C2C business model is essentially a transaction between individuals, their transaction processes and the formation mechanism of consumer trust may be very different. Therefore, it is necessary for this paper to choose one of the modes to study. Considering that the B2C model has developed well in China's second-hand car e-commerce market and is more likely to become the mainstream model, we decide to take the B2C model as the research scope of this paper.

The research on the second-hand car market originated from Akerlof's "The Market for Lemons: Quality Uncertainties and the Market Mechanism" published in 1970 [1]. He discussed and analyzed three industries with asymmetric information, including the analysis of lemon market problems caused by the second-hand car market, and pointed out that the reason why there are problems in the second-hand car market is that the seller has more information than the buyer. Information asymmetry is an important aspect that affects consumer trust. As a critical factor for the success of online enterprises, e-services,

trust has been proven to have a significant impact on customer behavioral intentions (Lee and Lee, 2005; Tajvidi et al., 2017), even in the context of second-hand cars [2,3].

Trust has been widely studied and considered as the driving factor of e-commerce (Alalwan et al., 2017) [4], but there is still relatively little attention to revealing how trust develops and its role in the second-hand car business. The unpredictable environment due to the lack of face-to-face communication is the main reason why previous e-commerce/s-commerce studies have explored the mechanism of trust formation (Gefen and Straub, 2003; Kim and Park, 2013) [5,6]. Factors such as social support, information quality and social presence (Chen and Shen, 2015; El Amri and Akrout, 2020) have been proved to be able to help sellers gain customers' trust [7,8]. However, there are huge differences between second-hand cars and general goods. Whether the mechanism of trust has changed and how it affects follow-up behavior is still unknown in the e-commerce of second-hand cars. We believe that business characteristics, product attributes and other factors can affect consumer trust, and website authentication can also promote consumer trust (Hillman, 2017) [9]. When consumer perception is consistent with product quality, consumer satisfaction will increase, and thus trust in the seller will also increase (Fang et al., 2014) [10]. Consumers have higher confidence in products with a quality certification or quality endorsement. When the transaction is at risk, consumers are willing to believe in policies and laws, and this effective governance can significantly improve consumer trust (Hartl et al., 2016) [11].

The existing research tends to regard trust as an aggregation structure (Wan et al., 2016; Jiang et al., 2019) [12,13]. The whole concept is problematic because the customer's behavior intention depends not only on the expectation of the product but also on their attitude towards the person who provides them with services (Kim and Park, 2013) and the service level of the service provider [14]. Jone (2014) takes perceived website quality, third-party authentication and network security performance as factors affecting e-commerce consumer trust [15]. In addition, personal experience factors cannot be ignored. Sutanonpaiboon (2008) divided the trust dimensions that directly affect consumers' purchases into media trust and trust in individual characteristics, including individual ability, kindness and honesty [16]. However, there is little research on how to form trust in the Internet market of second-hand cars. The relevant literature still lacks a micro-analysis of trust mechanisms and a deeper understanding of how they affect customer behavior. Therefore, in the context of second-hand car Internet platforms, we distinguish trust at the individual level, platform level and system level. These sources of trust are both different and interrelated. What is the internal relationship between them and the formation of consumer trust? This is the problem that we need to solve in our work. This paper has made some contributions in theory, mainly as follows: (1) Based on the consumption decision-making process, the consumer trust mechanism model has been constructed from the three levels of system, enterprise and individual, which is a beneficial extension of consumer trust theory; (2) Second-hand car e-commerce is a special type of e-commerce, which has developed rapidly in China. However, there has been no research on this issue in the past, so this paper has enriched the theoretical research of e-commerce.

This paper is organized as follows: Firstly, it analyzes the market background and research basis of the research. Section 2 establishes a theoretical model and puts forward assumptions. Section 3 conducts empirical analysis. Finally, it summarizes the research conclusions and emphasizes the management implications for enterprises.

2. Materials and Methods

2.1. Research Model

Moorman (1993) first proposed a three-stage model of network trust: trust influencing factors, trust generating process and trust outcomes [17]. Mayer's (1995) outcome model assumes that the characteristics of both the trusted party (competence, goodwill and honesty) and the trusting party (propensity to trust) have an impact on overall trust [18].

Later, Gefen and Straub (2004) extended the trust factor model [19]. The main research hypothesis is proposed based on the reading study of relevant literature.

2.1.1. Consumer Personal Factors

Personal factors are important aspects affecting trust formation, and personal factors include three dimensions: personal inherent trust tendency, personal vehicle knowledge level and personal online shopping experience.

1. Personal inherent trust tendency

Personal inherent trust tendency arises from the individual's past life experiences.

Lee (2001) found that trust tendency directly affects personal online trust [20]. Heyns and Rothmann (2015) concluded that a high level of personal inherent trust tendency would promote perceived trustworthiness [21]. The following hypothesis is proposed:

H1. *Consumers' personal inherent trust tendency fosters the consumer trust in B2C second-hand car e-commerce platforms*.

2. Personal vehicle knowledge level

In the transaction situation, the degree of consumer knowledge of a good can directly affect trust formation.

Luhmann (1979) believed that the more familiar consumers are, the easier it is to alleviate internal doubts and confusion, and thus the more likely they are to develop trust [22]. Wu Shaowei (2006) argued that the size of a consumer's knowledge base affects his ability to receive, process and perceive information [23]. All these indicate the important role of knowledge level for the formation of consumer trust.

For a commodity with many technical parameters such as automobiles, this paper argues that consumers who have more knowledge about vehicles are less likely to reject the second-hand car e-commerce transaction method. The following hypothesis is proposed:

H2. *Consumers' personal vehicle knowledge level increases the consumer trust in B2C second-hand car e-commerce platforms*.

3. Personal online shopping experience

Koufaris (2002) believed that consumers with more experience can better use online shopping as a consumption channel [24]. Chen Chen (2015) stated that those consumers who have experience in online shopping have a deeper understanding of e-commerce and are more receptive to new models [25]. This paper argues that consumers' previous online shopping experience can contribute to whether they choose to buy second-hand cars online. The following hypothesis is proposed:

H3. *Consumers' personal online shopping experience raises the consumer trust in B2C second-hand car e-commerce platforms*.

2.1.2. System Environmental Factors

In addition to individual subjective factors, objective environmental factors are also the main aspects affecting trust formation. The objective environment of second-hand car e-commerce transactions includes laws and regulations; third-party certification; and industry technology.

1. Laws and regulations

McKnight et al. (2000) believe that sound laws and regulations will affect consumers' trust level [26]. Chen Yini (2010) argued that a secure environment brings behavioral dependence to consumers [27]. There are many legal risks in second-hand car transactions, such as stolen cars, illegal unprocessed cars and concealed vehicle failure history. Therefore, the laws and regulations related to second-hand car network transactions are particularly important. It directly determines the consumer's sense of security, which in turn affects consumer trust. The following hypothesis is proposed:

H4. *Laws and regulations influence the consumer trust in B2C second-hand car e-commerce platforms*.

2. Third-party certification

The third-party certification mechanism is the basic condition for the explosive growth of e-commerce in China. For example, Taobao sets up crown certification for sellers and the 268V vehicle inspection service is provided by the CarEasy platform. Chen Xianyou (2013) believed that third-party certification would improve consumers' trust [28]. Yoon and Occeña (2015) pointed out that third-party certification significantly affects consumers' trust in e-commerce platforms [29]. Vehicle transactions involve a large number of technical parameters, which are a key basis for second-hand car valuation and consumer purchase decisions. Authoritative certifications make consumers more likely to trust e-commerce platforms. The following hypothesis is proposed:

H5. *Third-party certification of platforms promotes the consumer trust in B2C second-hand car e-commerce platforms*.

3. Industry technology level

Yan Zhonghua (2004) argued that technological trust is a subjective concept that facilitates transactions [30]. Wang Shouzhong (2007) pointed out that the Internet has been able to develop in China, which is inseparable from the developed financial system and logistics and distribution system, which are closely related to transactions [31]. Tian Zhaohui (2020) argued that second-hand car e-commerce platforms should facilitate transactions with the help of innovative technologies such as artificial intelligence to accomplish services such as product pricing, intelligent inspection and integration of logistics information [32]. The level of industrial technology referred to in this study is mainly that of the two industries, automotive and Internet. The following hypothesis is proposed:

H6. *Industry technology level may increase the consumer trust in B2C second-hand car e-commerce platforms*.

2.1.3. Website/APP factors

At the first step of forming online trust between the two sides of the transaction, those at both sides of the transaction have never met each other and are strangers to each other; the first impression or some details will affect the formation of trust.

1. Ease of use of the website/APP

Ease of use is essentially the cost of use for consumers. Stanford (2002) argued that a website that is designed to have consumers up and running quickly gives a good start to building consumer trust [33]. Zeng Guichuan (2015) showed that the ease of use of a mobile app significantly affects the user's usage behavior [34]. In this paper, we argue that the ease of use of the website/APP of second-hand car e-commerce platforms in terms of appearance design, navigation functions and related links affects consumers' perceptions and experiences. The following hypothesis is proposed:

H7. *The ease of use of the website/APP increases the consumer trust in the B2C second-hand car e-commerce platform*.

2. Security of website/APP

The security of a website/APP includes two aspects: transaction security and personal information security. Zhang Gaoliang (2014) showed that the level of security of online transactions has a significant positive impact on users' trust and satisfaction [35]. The importance of website/app security is accentuated by the high customer unit price of second-hand car transactions. The following hypothesis is proposed:

H8. *The security of a website/APP fosters the consumer trust in a B2C second-hand car e-commerce platform*.

2.1.4. Platform Company Factors

The background, reputation and level of operation of the e-commerce platform company in the B2C model are also factors that consumers consider.

1. Company size

The company size means the depth of the company's product offerings and the breadth of its services. Liu Junqing (2015) showed that the larger the e-commerce platform, the higher the level of trust generated [36]. Lv Xiaojing (2019) believes that the larger scale of e-commerce platforms means that they can provide better services, and they can better meet the needs of different consumers [37].

Larger second-hand car e-commerce platform companies generate stronger network externalities and attract more consumers' attention. Additionally, they have better second-hand car sources as well as supporting service providers, which further facilitate consumer experience and help generate trust. Therefore, the following hypothesis is proposed:

H9. *The strength of the platform company's size increases the consumer trust in a B2C second-hand car e-commerce platform*.

2. Company brand reputation

McKnight et al. (1998) argued that corporate reputation is a key factor for e-commerce merchants to build trust [38]. Xiang Luquan (2020) pointed out that the better a company's brand reputation, the more it can improve consumers' trust in the merchant [39]. The following hypothesis is proposed:

H10. *The brand reputation of the platform company increases the consumer trust in a B2C second-hand car e-commerce platform*.

Based on the research hypotheses established above, the research model shown in Figure 2 was constructed.

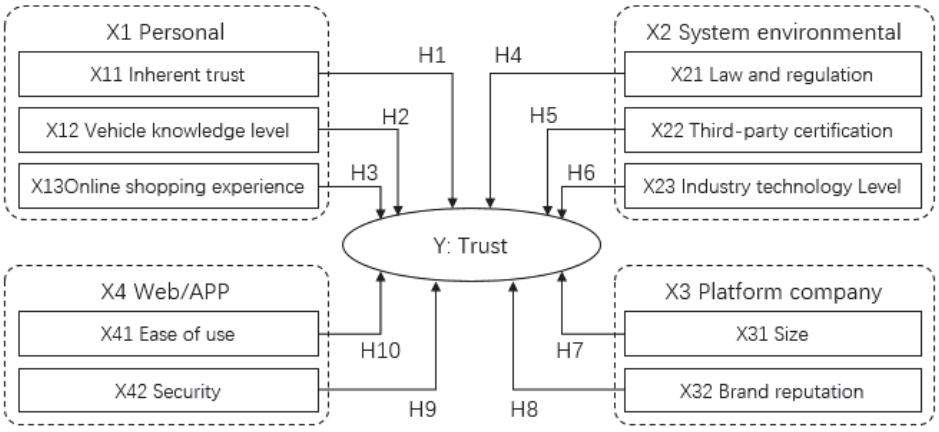

Figure 2. Consumer trust mechanism model of second-hand car e-commerce platforms.

2.2. Research Methodology

This study collected data by questionnaire. Based on the relevant literature and the consumer trust characteristics of a used-car e-commerce platform, the scale was developed and more than three questions were designed for each measurement variable to improve the validity of the questionnaire, as shown in Table 1. After the design and pre-test of the first draft of the questionnaire, the questionnaire that meets the needs of this study was finally formed.

Table 1. Variables and index.

Variables		Index
Personal trust tendency	PT1	I believe that in most cases, human nature is kind.
	PT2	Generally speaking, I usually trust a person or thing, even if I don't know much about it.
	PT3	I will not take the initiative to suspect a person until there is evidence that this person is not trustworthy.
Personal vehicle knowledge	PK1	I have the experience of buying vehicles and have a certain understanding of the nature of vehicles.
	PK2	I understand the basic knowledge of vehicles, such as engine, gearbox, chassis, etc.
	PK3	I understand the meaning of some vehicle performance parameters and can compare them, such as horsepower, torque, fuel consumption, etc.
Personal online shopping experience	PE1	When I have shopping needs, I will choose to use e-commerce to find goods and have done online shopping.
	PE2	I understand the process of online shopping, have dealt with customer service, and have tried after-sales service.
	PE3	During online shopping, I can smoothly complete the steps of product retrieval, order confirmation, online payment, etc.
Laws and regulations	LR1	I know more about the existing laws and regulations related to e-commerce industry and automobile industry in China
	LR2	I think the relevant e-commerce laws can effectively ensure the safety of online shopping.
	LR3	I think the relevant laws and regulations of the second-hand car industry can guarantee the rights and obligations of both parties.
Third-party certification	TR1	I think the third-party certification is very important for the used car e-commerce platform.
	TR2	I think the third-party authoritative certification provides guarantee for the capability and legal compliance of the second-hand car e-commerce platform.
	TR3	I believe that a third party can protect my rights and interests when the other party does not act in good faith.
Industrial technology	IT1	I usually pay attention to the development of some industrial technologies and future technologies.
	IT2	I think the technology of automobile industry can guarantee the quality of automobiles and meet my needs.
	IT3	I think the Internet night technology can enable me to use the Internet safely and efficiently.
Website/APP perceived ease of use	PU1	The rationality of website interface design or APP interactive interface design helps me believe that the website can be used for the sake of users.
	PU2	The timeliness of the response of the website or APP helps me believe in the authenticity of the platform's information.
	PU3	When browsing the website or APP, when I encounter problems, if I can find official guidance on the website APP, I will feel very convenient.
Website/APP perceived security	PS1	The authority and popularity of the certification party and partner of the website or APP will affect my judgment on the security of the website.
	PS2	When browsing the website or APP, if the website or APP will inform the user of the personal information protection policy, then I think it is safer to change the website.
	PS3	When confirming the order and paying, if it is a traditional payment method (WeChat, Alipay, UnionPay card, etc.), I will feel that the transaction payment is safer.

Table 1. *Cont.*

Variables		Index
company size	CS1	I think large companies can provide me with better products and services.
	CS2	I think a strong company can better meet my needs.
	CS3	If the brand awareness of the two companies is equal, I will choose the company with a larger market share.
Company brand reputation	CR1	I think companies with good reputation can be more honest and trustworthy with consumers.
	CR2	I think companies with high brand awareness pay more attention to consumer relationship maintenance.
	CR3	If both companies can meet my needs, I will choose the company with less negative comments.
Consumer trust	CT	I believe that the company has the intention and ability to provide products and services that satisfy me.

First, we interviewed second-hand car consumers and second-hand car experts, combined with existing theoretical scales, for the initial development of the questionnaire. It was distributed to neighboring friends as a trial fill and revised and finalized. At the same time, before we asked the respondents to fill in the questionnaire, we solicited the opinions of the respondents and explained the purpose of the questionnaire in detail. The questionnaire includes an introduction and body. In the introduction, we explained the purpose and significance of this study in detail, and emphasized that it is only for theoretical research, does not involve personal privacy and does not pose any risk to individuals and the public. The respondents could refuse to fill in the questionnaire. In the body, they did not need to fill in the identity information. Finally, we used the "Questionnaire Star" to make a questionnaire that is easy to fill in, and distributed it using online tools. Then, it was distributed to them using web tools, and, finally, 468 questionnaires were collected, of which 410 were valid.

After statistical analysis, it was found that 57.56% of the respondents were female and 42.44% were male, basically in line with the reality that women are the main group in e-commerce consumption. From the age distribution, it can be seen that 20–29 year-old plus 30–39 year-old people accounted for 69.27% of the respondents, and the younger group showed a stronger interest in new things. People with a bachelor's degree or above accounted for the majority, accounting for 67.07%.

The number of people who have had the experience of purchasing a car in the questionnaire survey is 237, accounting for 57.80%, more than those who have not had the experience of purchasing a car. The number of respondents who have a license is 68.78%, more than those who do not have a driver's license, basically in line with the proportion of people who have a driver's license in the total population. A total of 92.44% of the respondents maintain the habit of online shopping; only 7.56% said they do not shop online at all. People who have used a second-hand trading platform accounted for 39.27% of the interviewed population, of which only 7.56% have used a second-hand car e-commerce platform, indicating the low popularity of second-hand car e-commerce platforms. It can be found that the basic background of the interviewees is basically in line with the development pattern of Chinese society and the e-commerce industry, which lays the foundation for the subsequent analysis and research.

3. Empirical Analysis

3.1. Reliability and Validity Analysis

In the reliability analysis, the Cronbach's alpha coefficient of the measured questionnaire data is 0.919, which is greater than 0.8, indicating that the overall reliability of the questionnaire is very good. In the validity analysis, the value of sample KMO is 0.927,

which is higher than 0.7, indicating that there are more common factors among variables. The Bartlett's test of sphericity approximate chi-square value is 7755.876, the degree of freedom reaches 528 and the obtained result is significant, indicating that there are common factors in the correlation matrix of the group, based on which this questionnaire is considered suitable for factor analysis and the total amount reaches validity.

3.2. Model Test

3.2.1. Validation of the Structural Equation Model

In this study, the model was tested for goodness of fit using AMOS, and the chi-square test index of the model goodness of fit reached χ2/df 2.019, an RMSEA of 0.05, a TLI index of 0.928, a CFI index of 0.940, a PNFI index of 0.741 and a PGFI index of 0.783; all of these major indices reached a very high level. The GFI value is 0.887, the AGFI value is 0.856 and the NFI value is 0.889, and the regression levels of these three indices are within a reasonable range. See Table 2 for details. Based on the above indices, we can assume that the fit of the model can meet the needs of validation.

Table 2. Analysis of the results of the overall model fit test.

Indicator	Evaluation Indicators		Value	Judgment
	Able to Accept	Better		
χ^2/df	3~5	1~3	2.019	Better
RMSEA	0.08~0.10	<0.08	0.050	Better
GFI	0.80~0.90	>0.90	0.887	Able to accept
AGFI			0.856	Able to accept
NFI	0.80~0.90	>0.90	0.889	Able to accept
TLI			0.928	Better
CFI			0.940	Better
PNFI	>0.50		0.741	Better
PGFI			0.783	Better

In this study, the structural equation was chosen to test the paths of the two groups of consumer personal factors and system environmental factors; SPSS was chosen to conduct regression analysis on the website/APP factors and the platform company factors. The reason for this is that both consumer personal factors and system environmental factors contain three independent variables, which can be correlated two by two in the structural equation; both website/APP factors and platform company factors contain two independent variables, and if the structural equation is chosen to describe their paths, it will affect the overall fit and the quality of the path test. Based on this, the variables are divided into two groups and, using two methods, are tested below.

Using AMOS software, the degree of fit of the consumer trust part of the model was calculated by choosing the maximum likelihood method and the oblique rotation method, and the results are shown in Table 3.

Table 3. Table of the results of the overall goodness-of-fit test of the study model.

Indicators	χ^2/df	GFI	AGFI	CFI	TLI	RMSEA
Results	3.168	0.893	0.860	0.895	0.875	0.073
Judgment	True	True	True	True	True	True

The results of the path test for a total of six variables in two groups of factors, consumer personal factors and system environmental factors, are shown in Table 4.

Table 4. Consumer factors and system environmental factors—path coefficient results table.

Path	Estimate	B	S.E	C.R	ρ-Value	Sig.
H1: X_{11}→Y	0.043	0.083	0.034	1.285	0.199	No
H2: X_{12}→Y	0.121	0.333	0.021	5.810	***	Yes
H3: X_{13}→Y	0.202	0.520	0.027	7.564	***	Yes
H4: X_{21}→Y	−0.079	0.151	0.054	1.465	0.143	No
H5: X_{22}→Y	0.101	0.229	0.043	2.337	*	Yes
H6: X_{23}→Y	0.508	0.843	0.085	5.979	***	Yes

Note: In the ρ-value column, *** indicates $p < 0.001$ and * indicates $p < 0.05$.

In the above table, Estimate is the path coefficient, B marks the standardized path coefficient, S.E is the standard error of the regression sampling distribution and C.R and ρ-value are used to measure significance: less than 1.96 means it failed the significance test; C.R greater than 1.96, i.e., $p < 0.05$, means that the path coefficient is significant at the level of 0.05; C.R greater than 2.58, i.e., $p < 0.01$, represents that the path coefficient is significant at the level of 0.01; and C.R greater than 3.3, i.e., $p < 0.001$, represents that the path is significant at the level of 0.001. According to the results of path analysis, it can be found that personal vehicle knowledge level, personal online shopping experience, third-party certification and industry technology level have a significant positive influence on second-hand car e-commerce platform consumer trust; personal inherent trust tendency and laws and regulations cannot positively promote second-hand car e-commerce platform consumer trust.

3.2.2. Linear Regression Analysis

The relationship between the remaining two groups of variables and consumer trust was investigated using regression analysis.

1. Regression analysis of website/APP factors (X3) and consumer trust (Y)

Two sub-variables under the website/APP factor (X3), ease of use of the website/APP (X31) and security of the website/APP (X32), were regressed on the dependent variable consumer trust. The regression results are presented in the Table 5.

Table 5. Regression results of website/APP factors.

Variables	Non-Standardized Coefficients	Standardized Coefficients	t	Sig.	VIF
Constant	5.272		16.992	0.000	
X_{31}	0.318	0.468	9.526	0.000	2.186
X_{32}	0.231	0.328	6.676	0.000	
	Sig.F			Sig. = 0.000	
	R^2			0.552	
	Adjusted R^2			0.549	
	Durbin–Watson coefficient			1.826	

In the regression for the website/APP factor, the adjusted R^2 value of 0.549 is greater than 0.4, indicating that the ease of use of the website/APP (X31) and the security of the website/APP (X32) contribute to 54.9% of the degree of change in consumer trust (Y). The significance of the F-value in the regression results is under 0.05, which shows that the model has a good goodness of fit. Looking at the Durbin–Watson coefficient and VIF values, after the regression, the Durbin–Watson coefficient of ease of use of the website/APP (X31) and security of website/APP (X32) is 1.826, which is close to 2, and the VIF value is 2.186, which is in the 1–10 acceptable range. Based on the above two points, it can be concluded that the ease of use of the website/APP (X31) and the security of the website/APP (X32) do not have first-order autocorrelation and multicollinearity, and can support linear regression analysis.

The values of the standard coefficients of ease of use of the website/APP(X31) and the security of the website/APP (X32) are 0.468 and 0.328, respectively, indicating that they both have a positive effect on consumer trust, and that ease of use of the website/APP (X31) has the largest effect on consumer trust (Y). The significance of both variables is below 0.05, which shows that ease of use of the website/APP (X31) and the security of the website/APP (X32) have a significant positive relationship with consumer trust. The conclusion of the regression analysis verifies hypotheses H7 and H8. The standardized regression coefficients were used to establish the equation:

Consumer trust = 0.468 × ease of use of the website/APP (X31) + 0.328 × security of the website/APP (X32).

2. Regression analysis of platform company factors (X4) and consumer trust (Y)

Multiple regression analysis was conducted on the two sub-variables under the platform company factors (X4), company size (X41) and company brand reputation (X42), and the dependent variable consumer trust, and the regression analysis results are tabulated as Table 6.

Table 6. Regression results of platform company factors.

Variables	Non-Standardized Coefficients	Standardized Coefficients	t	Sig.	VIF
Constant	5.312		13.064	0.000	
X_{41}	0.221	0.312	5.232	0.000	2.465
X_{42}	0.293	0.372	6.247	0.000	
	Sig.F			Sig. = 0.000	
	R^2			0.414	
	Adjusted R^2			0.411	
	Durbin–Watson coefficient			2.013	

In the regression analysis of the platform company factors, the value of adjusted R^2 is 0.411, which is greater than 0.4. The company size (X41) and company brand reputation (X42) lead to a 41.1% degree of change in consumer trust, and the significance of the F-value in the regression results is under 0.05, which shows that the model has a good goodness of fit. Looking at the Durbin–Watson coefficient and VIF values, the Durbin–Watson coefficient of the company size (X41) and company brand reputation (X42) is 2.013, which is close to 2, and the VIF value is 2.465, which is between 1 and 10 in the acceptable range. Based on the above two points, it can be concluded that there is no first-order autocorrelation and multicollinearity between company size (X41) and company brand reputation (X42), which can support linear regression analysis.

The values of the standard coefficients of company size (X41) and company brand reputation (X42) are 0.312 and 0.372, respectively, indicating that they both have a positive effect on consumer trust, and that company brand reputation has the largest effect on consumer trust. The significance of t-values for both variables is below 0.05, which shows that company size (X41) and company brand reputation (X42) have a significant positive relationship with consumer trust. Hypotheses H9 and H10 pass the test. The standardized regression coefficients were used to establish the regression equation.

Consumer trust = 0.312 × company size (X41) + 0.372 × company brand reputation (X42).

3.3. Results Summary

A total of 10 hypotheses have been proposed in this paper. Except H1 and H4, all the other hypotheses have passed the verification. The explanation is as follows:

(1) The influence coefficient of consumers' personal trust tendency on the trust standardization path of a second-hand car e-commerce platform is 0.083, and the ρ-value is 0.199, which is greater than the minimum requirement of 0.05 for the significance test and fails to pass the significance test. Hypothesis H1 is not valid. This may be because people are more cautious about goods such as cars on virtual trading

platforms. Consumers' old trust mechanisms cannot be transferred to something as new as online second-hand car trading.

(2) The influence coefficient of consumers' personal vehicle knowledge on the standardized path of trust of a second-hand car e-commerce platform is 0.333, and the ρ-value is less than 0.001, passing the significance test, and the influence degree is 0.333, assuming H2 is valid. Its internal mechanism is as follows: people who know more about vehicle parameters will be more capable and confident to judge the quality of second-hand cars, so they are more likely to buy on second-hand car e-commerce platforms.

(3) The influence coefficient of consumers' personal online shopping experience on the standardized path of trust of a second-hand car e-commerce platform is 0.520, and the ρ-value is less than 0.001, passing the significance test, and the influence degree is 0.333. Hypothesis H3 is valid. A second-hand car e-commerce platform is essentially similar to online trading platforms for other commodities. In addition, a second-hand car e-commerce platform will design the transaction process and services in line with the habits of online shoppers. Therefore, consumers with more online shopping experience will have lower psychological barriers to a second-hand car e-commerce platform and will be more likely to have purchasing behaviors.

(4) The influence coefficient of laws and regulations on the standardized path of trust of a second-hand car e-commerce platform is −0.079, and the ρ-value is 0.143, which is greater than the minimum requirement of 0.05, and fails to pass the significance test. Hypothesis H4 is not valid. The reason may be that Chinese e-commerce law is not perfect, and it takes some time and process to popularize the law.

(5) The influence coefficient of the third-party certification on the standardized path of trust of a second-hand car e-commerce platform is 0.229, and the ρ-value is less than 0.01. It passes the significance test, and the influence degree is 0.229, assuming that H5 is valid. Third-party certification agencies can improve the trust in a second-hand car e-commerce platform in the eyes of consumers. The more authoritative the certification, the stronger the sense of trust.

(6) The influence coefficient of industrial technology on the trust standardization path of a second-hand car e-commerce platform is 0.508, and the ρ-value is less than 0.01. It passes the significance test, and the influence degree is 0.508. Hypothesis H6 is valid. The more technologically sophisticated the industry, the more trustworthy the commodity itself and the transaction itself. On the contrary, new energy vehicles are rarely traded on second-hand car trading platforms because their technology is not mature.

(7) The trust standard coefficient of perceived ease of use of the website/APP of a second-hand car e-commerce platform is 0.468, the ρ-value is less than 0.001, passing the significance test, and the influence degree is 0.508, assuming that H7 is valid. If the interaction design of a platform's website/APP allows consumers to learn quickly and find the information they want easily, it will be easier to build trust.

(8) The standard coefficient of trust of the perceived safety of the website/APP of a second-hand car e-commerce platform is 0.328, the ρ-value is less than 0.001, passing the significance test, and the influence degree is 0.328, assuming that H8 is valid. Consumers receive security information such as website/APP security agreement terms and privacy protection measures. The easier this information is perceived by consumers, the stronger the sense of trust will be.

(9) The standard coefficient of trust of the scale and strength of a company's platform of a second-hand car e-commerce platform is 0.312, and the ρ-value is less than 0.001, passing the significance test, and the influence degree is 0.312, assuming that H9 is valid. This is consistent with the general law of business, which is that the larger the company, the more people recognize its strength. Consumers are more likely to trade with large firms than small ones.

(10) The standard coefficient of trust of a company's brand reputation of a second-hand car e-commerce platform is 0.372, and the ρ-value is less than 0.001, which passes

the significance test, and the influence degree is 0.372. Hypothesis H10 is valid. The better a platform's brand reputation, the easier it is to create trust. Consumers tend to pay less attention to product performance and price due to brand trust.

4. Conclusions and Discussions

4.1. Theoretical Implications

Results of this study indicate that consumer trust in used-car e-commerce comes from many factors. In terms of personal factors, consumers' mastery of commodities and familiarity with online shopping are the internal factors that determine whether consumers choose to purchase second-hand cars on a second-hand car e-commerce platform. Therefore, businesses selling vehicles on a platform should be highly professional. In terms of system factors, technical level and authoritative certification are the external factors that determine whether consumers trust used-car e-commerce. It can be considered that the more mature the automobile industry is, the more likely it is to trade second-hand cars through the Internet, and the more likely it is to succeed in the e-commerce model of second-hand cars. On the contrary, when the industry itself is not mature, it may be impossible to conduct transactions through the network. Business factors such as enterprise scale, brand influence and user interface experience can affect the formation of consumer trust. Industry facts also show that it is difficult for used-car e-commerce enterprises to fully rely on their own resources and capabilities in the early stage and gradually accumulate customers in order to achieve endogenous development. They often introduce capital at an early stage, combine industry forces to rapidly increase the flow, and then iteratively optimize their products and services to achieve endogenous development.

4.2. Practical Implications

A second-hand car e-commerce platform has the characteristics of high unit price and low frequency. Therefore, establishing the initial trust of consumers and improving the degree of trust of consumers is the top priority to trigger the purchase behavior [40].

Broadly speaking, in order to strengthen the environment of trust in the second-hand car trade, the following should be considered:

- Improve the Internet legal system and standardize the trading order of the second-hand car e-commerce platform.
- Increase publicity of legal knowledge to improve consumers' cognition of second-hand car e-commerce trading rules.

In a narrow sense, a second-hand car e-commerce platform should improve its service management level, improve consumers' sense of experience on the service contact surface and thus increase the sense of trust. Specific measures are as follows:

- A platform should take consumer groups who prefer online shopping as the preferred target market.
- The selection and evaluation mechanism of service providers should be designed for the second-hand car e-commerce platform to ensure the service level of service providers.
- Introduce local third-party authoritative certifications, including second-hand car quality certification, e-commerce platform qualification certification, etc.
- The interface design of the platform should use colors and layouts that help consumers improve their trust and highlight information such as quality certification and transaction evaluation.
- Attach importance to brand image construction and maintenance, and constantly improve brand awareness and reputation.
- A second-hand car e-commerce platform should train the service team and improve the professional quality of the team.

4.3. Limitations and Future Research

This study is not free of limitations. First of all, some of the respondents used are mainly from the researcher's circle of friends, which may have some limitations. In the future, user feedback data can be obtained through more channels to improve sample quality. Second, this study only uses the questionnaire method, not the qualitative method, so the information obtained is still limited. Some representative used-car e-commerce enterprises can be selected to carry out in-depth case studies.

Author Contributions: Conceptualization, X.L. and J.M.; Methodology, X.L. and J.M.; Validation, J.M.; Investigation, X.L., J.M., X.Z. and R.Y.; Writing—original draft, X.L., J.M. and X.Z.; Writing—review & editing, J.M., X.Z. and R.Y.; Project administration, X.L. All authors have read and agreed to the published version of the manuscript.

Funding: This research received no external funding.

Institutional Review Board Statement: Not applicable.

Informed Consent Statement: Not applicable.

Data Availability Statement: Not applicable.

Conflicts of Interest: The authors declare no conflict of interest.

References

1. Akerlof, G.A. The Markets for "Lemons": Quality Uncertainty and The Market Mechanism. *Q. J. Econ.* **1970**, *84*, 485–500. [CrossRef]
2. Lee, S.M.; Lee, S. Consumers' initial trust toward second-hand products in the electronic market. *J. Comput. Inf. Syst.* **2005**, *46*, 85–98.
3. Tajvidi, M.; Wang, Y.; Hajli, N.; Love, P.E. Brand Value Co-creation in Social Commerce: The Role of Interactivity, Social Support, and Relationship Quality. *Comput. Hum. Behav.* **2021**, *115*, 105238. Available online: https://www.sciencedirect.com/science/article/abs/pii/S0747563217306271 (accessed on 8 November 2017). [CrossRef]
4. Alalwan, A.A.; Dwivedi, Y.K.; Rana, N.P. Factors influencing adoption of mobile banking by jordanian bank customers: Extending utaut2 with trust. *Int. J. Inf. Manag.* **2017**, *37*, 99–110. [CrossRef]
5. Gefen, D.; Straub, K.D.W. Trust and tam in online shopping: An integrated model. *MIS Q.* **2003**, *27*, 51–90. [CrossRef]
6. Kim, S.; Park, H. Effects of various characteristics of social commerce (scommerce) on consumers' trust and trust performance. *Int. J. Inf. Manag.* **2013**, *33*, 318–332. [CrossRef]
7. Chen, J.; Shen, X.L. Consumers' decisions in social commerce context: An empirical investigation. *Decis. Support Syst.* **2015**, *79*, 55–64. [CrossRef]
8. El Amri, D.; Akrout, H. Perceived design affordance of new products: Scale development and validation. *J. Bus. Res.* **2020**, *121*, 127–141. [CrossRef]
9. Hillman, S.; Neustaedter, C. Trust and Mobile Commerce in North America. *Comput. Hum. Behav.* **2017**, *70*, 10–21. [CrossRef]
10. Fang, Y.; Qureshi, I.; Sun, H.; McCole, P.; Ramsey, E.; Lim, K.H. Trust, Satisfaction, and Online Repurchase Intention: The Moderating Role of Perceived Effectiveness of E-commerce Institutional Mechanisms. *Mis Q.* **2014**, *38*, 407–427. [CrossRef]
11. Hartl, B.; Hofmann, E.; Kirchler, E. Do We Need Rules for "What's Mine is Yours"? Governance in Collaborative Consumption Communities. *J. Bus. Res.* **2016**, *69*, 2756–2763. [CrossRef]
12. Wan, J.; Lu, Y.; Wang, B.; Zhao, L. How attachment influences users'willingness to donate to content creators in social media: A socio-technical systems perspective. *Inf. Manag.* **2016**, *54*, 837–850. [CrossRef]
13. Jiang, C.; Rashid, R.M.; Wang, J. Investigating the role of social presence dimensions and information support on consumers' trust and shopping intentions. *J. Retail. Consum. Serv.* **2019**, *51*, 263–270. [CrossRef]
14. Masele, J.J.; Matama, R. Individual consumers' trust in B2C automobile e-commerce in Tanzania: Assessment of the influence of web design and consumer personality. *Electron. J. Inf. Syst. Dev. Ctries.* **2020**, *86*, e12115. [CrossRef]
15. Jone, K.; Leonard, F.N.K. Factors influencing buyer's trust in consumer to consumer E- commerce. *J. Comput. Inf. Syst.* **2014**, *54*, 71–79.
16. Sutanonpaiboon, J.; Abuhamdieh, A. Factors influencing trust in online consumer-to-consumer (C2C) transactions. *J. Internet Commer.* **2008**, *7*, 203–220. [CrossRef]
17. Moorman, C.; Zaltman, G. Factors affecting trust in market research relationships. *J. Mark.* **1993**, *57*, 81–101. [CrossRef]
18. Mayer, R.C.; Davis, J.H.; Schoorman, F.D. An Integrative Model of Organizational Trust. *Acad. Manag. Rev.* **1995**, *20*, 709–734. [CrossRef]
19. Gefen, D.; Straub, D.W. Consumer Trust in B2C E-commerce and the Importance of the Social Presence: Experiments E-Products and E-service. *Omega Inter-Natl. J. Manag. Sci.* **2004**, *8*, 1–18. [CrossRef]

20. Lee, M.K.O.; Turban, E. A Trust Model for Internet Shopping. *Int. J. Electron. Commer.* **2001**, *6*, 75–91. [CrossRef]
21. Heyns, M.; Rothmann, S. Dimensionality of trust: An analysis of the relations between propensity, trustworthiness and trust. *SA J. Ind. Psychol.* **2015**, *41*, 1–12. [CrossRef]
22. Luhmann, N. *Trust and Power*; John Wiley &Sons Vhichester: New York, NY, USA, 1979.
23. Wu, S. Analysis of Influencing Factors of Consumers' Online Trust. *Econ. Forum* **2006**, *23*, 43–46.
24. Koufaris, M. Applying the Technology Acceptance Model and Flow Theory to Online Consumer Behavior. *Inf. Syst. Res.* **2002**, *13*, 205–223. [CrossRef]
25. Chen, C. *Measurement Research on Influencing Factors of Taobao Consumer C2C Mobile E-Commerce Trust*; Nanjing University: Nanjing, China, 2015.
26. McKnight, D.H.; Choudhury, V.; Kacmar, C. Trust in e-commerce vendors: A two-stage model. In Proceedings of the Twenty-First International Conference on Information Systems, ICIS 2000, Brisbane, Australia, 10–13 December 2000; pp. 532–536.
27. Chen, Y.; Jin, X. Research on Customer Segmentation based on the perspective of trust and Distrust in online shopping. *Manag. Mod.* **2010**, *1*, 12–14.
28. Chen, X. Research on Main Factors Influencing Consumer Trust in B2C Online Shopping Based on third-party Evaluation. *J. Credit Res.* **2013**, *31*, 39–42.
29. Yoon, H.S.; Occeña, L.G. Influencing factors of trust in consumer-to-consumer electronic commerce with gender andage. *Int. J. Inf. Manag.* **2015**, *35*, 352–363. [CrossRef]
30. Yan, Z.; Guan, S.; Miganin. The theoretical research of B2B E-commerce trust Model based on system. *Sci. Res. Manag.* **2004**, *25*, 76–810.
31. Wang, S. *Empirical Analysis of Factors Influencing initial Trust of Chi-nese B2C Consumers*; Southwest Jiaotong University: Chengdu, China, 2008.
32. Tian, Z. Study on the operation mode of second-hand car e-commerce in the new retail era. *J. Fujian Jiangxia Univ.* **2020**, *10*, 28–35.
33. Shankar, V.; Urban, G.L.; Sultan, F. Online Trust: A stakeholder perspective, concepts, implications, and future directions. *J. Strateg. Inf. Syst.* **2002**, *11*, 325–344. [CrossRef]
34. Zeng, G. *Research on Influencing Factors of Consumer Trust in Group-Buying Websites in the Context of Mobile E-Commerce*; Yunnan University of Finance and Economics: Kunming, China, 2015.
35. Zhang, G.; Zhu, W.; Zhu, J. The formation mechanism of consumer trust in business online group-buying model. *Ergonomics* **2014**, *20*, 50–55.
36. Liu, J. Research on Influencing factors of Consumer trust in B2C E-commerce. *Mod. Commer. Ind.* **2015**, *36*, 61–62.
37. Lu, X. Research on Influencing Factors of Consumer Trust in B2C. *Logist. Eng. Manag.* **2019**, *41*, 114–115+60.
38. McKnight, D.H.; Cummings, L.L.; Chervany, N.L. Chervany: Initial trust formation in new organization relationships. *Acad. Manag. Rev.* **1998**, *23*, 473–490. [CrossRef]
39. Xiang, L. Construction of theoretical model of Influencing Factors of Consumer trust in B2C E-commerce. *China Bus. Theory* **2020**, *3*, 27–28.
40. Huang, X.; Le, Z.; Tang, X. Current Situation Analysis and Development Suggestions of Chinese Second-hand Car Market. *Intern. Combust. Engine Accessories* **2021**, *3*, 174–176.

sustainability

MDPI

Article

The Dynamic Impacts of Economic Growth, Financial Globalization, Fossil Fuel, Renewable Energy, and Urbanization on Load Capacity Factor in Mexico

Asif Raihan [1], Mamunur Rashid [2], Liton Chandra Voumik [3], Salma Akter [3] and Miguel Angel Esquivias [4,*]

[1] Institute of Climate Change, Universiti Kebangsaan Malaysia, Bangi 43600, Malaysia; asifraihan666@gmail.com
[2] Department of Information Technology, School of Business & Technology, Emporia State University, Emporia, KS 66801, USA; mrashid1210@gmail.com
[3] Department of Economics, Noakhali Science and Technology University, Noakhali 3814, Bangladesh; litonvoumik@gmail.com (L.C.V.); salmanstu97@gmail.com (S.A.)
[4] Department of Economics, Airlangga University, Surabaya 60286, Indonesia
* Correspondence: miguel@feb.unair.ac.id

Abstract: This study explores the interplay among economic growth, financial globalization, urbanization, fossil fuel consumption, and renewable energy usage and their combined impact on the load capacity factor in Mexico. This research employs the load capacity factor as a unique measure of ecological health, facilitating a comprehensive ecosystem assessment by sequentially evaluating biocapacity and ecological effects. Using time series data spanning from 1971 to 2018, this study employs the Autoregressive Distributed Lag (ARDL) method to analyze both long-term and short-term dynamics and cointegration. The findings reveal that economic growth, fossil fuel usage, and urbanization reduce Mexico's load capacity factor, thereby diminishing environmental quality. In contrast, the adoption of renewable energy sources and the influence of financial globalization exhibit positive effects on the load capacity factor over the long and short term. These outcomes remain consistent even when compared with alternative estimation techniques, including dynamic ordinary least squares (DOLS), fully modified least squares (FMOLS), and canonical cointegrating regression (CCR). As a priority, Mexican policymakers should accelerate the transition to renewable energy sources, encourage sustainable urban development, and foster a more ecologically conscious economic agenda. Furthermore, promoting greener technologies can enhance the load capacity and mitigate environmental degradation. Ultimately, Mexico can establish an environment conducive to expanding sustainable investments by encouraging cross-border investments, enabling global trade in financial services, and cultivating greater integration of capital and financial markets.

Keywords: load capacity factor; fossil fuel; ecological degradation; financial globalization; renewable energy; sustainable development

1. Introduction

Despite increased climate change awareness, emissions of greenhouse gases and other pollutants from fossil fuel use, industrial processes, transportation, and human activities persist at elevated levels. The public's better grasp of climate change has yet to reduce ecological harm [1,2]. The barrier to mitigating climate devastation partly endures due to a lack of affordable technical solutions, inadequate policy-making, and uncoordinated sustainability efforts [3,4]. In 2022, the International Energy Agency reported a record 36.8 gigatons of CO_2 emissions, up 0.9% from the prior year, driven by a growing global economy and energy demand [5,6]. Consequently, the UN Framework Convention on Climate Change emphasizes reinforcing the Paris Agreement via concerted state and collaborative efforts. Prominent nations like the UK, Brazil, France, Japan, Germany, and Mexico

have pledged substantial CO_2 reduction commitments despite ongoing environmental degradation [7,8].

The nexus of globalization, ecological preservation, and economic growth is a current debate [9,10]. Expanding global trade will likely elevate energy use and greenhouse gas emissions, particularly as developing nations seek economic advancement via integration and innovation [11,12]. Dreher's globalization index [13] and Gygli et al.'s extended version [14] illuminate these dynamics, including the ecological impacts of trade and finance globalization. Dreher's [13] calculations could not differentiate between the ecological effects of global trade and global finance. In contrast, using Gygli et al.'s calculations [14] allows us to distinguish between the ecological consequences of trade and financial globalization. This study employs the financial globalization index, encompassing de facto (e.g., reserves, overseas income payments) and de jure (e.g., investment agreements) dimensions to analyze if financial globalization and urbanization aid developing nations in achieving economic prosperity without ecological harm. Amid interconnected financial globalization, fossil fuels, renewable energy, and urbanization concerns, this research offers policy insights to address ecological degradation.

Carbon emissions are under intense study, revealing threats to environmental quality in developing nations like India, Mexico, Malaysia, the BRICS, and South Asian countries due to economic growth, global trade, population increase, and non-renewable resource usage [6,15–17]. However, Akinsola et al. [18] underline that carbon output, a significant GHG component, inadequately reflects ecological damage in both advanced and developing nations [19–21]. These analyses focus primarily on ecological impact, overlooking ecosystem resources [22]. Thus, finding a superior indicator for holistic environmental assessment is paramount, as was first proposed by Rees [23]. The load capacity factor, presented by Siche et al. [24], offers a more precise ecological insight. Calculated by dividing biocapacity (supply) by ecological footprint (demand), a factor above 1 indicates stability, while below 1 implies unsustainability [3]. Unlike carbon emissions or ecological impact, the load capacity factor provides a comprehensive index. This study advances comprehensive analysis by considering the broader ecological context.

Numerous studies have explored how environmental factors impact carbon emissions and ecological footprints across countries or groups [19–21]. However, there is a research gap in investigating the dynamic interactions of environmental variables with the load capacity factor, especially concerning Mexico. Earlier studies largely concur that financial development and greater renewable energy integration curb CO_2 emissions or ecological footprint [1,2,18]. In contrast, economic growth, non-renewable energy usage, urbanization, and trade openness often correlate with elevated CO_2 levels [2,9,25]. However, few studies have examined these variables' impact on CO_2 and biocapacity, yielding a more holistic environmental quality evaluation.

Moreover, existing literature requires more conclusive insights into the effects of urbanization and financial globalization on the load capacity factor. This study aims to bridge this gap by examining the dynamic relationships between economic growth, financial globalization, fossil fuel and renewable energy use, urbanization, and the load capacity factor. Utilizing the case of Mexico, one of the world's largest emerging economies, we employ the latest econometric techniques to provide comprehensive insights.

Mexico was chosen for this study due to significant factors. As of 2019, Mexico was Latin America's second-largest economy and ranked fifteenth globally, with a GDP of USD 1.25 trillion and a per capita income of USD 10,013 [26]. Mexico draws increased foreign investments as a G-20, OECD, and WTO member. Its financial globalization index rose from 40 to 69 points between 1970 and 2020, positioning it as one of Latin America's most globalized economies. Mexico's industrial and service sectors heavily rely on fossil fuels, ranking eleventh and thirteenth in crude production and net exports. The country is among the top 17 for oil reserves and is the fourth-largest oil supplier in the Americas [27]. This fossil-fuel dependence has led to one of the region's most polluted power grids and the highest annual energy consumption in Latin America [8,16]. Mexico ranks fifteenth

globally in energy consumption, with over 80% of its energy sourced from fossil fuels. In 2019, oil accounted for 45.20%, natural gas 37.84%, coal 6.44%, biofuels 5.02%, wind and solar 2.75%, nuclear 1.65%, and hydropower 1.13% of its energy supply.

In addition, urban and city areas hosted approximately 80% of Mexico's total population, growing by around 1.5% each year during the same period [26]. Rapid urbanization negatively affects Mexico's economic and social progress by driving business and residential construction, contributing to ecological degradation [8]. Accelerated urbanization threatens sustainable development via increased energy consumption and greenhouse gas emissions [28]. As the 12th largest global CO_2 emitter and the largest in Latin America, Mexico's extensive fossil fuel use generates around 1.3% of worldwide emissions [26]. Raihan and Tuspekova [27] highlighted that Mexico's rapid economic growth, urbanization, and tourism development are fueled by intensified fossil fuel energy use, causing a significant CO_2 emission rise in recent years. Despite relying on fossil fuels for over 80% of its energy, Mexico remains Latin America's most globalized nation, achieving an annual GDP growth rate of 4.7% in 2021 and setting ambitious renewable energy targets while grappling with rapid urbanization and environmental degradation.

Mexico, however, possesses multiple sources of green energy supported by governmental regulations. In line with its General Climate Change Law, the nation is poised to achieve its objective of producing 35% of its electricity from clean sources by 2024. Mexico's commitment to emission reduction has also intensified post-Paris Agreement. Its updated NDC outlines a more ambitious target of 35% lower GHG emissions by 2030, surpassing the previous 22% reduction goal established in 2020. Figure 1 illustrates Mexico's annual biocapacity, ecological footprint, and load capacity factor trends. Deteriorating environmental conditions contribute to diminishing biocapacity and expanding ecological footprint, leading to reduced load capacity. Hence, studying load capacity factors becomes imperative to attain ecological sustainability in Mexico and achieve its climate objectives.

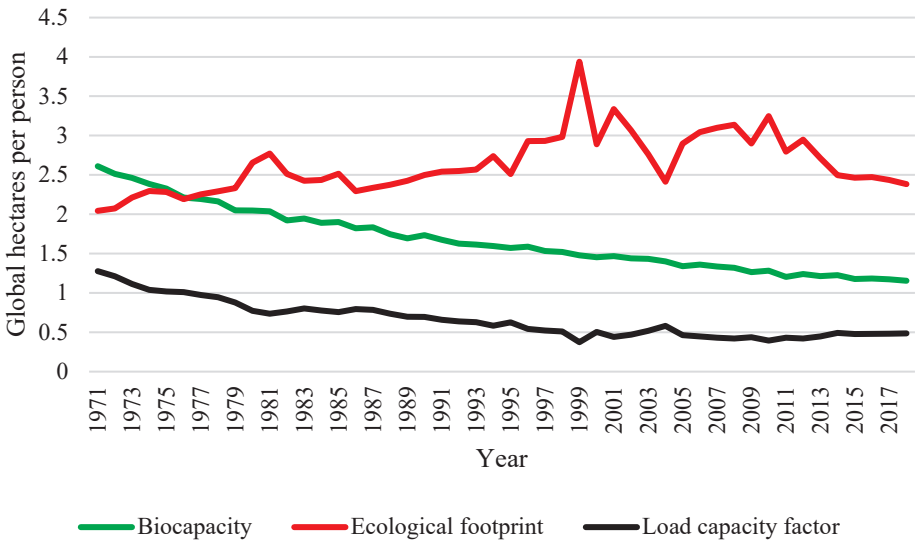

Figure 1. Biocapacity, ecological footprint, and load capacity factor in Mexico.

This research adds to the existing literature by providing much-needed context for the connection between load capacity factor and the interconnectedness of energy and economic systems, globalization, and the natural world in the context of developing countries. Second, when applied to Mexico's particular circumstances, the load capacity factor offers a nuanced perspective on the ecological balance within a nation that possesses a rich array of resources but also contends with environmental challenges stemming from fossil fuel utilization. Both supply and demand-side approaches to ecological issues are looked at in the study. Thirdly, how financial globalization, encompassing the flow of capital, investment, and financial services across international borders, intersects with

ecological well-being has remained relatively obscure. The adopted measure of financial globalization takes the consideration of environmentally responsible practices to a greater depth. Fourthly, the most up-to-date and extensive data collection was used for this study; it covered the period from 1971 to 2018. Three-unit root analyses (ADF, DF-GLS, and P-P) were implemented to determine the optimal data integration sequence. Finally, DOLS, FMOLS, and CCR have been implemented to confirm the ARDL procedure predicted values on the variables.

In addition to bolstering climate change adaptation and mitigation strategies, the findings of this study could aid other developing nations in formulating effective methods for achieving sustainable development. Finally, the outcomes of this investigation offer government officials with more complete and informative verification to implement successful approaches for the sectors of the carbon-free economy as a whole, advancement of green power, practical urban planning, and enhancement of financial globalization, all of which would guarantee a boost in load capacity factor along with ecological longevity in Mexico.

Here is how the rest of the article is laid out. The research pertinent to this article's topic is discussed in the second part, "Literature review", to provide context. The data, theoretical framework, empirical model creation, and estimation techniques used in this study are all described in depth under the "Methodology" of this publication. The practical assessment of the model's performance is extensive in the article's fourth part, "Results and Discussion", along with a discussion and comparison with the results of other research that has addressed similar questions. Finally, the study's findings and policy recommendations are summarized in the fifth part.

2. Literature Review

This particular part of the present study examines the research conducted on the relationship between economic growth, fossil fuel and renewable power, financial globalization, urbanization, and ecological mortification.

2.1. Economic Growth and Environment

Various countries have extensively explored the relationship between economic growth and environmental impact. The relationship between economic growth and CO_2 emissions is typically understood to involve increased emissions with higher economic activity, particularly for emerging countries [8]. However, the scenario becomes more complex when a broader measure of environmental quality, such as the load capacity, is considered instead of solely relying on CO_2 emissions [9]. Pata and Balsalobre-Lorente [29] studied Turkey's data from 1965 to 2017, revealing a negative correlation between economic development and the load capacity factor. Khan et al. [30] analyzed G7 and E7 countries from 1997 to 2018, finding that economic development corresponded with a reduction in the load capacity factor. Awosusi et al. [31] investigated South Africa from 1980 to 2017, uncovering an adverse association between economic prosperity and the load capacity factor. Shang et al. [32] examined ASEAN countries between 1980 and 2018, observing the adverse effects of economic expansion on load capacity factors.

In India, Akadiri et al. [33] discovered a short-term positive correlation between economic growth and the load capacity factor, shifting to a negative correlation in the long run. Pata's empirical analysis [3] used the ARDL method and identified an inverse relationship between economic growth and the load capacity factor in Japan and the United States from 1982 to 2016. Pata and Isik [34] focused on China from 1981 to 2017, finding that a growing economy adversely affects the load capacity factor.

Fareed et al. [35] investigated Indonesia's data spanning 1965 to 2014, observing that increased income led to a decrease in the load capacity factor. Majeed et al. [36] employed an asymmetric procedure to study Pakistan's economy from 1971 to 2014, showing a negative impact of economic expansion on environmental performance. However, Solarin et al. [37] employed the ARDL method for Nigeria from 1977 to 2016 and found that while economic

growth initially deteriorates the environment, it ultimately improved environmental quality in the long run. Examining countries with rapid economic expansion followed by significant slowdown, such as Mexico, is crucial to understanding the evolving dynamics between economic growth and environmental well-being.

2.2. Energy Use and Environment

Previous research emphasizes the significant influence of energy consumption and sources on determining the load capacity factor and its subsequent environmental consequences; however, the outcomes have demonstrated variability.

Huang et al. [38] in India, Pata and Balsalobre-Lorente [29] in Turkey, and Pata and Isik [34] in the case of China reveal that energy consumption, particularly non-renewable sources, adversely affects the load capacity factor, leading to ecological degradation. In the instances of those countries (all of which are emerging economies), the load capacity factor experienced a decline attributed to a rise in energy intensity. On the other hand, Alola et al. [9] find that a higher load capacity factor, achieved via enhanced renewable energy use, promotes ecological sustainability. Similar trends emerge as researchers examine different countries and regions. Guloglu et al. [39] in 26 OECD nations, Shang et al. [32] in Southeast Asia, Pata and Samsour [40] in 27 OECD nations, Pata [3] in the US and Japan, Zhao et al. [41] in the BRICS, and Awosusi et al. [31] in South Africa collectively suggest that the adoption of cleaner energy sources, such as green power, positively influences the load capacity factor, indicating an improvement in environmental quality.

Researchers have highlighted the challenges countries face in enhancing the load capacity factor while striking a balance between the utilization of renewable and fossil fuel energy sources [42]. Raihan et al. [27], Shang et al. [32], and Caglar et al. [39] found that the utilization of non-renewable energy sources negatively correlated with the load capacity factor, exacerbating ecological concerns. Still, using data from 1997 to 2018, Khan et al. [30] discovered a positive interaction between renewable energy and load capacity factor in the context of the G7 and E7 countries, similar to the findings of Fareed et al. [35] in Indonesia between 1965 and 2014. Shang et al. [32] also found that between 1980 and 2018, load capacity factors in ASEAN countries improved significantly due mainly to the elevated adoption of clean power, in line with the findings of Hakkak et al. [42] In Russia, Caglar et al.'s [43] study of 10 economies validated a positive relationship between non-renewable energies and carbon output; green energy and ecological effects had a negative feedback loop. Pata [44] also discovered that clean power negatively correlated with ecological damage from 1980 to 2016 in the United States.

These findings underscore the pivotal role of energy sources in shaping the load capacity factor and the subsequent environmental impact, with overall agreement that a higher load capacity factor enhances ecological sustainability by boosting renewable energy utilization. Similarly, the use of non-renewable energy generally appears to reduce load capacity. Still, several studies found an insignificant impact of renewable energy on load capacity factor (i.e., in Japan [3]) or a decreasing (even reversing) trend in the influence of renewable power on load capacity over time (i.e., Akadiri et al. [33] in India).

2.3. Urbanization and Environment

Another common challenge experienced by major emerging countries is the environmental pressure stemming from the rapid growth of urbanization, which is often linked to a substantial increase in energy demands [2,17,19,45]. The research of Guloglu et al. [39] revealed that as cities expanded, their load capacity factors diminished in 26 OECD countries from 1980 to 2018. Between 1980 and 2017, Rafique et al. [21] found that in 10 different economies, ecological effects negatively interacted with urbanization. Nathaniel [46] employed the ARDL procedure to find that between 1971 and 2014, the carbon footprint in Indonesia increased significantly in line with urbanization. Nathaniel et al. [45] provided more support for this analysis by citing studies they conducted in South Africa between 1965 and 2014. Ahmed et al. [47] looked at the G-7 countries from 1971 to 2014 to see

how urbanization influenced their ecosystems. The ecological footprint was found to be positively associated with urbanization.

However, Nathaniel and Khan [48] discovered a dissimilar conclusion regarding ASEAN economies. The researchers did not find significant evidence of the urbanization-energy-environment nexus for the developing ASEAN economies. For the time frame spanning 1977–2016, Solarin et al. [37] applied the ARDL method to the case of Nigeria. They reported that urbanization has no harmful impact on the environmental quality of Nigeria. By utilizing the data spanning 1991–2016, Ansari et al. [49] discovered a negative correlation between ecological footprint and urbanization, indicating that urbanization improves the quality of the environment in a panel of top renewable energy-consuming countries. Danish et al. [19] also found that urbanization alleviated the carbon footprint level. As highlighted by Ahmed et al. [47], urbanization can increase the ecological footprint, which suggests an enhanced capacity of the ecosystem to regenerate and provide essential resources. In this context, a larger ecological footprint can potentially mitigate the adverse impacts stemming from the heightened energy demand in urbanized regions.

2.4. Financial Globalization and Environment

Prior research on the finance–environment relationship suggests that financial development's attraction of Foreign Direct Investment (FDI) might amplify economic expansion and energy consumption, potentially harming the environment [18,20,50]. However, it is crucial to note that financial development can have a positive impact on curbing carbon emissions if FDI aligns with environmental goals. Enhanced access to financial markets can facilitate access to greener technologies, advanced expertise, and efficient energy utilization, potentially resulting in decreased CO_2 emissions. Some studies support the negative influence of FDI on CO_2 emissions via the adoption of energy-efficient technologies [20,51,52]. Nonetheless, empirical evidence on FDI's contribution to environmental quality is contradictory, with specific studies indicating that financial development correlates with reduced environmental quality [53,54]. This complexity underscores the need for further research to grasp the multifaceted interactions between finance, FDI, and environmental outcomes.

Still, the impact of financial globalization on ecological devastation is discussed relatively infrequently. Kihombo et al. [20] investigated the association between economic globalization and CO_2 emissions during the period spanning from 1970 to 2018 in India using the NARDL approach. The empirical findings suggest that a boost in financial globalization will diminish CO_2 emissions in India. Still, the release of more carbon dioxide will rise proportionately to the degree to which globalization is reduced. Ulucak et al. [51] implemented the ARDL and DOLS datasets spanning 1974 to 2016 to explore the association between rising nations' carbon footprint and globalized finance. They illustrated that globalization alleviated ecological damage. Examining 1996 to 2019, Shahzad et al. [52] determined that globalization in finance heightened ecological impacts, with financial and trade globalization amplifying pollution. Interconnections between environmental footprints, globalization, and economic complexity highlight the complicated globalization-environment nexus. Similar findings were supported by Kihombo et al. [55], who discovered that the economy in West Asia and the Middle East (WAME) region has an adverse link between economic globalization and its ecological footprint.

Nevertheless, in the case of India, Akadiri et al. [33] found that financial globalization positively influences the load capacity factor. Advocating for India's increased financial integration, Akadiri et al. [33] suggest governmental promotion of liberalization and international capital inflows, directing funds towards eco-friendly manufacturing as financial globalization positively impacts environmental quality. Ansari et al. [49] discovered a negative correlation between ecological footprint and globalization, indicating that globalization improves the quality of the environment in the top renewable energy-consuming countries. Considering these findings, it is imperative to explore whether financial globalization offers a similar avenue for Mexico to enhance its load capacity factor. The positive impact on the load capacity factor seen in India, where financial globalization was encouraged,

along with the improvement in environmental quality due to globalization, as observed in top renewable energy-consuming countries, warrants a closer examination of Mexico's potential in this regard.

The research mentioned above is an indispensable foundation for the expanding environmental challenges in emerging economies like Mexico. This complex web of interactions underscores the necessity to closely examine whether these factors could present a novel opportunity for Mexico to enhance its load capacity factor. By delving into these dynamics, Mexico can ascertain if harnessing economic growth, urbanization, and financial integration could provide a pathway to elevate its load capacity factor, aligning with broader global trends towards enhanced environmental sustainability. Research has yet to be mentioned on the impact of the load capacity factor in Mexico. Consequently, this research considers these aspects necessary for environmental and long-term sustainability. The present study used the latest time series data to apply the most up-to-date estimation techniques for filling the research gap in the existing literature.

3. Methodology

3.1. Data

Using data collected from 1971 to 2018, this study examines how load capacity factors changed in response to economic development, urbanization, financial globalization, fossil fuel, and renewable power. Data on financial globalization led to the selection of a period beginning in 1971; the lack of load capacity factor data through 2018 led to the choice of a period ending in 2018. The World Development Indicators database was mined for information on growing economies, increasing urbanization, fossil fuels, and renewable energy sources. The load capacity factor was sourced directly from the GFN. Lastly, information on globalization in the financial sector came from the "Swiss Economic Institute's (KOF) database". The observed series were transformed into their natural logarithms to minimize the potential for estimating mistakes. The series descriptions are compiled in Table 1.

Table 1. Specification of the variables.

Variables	Description	Logarithmic Forms	Measurement Units	Sources
LCF	Load capacity factor	LLCF	Global hectares per person	GFN
GDP	Economic growth	LGDP	GDP per capita (constant 2015 USD)	WDI
FFE	Fossil fuel energy use	LFFE	Percentage of total final energy use	WDI
RNE	Renewable energy use	LRNE	Percentage of total final energy use	WDI
FGL	Financial globalization	LFGL	Financial globalization index	KOF
URB	Urbanization	LURB	Urban population (% of the total population)	WDI

3.2. Conceptual Framework and Empirical Model

The environmental Kuznets curve (EKC) theory was suggested by Grossman and Krueger [56], and a reverse U-shaped connection is described between economic expansion and the environment. This relationship can be further broken down into three phases (size, composition, and technical). The size of the impact suggests that higher production levels result in environmental degradation. The compositional effect is indicative of a structural shift in the economy. While pollution rises throughout the move from agricultural to industry, it drops significantly as industries give way to services. Furthermore, the technical effect demonstrates that environmentally responsible technologies and manufacturing procedures can improve ecological conditions.

Despite being essential to economic prosperity, energy consumption is a major contributor to ecological deterioration [57]. Numerous fossil fuels exist, including coal, natural gas, and oil, used by nations worldwide to power economic development, urbanization, and industrialization, all of which negatively affect the environment [58]. Since emission levels have been rising recently, methods for reducing the buildup of these gases are urgently needed. However, there needs to be an agreement on the best strategies for preventing

severe environmental damage. However, renewable energy has become a serious contender to fossil fuels recently. The widespread availability of renewable energy options that do not contribute to climate change, like fossil fuels, is a big reason for their recent surge in popularity. It has been shown that switching to renewable power can save money, boost health, clean the air, and create new jobs [59]. Clean energy like solar, wind, geothermal, and biomass can be used locally to keep the lights on and reduce expensive imports.

Consequences of other factors, which include globalization, on the mix, scale, and methodology of these effects may be more explicit than those of economic growth alone. Thus, globalization is crucial to the correlation between growing economies and worsening ecological circumstances. The financial globalization viewpoint holds that the globalization of finance exacerbates numerous ecological issues. Globalization of the financial sector via the scale effect might boost spending and the economy. In addition, globalization in the financial sector encourages international trade and investment, which in turn stimulates the manufacturing sector within a country and, in turn, exacerbates environmental degradation. Increased consumer and company confidence, increased output and consumption, and a worsening of environmental degradation are all outcomes that can be expected to follow a period of strong stock market performance.

On the other hand, globalization of the financial sector has the potential to enhance environmental quality via technical and compositional impacts. As the population grows, the demand for natural resources rises, making urbanization a major contributor to the state of the planet. Thus, unchecked urbanization may negatively influence the ecology, while sustainable urbanization may help lessen those effects. Therefore, ecological degradation may come from poorly managed urbanization. We used this data to derive the following economic function, which we implemented inside the framework of the Cobb-Douglas production function [60] at time t:

$$LCF_t = f\ (GDP_t; FFE_t; RNE_t; FGL_t; URB_t) \quad (1)$$

This section details the experimental framework:

$$LCF_t = \tau_0 + \tau_1 GDP_t + \tau_2 FFE_t + \tau_3 RNE_t + \tau_4 FGL_t + \tau_5 URB_t + \varepsilon_t \quad (2)$$

where τ_0 is the intercept and ε_t is the error term at time t. In addition, τ_1, τ_2, τ_3, τ_4, and τ_5 characterize the coefficients. Moreover, LCF_t is the load capacity factor at time t, GDP_t is the economic growth at time t, FFE_t is fossil fuel energy use at time t, RNE_t is renewable energy use at time t, FGL_t is financial globalization at time t, and URB_t is urbanization at time t.

In addition, to normalize the time series data, the paper computed the natural log of every variable. Conclusions from log-linear models are more reliable and efficient than those from simple linear models in empirical studies. Here is the linear log model's enhanced multivariate production function:

$$LLCF_t = \tau_0 + \tau_1 LGDP_t + \tau_2 LFFE_t + \tau_3 LRNE_t + \tau_4 LFGL_t + \tau_5 LURB_t + \varepsilon_t \quad (3)$$

where $LLCF_t$ is the logarithm form of load capacity factor at time t, GDP_t is the logarithm form of economic growth at time t, FFE_t is the logarithm form of fossil fuel energy use at time t, RNE_t is the logarithm form of renewable energy use at time t, FGL_t is the logarithm form of financial globalization at time t, and URB_t is the logarithm form of urbanization at time t.

An overview of the estimating processes is shown in Figure 2.

3.3. Unit Root Test

Avoiding errors in the regression requires conducting unit root tests. In this test, we check to see if the regression variables are stable, and if they are, the paper uses equations for estimating the required stationary procedures. According to the data presented in the

empirical research, identifying the integration sequence is necessary before using cointegration techniques [61]. For this reason, the unit root test is implemented to guarantee that the variables in this portion are stable. Probability distributions for mean-variance and covariance of variable shifts over time; we say that the variable is non-stationary. Due to the power disparity between the tests and sample size, many researchers have suggested using various unit root tests to establish the integration order [62]. This research deployed three different tests for detecting the occurrence of an autoregressive unit root: the "Augmented Dickey–Fuller (ADF) "test designed by Dickey and Fuller [63], the "Dickey–Fuller generalized least squares (DF-GLS)" test generated by Elliott et al. [64], and the "Phillips–Perron (P-P)" test developed by Phillips and Perron [65].

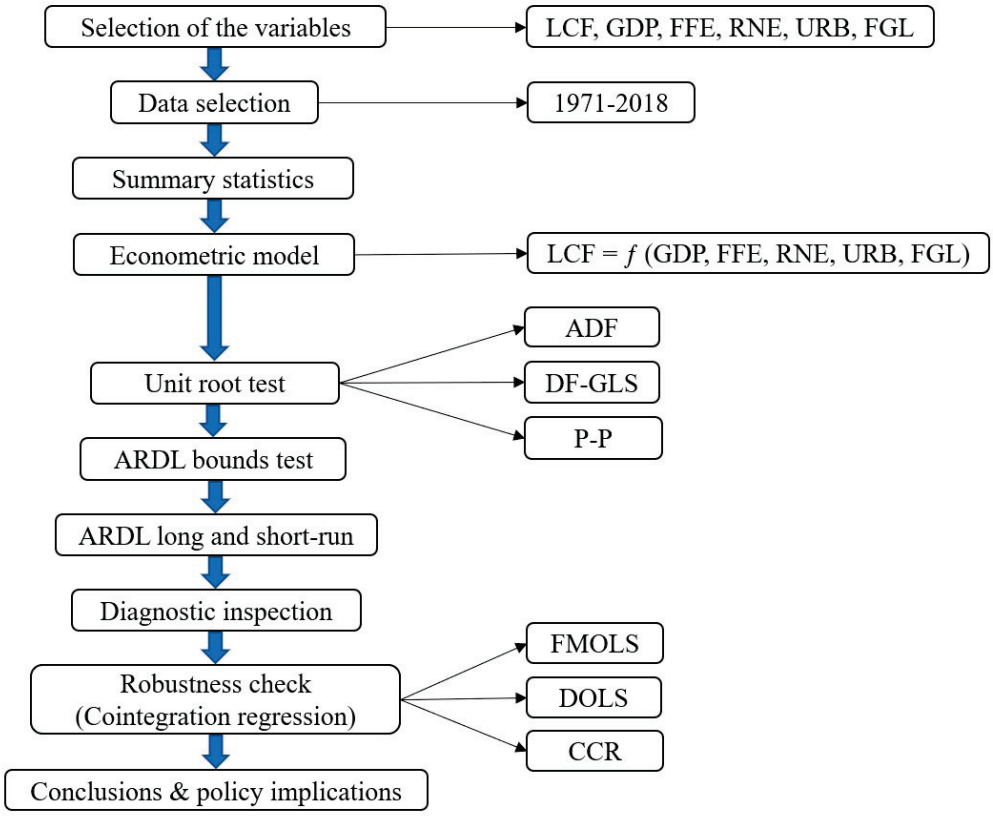

Figure 2. The methodological framework of the study.

This study employed the unit root test to confirm that no variable exceeded the order of integration required to verify the cointegration regressions (ARDL, DOLS, FMOLS, and CCR). A unit root test in statistics determines if a time series variable is non-stationary and has a unit root. The purpose of the test is to ascertain whether or not the stochastic component has a unit root or is stationary. The null hypothesis is characterized as the presence of a unit root, while the alternative hypothesis is either stationarity, trend stationarity, or explosive root, depending on the test employed. In general, the method of unit root testing implicitly presupposes that the to-be-tested time series (Y_t) can be expressed as follows:

$$Y_t = D_t + Z_t + \varepsilon_t \quad (4)$$

where D_t represents the deterministic (trend, seasonal component, etc.) component, Z_t represents the stochastic component, and ε_t describes the stationary error process.

3.4. ARDL Approach

This study implemented the ARDL-bound procedure Pesaran et al. [66] developed to determine the variables' integration. Comparing this strategy to earlier cointegration

techniques offers several benefits [67]. The integration feature of a series had required being established before using prior cointegration methods, but this technique does not call for such testing. The ARDL model can adjust for endogeneity while considering the variable's lag length. Second, it is appropriate in all situations involving the integration of investigative series. Even with few observations, the ARDL model continues to be viable. Employing the econometric framework depicted in Equation (5), the ARDL bound testing strategy might be designed.

$$\begin{aligned}\Delta LLCF_t = {} & \tau_0 + \tau_1 LLCF_{t-1} + \tau_2 LGDP_{t-1} + \tau_3 LFFE_{t-1} + \tau_4 LRNE_{t-1} + \tau_5 LFGL_{t-1} + \tau_6 LURB_{t-1} + \sum_{i=1}^{q} \gamma_1 \Delta LLCF_{t-i} \\ & + \sum_{i=1}^{q} \gamma_2 \Delta LGDP_{t-i} + \sum_{i=1}^{q} \gamma_3 \Delta LFFE_{t-i} + \sum_{i=1}^{q} \gamma_4 \Delta LRNE_{t-i} + \sum_{i=1}^{q} \gamma_5 \Delta LFGL_{t-i} \\ & + \sum_{i=1}^{q} \gamma_6 \Delta LURB_{t-i} + \varepsilon_t\end{aligned} \tag{5}$$

where q embodies the lag length of the series and Δ indicates the first difference operator.

Starting with Equation (5), we estimate the lagged variables' joint significance using OLS and the F-test. The goal of this method is to observe long-run cointegration. Where no long-run interactions among the variables are considered null hypotheses, upper and lower limits may be used as critical values against which comparison of F-statistics is feasible [66]. If the F-statistics are larger than the maximum critical value for rejecting the null hypothesis, then it can be concluded that the variables are linked over the long term. The null hypothesis is accepted if the F-statistic is less than the minimum acceptable value. The test is inconclusive if the F-statistics are seen to fall between the minimum and maximum thresholds.

Moreover, Pesaran et al. [66] described the ARDL procedure as promising for predicting the short and long-term associations among the model's variables after establishing their unit roots and cointegration. After establishing cointegration between the study's variables, the investigation used Equation (5) to predict an ARDL procedure of the long-run coefficient. Following the identification of the long-term connections, to look into the short-term behavior of the independent variables and the short-term adjustment rate toward the long-term rate, this study evaluated the error correction model (ECM). The ECM is integrated into the ARDL structure to accomplish this goal [68], illustrated in Equation (6), where θ is the ECM's coefficient. The equation shows how the series are linked across time and how error-correction dynamics work.

$$\begin{aligned}\Delta LLCF_t = {} & \tau_0 + \tau_1 LLCF_{t-1} + \tau_2 LGDP_{t-1} + \tau_3 LFFE_{t-1} + \tau_4 LRNE_{t-1} + \tau_5 LFGL_{t-1} + \tau_6 LURB_{t-1} + \sum_{i=1}^{q} \gamma_1 \Delta LLCF_{t-i} \\ & + \sum_{i=1}^{q} \gamma_2 \Delta LGDP_{t-i} + \sum_{i=1}^{q} \gamma_3 \Delta LFFE_{t-i} + \sum_{i=1}^{q} \gamma_4 \Delta LRNE_{t-i} + \sum_{i=1}^{q} \gamma_5 \Delta LFGL_{t-i} + \sum_{i=1}^{q} \gamma_6 \Delta LURB_{t-i} \\ & + \theta ECM_{t-1} + \varepsilon_t\end{aligned} \tag{6}$$

3.5. Robustness Check

Considering Equation (6), this study assessed the reliability of the ARDL conclusions by applying the DOLS test offered by Stock and Watson [69], the FMOLS test that was suggested by Phillips and Hansen [70], and the CCR test proposed by Park [71]. These approaches are used to estimate the long-run association by using a single cointegrating vector. Two major difficulties prompted the deployment of these solutions. FMOLS, DOLS, and CCR can be employed once the cointegration conditions among the I(1) parameters are met. Second, these techniques give consistent parameters even in the small sample size, overcome the problems of endogeneity, serial correlation, omitted variable bias, and measurement errors [72], and allow for heterogeneity in the long-run parameters. Therefore, the results it produces are asymptotically efficient.

4. Results and Discussion

4.1. Descriptive Statistics

Before performing the actual assessment (using methods like unit root, cointegration, and other analysis methods), it is necessary to determine the dataset's descriptive properties, particularly its normality. Table 2 lists the dataset's defining characteristics across its 48 years. The outcomes demonstrate that the means of the variables are typically distributed, demonstrating the absence of outliers in the data set. According to the calculated standard deviation values, the findings for the examined parameters indicate an appropriate amount of volatility so far. Moreover, all the applied parameters' anticipated skewness between +1 and −1. The load capacity factor and renewable power data are positively skewed, while financial globalization, urbanization, economic growth, and fossil fuel energy utilization are negatively skewed. Nature is platykurtic, as evidenced by all observable series having kurtosis values below 3. Since the Jarque–Bera test and the probability value for each series agree that the data follows a normal distribution, we may conclude that all observed series follow a normal distribution. The confirmation of data normality led us to the next step of the analysis, which is the unit root test for data stationarity.

Table 2. Descriptive statistics of the variables.

Variables	LLCF	LGDP	LFFE	LRNE	LFGL	LURB
Mean	−0.471092	8.987041	4.482117	2.417434	3.927990	4.272897
Median	−0.504034	8.993692	4.485016	2.413601	3.946589	4.292871
Maximum	0.244597	9.222305	4.511486	2.821840	4.193552	4.383975
Minimum	−0.979550	8.602729	4.421154	2.193886	3.676873	4.090654
Std. Dev.	0.330707	0.153684	0.021005	0.165563	0.176163	0.082632
Skewness	0.424271	−0.642277	−0.712863	0.484865	−0.054002	−0.601856
Kurtosis	2.077219	2.753942	2.830229	2.190244	1.519375	2.293941
Jarque–Bera	3.143097	3.421245	3.406817	3.192163	3.407829	3.894889
Probability	0.207723	0.180753	0.130791	0.202689	0.110370	0.142638
Observations	48	48	48	48	48	48

4.2. Findings of Unit Root Tests

Before using cointegration, unit root testing should be performed often to ensure that the variables are stationary, and then use descriptive statistics to check that the data is normally distributed. This is a crucial stage since it determines whether the applied variable is stationary and helps researchers choose the most appropriate test. In this investigation, we employed the utilization of the ADF, DF-GLS, and P-P unit root testing techniques. As shown in Table 3, all relevant metrics are constant after the initial difference. Therefore, the ARDL estimator and cointegration are viable options for these data.

Table 3. The outcomes of unit root tests.

Logarithmic Form of the Variables	ADF		DF-GLS		P-P	
	Log Levels	Log First Difference	Log Levels	Log First Difference	Log Levels	Log First Difference
LLCF	2.286	−9.520 ***	−0.186	−9.391 ***	−2.120	−9.492 ***
LGDP	−2.256	−5.705 ***	0.397	−4.831 ***	−2.211	−5.650 ***
LFFE	−3.076 **	−6.687 ***	−0.673	−4.111 ***	−2.971 **	−6.727 ***
LRNE	−2.503	−7.385 ***	−0.851	−3.662 ***	−2.520	−7.367 ***
LFGL	−0.971	−6.324 ***	−0.234	−6.348 ***	−0.414	−11.611 ***
LURB	−1.253	−3.518 ***	0.650	−3.171 ***	−2.477	−12.497 ***

*** and ** signify 1% and 5% significance, correspondingly.

4.3. The ARDL Bounds Analysis Outcomes

After validating stationarity characteristics, this research then estimated the ARDL framework. This investigation was selected using the Akaike Information Criterion (AIC)

minimum values to calculate an F-statistic and then perform an ARDL bounds test; this requires a suitable lag time for the AIC for cointegration assessment. Table 4 shows the conclusions obtained from examining the ARDL bounds to establish whether the variables integrate. The existence of a long-term interaction within the variables may be inferred if the value that the F-test predicts is more than both of the threshold values, then the test is significant. The projected F-statistic value (9.193444), which shows a long-run association between related factors, is more than the 10%, 5%, 2.5%, and 1% of the crucial upper limit in the I(0) and I(1).

Table 4. ARDL bounds test results.

F-Bounds Test		**Null Hypothesis: No Degrees of Relationship**		
Test Statistic	**Estimate**	**Significance**	**I(0)**	**I(1)**
F-statistic	9.193444	At 10%	2.08	3.00
K	5	At 5%	2.39	3.38
		At 2.5%	2.70	3.73
		At 1%	3.06	4.15

4.4. Conclusions Drawn from ARDL's Short-Run and Long-Run Analyses

Given the apparent cointegration relationship, the ARDL method assessed these regressors' long- and short-term effects on load capacity. The computed values are shown in Table 5. The expansion of the Mexican economy is projected to reduce the country's load capacity factor. The short- and long-term data indicated that economic prosperity negatively correlates with the load capacity factor. A one percent increase in GDP would reduce load capacity by 0.63% in the long term and 0.23% in the short term. Consequently, economic prosperity degrades the character of the ecology over time. The finding is realistic from the theoretical point of view as the developing economies are heavily dependent on fossil fuels that lead to environmental degradation. Several studies reported a detrimental relationship between economic development and load capacity factor, consistent with the present study's finding. For example, Xu et al. [2] for Brazil; Pata and Balsalobre-Lorente [29] for Turkey; Khan et al. [30] in the context of G7 and E7 countries; Awosusi et al. [31] for South Africa; Shang et al. [32] for ASEAN countries; Akadiri et al. [33] for India; Pata [3] in Japan and the United States; Pata and Isik [34] for China; Fareed et al. [35] for Indonesia; and Majeed et al. [36] for Pakistan. However, the present study's findings contradict Solarin et al. [37], who reported that urbanization has no harmful impact on the environmental quality of Nigeria.

Table 5. ARDL long and short-run findings.

Variables	**Long-Run**			**Short-Run**		
	Coefficient	**t-Statistic**	***p*-Value**	**Coefficient**	**t-Statistic**	***p*-Value**
LGDP	−0.628 ***	−3.932	0.004	−0.234 ***	−3.773	0.006
LFFE	−6.779 ***	−5.311	0.001	−1.381 ***	−4.784	0.003
LRNE	1.026 ***	7.184	0.000	0.178 ***	3.947	0.001
LFGL	0.130 ***	5.686	0.000	0.009 ***	3.580	0.000
LURB	−2.314 ***	−5.195	0.001	−1.252 ***	−3.546	0.002
C	35.711	5.807	0.156	-	-	-
ECM (−1)	-	-	-	−0.541 ***	−3.953	0.000
R^2	0.9259					
Adjusted R^2	0.9190					

*** designates 1% significance, correspondingly.

The fact that Mexico is presently at the scale phase demonstrates that the nation is working toward achieving its pro-growth goals. Mexico's economic growth results from ecological issues like land, sea, and air pollution. As a developing economy, Mexico draws on a significant quantity of its resources and depends on forms of energy that produce much

carbon to promote its economy [8]. To no one's surprise, ecological problems have arisen due to Mexico's rapid economic growth, driven by intensive on-resources manufacturing that has now achieved export saturation. Therefore, the growth of Mexico's economy, especially after the turn of the century, has contributed to the acceleration of environmental degradation. This highlights that an increase in income per person is not necessarily a good predictor of ecological sustainability; consequently, the government of Mexico needs to enact ecological regulations around energy use.

This study discovered that fossil fuel energy has a detrimental and statistically significant relationship with Mexico's load capacity factor in both the short and long term. A one percent boost in fossil power would reduce the load capacity factor by 6.78% in the long run and 1.38% in the short run. In Brazil, Xu et al. [2] observed that the rising demand for fossil fuels detrimentally impacts the LCF. Comparable outcomes were highlighted for Turkey by Pata and Balsalobre-Lorente [29] and South Africa, as indicated by Awosusi et al. [31]. Developing Asian countries exhibited analogous adverse connections between non-renewable energy consumption and LCF, as noted in Pata and Isik [30], Fareed et al. [35] for Indonesia, and Huang et al. [34] for China. However, our findings diverge from Alola et al. [9], who suggested that non-renewable energy efficiency advances environmental sustainability by elevating the load capacity factor.

The present study's result is not surprising as about 90 percent of Mexico's energy bundle comprises fossil fuels [26], the economic engines driving manufacturing, and output. Since the energy policy of Mexico includes the production of oil, natural gas, and coal that promotes economic growth based on fossil fuels is unavoidable. Therefore, industrial production and domestic business substantially impact the environment. An additional cause for concern is that overusing fossil power will inevitably lead to their depletion, and economies that rely only on them will eventually collapse. Mexico's extensive reliance on fossil power causes pollution and contributes to the country's mounting ecological issues by contaminating the atmosphere, reducing soil quality, and poisoning aquatic organisms. Hence, the foremost strategic imperative is to build a robust and advanced renewable energy infrastructure, ultimately phasing out the reliance on fossil fuels [73]. Mexico has been developing green power sources for decades while maintaining a fossil fuel-based power generation system.

However, this research showed that renewable power has a positive and statistically strong correlation with the load capacity factor throughout the entire load life cycle. The outcomes suggest using green energy could benefit Mexico's load capacity factor. The load capacity factor would rise by 1.03% over the long run and 0.18% over the short term, with a 1% boost in green power. Evidence from developed countries supports a positive correlation between the proportion of green power in total energy usage and the load capacity factor, as demonstrated in Pata [3] in Japan and the United States; Khan et al. [30] in the context of the G7; and Pata and Samsour [40] and Guloglu et al. [39] for OECD nations. Furthermore, comparable effects are observed within emerging economies, particularly in Asia, as highlighted by Shang et al. [32] in the Southeast Asia region, Fareed et al. [35] for Indonesia, Alola et al. [9] for India, and Zhao et al. [41] for BRICS-T nations. All observed a correlation between the ratio of green power to total energy usage and the load capacity factor; therefore, our findings align with theirs. However, our results oppose Akadiri et al. [33], who found that using renewable power sources temporarily lowers the load capacity factor in India.

The findings of this study hold both theoretical and practical validity, as the shift from fossil fuels to renewable and green energy sources could alleviate Mexico's environmental impact. Likewise, these findings are likely relevant to other developing nations grappling with environmental challenges. Using renewable energies for electricity generation is crucial to forestall potentially catastrophic climate change and guarantee ecologically sound growth. Increased energy accessibility, improved power, and utilizing locally available energy sources are just some of the many economic benefits of renewable energy [74,75]. Be-

cause of rising global environmental consciousness, Mexico must shift its energy spending toward renewables to facilitate the development of a green economy.

Mexico is on track to produce 35% of its electricity from clean energy sources by 2024, as the country's General Climate Change Law mandates. Diversifying Mexico's energy supply into clean power, including wind, solar, biofuel, geothermal, hydropower, and nuclear power, might bring in vast investment. Investment in Mexico's renewable energy sector could increase if current market circumstances persist. However, natural coupling and utilization of these deposits are hindered by a wide range of specialized terminology and organizational, social, political, and economic limitations. Mexico requires an all-encompassing plan to boost the electricity it generates from green power to reach ecological sustainability.

In addition to the impact of renewables, this research found a positive correlation between financial globalization and load capacity factor, with a 1% rise in financial globalization predicted to enhance load capacity factor by 0.13% in the long run and 0.01% in the short run. Therefore, globalization of the financial sector is essential to the long-term changes and fluctuations of Mexico's ecosystems. Xu et al. [2] and Akadiri et al. [33] revealed a positive association between financial globalization and load capacity factor in Brazil and India, respectively, lending further credence to this assessment. This result is sound, as foreign investment can introduce advanced technology that enhances productivity even in resource-constrained environments. From a theoretical perspective, financial globalization signifies the advancement of a nation's financial sector, where a well-developed financial system would prioritize investments for environmental sustainability rather than pursuing a developmental trajectory that harms the environment. The availability of funds also facilitates the promotion of green energy initiatives, leading to improved sustainable development.

In addition, this study found that the load capacity factor is negatively related to urbanization. The results showed that for every 1% increase in urban population, the load capacity factor dropped by 2.31 percent in the longer term and 1.25 percent in the shorter term. The finding aligns with both a theoretical and practical standpoint, as the rise in urban population contributes to environmental deterioration via intensified energy consumption, waste production, water utilization, electricity usage, air and noise pollution, deforestation, soil erosion, and alterations in land use. The present study's result agrees with Guloglu et al. [39] for OECD nations, Zhao et al. [41] for Indonesia, and Pata [44] for E-7 countries, who found that urbanization adversely interacts with the load capacity factor leads to more degradation of the environment. This finding explains why Mexico's rapid urbanization due to rural-to-urban migration constitutes a risk to the country's environment. The findings point to a rise in GHG emissions from the usage of electrical devices, the construction of homes and factories, and the operation of automobiles due to Mexico's rapid urbanization. Economic growth, which urbanization facilitates, can lead to environmental degradation [76]. As a result, Mexico's urbanization can only be maintained for a little while, calling for adopting a strategy for such growth.

However, our results contradict Solarin et al.'s [37] theory that non-renewable energy efficiency promotes environmental sustainability by increasing load capacity. Similarly, our results contrast with Danish et al.'s [19] argument that urbanization reduces the ecological footprint of BRICS countries. These studies [19,37,61] argue that these major emerging nations could reduce emissions by prioritizing sustainable energy use, responsible natural resource management, increasing the share of renewable energy, managing urbanization, and aligning these efforts with income growth. Thus, Mexico must promote a more rapid transition to cleaner energy alongside income growth to enable the adoption of cleaner technologies and sustainable urban investments.

The error correction coefficient suggests that the model's short-term equilibrium deviations will cancel out over the long run. The calculated coefficient value of 0.611 demonstrated that the rate of change from short-run stability to long-term stability is 61% per year, which is steady. Furthermore, the proposed regression model fits the data well, as shown

by the long-run estimation R^2 of 0.9259 and the corrected R^2 of 0.9190. This indicated that the independent variable could explain the changes in the dependent variable caused in 92% of cases.

4.5. Diagnostic Inspection

This investigation employed the ARDL test outcomes that need to be confirmed by various diagnostic tools before they can be considered reliable. Table 6 displays the results of applying the Breusch–Godfrey Langrage Multiplier (LM) to investigate the possibility of serial correlation. The findings suggest no sequential relationship. Heteroscedasticity was tested using the Breusch-Pagan-Godfrey statistic, and it was found that the data were not heteroscedastic. The Jarque–Bera Normality test examined the series' potential for normality. The *p*-value and Jarque–Bera statistic both pointed to a normally distributed residual. The "cumulative sum (CUSUM) and cumulative sum of squares (CUSUMSQ) tests" are applied to the recursive residuals to assess the consistency of the short-run beta coefficients in the ARDL technique. Figure 3 shows that according to the outcomes of the CUSUM and CUSUM square tests, the paper finds no evidence of a fundamental inconsistency (at the 5% level) within GHG emissions and independent variables. The testing validated the reliability of the model.

Table 6. The outcome of diagnostic tests.

Diagnostic Tests	Coefficient	*p*-Value	Decision
Jarque-Bera test	2.715821	0.2572	Residuals are normally distributed
Breusch-Godfrey LM test	2.657845	0.1028	No serial correlation exits
Breusch-Pagan-Godfrey test	0.574111	0.9016	No heteroscedasticity exists
Ramsey RESET test	1.254856	0.2276	The model is specified correctly

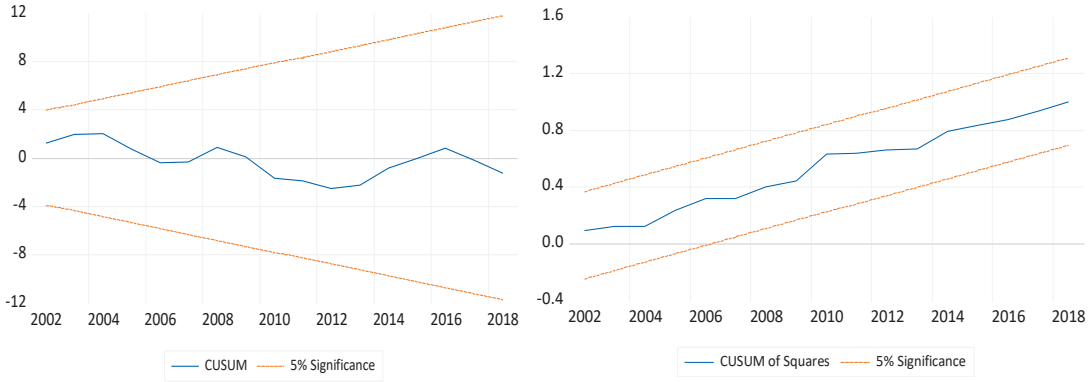

Figure 3. The plots of CUSUM and CUSUMQ tests.

4.6. Results of Robustness Check

Longitudinal evaluations employing the DOLS, FMOLS, and CCR assessments were also performed on the ARDL procedure conclusions. The anticipated outcomes from using DOLS, FMOLS, and CCR are shown in Table 7. Conclusions from DOLS, FMOLS, and CCR were all demonstrated to be consistent and reliable. The outcomes showed that Mexico's load capacity factor drops as economic expansion, fossil power, and urbanization boost but rises with renewable energy and financial globalization. These findings are comparable with those from the ARDL simulations, with some minor differences statistically and in terms of the size of the coefficients. Given these results, it seems reasonable to determine that the ARDL analysis's findings are credible and consistent.

Table 7. The results of the robustness check.

Variables	DOLS		FMOLS		CCR	
	Coefficient	**t-Statistic**	**Coefficient**	**t-Statistic**	**Coefficient**	**t-Statistic**
LGDP	−0.639 ***	−3.387	−0.665 ***	−3.418	−0.631 ***	−3.329
LFFE	−5.531 **	−2.670	−6.671 **	−2.688	−6.995 **	−2.762
LRNE	0.497 ***	3.409	0.650 ***	3.534	0.707 ***	3.507
LFGL	0.145 ***	3.709	0.085 **	2.320	0.139 ***	3.482
LURB	−2.119 ***	−3.765	−3.029 **	−2.511	−3.168 **	−2.448
C	13.719	0.846	13.365	0.877	14.874	0.924
R^2	0.9267		0.9159		0.9146	
Adjusted R^2	0.9180		0.9057		0.9041	

*** and ** denote significance at 1% and 5% levels, respectively.

5. Conclusions and Policy Implications

5.1. Conclusions

The rapid growth of Mexico's economy has made it a developing country with severe ecological problems. Carbon emissions, ecological footprint, and greenhouse gas emissions are the most often used measures to compare environmental degradation in rich and developing nations. The "Sustainable Development Goals (SDGs)" and mitigating ecological concerns depend on a broader and more comprehensive ecological evaluation. Therefore, the load capacity factor was used as an independent proxy for environmental deterioration and offered a comprehensive evaluative measurement of the environment by simultaneously contrasting biocapacity and ecological footprint. The load capacity factor also gives the integrated environmental demand and supply features.

Focusing on Mexico, this study looked at load capacity from 1971 to 2018 to see how economic growth, urbanization, financial globalization, and fossil and renewable power usage influenced it. These connections were uncovered using an array of techniques. The "ADF, DF-GLS, and P-P unit root tests" were conducted to examine the stability and stationarity of each variable. The variables were shown to be cointegrated across long periods; ARDL-bound test outcomes point in this direction. Economic growth, fossil fuel, and urbanization negatively influence Mexico's load capacity factor, based on the ARDL method's findings, while using renewable power sources and financial globalization have a favorable effect. The utilization of DOLS, FMOLS, or CCR methods robustly confirms that the estimated results remain unaffected.

5.2. Policy Implications

Given the negative coefficients within GDP and the load capacity factor, policymakers in Mexico should focus on promoting sustainable and resource-efficient economic growth. Instead of solely pursuing traditional economic indicators, the emphasis should be on inclusive development, prioritizing energy efficiency and clean technologies. Encouraging investments in green sectors, fostering innovation, and supporting businesses adopting sustainable practices can maximize the load capacity factor while achieving robust GDP growth. Additionally, targeted policies that stimulate research and development in renewable energy and sustainable infrastructure can further enhance the country's economic performance while reducing its energy intensity and environmental impact.

Based on the negative coefficients between fossil fuel consumption and the load capacity factor, Mexico should prioritize policies to reduce reliance on fossil fuels for energy consumption. Implementing measures to transition towards cleaner and renewable energy sources will mitigate environmental impacts, enhance energy security, and reduce the strain on the electricity grid. Policymakers can consider incentivizing the adoption of renewable power knowledge, setting targets for clean power integration in the energy mix, and phasing out subsidies for fossil fuels. Additionally, promoting energy conservation and efficiency initiatives across industries and the transportation sector will further support

efforts to minimize the load capacity factor and move Mexico towards enhanced energy security and sustainability.

With the positive coefficients observed in both renewable power and the load capacity factor, Mexico's priority should be formulating policies to accelerate the implementation and integration of renewable energy sources. Policymakers can introduce supportive measures like feed-in tariffs, tax incentives, and grants, fostering investments in clean power projects. Streamlining the approval process for renewable energy initiatives and bolstering grid infrastructure to accommodate higher levels of renewable energy penetration become crucial steps in maximizing the load capacity factor. Additionally, initiatives focused on public awareness and knowledge dissemination can play a vital role in encouraging the utilization of green power among individuals and businesses, thereby fostering the adoption of clean energy technologies and enhancing the overall dependability and sustainability of Mexico's energy infrastructure.

Mexico can leverage the strong coefficients connecting financial globalization and the load capacity factor. This presents an opportunity to bolster its energy infrastructure and capacity. Prioritizing the attraction of FDI in the power sector, particularly in projects promoting renewable energy and energy efficiency, becomes crucial. Facilitating cross-border capital flows and nurturing international partnerships will expedite the adoption of advanced technologies and energy management best practices. Establishing comprehensive regulatory frameworks is essential to ensure sustainable and fair benefits from financial globalization, guarding against instability. Achieving equilibrium between open global financial interactions and effective regulations enables Mexico to tap into the potential of financial globalization. This approach will maximize the load capacity factor, driving Mexico's energy transition objectives.

Given the negative coefficients between urbanization and the load capacity factor, policymakers in Mexico should prioritize sustainable and smart urban planning to mitigate the strain on the electricity grid. Encouraging compact and well-connected urban development and promoting green spaces and public transportation can reduce energy demand and enhance energy efficiency in cities. Implementing energy-efficient building codes and standards, and incentivizing the implementation of green power technologies in urban infrastructure can further support the goal of minimizing the load capacity factor. Additionally, integrating urban planning with energy management strategies and considering the environmental impacts of urbanization will be essential in ensuring a balanced approach to sustainable urban development and a more resilient energy future for Mexico.

5.3. Future Research Directions and Study Limitations

This study analyzes the varied effects of economic expansion, fossil power, clean power, financial globalization, and urbanization on load capacity factors in Mexico, which have several notable limitations. Firstly, the study's reliance on available data sources may have restricted the depth of analysis and precision of results. To overcome this, more in-depth data should be collected in the future, and up-to-date data to enhance the accuracy of findings. Additionally, the research may have been constrained by the complexities and interdependencies of the factors under investigation. Future studies could employ advanced econometric models and causal analysis techniques to better discern the causal relationships among these variables. Moreover, the impact of external factors, such as government policies and technological advancements, could have been overlooked in this study. Future research might delve into the drive of these external factors on load capacity factor and its interaction with the studied variables. Furthermore, considering Mexico's geographical diversity and regional disparities, future research could adopt a more granular approach to explore how load capacity factors vary across different states or cities. Lastly, the study primarily focused on the quantifiable aspects of energy and economic factors, leaving scope for future investigations into the ecological and societal implications of pursuing renewable power and urbanization. By addressing these limitations and pursuing more comprehensive research, policymakers and stakeholders can make better-informed

decisions to facilitate sustainable energy development and efficient energy utilization in Mexico.

Author Contributions: Conceptualization, A.R. and L.C.V.; methodology, A.R. and S.A.; software, M.R.; validation, M.R.; formal analysis, S.A.; investigation, S.A.; resources, M.A.E.; data curation, L.C.V.; writing—original draft preparation, M.R. and L.C.V.; writing—review and editing, A.R. and M.A.E.; visualization, M.R.; funding acquisition, M.A.E. All authors have read and agreed to the published version of the manuscript.

Funding: This research was funded by Airlangga University. The APC was funded by Airlangga University.

Institutional Review Board Statement: Not applicable.

Informed Consent Statement: Not applicable.

Data Availability Statement: Data obtained from the World Development Indicators (WDI); Data series by The World Bank Group; The World Bank: Washington, DC, USA. Retrieved from https://databank.worldbank.org/source/world-development-indicators, accessed on 25 January 2023.

Conflicts of Interest: The authors declare no conflict of interest.

References

1. Usman, M.; Makhdum, M.S.A.; Kousar, R. Does financial inclusion, renewable and non-renewable energy utilization accelerate ecological footprints and economic growth? Fresh evidence from 15 highest emitting countries. *Sustain. Cities Soc.* **2021**, *65*, 102590. [CrossRef]
2. Xu, D.; Salem, S.; Awosusi, A.A.; Abdurakhmanova, G.; Altuntaş, M.; Oluwajana, D.; Kirikkaleli, D.; Ojekemi, O. Load Capacity Factor and Financial Globalization in Brazil: The Role of Renewable Energy and Urbanization. *Front. Environ. Sci.* **2022**, *9*, 823185. [CrossRef]
3. Pata, U.K. Do renewable energy and health expenditures improve load capacity factor in the USA and Japan? A new approach to environmental issues. *Eur. J. Health Econ.* **2021**, *22*, 1427–1439. [CrossRef] [PubMed]
4. Rahman, A.; Richards, R.; Dargusch, P.; Wadley, D. Pathways to reduce Indonesia's dependence on oil and achieve longer-term decarbonization. *Renew. Energy* **2023**, *202*, 1305–1323. [CrossRef]
5. Muhammad, I.; Ozcan, R.; Jain, V.; Sharma, P.; Shabbir, M.S. Does environmental sustainability affect the renewable energy consumption? Nexus among trade openness, CO_2 emissions, income inequality, renewable energy, and economic growth in OECD countries. *Environ. Sci. Pollut. Res.* **2022**, *29*, 90147–90157. [CrossRef]
6. Ghosh, S.; Hossain, M.S.; Voumik, L.C.; Raihan, A.; Ridzuan, A.R.; Esquivias, M.A. Unveiling the spillover effects of democracy and renewable energy consumption on the environmental quality of BRICS countries: A new insight from different quantile regression approaches. *Renew. Energy Focus* **2023**, *46*, 222–235. [CrossRef]
7. EIA. *Annual Energy Outlook 2020*; Energy Information Administration: Washington, DC, USA, 2020; pp. 1672–1679. Available online: https://www.eia.gov/outlooks/aeo/pdf/AEO2020%20Full%20Report.pdf (accessed on 10 March 2023).
8. Nahrin, R.; Rahman, M.H.; Majumder, S.C.; Esquivias, M.A. Economic Growth and Pollution Nexus in Mexico, Colombia, and Venezuela (G-3 Countries): The Role of Renewable Energy in Carbon Dioxide Emissions. *Energies* **2023**, *16*, 1076. [CrossRef]
9. Alola, A.A.; Özkan, O.; Usman, O. Role of Non-Renewable Energy Efficiency and Renewable Energy in Driving Environmental Sustainability in India: Evidence from the Load Capacity Factor Hypothesis. *Energies* **2023**, *16*, 2847. [CrossRef]
10. Shahbaz, M.; Balcilar, M.; Mahalik, M.K.; Akadiri, S.S. Is causality between globalization and energy consumption bidirectional or unidirectional in top and bottom globalized economies? *Int. J. Financ. Econ.* **2023**, *28*, 1939–1964. [CrossRef]
11. Xia, W.; Apergis, N.; Bashir, M.F.; Ghosh, S.; Doğan, B.; Shahzad, U. Investigating the role of globalization, and energy consumption for environmental externalities: Empirical evidence from developed and developing economies. *Renew. Energy* **2022**, *183*, 219–228. [CrossRef]
12. Behera, P.; Haldar, A.; Sethi, N. Achieving carbon neutrality target in the emerging economies: Role of renewable energy and green technology. *Gondwana Res.* **2023**, *121*, 16–32. [CrossRef]
13. Dreher, A. Does globalization affect growth? Evidence from a new index of globalization. *Appl. Econ.* **2006**, *38*, 1091–1110. [CrossRef]
14. Gygli, S.; Haelg, F.; Potrafke, N.; Sturm, J.-E. The KOF Globalisation Index—Revisited. *Rev. Int. Organ.* **2019**, *14*, 543–574. [CrossRef]
15. Begum, R.A.; Raihan, A.; Said, M.N.M. Dynamic Impacts of Economic Growth and Forested Area on Carbon Dioxide Emissions in Malaysia. *Sustainability* **2020**, *12*, 9375. [CrossRef]
16. Salazar-Núñez, H.F.; Venegas-Martínez, F.; Lozano-Díez, J.A. Assessing the interdependence among renewable and non-renewable energies, economic growth, and CO_2 emissions in Mexico. *Environ. Dev. Sustain.* **2022**, *24*, 12850–12866. [CrossRef]

17. Voumik, L.C.; Mimi, M.B.; Raihan, A. Nexus Between Urbanization, Industrialization, Natural Resources Rent, and Anthropogenic Carbon Emissions in South Asia: CS-ARDL Approach. *Anthr. Sci.* **2023**, *2*, 48–61. [CrossRef]
18. Akinsola, G.D.; Awosusi, A.A.; Kirikkaleli, D.; Umarbeyli, S.; Adeshola, I.; Adebayo, T.S. Ecological footprint, public-private partnership investment in energy, and financial development in Brazil: A gradual shift causality approach. *Environ. Sci. Pollut. Res.* **2022**, *29*, 10077–10090. [CrossRef]
19. Danish; Ulucak, R.; Khan, S.U.-D. Determinants of the ecological footprint: Role of renewable energy, natural resources, and urbanization. *Sustain. Cities Soc.* **2020**, *54*, 101996. [CrossRef]
20. Kihombo, S.; Ahmed, Z.; Chen, S.; Adebayo, T.S.; Kirikkaleli, D. Linking financial development, economic growth, and ecological footprint: What is the role of technological innovation? *Environ. Sci. Pollut. Res.* **2021**, *28*, 61235–61245. [CrossRef]
21. Rafique, M.Z.; Nadeem, A.M.; Xia, W.; Ikram, M.; Shoaib, H.M.; Shahzad, U. Does economic complexity matter for environmental sustainability? Using ecological footprint as an indicator. *Environ. Dev. Sustain.* **2022**, *24*, 4623–4640. [CrossRef] [PubMed]
22. Galli, A.; Wiedmann, T.; Ercin, E.; Knoblauch, D.; Ewing, B.; Giljum, S. Integrating Ecological, Carbon and Water footprint into a "Footprint Family" of indicators: Definition and role in tracking human pressure on the planet. *Ecol. Indic.* **2012**, *16*, 100–112. [CrossRef]
23. Rees, W.E. Ecological footprints and appropriated carrying capacity: What urban economics leaves out. *Environ. Urban.* **1992**, *4*, 121–130. [CrossRef]
24. Siche, R.; Pereira, L.; Agostinho, F.; Ortega, E. Convergence of ecological footprint and emergy analysis as a sustainability indicator of countries: Peru as case study. *Commun. Nonlinear Sci. Numer. Simul.* **2010**, *15*, 3182–3192. [CrossRef]
25. Wang, Q.; Sun, J.; Li, R.; Korkut Pata, U. Linking trade openness to load capacity factor: The threshold effects of natural resource rent and corruption control. *Gondwana Res.* **2023**, S1342937X23001557. [CrossRef]
26. World Bank. *World Development Indicators (WDI)*; World Bank: Washington, DC, USA, 2023. Available online: https://databank.worldbank.org/source/world-development-indicators (accessed on 17 February 2023).
27. Raihan, A.; Tuspekova, A. Towards sustainability: Dynamic nexus between carbon emission and its determining factors in Mexico. *Energy Nexus* **2022**, *8*, 100148. [CrossRef]
28. Cai, J.; Zheng, H.; Vardanyan, M.; Shen, Z. Achieving carbon neutrality through green technological progress: Evidence from China. *Energy Policy* **2023**, *173*, 113397. [CrossRef]
29. Pata, U.K.; Balsalobre-Lorente, D. Exploring the impact of tourism and energy consumption on the load capacity factor in Turkey: A novel dynamic ARDL approach. *Environ. Sci. Pollut. Res.* **2022**, *29*, 13491–13503. [CrossRef] [PubMed]
30. Khan, U.; Khan, A.M.; Khan, M.S.; Ahmed, P.; Haque, A.; Parvin, R.A. Are the impacts of renewable energy use on load capacity factors homogeneous for developed and developing nations? Evidence from the G7 and E7 nations. *Environ. Sci. Pollut. Res.* **2022**, *30*, 24629–24640. [CrossRef]
31. Awosusi, A.A.; Kutlay, K.; Altuntaş, M.; Khodjiev, B.; Agyekum, E.B.; Shouran, M.; Elgbaily, M.; Kamel, S. A Roadmap toward Achieving Sustainable Environment: Evaluating the Impact of Technological Innovation and Globalization on Load Capacity Factor. *Int. J. Environ. Res. Public Health* **2022**, *19*, 3288. [CrossRef]
32. Shang, Y.; Razzaq, A.; Chupradit, S.; Binh An, N.; Abdul-Samad, Z. The role of renewable energy consumption and health expenditures in improving load capacity factor in ASEAN countries: Exploring new paradigm using advance panel models. *Renew. Energy* **2022**, *191*, 715–722. [CrossRef]
33. Akadiri, S.S.; Adebayo, T.S.; Riti, J.S.; Awosusi, A.A.; Inusa, E.M. The effect of financial globalization and natural resource rent on load capacity factor in India: An analysis using the dual adjustment approach. *Environ. Sci. Pollut. Res.* **2022**, *29*, 89045–89062. [CrossRef] [PubMed]
34. Pata, U.K.; Isik, C. Determinants of the load capacity factor in China: A novel dynamic ARDL approach for ecological footprint accounting. *Resour. Policy* **2021**, *74*, 102313. [CrossRef]
35. Fareed, Z.; Salem, S.; Adebayo, T.S.; Pata, U.K.; Shahzad, F. Role of Export Diversification and Renewable Energy on the Load Capacity Factor in Indonesia: A Fourier Quantile Causality Approach. *Front. Environ. Sci.* **2021**, *9*, 770152. [CrossRef]
36. Majeed, M.T.; Tauqir, A.; Mazhar, M.; Samreen, I. Asymmetric effects of energy consumption and economic growth on ecological footprint: New evidence from Pakistan. *Environ. Sci. Pollut. Res.* **2021**, *28*, 32945–32961. [CrossRef]
37. Solarin, S.A.; Nathaniel, S.P.; Bekun, F.V.; Okunola, A.M.; Alhassan, A. Towards achieving environmental sustainability: Environmental quality versus economic growth in a developing economy on ecological footprint via dynamic simulations of ARDL. *Environ. Sci. Pollut. Res.* **2021**, *28*, 17942–17959. [CrossRef]
38. Huang, Y.; Villanthenkodath, M.A.; Haseeb, M. The nexus between eco-friendly technology and environmental degradation in India: Does the N or inverted N-shape load capacity curve(LCC) hypothesis hold? *Nat. Resour. Forum* **2023**, *47*, 276–297. [CrossRef]
39. Guloglu, B.; Emre Caglar, A.; Korkut Pata, U. Analyzing the determinants of the load capacity factor in OECD countries: Evidence from advanced quantile panel data methods. *Gondwana Res.* **2023**, *118*, 92–104. [CrossRef]
40. Pata, U.K.; Samour, A. Assessing the role of the insurance market and renewable energy in the load capacity factor of OECD countries. *Environ. Sci. Pollut. Res.* **2023**, *30*, 48604–48616. [CrossRef]
41. Zhao, W.-X.; Samour, A.; Yi, K.; Al-Faryan, M.A.S. Do technological innovation, natural resources and stock market development promote environmental sustainability? Novel evidence based on the load capacity factor. *Resour. Policy* **2023**, *82*, 103397. [CrossRef]

42. Hakkak, M.; Altintaş, N.; Hakkak, S. Exploring the relationship between nuclear and renewable energy usage, ecological footprint, and load capacity factor: A study of the Russian Federation testing the EKC and LCC hypothesis. *Renew. Energy Focus* **2023**, *46*, 356–366. [CrossRef]
43. Caglar, A.E.; Mert, M.; Boluk, G. Testing the role of information and communication technologies and renewable energy consumption in ecological footprint quality: Evidence from world top 10 pollutant footprint countries. *J. Clean. Prod.* **2021**, *298*, 126784. [CrossRef]
44. Pata, U.K. Renewable and non-renewable energy consumption, economic complexity, CO_2 emissions, and ecological footprint in the USA: Testing the EKC hypothesis with a structural break. *Environ. Sci. Pollut. Res.* **2021**, *28*, 846–861. [CrossRef] [PubMed]
45. Nathaniel, S.; Nwodo, O.; Adediran, A.; Sharma, G.; Shah, M.; Adeleye, N. Ecological footprint, urbanization, and energy consumption in South Africa: Including the excluded. *Environ. Sci. Pollut. Res.* **2019**, *26*, 27168–27179. [CrossRef] [PubMed]
46. Nathaniel, S.P. Ecological footprint, energy use, trade, and urbanization linkage in Indonesia. *GeoJournal* **2021**, *86*, 2057–2070. [CrossRef]
47. Ahmed, Z.; Zafar, M.W.; Ali, S. Danish Linking urbanization, human capital, and the ecological footprint in G7 countries: An empirical analysis. *Sustain. Cities Soc.* **2020**, *55*, 102064. [CrossRef]
48. Nathaniel, S.; Khan, S.A.R. The nexus between urbanization, renewable energy, trade, and ecological footprint in ASEAN countries. *J. Clean. Prod.* **2020**, *272*, 122709. [CrossRef]
49. Ansari, M.A.; Haider, S.; Masood, T. Do renewable energy and globalization enhance ecological footprint: An analysis of top renewable energy countries? *Environ. Sci. Pollut. Res.* **2021**, *28*, 6719–6732. [CrossRef]
50. Shahbaz, M.; Dogan, M.; Akkus, H.T.; Gursoy, S. The effect of financial development and economic growth on ecological footprint: Evidence from top 10 emitter countries. *Environ. Sci. Pollut. Res.* **2023**, *30*, 73518–73533. [CrossRef]
51. Ulucak, Z.Ş.; İlkay, S.Ç.; Özcan, B.; Gedikli, A. Financial globalization and environmental degradation nexus: Evidence from emerging economies. *Resour. Policy* **2020**, *67*, 101698. [CrossRef]
52. Shahzad, U.; Ferraz, D.; Nguyen, H.-H.; Cui, L. Investigating the spill overs and connectedness between financial globalization, high-tech industries and environmental footprints: Fresh evidence in context of China. *Technol. Forecast. Soc. Chang.* **2022**, *174*, 121205. [CrossRef]
53. Shahbaz, M.; Balsalobre, D.; Shahzad, S.J.H. The Influencing Factors of CO_2 Emissions and the Role of Biomass Energy Consumption: Statistical Experience from G-7 Countries. *Environ. Model. Assess.* **2019**, *24*, 143–161. [CrossRef]
54. Tang, C.F.; Tan, B.W. The impact of energy consumption, income and foreign direct investment on carbon dioxide emissions in Vietnam. *Energy* **2015**, *79*, 447–454. [CrossRef]
55. Kihombo, S.; Vaseer, A.I.; Ahmed, Z.; Chen, S.; Kirikkaleli, D.; Adebayo, T.S. Is there a tradeoff between financial globalization, economic growth, and environmental sustainability? An advanced panel analysis. *Environ. Sci. Pollut. Res.* **2022**, *29*, 3983–3993. [CrossRef] [PubMed]
56. Grossman, G.M.; Krueger, A.B. *Environmental Impacts of a North American Free Trade Agreement*; NBER Working Paper Series; National Bureau of Economic Research: Cambridge, MA, USA, 1991.
57. Fatima, T.; Mentel, G.; Doğan, B.; Hashim, Z.; Shahzad, U. Investigating the role of export product diversification for renewable, and non-renewable energy consumption in GCC (gulf cooperation council) countries: Does the Kuznets hypothesis exist? *Environ. Dev. Sustain.* **2022**, *24*, 8397–8417. [CrossRef] [PubMed]
58. Chen, H.; Tackie, E.A.; Ahakwa, I.; Musah, M.; Salakpi, A.; Alfred, M.; Atingabili, S. Does energy consumption, economic growth, urbanization, and population growth influence carbon emissions in the BRICS? Evidence from panel models robust to cross-sectional dependence and slope heterogeneity. *Environ. Sci. Pollut. Res.* **2022**, *29*, 37598–37616. [CrossRef]
59. Paramati, S.R.; Shahzad, U.; Doğan, B. The role of environmental technology for energy demand and energy efficiency: Evidence from OECD countries. *Renew. Sustain. Energy Rev.* **2022**, *153*, 111735. [CrossRef]
60. Cobb, C.W.; Douglas, P.H. A theory of production. *Am. Econ. Rev.* **1928**, *18*, 139–165.
61. Sahoo, M.; Sethi, N. The dynamic impact of urbanization, structural transformation, and technological innovation on ecological footprint and PM2.5: Evidence from newly industrialized countries. *Environ. Dev. Sustain.* **2022**, *24*, 4244–4277. [CrossRef]
62. Raihan, A.; Tuspekova, A. Toward a sustainable environment: Nexus between economic growth, renewable energy use, forested area, and carbon emissions in Malaysia. *Resour. Conserv. Recycl. Adv.* **2022**, *15*, 200096. [CrossRef]
63. Dickey, D.A.; Fuller, W.A. Distribution of the estimators for autoregressive time series with a unit root. *J. Am. Stat. Assoc.* **1979**, *74*, 427–431.
64. Elliott, G.; Rothenberg, T.J.; Stock, J.H. *Efficient Tests for an Autoregressive Unit Root*; National Bureau of Economic Research: Cambridge, MA, USA, 1992.
65. Phillips, P.C.B.; Perron, P. Testing for a unit root in time series regression. *Biometrika* **1988**, *75*, 335–346. [CrossRef]
66. Pesaran, M.H.; Shin, Y.; Smith, R.J. Bounds testing approaches to the analysis of level relationships. *J. Appl. Econom.* **2001**, *16*, 289–326. [CrossRef]
67. Sharif, A.; Kartal, M.T.; Bekun, F.V.; Pata, U.K.; Foon, C.L.; Kılıç Depren, S. Role of green technology, environmental taxes, and green energy towards sustainable environment: Insights from sovereign Nordic countries by CS-ARDL approach. *Gondwana Res.* **2023**, *117*, 194–206. [CrossRef]
68. Luqman, M.; Li, Y.; Khan, S.U.-D.; Ahmad, N. Quantile nexus between human development, energy production, and economic growth: The role of corruption in the case of Pakistan. *Environ. Sci. Pollut. Res.* **2021**, *28*, 61460–61476. [CrossRef]

69. Stock, J.H.; Watson, M.W. A Simple Estimator of Cointegrating Vectors in Higher Order Integrated Systems. *Econometrica* **1993**, *61*, 783. [CrossRef]
70. Phillips, P.C.; Hansen, B.E. Statistical inference in instrumental variables regression with I (1) processes. *Rev. Econ. Stud.* **1990**, *57*, 99–125.
71. Park, J.Y. Canonical Cointegrating Regressions. *Econometrica* **1992**, *60*, 119. [CrossRef]
72. Yao, S.; Zhang, S.; Zhang, X. Renewable energy, carbon emission and economic growth: A revised environmental Kuznets Curve perspective. *J. Clean. Prod.* **2019**, *235*, 1338–1352. [CrossRef]
73. Peyerl, D.; Barbosa, M.O.; Ciotta, M.; Pelissari, M.R.; Moretto, E.M. Linkages between the Promotion of Renewable Energy Policies and Low-Carbon Transition Trends in South America's Electricity Sector. *Energies* **2022**, *15*, 4293.
74. Sahoo, M.; Sethi, N.; Angel Esquivias Padilla, M. Unpacking the dynamics of information and communication technology, control of corruption and sustainability in green development in developing economies: New evidence. *Renew. Energy* **2023**, *216*, 119088. [CrossRef]
75. Rahman, M.M.; Alam, K. Life expectancy in the ANZUS-BENELUX countries: The role of renewable energy, environmental pollution, economic growth and good governance. *Renew. Energy* **2022**, *190*, 251–260. [CrossRef]
76. Ahmad, M.; Zhao, Z.-Y. Empirics on linkages among industrialization, urbanization, energy consumption, CO_2 emissions and economic growth: A heterogeneous panel study of China. *Environ. Sci. Pollut. Res.* **2018**, *25*, 30617–30632. [CrossRef] [PubMed]

sustainability

MDPI

Review

Bibliometrics and Knowledge Map Analysis of Research Progress on Biological Treatments for Volatile Organic Compounds

Yuan Wang [1,2,3], Bin Zhou [4], Mengrong Yang [2,3,5], Gao Xiao [1], Hang Xiao [2,3,*] and Xiaorong Dai [2,3,6,*]

[1] College of Environmental and Safety Engineering, Fuzhou University, Fuzhou 350108, China
[2] Key Laboratory of Urban Environment and Health, Institute of Urban Environment, Chinese Academy of Sciences, Xiamen 361021, China
[3] Zhejiang Key Laboratory of Urban Environmental Processes and Pollution Control, Ningbo (Beilun) Zhongke Haixi Industrial Technology Innovation Center, Ningbo 315800, China
[4] Zhejiang Provincial Animal Husbandry Technology Extension and Breeding Livestock and Poultry Monitoring Station, Hangzhou 310020, China
[5] University of Chinese Academy of Sciences, Beijing 100049, China
[6] College of Biological and Environmental Sciences, Zhejiang Wanli University, Ningbo 315100, China
* Correspondence: hxiao@iue.ac.cn (H.X.); xrdai@zwu.edu.cn (X.D.)

Abstract: The emission of volatile organic compounds (VOCs) has resulted in increasingly severe harm to the environment and human health. In recent years, biological methods have become the preferred technology for VOC removal due to their environmental friendliness and economic advantages. Based on the theory of bibliometrics, this study analyzed research articles and reviews on biological methods for VOC removal published in the Web of Science Core Collection (WOSCC) database from 1966 to 2021. The knowledge map visualization software CiteSpace was utilized to analyze research progress in different countries, co-citation clustering, co-citation bursts, and keyword clustering in the literature data. The results indicated that early research on VOC biological treatment focused on the removal of odorous gases and single components of volatile organic waste gases. Subsequently, benzene contents (BTEX), hydrophobic VOCs, and multi-component VOCs have gradually become the focus of research. In recent years, improving VOC removal efficiency by studying packing materials and microbial communities has become an important research topic both domestically and internationally. Future research should focus on continuously improving the performance of reactors, developing novel reactors, and investigating technologies for treating complex and recalcitrant VOCs.

Keywords: volatile organic compounds; biological methods; bibliometrics; CiteSpace; clustering analysis

1. Introduction

Volatile organic compounds (VOCs) are a class of gaseous pollutants widely present in the atmosphere. According to the definition of the World Health Organization, VOCs are various organic compounds with boiling points ranging from 50 °C to 260 °C at standard atmospheric pressure. VOCs emanate from a diverse range of sources. Outdoor sources of pollution include effluent gases from chemical, paper, pharmaceutical, electronic, and other industries [1], as well as automobile exhaust produced by transportation. Indoor emissions primarily originate from activities such as coal burning, natural gas combustion, and building decoration. In the atmosphere, VOCs are not only precursors for the formation of secondary pollutants, such as $PM_{2.5}$ and O_3, but also react with other substances in the air to cause air pollution problems, such as haze and photochemical smog [2]. In addition, the majority of VOCs are irritant, toxic, teratogenic, and carcinogenic, not only causing sensory discomfort but also inflicting severe harm. For instance, formaldehyde, a

pollutant emitted by indoor decorations, can trigger headaches and nausea when present at a concentration above a certain threshold. Moreover, it can lead to coma and harm the human respiratory and nervous systems [3]. Benzene series are very harmful to human blood, viscera, and nerves and can cause teratogenic, carcinogenic, and mutagenic effects in severe cases [4]. In 1979, the United Nations Economic Commission for Europe convened a transnational conference on air pollution in Geneva, which centered on the management of VOCs. Currently, with the aggravation of air pollution worldwide, nations are increasingly recognizing the impact of VOCs. Laws and regulations regarding emissions are being regulated, and treatment technologies are being gradually improved.

VOC treatment technologies are mainly divided into two categories: recovery and removal methods. The recovery methods involve physical techniques, such as adsorption [5] and condensation [6], to adsorb or separate VOCs. However, these methods only transfer pollutants from the gas phase to the liquid or solid phase [7]. Since VOCs cannot be completely eliminated, further treatment is required to mitigate their impact. The removal methods for VOCs comprise combustion [8], photocatalysis [9], plasma technology [10], and biological methods [11]. These methods primarily involve chemical or biochemical reactions that utilize light, heat, microorganisms, and catalysts to degrade pollutants into harmless inorganic substances, such as CO_2 and H_2O. In recent years, the biological method has undergone widespread development and application due to its low economic cost and environmentally friendly advantages. The primary processes include biofiltration, biotrickling filtration, and bioscrubbing [12]. Among these processes, biofiltration is the most extensively employed and is suitable for treating low flow rates of waste gas [13]. Biotrickling filtration is effective in treating high loads of VOCs and malodorous gases [14]. Bioscrubbing is appropriate for the removal of organic waste gas with good water solubility [15]. Given the rapid development of testing technology and biotechnology, the objects and process technologies of biological methods are also constantly changing. However, the current research still has some limitations. The removal efficiency of complex and difficult-to-degrade acid gas is relatively low; studies on the mechanism of biofilm formation and microbial community evolution in the reactor are not systematic and perfect. Hence, it is necessary to conduct a comprehensive review of related research to provide a reference for the improvement and development of biotechnology.

The traditional literature review involves collecting relevant papers in the field and summarizing, organizing, and reviewing the information. Bibliometrics is the science of quantitatively analyzing knowledge carriers using mathematical and statistical methods, with the primary objects of analysis being the volume of literature, author information, and vocabulary count. This article employs the theoretical framework of bibliometrics and utilizes the knowledge mapping visualization software CiteSpace [16], developed by Professor Chaomei Chen, to quantitatively analyze and model papers published on a global scale and over an extended period in the research field of VOC biological removal. The article outlines the knowledge structure, developmental lineage, and research trends in this field. By mining key studies in the literature and newly published articles, the research focus and development direction in this field are further summarized to provide ideas and references for future research.

2. Data Sources and Analysis Methods

2.1. Data Sources

The literature data used in this paper are from the Web of Science core collection (WOSCC) database, encompassing authoritative and high-impact academic journals across various subject areas. Abstract and keyword information was not included in the WOSCC data for articles published in 1990 and before. As a result, the search strategy was divided into two parts. In the first part, the search term "TS = (biofilter* OR biofiltration*) AND TS = (VOCs* OR volatile organic compounds*)" was used, and the publication types "Article" and "Review" were selected. The literature retrieval period was set from 1 January 1990 to 31 July 2021, and this resulted in obtaining a total of 824 publications. The first part

of the literature was used as the primary data for analyzing the progress of related research using the visualization software CiteSpace. The search strategy in the second part was altered to "TI = (biofilter* OR soil bed)", with the publication types "Article" and "Review" selected. The retrieval period time was set from 1900 to 1989. A total of 114 search results were obtained, and after manually screening papers related to the topic, 13 papers were selected to understand the developmental history of global biofiltration. As the data in the second part lacked citation information, they were not imported into CiteSpace, and only the relevant contents were directly reviewed.

2.2. Analysis Method

Initially, the number of published papers in the country was manually imported into Microsoft Excel 2019 to calculate the number of published papers all over the world. The WOSCC retrieved documents were downloaded in the format of "full record and cited references" and saved as a plain text (txt) file. The data were imported into the online platform https://bibliometric.com/ (accessed on 9 August 2022) and CiteSpace (5.7.R5). By setting different node types, we were able to visualize the data information, such as the publication volume trends, the cooperation networks of countries and institutions, co-citation clustering, and keyword time zones. We obtained a knowledge map to analyze the distribution characteristics and knowledge structure of papers in the research field, the key research contents and evolution process, the state of research and important studies, as well as the research hotspots and future development trends. The data analysis process is presented in Figure 1.

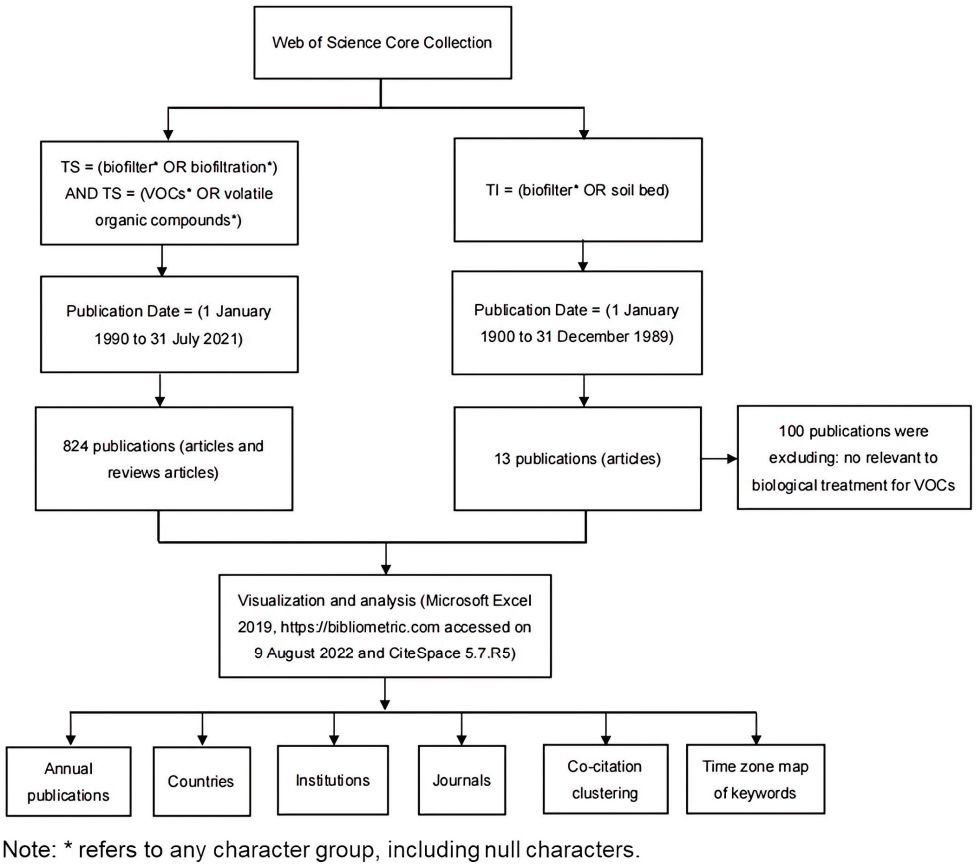

Figure 1. Flow chart for the analysis of VOC removal by biological treatment.

3. General Overview

3.1. Number of Published Studies in the Literature

Figure 2 illustrates the annual number of studies published worldwide in the literature retrieved from WOSCC. The results indicate that the number of studies increased slowly until 1997. The initial publication in 1966 by Carlson and Leiser [17] used biofiltration to remove odor and emphasized the crucial role of microorganisms in the soil in odor removal. This was followed by the promotion and application of biological treatment technologies in European countries through the 1980s. From 1997 onwards, there was a substantial increase in the number of published papers, which exhibited an upward trend. Among the published papers, the most-cited article is the review published by Faisal and Aloke in 2000, titled "Removal of Volatile Organic Compounds from polluted air" [18]. They presented and evaluated each technology for VOC control in detail and concluded that biofiltration would be the most popular option in the future.

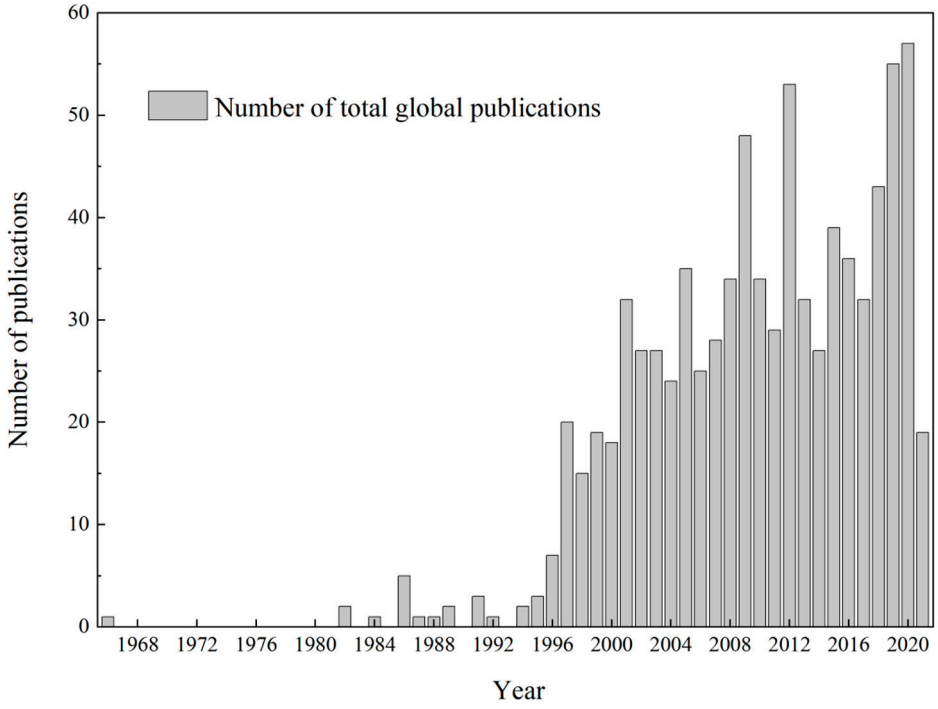

Figure 2. Annual number of publications (as of 31 July 2021).

3.2. Country Cooperation Network

The collaboration network of countries was established based on country collaborations in the cited literature, and collaboration was considered to exist when authors from two different countries contributed to the same article. Based on the publications related to the research topic that appeared between 1900 and 2021, the countries with more than 10 publications and the network of collaborations between them are shown in Figure 3. The circle color scale radiating outward from the center corresponds to the year of publication. The color ranges from dark purple to yellow-green, indicating early to recent years, respectively. In addition, the color of the circle's center represents the earliest year of publications, while the thickness of the color scale corresponds to the number of publications in the respective years. The United States' and Canada's circle centers are dark purple, indicating that relevant research was conducted at the earliest time. The average annual number of publications in the United States is evenly distributed, suggesting that there are continuous research outcomes published in this field. On the other hand, China's and Spain's circle centers are dark green, signifying that research in these countries started later. The color levels for China are predominantly from light green to yellow, implying that the main research results have been published in recent years. The size of the circles

corresponds to the total number of publications. As shown in the figure, the number of publications in the United States is significantly higher than that in other countries, indicating that the United States holds a leading position in the field of biological VOC removal research. Additionally, several countries in the figure have nodes encompassed by rosy-red circles outside, which denote points with high intermediary centrality in the network. Intermediary centrality is a commonly used indicator for centrality measurement, representing a pivotal node with strong connections to other nodes. Countries such as the United States, Spain, and Canada have more interactions and collaborations with scholars from other countries in this field.

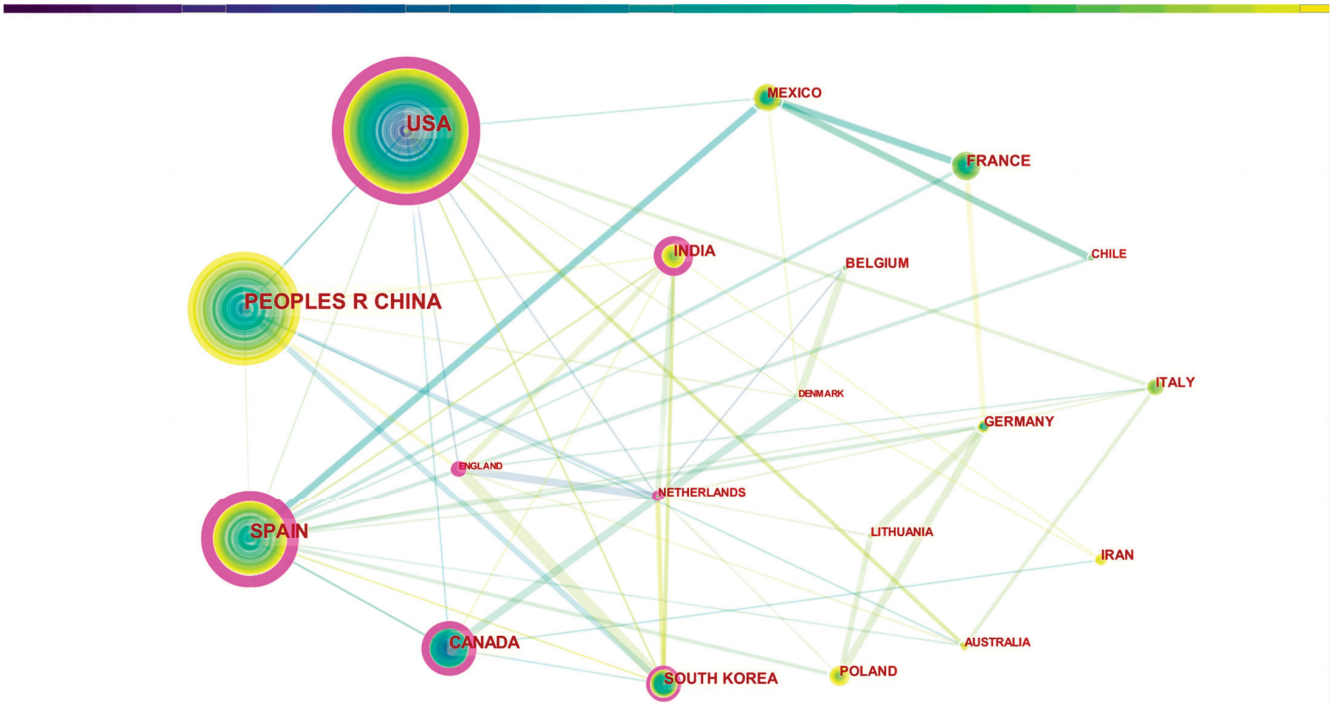

Figure 3. Country Cooperation Network.

3.3. Research Institutions

Table 1 shows the primary institutions and analytical indicators concerning global research on biological VOC removal from 1990 to 2021. The University of Cincinnati held the top spot in the United States based on the combined count of publications and citations, while Hunan University ranked first in terms of the average number of citations. The institutions in the table are the main forces in the research field and have a strong influence on biological treatment research.

Table 1. Major research institutions.

Rank	Institution	Number of Published Articles	Total Number of Citations	Total Citation Rank	Average Number of Citations
1	Univ Cincinnati University of Cincinnati (USA)	41	475	1	11.59
2	Tsinghua Univ Tsinghua University (China)	36	205	6	5.69
3	Chinese Acad Sci Chinese Academy of Sciences (China)	34	152	11	4.47
4	Univ Ghent University of Ghent (Belgium)	28	129	15	4.61

Table 1. *Cont.*

Rank	Institution	Number of Published Articles	Total Number of Citations	Total Citation Rank	Average Number of Citations
5	Univ Valladolid University of Valladolid (Spain)	27	237	5	8.78
6	Hunan Univ Hunan University (China)	25	443	2	17.72
7	Univ Sherbrooke Shebuch University (Canada)	25	308	4	12.32
8	Univ A Coruna University of A Coruña (Spain)	24	376	3	15.67
9	Univ Technol Sydney University of Technology Sydney (Australia)	19	117	18	6.16
10	Tianjin Univ Tianjin University (China)	18	52	40	2.89

3.4. Highly Published Journals

The top 10 journals based on the number of publications are shown in Table 2, with the *Journal of Chemical Technology and Biotechnology* (JCTB) and *Chemosphere* (CHEMOSPHERE) being tied for first place with 43 publications. The total number of citations reflects the academic influence of the journals, as illustrated in the table. The *Journal of the Air Waste Management Association* (JAWMA), the *Journal of Chemical Technology and Biotechnology* (JCTB), and the *Journal of Hazardous Materials* (JHM) are the three most influential journals in this research area. This is important information for new researchers regarding submissions.

Table 2. Top 10 journals in terms of published articles.

Rank	Journal	Number of Published Articles	Total Number of Citations	Total Citation Rank	Average Number of Citations
1	*Journal of Chemical Technology and Biotechnology* (JCTB)	43	368	2	8.56
2	*Chemosphere* (CHEMOSPHERE)	43	189	7	4.40
3	*Journal of the Air Waste Management Association* (JAWMA)	40	401	1	10.03
4	*Journal of Hazardous Materials* (JHM)	31	343	3	11.06
5	*Chemical Engineering Journal* (CEJ)	30	296	4	9.87
6	*Bioresource Technology* (BT)	30	212	5	7.07
7	*Environmental Technology* (ET)	27	104	18	3.85
8	*Water Science and Technology* (WST)	25	128	16	5.12
9	*Biochemical Engineering Journal* (BEJ)	19	133	15	7.00
10	*Biotechnology and Bioengineering* (BB)	18	198	6	11.00

4. Research Themes and Key Studies

4.1. Co-Citation Clustering

Co-citation clustering refers to cases where two or more authors are cited by one or more subsequent papers simultaneously, leading to a co-citation relationship between them. The 30 publications with the highest number of citations every two years were selected in CiteSpace to construct a citation network from 1990 to 2021. Multiple networks were synthesized to obtain a citation network with 263 nodes and 412 connected lines. The clustering function generates knowledge clusters based on the log-likelihood algorithm and assigns labels for the clusters based on the title subject terms of the cited studies in each cluster, as shown in the Figure 4. Clustering aids researchers in identifying the subdomains of a research topic. The modularity and the weighted mean silhouette are the metrics used

to assess whether the clustering is optimal. In Figure 4, these are 0.84 and 0.94, signifying that the subdomains of clustering and the classification results are evident [19].

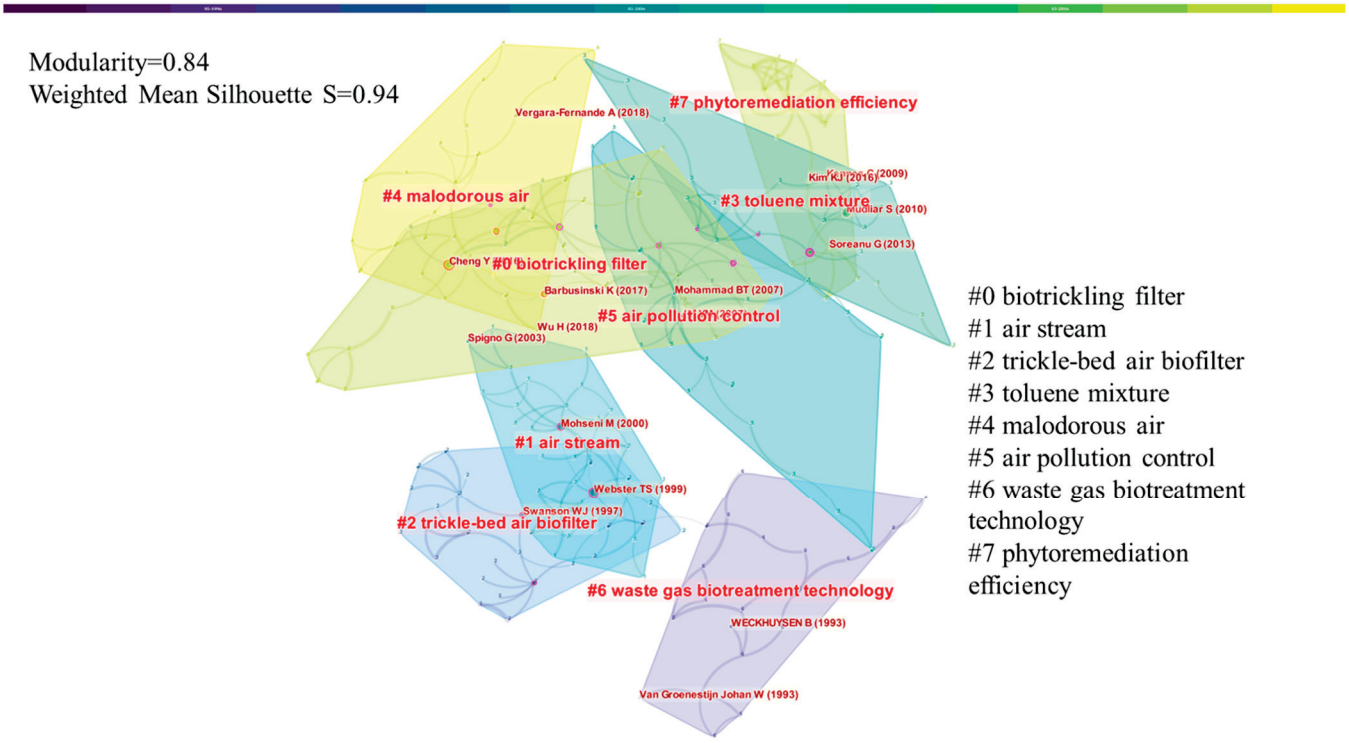

Figure 4. Co-citation clustering.

Table 3 shows the details of the eight main clusters, including the cluster silhouette, the average year, and the topic identifiers. The cluster silhouette serves as an assessment metric for the clustering function, and the closer it is to 1, the better the clustering performance. The average year represents the period when more research outcomes were published. Cluster identifier words are generated according to the publication titles with the highest number of citations in each cluster. Through the color clustering in the co-citation map combined with the literature reading before 1990, we can understand the development of the research field of biological removal of VOCs.

Table 3. Clustering information.

Cluster Number	Number of Studies	Clustering Silhouette	Average Year	Subject Identifier
0	36	0.988	2015	Biotrickling Filter
1	30	0.946	2001	Air Stream
2	27	0.975	1996	Trickle-bed Air Biofilter
3	24	0.924	2009	Toluene Mixture
4	24	0.957	2016	Malodorous Air
5	21	1	2006	Air Pollution Control
6	20	0.931	1994	Waste Gas Biotreatment Technology
7	17	1	2016	Phytoremediation Efficiency

The first stage, before 1990, was characterized by the nascent phase of biological treatment technology. Even though the concept of biological treatment of waste gas was first proposed by Bach [20] as early as the 1820s, this technology did not receive much attention, and its development remained slow. It was not until the 1970s that the biological method was adopted in industries to address issues related to odor and organic and

inorganic pollutants. In the 1980s, Germany applied the biological method in chemical, printing, coating, and other industries, attaining favorable outcomes [21].

In the second stage, the identifying keywords included "waste gas biological treatment technology" (cluster 6) and "trickle-bed air biofilter" (cluster 2). In this stage, the application of biological methods expanded to include more advanced research areas. The implementation of the Clean Air Act Amendment in 1990 prompted the United States and other developed countries to deepen their research on VOCs, which comprise the vast majority of air pollutants and are categorized into various groups based on their chemical structure, such as alkanes, aromatics, alkenes, halocarbons, esters, aldehydes, ketones, and others. Aromatic compounds, which are complex and difficult to deal with, are commonly found in VOC emissions [22]. Most studies on removing VOCs using biological methods focus on benzene series compounds, particularly toluene. Other commonly studied compounds include chlorobenzene [23], ethyl acetate [24], and methyl tert-butyl ether [25], as well as various mixed organic waste gases. According to a survey, biotechnology accounted for 78% of the German deodorant market in 1994 [26], highlighting the efficacy of biotreatment technologies for waste gas treatment and air pollution control. In their review article "Waste gas biotreatment technology," Kennes et al. [27] introduced the three most widely used processes in waste gas biotreatment technology and provided application examples with different compounds. Meanwhile, Lu et al. [28] employed a trickle-bed biofilter to effectively remove ethyl acetate under low- to high-load conditions.

The third stage is characterized by the identifying keywords "air stream" (cluster 1), "air pollution control" (cluster 5), and "toluene mixture" (cluster 3). The period for this cluster is 2001–2009, and the research during this stage mainly focuses on the development of bioreactors, including innovative bioreactors in practical applications and laboratory development stages. In his review article "Bioprocesses for air pollution control," Kennes [29] provides a detailed analysis of the advantages and disadvantages of various reactor installations.

Stage four is characterized by the identifying keywords "biotrickling filter" (cluster 0), "malodorous air" (cluster 4), and "phytoremediation efficiency" (cluster 7). Compared with previous biological methods, this stage emphasizes the importance of low cost and environmental friendliness in effectively removing VOCs. The reactors commonly used during this stage are biotrickling filters, with internal fillers made of inorganic materials, such as ceramics or plastics. A biotrickling filtration system supplemented with a nutrient solution is added to better regulate the growth of microorganisms, which has a good effect on the treatment of high-load organic waste gas, hydrogen sulfide, and malodorous gas [30]. For instance, Yang et al. [31] explored the performance and degradation efficiency of biotrickling filters for treating chemical fiber VOCs and demonstrated that biotrickling filtration is a lower-cost and effective VOC control scheme compared with adsorption technology and regenerative catalytic oxidation technology. Zhang et al. [32] studied the treatment of ethyl acetate organic matter discharged from the pharmaceutical industry by biological drip filters and found that the average removal rate could reach 95% when the residence time of the empty bed was 17 s. In the review article "Technologies for Deodorization of Malodorous Gases", Wysocka et al. [33] compared various gas deodorization technologies and concluded that biological gas is a relatively low-cost method, but it should be considered when removing gases with high concentrations and complex components. Phytoremediation efficiency is usually used to deal with indoor formaldehyde and other harmful VOCs produced during the decoration process to create a better living environment for people. Irga et al. [34] evaluated the effectiveness of various common plant species in removing two major groups of VOCs. This study provides a baseline indication of the removal efficiency of plant species for modeling hydrophobic and hydrophilic VOCs. The findings show that it is feasible to select plants for target pollutant-dependent plant biofilters.

4.2. Key Studies

The burst detection feature provided by CiteSpace detects publications with a rapid increase in citations over a short period. These are referred to as high-burst papers, reflecting the research topic bias during that particular period. The 10 papers with the highest burst intensity calculated by CiteSpace and their related information are listed in Table 4, all of which relate to the subject of biological VOC treatment. The paper with the highest emergent intensity is "Challenges and solutions for biofiltration of hydrophobic volatile organic compounds" published by Cheng et al. in 2016 [35]. This review paper examined the factors influencing the biological removal of hydrophobic VOCs in five aspects: surfactant incorporation, application of fungal biocatalysts, pretreatment biofiltration, novel bioreactors, and utilization of hydrophilic compounds.

Table 4. High-burst publications.

Publication Title	Type of Publication	Specific Information	Total Citations	Strength	Burst Year
Challenges and Solutions for Biofiltration of Hydrophobic Volatile Organic Compounds [35]	Review	Cheng, Y., 2016, Biotechnol Adv, V34, P1091	214	20.20	2017–2021
Biofiltration for Air Pollution Control [36]	Book	Devinny J S, 1999, Biofiltration Air Po, V0, P0	277	17.71	1999–2004
Bioreactors for Treatment of VOCs and Odours—A Review [37]	Review	Mudliar S, 2010, J Environ Manage, V91, P1039	349	17.49	2011–2016
Biofiltration of Mixtures of Hydrophilic and Hydrophobic Volatile Organic Compounds [38]	Article	Mohseni M, 2000, Chem Eng Sci, V55, P1545	164	12.03	2001–2006
Biological Methods for Odor Treatment—A Review [39]	Review	Barbusinski K, 2017, J Clean Prod, V152, P223	92	11.06	2019–2021
Simultaneous Removal of Multicomponent VOCs in Biofilters [40]	Review	Yang C P, 2018, Trends Biotechnol, V36, P673	89	10.61	2019–2021
A Comparative Study of Fungal and Bacterial Biofiltration Treating a VOC Mixture [41]	Article	Estrada J M, 2013, J Hazard Mater, V250, P190	68	9.82	2015–2018
Bioprocesses for Air Pollution Control [29]	Review	Kennes C, 2009, J Chem Technol Biot, V84, P1419	199	9.52	2011–2014
Biodegradation of BTEX in a Fungal Biofilter: Influence of Operational Parameters, Effect of Shock-Loads and Substrate Stratification [42]	Article	Rene E R, 2012, Bioresource Technol, V116, P204	78	8.86	2015–2018
Biofiltration of Toluene Vapor Under Steady-State and Transient Conditions: Theory and Experimental Results [43]	Article	Shareefdeen Z, 1994, Chem Eng Sci, V49, P4347	149	8.18	1997–2000

Papers 3, 5, 6, and 8 in the list are all reviews. Mudliar et al. [37] offered an overview of various bioreactors for the degradation of VOCs and malodorous gases. They provided detailed descriptions of their configurations and designs, operating mechanisms, and microbial degradation processes and of future research and development needs in this field. Barbusinski et al. [39] compared the variations in equipment design and the application scope of different odor treatment technologies by providing an overview of the available technologies, process principles, and characteristics. Yang et al. [40] conducted a review of the interactions between multiple target pollutants in the degradation of VOCs and proposed ways to mitigate the antagonistic effects by improving bioavailability and

biodegradability. Kennes et al. [29] introduced the biodegradation process, as well as the types and relative merits of innovative bioreactors that are in application or still in the experimental stage.

Papers 4, 7, 9, and 10 in the list are studies on the influencing factors and optimization methods in the removal of VOCs by biological methods. Mohseni et al. [38] discovered that the removal efficiency of two pollutants in mixed VOCs influenced each other, and the lipophilic properties of biofilms contributed to the high removal rate in the removal of VOCs. Estrada et al. [41] compared the efficiency of fungal and bacterial biodegradation of VOC mixtures (propionaldehyde, methyl isobutyl ketone, toluene, and hexanol) under the same operating conditions. In general, the removal capacity of fungal biofilters was lower than that of bacterial biofilters, and the implementation of coupled fungal/bacterial systems did not significantly enhance the performance of VOC removal. Rene et al. [42] examined the effectiveness of biological methods for removing a mixture of benzene pollutants and compared the conditions required for achieving optimal removal under various influencing factors. Shareefdeen et al. [43] conducted a parameter sensitivity study using a model and validated the feasibility of the model through experiments on the removal of toluene vapor by gas-phase biofilters.

In addition, the second publication in the list was compiled by Devinny et al. [36] in 1999 and comprises chapters on biofiltration mechanisms, biofiltration media, factors affecting and controlling biofiltration, microbial ecology in biofiltration, and biofiltration models, designs, and costs.

5. Research Hotspots and Trend Analysis

5.1. Analysis of Research Hotspots

A statistical analysis of the co-occurrence of keywords from 1990 to 2021 was performed. The basic information of the 30 most frequently used keywords is listed in Table 5 and can be roughly divided into the following categories:

Table 5. High-burst publications.

Rank	Keywords	Category	Frequency	Rank	Keywords	Category	Frequency
1	Biofiltration	Removal efficiency	510	16	Bioreactor	Reactor type	43
2	Biofilter	Reactor type	346	17	Odor	Pollutant	40
3	Volatile organic compound	Pollutant	283	18	Vapor	Removal efficiency	33
4	Removal	Removal efficiency	266	19	Waste gas	Environmental media	31
5	Toluene	Pollutant	232	20	Packing material	Principle	25
6	Biodegradation	Principle	206	21	Microbial community	Principle	24
7	VOC	Pollutant	206	22	Gas	Environmental media	23
8	Performance	Removal efficiency	195	23	Model	Removal efficiency	22
9	Air	Environmental media	157	24	Activated carbon	Principle	21
10	Biotrickling filter	Reactor type	132	25	BTEX	Pollutant	20
11	Degradation	Principle	129	26	Bacteria	Principle	19
12	Emission	Environmental media	67	27	Abatement	Removal efficiency	19
13	Hydrogen sulfide	Pollutant	60	28	Adsorption	Principle	18
14	Mixture	Pollutant	56	29	Biofilm	Principle	18
15	Benzene	Pollutant	54	30	Waste gas	Environmental media	17

The classification of environmental media can be identified with keywords, such as "air", "emission", "waste gas", and so forth. VOC pollutants are significant components of air pollution. Their sources can be categorized into natural and anthropogenic. Natural sources include activities such as volcanic eruptions, forest fires, and decay of animal and plant remains. Anthropogenic sources can be further subcategorized into mobile and stationary sources, with mobile sources mainly referring to vehicle exhaust emissions and stationary sources referring to the release of exhaust gases during industrial, agricultural,

and other production processes. VOCs participate in the formation of ozone and secondary aerosols in the atmosphere and act as important precursors to haze and photochemical smog pollution [44]. Due to their strong volatility and human activities, the majority of VOCs accumulate, migrate, and diffuse into the atmosphere, leading to harmful impacts on the environment and human health.

The high-frequency keywords related to reactor types are "biofilter", "biotrickling filter", and "bioreactor". A biofilter typically consists of packing material that offers attachment sites for the growth and reproduction of microorganisms. The exhaust gas flows through the packing bed, comes into contact with the biofilm, and is degraded by microorganisms [45]. The biotrickling filter has a similar structure to the biofilter and is humidified by a circulating water system with a spray at the top. The exhaust gas enters the system from the bottom of the unit and comes into contact with the microorganisms. In a two-phase bioreactor, the gas phase is separated from the aqueous phase in the device by a membrane. The gas phase is contaminated air, which usually contains a carbon source, while the aqueous phase serves as the nutrient source for the biofilm that grows on the water side of the membrane surface [29].

The keywords of the pollutant categories are "toluene", "benzene", "BTEX", "hydrogen sulfide", etcetera, with toluene being the most frequently occurring pollutant. Toluene is a colorless, volatile liquid with a distinct odor that is widely used in industrial production, decoration products, chemical synthesis, and pesticides [46]. With toluene as a research object, new technologies are being developed. Hybrid biological treatment technologies, such as biofiltration and adsorption, can be effective in treating VOCs [47]. The biofiltration system of Streptomyces griseus immobilized on activated carbon is feasible for removing toluene and increasing the reuse rate, providing a new solution for industrial applications [48]. The microbial activity of the planted biofilter is significantly higher than that of the nonplanted biofilter, and the growth of ryegrass in the biofilter enhances the biodegradation of toluene [49]. The high-frequency keyword "mixture" refers to mixed waste gas, where various pollutants are often mixed in the discharge. Traditional biofilters are inefficient at treating mixed waste gas, so many scholars are investigating ways to enhance the performance of bioreactors for removing mixed waste gas. Some of the findings include: a single-stage biotrickling filter that can effectively treat both hydrogen sulfide and toluene [50]; and that the mixing of hydrophilic and hydrophobic VOCs can improve the mutual degradation rate [51]. Furthermore, the two-stage bioreactor is highly effective in treating mixed waste gases [52].

The keywords to explore the principle of biofiltration are "biofilm", "adsorption", and "biodegradation", to name a few. The basic principle of the biological method includes the following steps: firstly, the organic pollutants in the gas phase are transferred to the liquid phase; these organic compounds react with compounds in the liquid phase or adsorb on the packing materials and the biofilm on the surface of the packing materials through the liquid film; finally, pollutants are decomposed, transformed, or synthesized into part of the cytoplasm through biodegradation, producing intermediate metabolites, water, and carbon dioxide, as well as inorganic small molecules.

The keywords related to exploring the efficiency of the bioreactor are "removal", "performance", etcetera. The performance parameters of bioreactor operation include removal efficiency, surface loading, and empty bed residence time. The empty bed residence time refers to the time required for the gas to pass through the bioreactor, while effective residence time refers to the time required for the gas to pass through the filled packing layer. The empty bed residence time is usually considered in the design of bioreactors, and this parameter is related to the removal efficiency and volume of the bioreactor. The surface load is the gas flow rate per unit area of the reactor, and the longer the empty bed residence time, the lower the surface load. The removal efficiency is the most intuitive parameter for evaluating the performance of a bioreactor, and the pollutant removal efficiency of a successful bioreactor is generally 95~99% [53].

5.2. Analysis of Research Trends

The time-zone diagram in Figure 5 also allows for the analysis of research trends related to a particular subject keyword in the development of biological methods for treating VOCs, primarily in terms of bioreactor types, pollutant categories, and research methods.

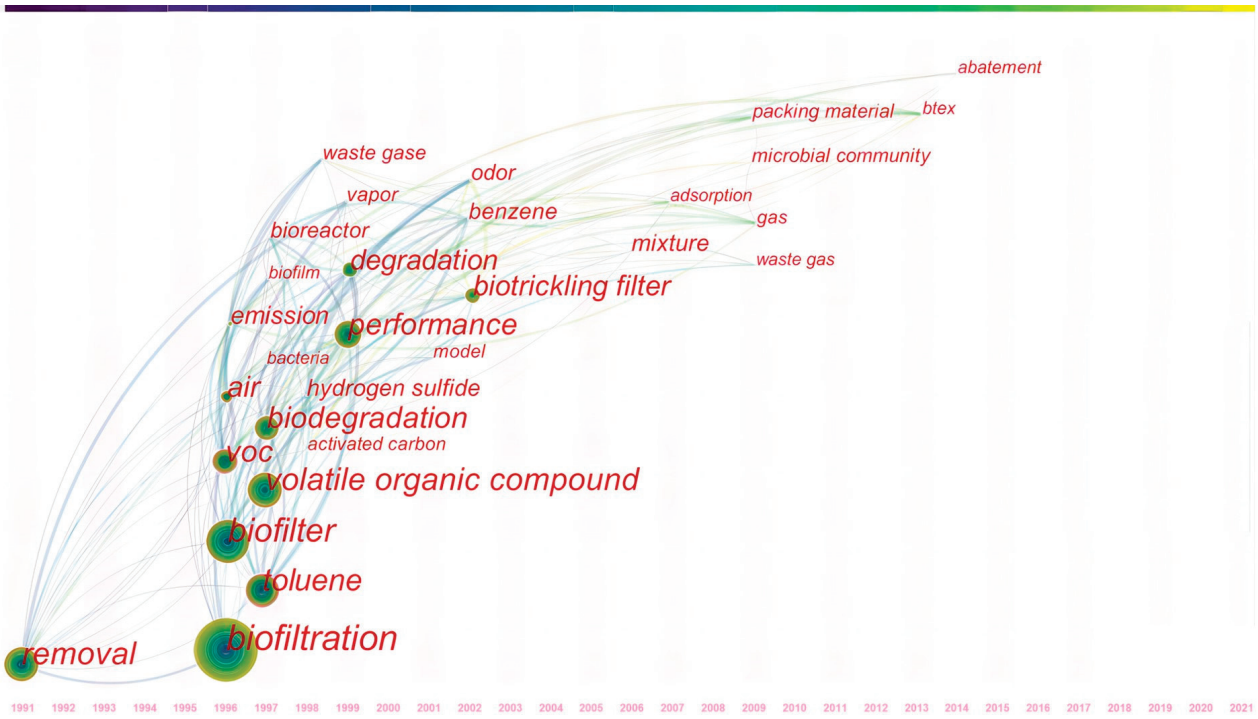

Figure 5. Time-zone map of keywords.

The type of treatment device shifted from biofilters to biotrickling filters from 1996 to 2002. Traditional biofilters are widely used for odor and VOC removal, having the advantages of simple operation and low operating costs. However, they have limitations in treating large flow rates and hard-to-degrade VOCs. The waste gas must meet the following requirements: hydrophilicity, easy biodegradability, and low concentration of particulate matter [54]. To improve the transfer efficiency of pollutants from the gas phase to the liquid phase, the biotrickling filter was developed. It solves the problems of degradation of packing materials and easy clogging when the pollutant load is high [55]. It can also better regulate the growth of microorganisms.

Around the year 2000, biological methods were primarily applied for the removal of single-component pollutants, such as hydrogen sulfide and toluene. However, with the increase in VOC pollution, the removal of single VOCs is insufficient for pollution control. As a result, benzene pollutants and mixed waste gases gradually became the mainstream targets of biological methods for studying treatments and their functionality. The keyword "BTEX" includes VOCs composed of benzene, toluene, ethylbenzene, xylene, etcetera [56]. BTEX has been a major research hotspot in the field of biological methods in recent years, and related studies are maturing. In industrial waste gas, BTEX is often emitted as a multicomponent mixture; thus, there are synergistic or antagonistic effects among the components in the biodegradation process [57,58]. Susant et al. [59] discovered that the presence of xylene promoted the removal of toluene from the mixture. Raboni et al. [60] achieved an average removal rate of over 96% when treating BTEX with bacteria and fungi in combination. To simultaneously improve the removal of BTEX, Mathur et al. [61] attempted to remove BTEX using a mixture of compost, bagasse, and granular activated carbon filters, and the removal of BTEX was almost 100% under suitable operating conditions. Klapková et al. [62] found that, in the removal of BTEX, bacterial strains

inoculated with toluene and xylene performed better than the indigenous microorganisms of the packing materials themselves. However, due to the very similar chemical structure and metabolism of BTEX, they showed more mutual inhibition in the process of biodegradation [63]. Inés et al. [64] experimentally demonstrated that the mixing of multiple waste gases in the reactor reduced the biodegradation rate of each pollutant and the overall biodegradation rate. Plessis et al. [65] found that toluene inhibited the removal of benzene and ethylbenzene in a biofilter inoculated with toluene-dominated bacteria.

The keyword at the research method level is "modeling", which refers to the use of computer and mathematical methods to model the waste gas treatment process and verify the feasibility of the model using experimental results. There have been numerous studies on this subject since the beginning of biological methods. Douglas et al. [66] described the transfer between gas and water phases, and the biodegradation process of substrates. Basil et al. [67] considered the mutual kinetics between pollutants and the effect of oxygen on biodegradation. Based on this, a model was developed for the treatment of mixed gas streams of VOCs in biofilters. Kyungnan et al. [68] utilized mathematical models to determine the results of vinyl acetate removal at different organic loading rates, solid residence times, and dissolved oxygen concentrations. Currently, the method of predicting and evaluating bioreactor operating parameters and effectiveness by constructing models needs further exploration and investigation.

In addition, both the "packing material" and the "microbial community" in the figure are hot topics and major trends of research in recent years. The previous biological methods were limited in treating high concentrations of organic and mixed waste gases. Therefore, the performance of bioreactors has been increasingly researched in recent years, mainly in the exploration of composite functional packing materials and functional microbial communities. The packing material is a solid medium for microbial growth and biofilm formation, and its characteristics, such as its nature, particle size, and moisture content [69], affect the performance of bioreactors. The nutrient level in the packing material [70] guarantees microbial growth and metabolism. The organic packing materials in the biological methods are generally compost [71,72], peat [73], soil [74], etc., while inorganic packing materials include perlite, ceramic, etc. When selecting packing materials, attention should be given to the characteristics of large specific surface area, high porosity, and strong water-retention capacity. To improve the removal efficiency and service life of packing materials, composite materials and new functional packing materials have been continuously developed. Dumont et al. [75] composited calcium carbonate, urea, phosphoric acid, and other materials to form a new type of packing material, with a removal rate of more than 90% of organic waste gas. A composite material can compensate for the shortcomings of a single material and enhance the efficiency of composite pollutant removal [76]. Han et al. filled a biofilter with perlite and a high-strength 3D matrix material, which not only has a higher mass transfer efficiency [77] but also has a lower pressure drop and can maintain long-term performance [78].

The microbial community is a crucial parameter in bioreactors, and the species and growth of microorganisms are closely related to the degradation of pollutants. Therefore, the analysis of the microbial community in the system is a key point to increase the scope of application and removal efficiency of biological methods. Bacteria and fungi are among the microbial species that are used in biological methods. The genus Pseudomonas is suitable for the removal of VOCs and malodorous gases; the genus Rhodococcus is suitable for the removal of toluene, naphthalene, and other substances [79]. The genera Saccharomyces, Mycobacterium, and Serratia in fungi [80] can also be used in bioreactors. Fungal microorganisms have a filamentous structure and a strong ability to adsorb VOCs, which enhance the removal efficiency of exhaust gases [81]. Currently, the microorganisms used in biological systems are mainly bacteria, but their practical application varies depending on the pollutants to be removed and the environmental conditions. For instance, Zheng et al. [82] discovered that the microbial community in bioreactors depends on the inlet load of pollutants and the characteristics of packing materials. Liu et al. [83] constructed a novel

three-stage biofilter composed of acidophilic bacteria, fungi, and heterotrophic bacteria, which could achieve high and stable removal of ammonia, hydrogen sulfide, and VOCs. With the advancement of biotechnology and new materials, the screening and cultivation of functional microorganisms and the development of 3D porous composites will be future research trends.

6. Conclusions and Outlook

In this paper, the biological removal of VOCs was taken as the subject of research, and the bibliometric software CiteSpace was employed to analyze 837 research articles and reviews in the core WOSCC database. The analysis indicated that between 1966 and 2021, the number of papers in the field of biological methods to remove VOCs increased significantly after 1997. The United States, Spain, and other countries have close cooperation with other countries, and leading research institutions are primarily located in countries such as the United States, China, Belgium, and Spain. They have made significant contributions to the research in this field.

According to the analysis of research hotspots and trends, the field of biological treatment of VOCs concentrated on the removal of malodorous gases and single species of VOCs in the early stage. However, with the growing demand for the treatment of refractory organic waste gases, research on the inadequacy of conventional biofilters for the removal of organic waste gases has intensified and expanded. Benzene, hydrophobic compounds, and multi-component mixed waste gases have been the most prevalent types of pollutants studied. Current research focuses on the interactions of mixed VOCs during the removal process, microbial communities, and packing material innovations.

To achieve more efficient and energy-saving purposes, future research on biological methods for VOC removal should be based on theoretical knowledge, such as the operating mechanisms of bioreactors, combined with practical application experience of existing biological treatment technologies. The focus should be on developing new biological treatment reactors and their processes, as well as improving the efficiency of bioreactors by strengthening the development of new composite packing materials and the screening and cultivation of functional microorganisms for degrading specific pollutants. This will enable us to meet practical application requirements and actively respond to air pollution concerns.

Author Contributions: Conceptualization, X.D. and H.X.; methodology, Y.W.; validation, M.Y.; formal analysis, Y.W.; investigation, Y.W.; writing—original draft preparation, Y.W.; writing—review and editing, X.D., G.X., M.Y. and H.X.; visualization, Y.W.; supervision, H.X.; project administration, B.Z. All authors have read and agreed to the published version of the manuscript.

Funding: This study was funded by the Basic Public Welfare Research Project of Zhejiang Province (LTGS23C170001) and the Department of Agriculture and Rural Affairs of Zhejiang Province (2022SNJF055).

Institutional Review Board Statement: Not applicable.

Informed Consent Statement: Not applicable.

Data Availability Statement: Not applicable.

Conflicts of Interest: The authors declare no conflict of interest.

References

1. Josiane, N.; Paul-andré, D.; Michèle, H. Elimination of volatile organic compounds by biofiltration: A review. *Rev. Environ. Health* **2007**, *22*, 273–294.
2. Christensen, C.S.; Skov, H.; Palmgren, F. C_5–C_8 non-methane hydrocarbon measurements in Copenhagen: Concentrations, sources and emission estimates. *Sci. Total Environ.* **1999**, *236*, 163–171. [CrossRef]
3. Zhao, L.; Zhang, Y.F.; Li, R.H.; Ma, Z.C. Harms, recycling and treatment technology of VOC. *Chin. J. Chem. Educ.* **2015**, *36*, 1–6. (In Chinese)
4. Bari, M.A.; Kindzierski, W.B. Ambient volatile organic compounds (VOCs) in communities of the Athabasca oil sands region: Sources and screening health risk assessment. *Environ. Pollut.* **2018**, *235*, 602–614. [CrossRef] [PubMed]

5. An, Y.; Fu, Q.; Zhang, D.; Wang, Y.; Tang, Z. Performance evaluation of activated carbon with different pore sizes and functional groups for VOC adsorption by molecular simulation. *Chemosphere* **2019**, *227*, 9–16. [CrossRef] [PubMed]
6. Belaissaoui, B.; Moullec, Y.L.; Favre, E. Energy efficiency of a hybrid membrane/condensation process for VOC (Volatile Organic Compounds) recovery from air: A generic approach. *Energy* **2016**, *95*, 291–302. [CrossRef]
7. Giuseppina, O.; Tiziano, Z.; Vincenzo, N.; Raul, M.; Raquel, L.; Roxana, A.; Vincenzo, B. Comparative Analysis of Aops and Biological Processes for the Control of Vocs Industrial Emissions. *Chem. Eng. Trans.* **2018**, *68*, 451–456.
8. Barabad, M.L.M.; Jung, W.; Versoza, M.E.; Lee, Y.-I.; Choi, K.; Park, D. Characteristics of Particulate Matter and Volatile Organic Compound Emissions from the Combustion of Waste Vinyl. *Int. J. Environ. Res. Public Health* **2018**, *15*, 1390. [CrossRef]
9. Zou, W.; Gao, B.; Ok, Y.S.; Dong, L. Integrated adsorption and photocatalytic degradation of volatile organic compounds (VOCs) using carbon-based nanocomposites: A critical review. *Chemosphere* **2019**, *218*, 845–859. [CrossRef]
10. Adelodun, A.A. Influence of Operation Conditions on the Performance of Non-thermal Plasma Technology for VOC Pollution Control. *J. Ind. Eng. Chem.* **2020**, *92*, 41–55. [CrossRef]
11. Xi, J.Y.; Hu, H.Y. Performance of biofilters for the removal of VOCs. *Environ. Sci. Technol.* **2006**, *29*, 106–108+121. (In Chinese)
12. He, F.F. Study on biological treatment of volatile organic waste gas. *Chem. Eng. Des. Commun.* **2020**, *46*, 80–81. (In Chinese)
13. Li, Y.X.; Guo, B.; Liu, S. Recent progress and perspectives in biological treatment for gaseous pollutants. *Microbiol. China* **2019**, *46*, 3475–3482. (In Chinese)
14. Vikromvarasiri, N.; Pisutpaisal, N. Hydrogen sulfide removal in biotrickling filter system by *Halothiobacillus neapolitanus*. *Int. J. Hydrog. Energy* **2016**, *41*, 15682–15687. [CrossRef]
15. Le Cloirec, P.; Humeau, P.; Ramirez-Lopez, E.M. Biotreatments of odours: Control and performances of a biofilter and a bioscrubber. *Water Sci. Technol.* **2001**, *44*, 219–226. [CrossRef]
16. Chen, C.; Chen, Y.; Hou, J.; Liang, Y. CiteSpace II: Detecting and visualizing emerging trends and transient patterns in scientifc literature. *J. China Soc. Sci. Tech. Inf.* **2009**, *28*, 401–421. [CrossRef]
17. Carlson, D.A.; Leiser, C.P. Soil beds for control of sewage odors. *J. Water Pollut. Control Fed.* **1966**, *38*, 829–840.
18. Khan, F.I.; Ghoshal, A.K. Removal of Volatile Organic Compounds from polluted air. *J. Loss Prev. Process Indust.* **2000**, *13*, 527–545. [CrossRef]
19. Rousseeuw, P.J. Silhouettes: A graphical aid to the interpretation and validation of cluster analysis. *JCoAM* **1987**, *20*, 53–65. [CrossRef]
20. Bach, H. Schwefel im Abwasser. *Gesundheits-Ingenieur* **1923**, *46*, 370.
21. Leson, G.; Winer, A.M. Biofiltration: An innovative air pollution control technology for VOC emissions. *J. Air Waste Manag. Assoc.* **1991**, *41*, 1045–1054. [CrossRef] [PubMed]
22. Huang, L.K.; Wang, G.Z. Study on Species and Distribution of Volatile Organic Compounds in WWTP. *Adv. Mater. Res.* **2014**, *2914*, 2035–2038. [CrossRef]
23. Wang, C.; Xi, J.Y.; Hu, H.Y.; Yao, Y. Stimulative effects of ozone on a biofilter treating gaseous chlorobenzene. *Environ. Sci. Technol.* **2009**, *43*, 9407–9412. [CrossRef] [PubMed]
24. Covarrubias-García, I.; Jonge, N.D.; Arriaga, S.; Nielsen, J.L. Effects of ozone treatment on performance and microbial community composition in biofiltration systems treating ethyl acetate vapours. *Chemosphere* **2019**, *233*, 67–75. [CrossRef] [PubMed]
25. Moussavi, G.; Bahadori, M.B.; Farzadkia, M.; Yazdanbakhsh, A.; Mohseni, M. Performance evaluation of a thermophilic biofilter for the removal of MTBE from waste air stream: Effects of inlet concentration and EBRT. *Biochem. Eng. J.* **2009**, *45*, 152–156. [CrossRef]
26. Guievsse, B.; Hort, C.; Platel, V. Biological treatment of indoor air for VOC removal: Potential and challenges. *Biotechnol. Adv.* **2008**, *26*, 398–410. [CrossRef] [PubMed]
27. Kennes, C.; Thalasso, F. Review: Waste gas biotreatment technology. *J. Chem. Technol. Biotechnol.* **1998**, *72*, 303–319. [CrossRef]
28. Lu, C.; Lin, M.R.; Lin, J.; Chang, K. Removal of ethylacetate vapor from waste gases by a trickle-bed air biofilter. *J. Biotechnol.* **2001**, *87*, 123–130. [CrossRef]
29. Kennes, C.; Rene, E.R.; Veiga, M.C. Bioprocesses for air pollution control. *J. Chem. Technol. Biotechnol.* **2009**, *84*, 1419–1436. [CrossRef]
30. Cox, H.H.J.; Deshusses, M.A.; Converse, B.M.; Schroeder, E.D.; Iranpour, R. Odor and Volatile Organic Compound Treatment by Biotrickling Filters: Pilot-Scale Studies at Hyperion Treatment Plant. *Water Environ. Res.* **2002**, *74*, 557–563. [CrossRef]
31. Yang, Z.; Li, J.; Liu, J.; Cao, J.; Sheng, D.; Cai, T. Evaluation of a pilot-scale bio-trickling filter as a VOCs control technology for the chemical fibre wastewater treatment plant. *J. Environ. Manag.* **2019**, *246*, 71–76. [CrossRef] [PubMed]
32. Zhang, Y.; Liu, J.; Deng, W.; Qin, Y.; Xing, Y.; Li, J. Research on pressure drop solution and pilot-scale application of bio-trickling filter for the treatment of butan-2-yl ethanoate. *Process Biochem.* **2019**, *79*, 118–126. [CrossRef]
33. Wysocka, I.; Gebicki, J.; Namiesnik, J. Technologies for deodorization of malodorous gases. *Environ. Sci. Pollut.* **2019**, *26*, 9409–9434. [CrossRef] [PubMed]
34. Irga, P.J.; Pettit, T.; Irga, R.F. Does plant species selection in functional active green walls influence VOC phytoremediation efficiency? *Environ. Sci. Pollut.* **2019**, *26*, 12851–12858. [CrossRef] [PubMed]
35. Cheng, Y.; He, H.; Yang, C.; Zeng, G.; Li, X.; Chen, H.; Yu, G. Challenges and solutions for biofiltration of hydrophobic volatile organic compounds. *Biotechnol. Adv.* **2016**, *34*, 1091–1102. [CrossRef]
36. Devinny, J.S.; Deshusses, M.A.; Webster, T.S. *Biofiltration for Air Pollution Control*; Lewis Publishers: Boca Raton, FL, USA, 1999.

37. Mudliar, S.; Giri, B.; Padoley, K.; Satpute, D.; Dixit, R.; Bhatt, P.; Pandey, R.; Juwarkar, A.; Vaidya, A. Bioreactors for treatment of VOCs and odours—A review. *J. Environ. Manag.* **2010**, *91*, 1039–1054. [CrossRef]
38. Mohseni, M.; Allen, D.G. Biofiltration of mixtures of hydrophilic and hydrophobic volatile organic compounds. *Chem. Eng. Sci.* **2000**, *55*, 1554–1558. [CrossRef]
39. Barbusinski, K.; Kalemba, K.; Kasperczyk, D.; Urbaniec, K.; Kozik, V. Biological methods for odor treatment—A review. *J. Clean. Prod.* **2017**, *152*, 223–241. [CrossRef]
40. Yang, C.P.; Qian, H.; Li, X.; Cheng, Y.; He, H.J.; Zeng, G.M.; Xi, J.Y. Simultaneous removal of multicomponent VOCs in biofilters. *Trends Biotechnol.* **2018**, *36*, 673–685. [CrossRef]
41. Estrada, J.M.; Hernandez, S.; Munoz, R.; Revah, S. A comparative study of fungal and bacterial biofiltration treating a VOC mixture. *J. Hazard. Mater.* **2013**, *250*, 190–197. [CrossRef]
42. Rene, E.R.; Mohammad, B.T.; Veiga, M.C.; Kennes, C. Biodegradation of BTEX in a fungal biofilter: Influence of operational parameters, effect of shock-loads and substrate stratification. *Bioresour. Technol.* **2012**, *116*, 204–213. [CrossRef] [PubMed]
43. Shareefdeen, Z.; Baltzis, B.C. Biofiltration of toluene vapor under steady-state and transient conditions: Theory and experimental results. *Chem. Eng. Sci.* **1994**, *49*, 4347–4360. [CrossRef]
44. Atkinson, R. Atmospheric chemistry of VOCs and NOx. *Atmos. Environ.* **2000**, *34*, 2063–2101. [CrossRef]
45. Detchanamurthy, S.; Gostomski, P.A. Biofiltration for treating VOCs: An overview. *Rev. Environ. Sci. Bio./Technol.* **2012**, *11*, 231–241. [CrossRef]
46. Hassan, A.A.; Sorial, G. Biological treatment of benzene in a controlled trickle bed air biofilter. *Chemosphere* **2009**, *75*, 1315–1321. [CrossRef]
47. Hort, C.; Platel, V.; Sochard, S.; Munoz, A.T.L.; Ondarts, M.; Reguer, A.; Barona, A.; Elias, A. A hybrid biological process of indoor air treatment for toluene removal. *J. Air Waste Manag. Assoc.* **2014**, *64*, 1403–1409. [CrossRef]
48. Mohamed, E.F.; Awad, G.; Andriantsiferana, C.; El-Diwany, A.I. Biofiltration technology for the removal of toluene from polluted air using Streptomyces griseus. *Environ. Technol.* **2016**, *37*, 1197–1207. [CrossRef]
49. Xu, Z.; Wu, M.; He, Y. Toluene biofiltration enhanced by ryegrass. *Bull. Environ. Contam. Toxicol.* **2013**, *90*, 646–649. [CrossRef]
50. Cox, H.H.J.; Deshusses, M.A. Co-treatment of H_2S and toluene in a biotrickling filter. *Chem. Eng. J.* **2002**, *87*, 101–110. [CrossRef]
51. Zehraoui, A.; Hassan, A.A.; Sorial, G.A. Biological treatment of n-hexane and methanol in trickle bed air biofilters under acidic conditions. *Biochem. Eng. J.* **2013**, *77*, 129–135. [CrossRef]
52. Rene, E.R.; Jin, Y.; Veiga, M.C.; Kennes, C. Two-stage gas-phase bioreactor for the combined removal of hydrogen sulphide, methanol and α-pinene. *Environ. Technol.* **2009**, *30*, 1261–1272. [CrossRef] [PubMed]
53. Swanson, W.J. Biofiltration: Fundamentals, Design and Operations Principles, and Applications. *J. Environ. Eng.* **1997**, *123*, 538–546. [CrossRef]
54. Zhao, L.C. Advances in biological treatment of volatile organic waste gas. *Mod. Chem. Ind.* **2021**, *41*, 72–76. (In Chinese)
55. Alonso, C.; Zhu, X.; Suidan, M.T.; Kim, B.R.; Kim, B.J. Parameter Estimation in Biofilter Systems. *EnST* **2000**, *34*, 2318–2323. [CrossRef]
56. Mathur, A.K.; Balomajumder, C. Biological treatment and modeling aspect of BTEX abatement process in a biofilter. *Bioresour. Technol.* **2013**, *142*, 9–17.
57. Trigueros, D.E.G.; Módenes, A.N.; Kroumov, A.D.; Espinoza-Quiñones, F.R. Modeling of biodegradation process of BTEX compounds: Kinetic parameters estimation by using Particle Swarm Global Optimizer. *Process Biochem.* **2010**, *45*, 1355–1361. [CrossRef]
58. Jo, M.-S.; Rene, E.R.; Kim, S.-H.; Park, H.-S. Removal of BTEX compounds by industrial sludge microbes in batch systems: Statistical analysis of main and interaction effects. *World J. Microbiol. Biotechnol.* **2008**, *24*, 73–78. [CrossRef]
59. Padhi, S.K.; Gokhale, S. Treatment of gaseous volatile organic compounds using a rotating biological filter. *Bioresour. Technol.* **2017**, *244*, 270–280. [CrossRef]
60. Raboni, M.; Torretta, V.; Viotti, P. Treatment of airborne BTEX by a two-stage biotrickling filter and biofilter, exploiting selected bacterial and fungal consortia. *Int. J. Environ. Sci. Technol.* **2017**, *14*, 19–28. [CrossRef]
61. Mathur, A.K.; Majumder, C.B.; Chatterjee, S. Combined removal of BTEX in air stream by using mixture of sugar cane bagasse, compost and GAC as biofilter media. *J. Hazard. Mater.* **2007**, *148*, 64–74. [CrossRef]
62. Klapková, E.; Halecký, M.; Fitch, M.; Soccol, C.R.; Paca, J. Impact of biocatalyst and moisture content on toluene/xylene mixture biofiltration. *Braz. Arch. Biol. Technol.* **2006**, *49*, 1001–1006. [CrossRef]
63. Smith, M.R. The biodegradation of aromatic hydrocarbons by bacteria. *Biodegradation* **1990**, *1*, 191–206. [CrossRef] [PubMed]
64. García-Peña, I.; Ortiz, I.; Hernández, S.; Revah, S. Biofiltration of BTEX by the fungus Paecilomyces variotii. *Int. Biodeterior. Biodegrad.* **2008**, *62*, 442–447. [CrossRef]
65. Plessis, C.A.D.; Strauss, J.M.; Riedel, K.-H.J. BTEX catabolism interactions in a toluene-acclimatized biofilter. *Appl. Microbiol. Biotechnol.* **2001**, *55*, 122–128. [CrossRef] [PubMed]
66. Hodge, D.S. Modeling Removal of Air Contaminants by Biofiltration. *J. Environ. Eng.* **1995**, *121*, 21–32. [CrossRef]
67. Baltzis, B.C. Modeling Biofiltration of VOC Mixtures under Steady-State Conditions. *J. Environ. Eng.* **1997**, *123*, 599–605. [CrossRef]
68. Min, K.; Ergas, S.J. Volatilization and Biodegradation of VOCs in Membrane Bioreactors (MBR). *Water Air Soil Pollut. Focus* **2006**, *6*, 83–96. [CrossRef]

69. Ranasinghe, M.A.; Gostomski, P.A. A novel reactor for exploring the effect of water content on biofilter degradation rates. *Environ. Prog.* **2003**, *22*, 103–109. [CrossRef]
70. Son, H.K.; Striebig, B.A.; Regan, R.W. Nutrient limitations during the biofiltration of methyl isoamyl ketone. *Environ. Prog.* **2005**, *24*, 75–81. [CrossRef]
71. Rands, M.B.; Cooper, D.E.; Woo, C.; Fletcher, G.C.; Rolfe, K.A. Compost filters for H_2S removal from anaerobic digestion and rendering exhausts. *J. Chem. Technol. Biotechnol.* **1981**, *53*, 185–189.
72. Webster, T.S.; Devinny, J.S.; Torres, E.M.; Basrai, S.S. Microbial ecosystems in compost and granular activated carbon biofilters. *Biotechnol. Bioeng.* **1997**, *53*, 296–303. [CrossRef]
73. Togashi, I.; Suzuki, M.; Hirai, M.; Shoda, M.; Kubota, H. Removal of NH_3 by a peat biofilter without and with nitrifier. *J. Ferment. Technol.* **1986**, *64*, 425–432. [CrossRef]
74. Chou, M.S.; Cheng, W.H. Screening of Biofiltering Material for VOC Treatment. *J. Air Waste Manag. Assoc.* **2012**, *47*, 674–681. [CrossRef] [PubMed]
75. Dumont, E.; Andrès, Y.; Cloirec, P.L.; Gaudin, F. Evaluation of a new packing material for H_2S removed by biofiltration. *Biochem. Eng. J.* **2008**, *42*, 120–127. [CrossRef]
76. Ottengraf, S.P.P.; Meesters, J.J.P.; Oever, A.H.C.; Rozema, H.R. Biological elimination of volatile xenobiotic compounds in biofilters. *Bioprocess. Eng.* **1986**, *1*, 61–69. [CrossRef]
77. Han, M.-F.; Wang, C.; Yang, N.-Y.; Li, Y.-F.; Hu, X.-R.; Duan, E.-H. Determination of filter bed structure characteristics and influence on performance of a 3D matrix biofilter in gaseous chlorobenzene treatment. *Biochem. Eng. J.* **2021**, *165*, 107829. [CrossRef]
78. Han, M.F.; Wang, C.; Yang, N.Y.; Hu, X.R.; Wang, Y.C.; Duan, E.H.; Ren, H.W.; Hsi, H.C.; Deng, J.G. Performance enhancement of a biofilter with pH buffering and filter bed supporting material in removal of chlorobenzene. *Chemosphere* **2020**, *251*, 126358. [CrossRef]
79. Chen, P.; Yan, J.B.; Wu, W.L.; Hu, Q.Q. Separation and biodegradation characteristics of a o-xylene degrading strain. *Chem. Ind. Eng. Prog.* **2016**, *35*, 565–569. (In Chinese)
80. Schiavon, M.; Ragazzi, M.; Rada, E.C.; Torretta, V. Air pollution control through biotrickling filters: A review considering operational aspects and expected performance. *Crit. Rev. Biotechnol.* **2016**, *36*, 1143–1155. [CrossRef]
81. Lu, L.C.; Jia, Q.; Cheng, Z.W.; Liu, W.; Bu, Y.F. Progress on biodegradation of volatile organic compounds by fungi. *Environ. Pollut. Control* **2014**, *36*, 78–83. (In Chinese)
82. Zheng, T.; Li, L.; Chai, F.; Wang, Y. Factors impacting the performance and microbial populations of three biofilters for co-treatment of H_2S and NH_3 in a domestic waste landfill site. *Process Saf. Environ. Prot.* **2021**, *149*, 410–421. [CrossRef]
83. Liu, J.; Yue, P.; Zang, N.; Lu, C.; Chen, X. Removal of odors and VOCs in municipal solid waste comprehensive treatment plants using a novel three-stage integrated biofilter: Performance and bioaerosol emissions. *Front. Environ. Sci. Eng.* **2021**, *15*, 48. [CrossRef] [PubMed]

sustainability

MDPI

Article

Population Mobility and Urban Air Quality: Causal Inference and Impact Measurement

Fu Huang [1,2], Qiang Wu [1,2,*] and Pei Wang [1,2]

[1] Yangtze River Delta Economics and Social Development Research Center, Nanjing University, Nanjing 210093, China; dg20020029@smail.nju.edu.cn (F.H.)
[2] School of Economics, Nanjing University, Nanjing 210093, China
* Correspondence: qiangwu@nju.edu.cn; Tel.: +86-139-1296-1567

Abstract: This paper treats the lockdown of Hubei Province during the outbreak of COVID-19 in early 2020 as a quasi-experiment, and uses the prefecture-level data of 328 cities in China to identify the causal effects of population mobility and urban air quality. This paper uses the DID model to eliminate the 'Spring Festival effect' with data from the same period of the lunar calendar in 2019 as the control group, and finds the reduction in population mobility has a clear causal impact on the improvement of urban air quality. The vast majority of air pollutants decreased, but ozone, which has a special generation mechanism, increased. This paper also constructs 29-day panel data of 328 prefecture-level cities from January to February in 2020 to quantitatively estimate the impact of population flow on urban air quality. After controlling for fixed effects, the results reveal that 1% increases in intra-city and inter-city population flows correspond to respective increases of 0.433% and 0.201% in the urban air quality index. Compared with inter-city flow, intra-city population flow increases air pollution more severely.

Keywords: population mobility; urban air quality; quasi-natural experiment

1. Introduction

As China's urbanization level continues to improve, economic activities are becoming more and more concentrated at the spatial scale of cities, and urban air pollution is becoming increasingly serious. Urban air quality is an important issue for people's livelihoods and is closely related to the health and well-being of urban residents, which is why the issue of urban air quality has received widespread attention from all sectors of society in recent years. The Chinese government attaches great importance to this issue, and green development has become an important part of its new development concept. The Fifth Plenary Session of the 19th Central Committee of the Communist Party of China proposed that the 14th Five-Year Plan period should achieve new progress in the construction of ecological civilization, a continuous reduction in the total emissions of major pollutants, and a continuous improvement in the ecological environment. Urban air quality has become one of the binding indicators for China's economic and social development in the 14th Five-Year Plan, and the ratio of good air quality days in cities at the prefecture level and above should be increased to 87.5% (according to the 14th Five-Year Plan and the Long-Range Objectives Through the Year 2035 for the National Economic and Social Development of the People's Republic of China). Therefore, it is important to study the main determinants of urban air quality, identify the causal impact of these factors on urban air quality, and quantify the magnitude of their impact in order to scientifically formulate policies to solve urban air pollution problems.

Theoretical research into the determinants of urban air quality in China has produced a wealth of results. The foremost determinants are urban traffic conditions and transport infrastructure. Traffic congestion increases vehicle emissions and contributes to air

pollution [1], while increased investment in transport infrastructure will improve urban air quality by increasing road space [2]. For intra-city travel, the opening of rail lines is effective in combating urban air pollution [3], but car restriction policies do not significantly improve urban air quality [4]; for inter-city travel, the opening of high-speed rail significantly improves urban air quality, and the more extensive the high-speed rail network, the more significant the emission reduction effect brought by high-speed rail [5,6]. The second most important determinants of urban air quality are population concentration and urban expansion. Xu et al. [7] argued that population agglomeration has a "U"-shaped effect on environmental pollution emissions, Zhou and Zhang [8] found that new urbanization aggravates air pollution through population and production factors, and Wang and Shi [9] pointed out that low-carbon city construction can reduce haze pollution. Current research on the impact of urban expansion on urban air quality has different views, with some studies suggesting that urban expansion has a suppressive effect on environmental pollution [10] and others arguing that urban expansion exacerbates urban air pollution [11] and that urbanization is an important factor affecting urban air quality [12]. Some scholars have also studied the effects of factors such as official turnover [13,14], export trade [15], government behavior [16], and environmental regulation [17] on urban air quality. In addition, some scholars have conducted research on the urban heat island effect [18] and the impact of human activities on the ecological environment [19].

This paper seeks to examine the impact of population movements on urban air quality. Within the city limits, human activity is clearly the most significant factor influencing air quality, and the types of factors studied in the literature above are a reflection of human activity. Population movement, which is directly related to urban traffic conditions and transport infrastructure, is the underlying behavior in these human activities, and the movement of people within and between cities forms the micro-foundation of population clustering and urban expansion. In this sense, population movement may be a key factor affecting urban air quality at a deeper level.

However, when identifying the causal impact of population mobility on urban air quality, one faces endogeneity and estimation biases due to reverse causality. Numerous studies have shown that urban air pollution has a significant negative impact on the employment location of mobile populations [20], that population mobility prefers cities with good ecological construction [21], and that a good environment attracts environmental migrants and provides sustainable human capital for local economic development [22], especially for high-human capital groups [23]. After the outbreak of COVID-19 in early 2020, the Chinese government promptly took various preventive and control measures to effectively control the spread of the epidemic, one of the most significant measures being the lockdown of cities. City closures are exogenous in that they directly reduce the scale of population movement, both within and between cities, which cuts off the reverse causal effect of urban air quality on population movement and provides a key exogenous window of impact event for accurately identifying the causal effect of population movement on urban air quality. It is due to this exogeneity that some foreign scholars have begun to study the impact of various types of closure measures taken for epidemic prevention and control on local air quality [24,25] and on major air pollutants [26]; some Chinese scholars have also focused on the economic effects of epidemic prevention and control measures [27,28]. However, no results have yet emphasized the identification of causal relationships between population movements and urban air quality, or the role of exogenous measures such as city closures; additionally, quantitative measures of such causal effects are also lacking.

The possible marginal contributions of this paper lie in three areas. First, the topic is novel, as although there is a large literature on the factors influencing urban air quality, there are relatively few studies that have analyzed it from the perspective of population mobility, and few studies that have quantified this effect. Second, a standard DID model is used for causal identification, and data from the same period of the 2019 lunar calendar is used as a control group to eliminate the "Chinese New Year effect". Third, data crawling is combined with matching use. This paper uses Python crawling techniques to obtain

data on population movement, air quality and weather conditions, and matches these data according to city names.

2. Data and Methods

2.1. Theoretical Framework

The difficulty in identifying the causal impact of population movements on urban air quality is twofold. On the one hand, it is difficult to have a window period in which population movement changes dramatically, and it is common for population movement data to have a low degree of variability over sample periods; on the other hand, urban air quality changes can, in turn, affect population movement behavior, increasing the potential for endogeneity bias due to reverse causation. In early 2020, to prevent the spread of COVID-19, cities in Hubei Province took measures to close the city under the unified deployment and leadership of the Chinese government. Wuhan COVID-19 Pandemic Prevention and Control Headquarters first issued Circular No. 1 on 23 January, suspending public transport in the city and restricting passage out of Wuhan; subsequently, cities in Hubei issued city lockdown circulars one after another, until Xiangyang was officially closed on 28 January and all cities in the whole of Hubei went into lockdown. This paper uses the city closure policy adopted by Hubei cities as an exogenous shock event which both directly reduces population movement and does not have the reverse causal endogeneity of urban air quality affecting population movement, providing a valuable window period for identifying the impact of population movement on urban air quality. Therefore, this paper employs the difference-in-differences (DID) method for modeling. The difference-in-differences (DID) method is a commonly used analytical approach for policy research, and its underlying principle is similar to that of a natural experiment. It treats the implementation of a particular policy as a natural experiment, comparing and analyzing the treatment group, which is subject to the policy, with the control group, which is not affected by the policy, in order to examine the net impact of the policy on the analyzed variables.

At the same time, as the outbreak of COVID-19 in early 2020 coincided with the Chinese Lunar New Year holiday, the causal identification in this paper must take into account the fact that, during the Lunar New Year holiday, most of China celebrates the Chinese New Year, shutting down production and naturally reducing air pollution levels [29]. Therefore, in this paper, we use data from 2020 and 2019, rather than just 2020, to avoid the "Chinese New Year effect" [30]. Specifically, this paper uses data from the 23rd day of the 23rd month of the lunar calendar to the 28th day of the first month of the lunar calendar in Hubei in 2020 and data from cities outside Hubei in the same period of the 2019 lunar calendar, with the 2020 Hubei cities as the treatment group and the rest of the Chinese cities in the same period of the 2019 lunar calendar as the control group. In the baseline regression part of the causal identification, considering that, although the cities in Hubei declared city closures in a slight sequence, most Hubei cities declared city lockdowns on 24 January, with six cities declaring city lockdowns, and the vast majority of Hubei cities declaring city closures two days before and after 24 January, this paper chooses to take 24 January, i.e., Lunar New Year's Eve, as the time point of the policy shock. This is also, in fact, the most critical date for all cities in Hubei Province to actually adopt the city lockdown policy.

Analyzing the actual situation, the five Hubei cities that announced the implementation of city lockdowns on 25 and 28 January were actually close to the status of city lockdown after other cities had announced it. Therefore, the choice of Lunar New Year's Eve as the policy impact point in the benchmark regression is in line with the real situation of city lockdown in Hubei. However, in terms of the timing of the announcement, Wuhan and Ezhou were closed on 23 January; Huangshi, Jingmen, Jingzhou, Huanggang, Xianning, and Enshi were closed on 24 January; Shiyan, Yichang, Xiaogan, and Suizhou were closed on 25 January; and Xiangyang was closed on 28 January. The timing of the announcement of the city closure in each city in Hubei is sequential, and using 24 January as the timing of the policy shock uniformly may weaken the credibility of the causal identification. There-

fore, this paper also constructs a multi-period DID model to verify the robustness of the benchmark regression by using the city lockdown dates announced by each city in Hubei as the respective policy shock points.

In terms of specifically quantifying the magnitude of the impact of population movement on urban air quality, this paper divides population movement at the city level into two components: intra-city population flow, which refers to population moving within cities, and inter-city population flow, which refers to population moving between cities. The magnitude of the impact of these two types of population movement on urban air quality may differ and needs to be measured separately. Based on this, this paper introduces the intra-city population flow variable, $lnincity$, and the inter-city population flow variable, $lnoutcity$. Baidu Migration provides data on the scale of these two types of population flow, so this paper takes the intra-city travel intensity recorded by Baidu Migration, absolutizes the index using the approach of Fang et al. [31], and then takes its logarithmic value as the intra-city population flow variable, $lnincity$; then, the city in-migration scale index and city out-migration scale index of Baidu Migration are absolutized, and their logarithmic values are taken after summing to obtain a measure of the inter-city population mobility variable, $lnoutcity$. In this section, intra-city population flow and inter-city population flow are used as the main explanatory variables in turn, and static panel fixed effects models are used to measure the magnitude of the specific effects of these two on urban air quality, respectively.

2.2. Model Selection

The baseline regression component of the causal identification in this paper sets up a DID model, as shown in Equation (1), to identify whether a reduction in population movement can have a causal impact on urban air quality improvement.

$$Urpollu_{it} = \alpha + \beta treat_i * post_t + \gamma X_{it} + u_i + \eta_t + \varepsilon_{it} \quad (1)$$

Here, i and t denote city and time, respectively. The explanatory variable for urban air quality, $Urpollu_{it}$, is measured using a set of indicators, specifically the urban air quality index, AQI, and levels of six major air pollutants, $PM2.5$, $PM10$, SO_2, CO, NO_2, and O_3. The main explanatory variable is $treat_i * post_t$, where $treat_i$ is a dummy variable for the treatment group within Hubei Province and $post_t$ is a dummy variable for the implementation of the city closure policy in Hubei, with a value of 1 for New Year's Eve and beyond and 0 for before New Year's Eve. X_{it} is a set of control variables specifically including the local maximum and minimum temperatures, wind levels, and their squared terms for that day. This paper further controls for city fixed effects, u_i, and time fixed effects, η_t, while ε_{it} is a random error term.

In this paper, a multi-period DID model, as shown in Equation (2), is set up in the causal identification robustness test section.

$$Urpollu_{it} = \alpha + \beta D_{it} + \gamma X_{it} + u_i + \eta_t + \varepsilon_{it} \quad (2)$$

The main explanatory variable, D_{it}, is the cross multiplier between cities in Hubei Province and the implementation of city closure policies; if city i in Hubei Province announces the implementation of the city closure policy at time t, then the value of D_{it} for that city at time t and later will be 1, otherwise it will be 0. The explanatory variable, $Urpollu_{it}$, remains logarithmic, and the control variables and fixed effects are set as shown in Equation (1).

Based on the causal identification, Equation (3) is set up in this paper to estimate the magnitude of the effect of population movement on urban air quality.

$$Urpollu_{it} = \alpha + \beta X_{it} + \gamma Z_{it} + \varepsilon_{it} \quad (3)$$

Here, i and t denote area and time, respectively. The explanatory variable, $Urpollu_{it}$, is also a set of indicators measuring urban air quality from various aspects, specifically the urban air quality index, $lnAQI$, and the main air pollutants, $lnPM2.5$, $lnPM10$, $lnSO_2$, $lnCO$, $lnNO_2$, and lnO_3, all of which are taken as logarithmic values. The main explanatory variable, X_{it}, is the intra-city population flow variable, $lnincity$, and the inter-city population flow variable, $lnoutcity$, in that order. Z_{it} is a set of control variables specifically including the local maximum and minimum temperatures, as well as the wind level and its squared term on a given day, while ε_{it} is a random error term. This paper uses a static panel fixed effects model to estimate Equation (3), with standard error clustering at the city level.

2.3. Data Sources

This paper constructs panel data covering 36 days for 328 prefecture-level cities in China, matching three aspects: air quality, weather, and population movement. The air quality-related data are crawled from the historical data of the China Air Quality Online Monitoring and Analysis Platform (www.aqistudy.cn), including AQI, $PM2.5$, $PM10$, SO_2, CO, NO_2, and O_3 levels. Higher values of these data indicate poorer air quality. Weather-related data were crawled from weather.com (www.tianqi.com) historical data, specifically including the highest temperature of the day, the lowest temperature of the day, and wind; population movement data were crawled from Baidu Migration (qianxi.baidu.com) historical data, specifically including the urban migration size index and intra-city travel intensity. The treatment group includes data for cities in Hubei for 36 consecutive days from 17 January to 21 February 2020, and the control group includes data for cities outside Hubei for 36 consecutive days from 28 January to 4 March 2019. The population movement data in this paper is sourced from Baidu Migration, which may lead to a potential underestimation of population movement, as Baidu Migration is unable to track the movements of every individual. However, this is the closest approximation of population movement data available for this study.

As the population migration data in Baidu Migration are all relative indicators, this paper follows the approach of Fang et al. [31] and absolutizes them. Fang et al. [31] first collected the actual number of people entering and leaving Shanghai from 6–22 February 2020 from the National Earth System Science Data Centre, then compared the in-migration scale and out-migration scale indices of Shanghai in Baidu Migration in the same period, and estimated that the actual number of people corresponding to each unit of the city in-migration and out-migration scale indices was 90,848 and the actual number of people corresponding to each unit of intra-city travel intensity was 2,182,264 persons. This paper uses their estimated conversion values and converts them to obtain the actual number of people moving in and out of each city per day. Table 1 shows the descriptive statistics of the raw data for the variable measures. In Table 1, "Unit" represents the unit of measurement for the variable. "AQI" is a dimensionless index that does not have a unit. "Wind" is categorized by wind strength levels and does not have a unit. "N" represents the sample size.

Table 1. Definition of variables and descriptive statistics.

Variable	Unit	N (Sample Size)	Mean	Std. Dev.	Min	Max
AQI	/	11,808	83.693	56.235	0	500
PM2.5	$\mu g/m^3$	11,808	56.134	46.426	0	536
PM10	$\mu g/m^3$	11,808	84.740	66.863	0	1141
SO_2	$\mu g/m^3$	11,808	13.497	12.797	0	362
CO	mg/m^3	11,808	0.982	0.436	0.1	4.4
NO_2	$\mu g/m^3$	11,808	26.738	16.542	0	110
O_3	$\mu g/m^3$	11,808	71.397	24.838	4	294
Highest temperature	°C	11,808	8.944	8.851	−25	33
Lowest temperature	°C	11,808	−0.091	9.756	−38	25
Wind	/	11,808	2.156	0.769	0	6
Num of people moving into city	10 K people	11,808	12.216	17.039	0.008	237.639
Num of people moving out of city	10 K people	11,808	12.167	15.314	0.017	199.394
Num of people traveling within the city	10 K people	11,808	964.674	226.978	125.240	1922.706

3. Results

3.1. Baseline Regression Test

Table 2 shows the estimation results of Equation (1), with the explanatory variables in Columns (1)–(7) being AQI, $PM2.5$, $PM10$, SO_2, CO, NO_2, and O_3, respectively. Meanwhile, Figure 1 displays the visualized results of the magnitude of the coefficient estimates and their confidence intervals for the seven explanatory variables.

Table 2. Baseline regression for causal identification of reduced population movement to improve urban air quality.

	(1) *AQI*	(2) *PM2.5*	(3) *PM10*	(4) SO_2	(5) *CO*	(6) NO_2	(7) O_3
$treat_i * post_t$	−40.129 ***	−36.190 ***	−37.691 ***	−0.282	−0.174 ***	−16.635 ***	6.193 ***
	(5.445)	(4.228)	(4.139)	(0.524)	(0.038)	(0.950)	(1.878)
Lowest temperature	0.530 **	0.657 ***	0.624 **	−0.128 ***	0.000	0.030	−0.841 ***
	(0.261)	(0.204)	(0.294)	(0.047)	(0.002)	(0.062)	(0.155)
Highest temperature	2.917 ***	2.323 ***	3.603 ***	0.306 ***	0.023 ***	0.748 ***	1.416 ***
	(0.337)	(0.261)	(0.398)	(0.104)	(0.003)	(0.072)	(0.136)
Wind	−13.824 ***	−8.991 ***	−16.962 ***	0.092	−0.115 ***	−5.717 ***	−2.050
	(2.737)	(1.997)	(3.295)	(0.661)	(0.025)	(0.732)	(1.251)
Lowest temperature^2	0.026 ***	0.021 **	0.038 ***	0.001	0.000 *	0.011 ***	−0.022 ***
	(0.010)	(0.008)	(0.012)	(0.002)	(0.000)	(0.003)	(0.005)
Highest temperature^2	−0.016	−0.007	−0.034 ***	0.006	−0.000 ***	0.006 **	0.057 ***
	(0.011)	(0.009)	(0.012)	(0.005)	(0.000)	(0.003)	(0.005)
Wind^2	1.350 **	0.228	2.588 ***	−0.335 ***	0.003	0.119	0.380
	(0.526)	(0.378)	(0.653)	(0.127)	(0.004)	(0.144)	(0.232)
Constant	103.052 ***	71.869 ***	93.102 ***	7.790 ***	0.972 ***	50.886 ***	51.997 ***
	(4.125)	(3.176)	(4.945)	(0.815)	(0.034)	(1.014)	(2.185)
Sample size	11,808	11,808	11,808	11,808	11,808	11,808	11,808
R-squared	0.566	0.594	0.602	0.618	0.575	0.738	0.508
Time FE	YES	YES	YES	YES	YES	YES	YES
Urban FE	YES	YES	YES	YES	YES	YES	YES

Note: Figures in brackets are clustering robustness criteria errors; *, **, and *** denote significance levels of 10%, 5%, and 1%, respectively.

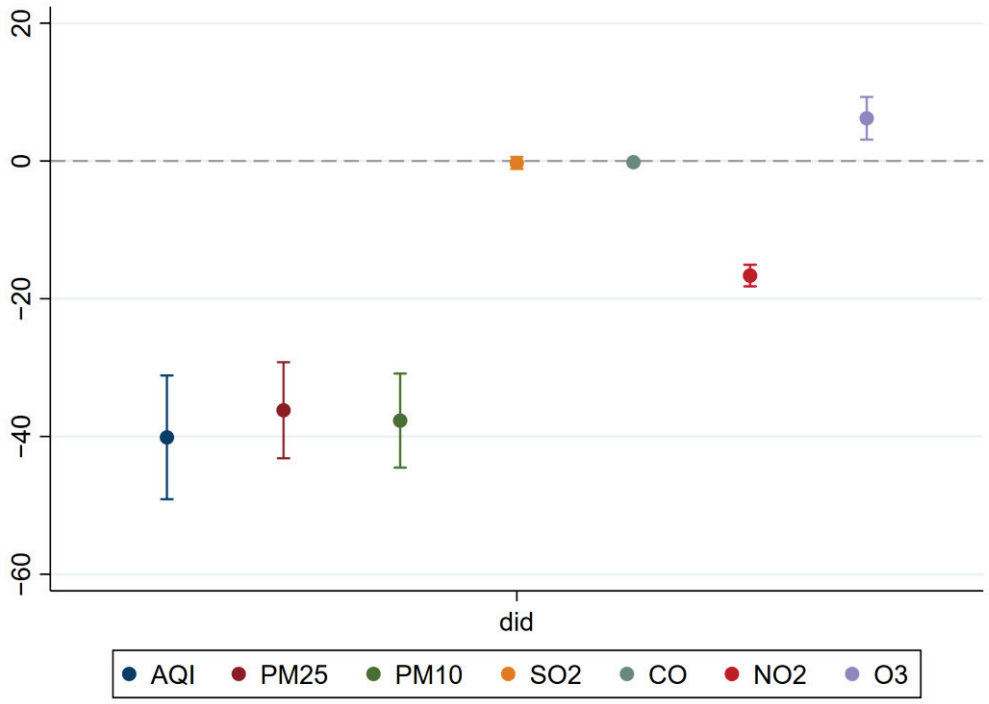

Figure 1. The coefficient estimates and confidence intervals for the seven explanatory variables. Note: "did" represents the interaction term "treat ∗ post".

In Table 2, when the explanatory variable is the AQI, the $treat_i * post_t$ coefficient is significantly negative, indicating that the reduction in population movement has led to an overall improvement in urban air quality. The $treat_i * post_t$ coefficients are also significantly negative when the explanatory variable is one of the major air pollutant indicators ($PM2.5$, $PM10$, CO, and NO_2), indicating that the reduction in population movement has led to a significant reduction in the concentration of these four major air pollutants in the air. When the explanatory variable is SO_2, the $treat_i * post_t$ coefficient is negative but not significant. Although the reduction in population movement leads to a reduction in the concentration of SO_2 in the air, this causal effect is weak and does not pass the statistical significance test. In addition, the $treat_i * post_t$ coefficient is significantly positive when the explanatory variable is O_3, indicating that the reduction in population movement leads to a significant increase in the concentration of O_3 in the air instead.

3.2. Parallel Trend Hypothesis Test

For the results of the DID method test to be unbiased and reliable, its experimental and treatment groups must satisfy the parallel trend assumption. In this paper, we adopt the event study method, referring to Luo et al. [32], use New Year's Eve as the event impact point, and select four days before and after for the parallel trend test. If the parallel trend hypothesis holds, then there should be no significant difference in the trend of urban AQI changes between the treatment and control groups before New Year's Eve. Figure 2 shows the results when the explanatory variable is the urban AQI. The x-axis represents the time before and after policy implementation, while the y-axis represents the impact of the policy effects. The results indicate that there is no significant difference in the overall urban air quality change trend between the treatment and control groups before the policy shock, i.e., the parallel trend hypothesis holds; after the policy shock occurs, there is a significant negative effect on the urban AQI. To save space, we have provided the parallel trend hypothesis test results for the six major air pollutants as explanatory variables in Appendix A. Please refer to Figures A1–A6 for details. Five of major air pollutants passed the parallel trend hypothesis test, demonstrating that, overall, the baseline regression results in Table 2 are plausible. Only SO_2 does not pass this test, which does

not fundamentally change the conclusions, as the interaction term $treat_i * post_t$ is also not significant when the explanatory variable in the baseline regression is SO_2. This is another way of demonstrating the heterogeneous causal impact of reduced population movements on different air pollutants.

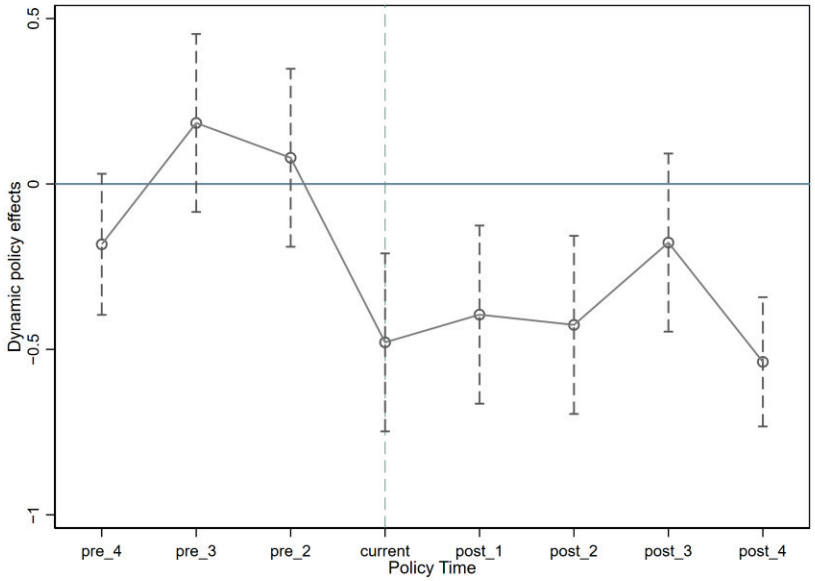

Figure 2. Results of parallel trend hypothesis testing where the explanatory variable is AQI. Note: Data for the pre_1 period is not available in the graph, as the first period before the policy shock is used as the base group.

3.3. Placebo Test

There may be other unobservable events prior to the occurrence of the city lockdown policy in Hubei cities in early 2020 that affect the veracity of the estimation results in this paper. To rule out the potential influence of such unobservable times on the estimation results, this paper uses a dummy policy shock point in time as a placebo method to identify whether such potential influence is real. A placebo test was conducted by using January 15, the date when the Chinese National Center for Disease Control and Prevention (CDC) initiated the Level 1 response, January 11, the date when the CDC provided PCR test strips to Wuhan, and January 8, the middle date of the two sessions in Wuhan, as the dummy shock dates in the original sample interval. To save space, we present the empirical results in Appendix B. The results of the placebo test for the explanatory variable AQI are shown in Table A1, where the $treat_i * post_t$ coefficients for Columns (1)–(3) were 1.038, 3.626, and −2.036, respectively, which did not pass the significance test, indicating that using these three time points as the policy shock dates did not have a significant impact on the overall air quality of the city. This suggests that using these three time points as policy shock dates did not have a significant effect on the overall urban air quality. The exogenous policy shocks in this paper are valid and the findings are robust, given that the causal effect of reduced population movement on urban air quality improvement due to the city lockdown policy in Hubei is real.

3.4. Robustness Tests

To further test whether the causal effect of reduced population mobility on urban air quality improvement is robust and reliable, this paper conducts robustness tests in two ways. Firstly, this paper replaces the explanatory variables. In this paper, the DID model of Equation (1) is estimated again by taking the logarithmic values of each measure of urban air quality in the baseline regression, and the results obtained are shown in Appendix C. Secondly, this paper uses a multi-period DID model. In this paper, the multi-period DID model of Equation (2) is estimated, and the results are shown in Appendix D.

The $treat_i * post_t$ coefficients of interest in this paper in Appendix C Table A2 are significantly negative when the explanatory variables are $lnAQI$, $lnPM2.5$, $lnPM10$, $lnSO_2$, $lnCO$, and $lnNO_2$, indicating that under the influence of reduced population movement, the urban air quality index, AQI, is significantly lower and the concentrations of the major air pollutants $PM2.5$, $PM10$, SO_2, CO, and NO_2 in the air are also significantly lower. Compared to the baseline regression, the interaction term ($treat_i * post_t$) coefficient, although becoming significant, is only significant at the 10% level when the explanatory variable is $lnSO_2$. When the explanatory variable is lnO_3, the interaction term ($treat_i * post_t$) is significantly positive, implying that the concentration of the main air pollutant (O_3) in the air increases significantly under the influence of reduced population movement, which is consistent with the baseline regression and the results are robust.

From the results in Appendix D Table A3, the results obtained from the D_{it} coefficients of interest in this paper remain consistent with the baseline regression under multi-period double difference estimation, again confirming the robustness of the causal identification results in this paper. Reduced population mobility does have a significant causal impact on urban air quality improvement.

3.5. Measuring the Impact of Intra-City Population Flow on Urban Air Quality

This paper empirically tests Model (3) with $lnAQI$, a measure of urban air quality, and $lnPM2.5$, $lnPM10$, $lnSO_2$, $lnCO$, $lnNO_2$, and lnO_3, the main explanatory variables, as the explanatory variables, respectively, and $lnincity$, a measure of intra-city population flow, as shown in Table 3.

Table 3. Results of measuring the impact of intra-city population flow on urban air quality.

	(1) *lnAQI*	(2) *lnPM2.5*	(3) *lnPM10*	(4) $lnSO_2$	(5) *lnCO*	(6) $lnNO_2$	(7) lnO_3
lnincity	0.433 ***	0.593 ***	0.516 ***	0.285 ***	0.273 ***	0.474 ***	0.050 ***
	(0.034)	(0.041)	(0.039)	(0.023)	(0.023)	(0.019)	(0.014)
Lowest temperature	0.001	0.021 ***	0.012 ***	−0.009 ***	0.013 ***	0.014 ***	−0.032 ***
	(0.002)	(0.003)	(0.003)	(0.002)	(0.002)	(0.002)	(0.001)
Highest temperature	0.010 ***	0.010 **	0.015 ***	0.017 ***	0.010 ***	0.025 ***	0.024 ***
	(0.003)	(0.004)	(0.003)	(0.003)	(0.002)	(0.002)	(0.001)
Wind	−0.118 ***	−0.171 ***	−0.164 ***	−0.147 ***	−0.110 ***	−0.211 ***	0.014
	(0.028)	(0.041)	(0.040)	(0.027)	(0.024)	(0.024)	(0.014)
Lowest temperature^2	−0.000 ***	0.000	0.000	−0.000 ***	0.000	0.000 **	−0.001 ***
	(0.000)	(0.000)	(0.000)	(0.000)	(0.000)	(0.000)	(0.000)
Highest temperature^2	−0.000	−0.000	0.000	0.000	−0.001 ***	−0.000 ***	0.001 ***
	(0.000)	(0.000)	(0.000)	(0.000)	(0.000)	(0.000)	(0.000)
Wind^2	0.002	−0.020 **	0.010	0.001	−0.008	−0.005	−0.004
	(0.005)	(0.009)	(0.008)	(0.006)	(0.005)	(0.005)	(0.002)
Constant	−2.403 ***	−5.251 ***	−3.951 ***	−2.062 ***	−4.196 ***	−4.395 ***	3.286 ***
	(0.523)	(0.639)	(0.598)	(0.347)	(0.360)	(0.290)	(0.210)
Sample size	9508	9508	9507	9508	9508	9508	9508
R-squared	0.125	0.212	0.127	0.187	0.194	0.428	0.265
FE	YES	YES	YES	YES	YES	YES	YES

Note: Figures in brackets are clustering robustness criteria errors; **, and *** denote significance levels of 5%, and 1%, respectively.

The results in Table 3 show that intra-city population flow does increase urban air pollution, both in terms of the urban air quality index indicator, $lnAQI$, and the main air pollutant indicators, $lnPM2.5$, $lnPM10$, $lnSO_2$, $lnCO$, $lnNO_2$, and lnO_3; all indicators increase with an increase in the intra-city population flow, and all results pass the 1% significance test.

3.6. Measuring the Impact of Inter-City Population Flow on Urban Air Quality

This paper empirically tests model (3) with $lnAQI$, a measure of urban air quality, and $lnPM2.5$, $lnPM10$, $lnSO_2$, $lnCO$, $lnNO_2$ and lnO_3, the main explanatory variables, as the explanatory variables, respectively, and $lnoutcity$, a measure of inter-city population flow, as shown in Table 4.

Table 4. Measured impact of inter-city population flow on urban air quality.

	(1)	(2)	(3)	(4)	(5)	(6)	(7)
	lnAQI	***lnPM2.5***	***lnPM10***	$\boldsymbol{lnSO_2}$	***lnCO***	$\boldsymbol{lnNO_2}$	$\boldsymbol{lnO_3}$
lnoutcity	0.201 ***	0.324 ***	0.235 ***	0.127 ***	0.158 ***	0.166 ***	0.043 ***
	(0.014)	(0.017)	(0.016)	(0.010)	(0.010)	(0.009)	(0.007)
Lowest temperature	0.005 **	0.028 ***	0.017 ***	−0.007 ***	0.016 ***	0.017 ***	−0.031 ***
	(0.002)	(0.003)	(0.003)	(0.002)	(0.002)	(0.002)	(0.001)
Highest temperature	0.011 ***	0.011 ***	0.015 ***	0.017 ***	0.010 ***	0.025 ***	0.025 ***
	(0.003)	(0.004)	(0.003)	(0.003)	(0.002)	(0.002)	(0.001)
Wind	−0.110 ***	−0.160 ***	−0.155 ***	−0.142 ***	−0.104 ***	−0.204 ***	0.016
	(0.028)	(0.040)	(0.039)	(0.026)	(0.023)	(0.024)	(0.014)
Lowest temperature^2	−0.000 ***	0.000	0.000	−0.000 ***	0.000 *	0.000 ***	−0.001 ***
	(0.000)	(0.000)	(0.000)	(0.000)	(0.000)	(0.000)	(0.000)
Highest temperature^2	0.000	0.000	0.000 **	0.000	−0.001 ***	−0.000	0.001 ***
	(0.000)	(0.000)	(0.000)	(0.000)	(0.000)	(0.000)	(0.000)
Wind^2	0.003	−0.018 **	0.010	0.001	−0.007	−0.005	−0.003
	(0.005)	(0.008)	(0.007)	(0.005)	(0.005)	(0.005)	(0.002)
Constant	2.245 ***	0.619 ***	1.635 ***	1.049 ***	−1.593 ***	1.252 ***	3.617 ***
	(0.138)	(0.176)	(0.159)	(0.101)	(0.096)	(0.093)	(0.069)
Sample size	9508	9508	9507	9508	9508	9508	9508
R-squared	0.131	0.239	0.130	0.187	0.220	0.396	0.271
FE	YES	YES	YES	YES	YES	YES	YES

Note: Figures in brackets are clustering robustness criteria errors, *, ** and *** denote significance levels of 10%, 5% and 1%, respectively.

The results in Table 4 show that inter-city population flow increases urban air pollution. The urban air quality index indicator, $lnAQI$, and the main air pollutant indicators, $lnPM2.5$, $lnPM10$, $lnSO_2$, $lnCO$, $lnNO_2$, and lnO_3, all increase with inter-city population flow and are significant at the 1% level.

4. Discussion

4.1. Reduced Population Movements Significantly Improve Urban Air Quality

The results in the causal identification section of this paper confirm that a reduction in population movement can significantly improve urban air quality. After excluding the Chinese New Year effect, the strict city lockdown policies in Hubei cities exogenously restrict population movement, which fundamentally reduces all types of socio-economic activities and, in turn, reduces the emission levels of most air pollutants, resulting in significant improvements in urban air quality in the treatment group. However, it is also important to highlight that there is variability in the causal impact of exogenous reductions in population movement on various air pollutants, with significant reductions in $PM2.5$, $PM10$, CO, and NO_2 concentrations in the air, a statistically insignificant reduction in SO_2 concentrations, and a statistically significant increase in concentrations of O_3, which has a complex generation mechanism. The lack of significant reduction in SO_2 may be attributed to the fact that the lockdown measures primarily targeted vehicle exhaust emissions, while the emissions of sulfur dioxide could be more closely linked to heavy industries such as steel plants and coal-fired power stations that continued operating during the lockdown period.

Ozone concentrations increased significantly due to its specific generation mechanism. Environmental science research explains that this is partly due to a reduction in NO_x concentrations from human activities due to city lockdown policies, which slows down the rate of ozone decomposition, while increased human activity in the home leads to an increase in VOC_s concentrations; together, these factors accelerate ozone accumulation [33]. On the other hand, reduced haze due to reduced PM2.5 leads to easier penetration of sunlight into the air, providing more energy for surface ozone production [34]. Lv et al. [35], when studying why the greatly reduced traffic volume during the COVID-19 lockdown in Beijing did not effectively reduce haze pollution, found that the reduction in traffic volume resulted in a large-scale reduction in NOx emissions, but due to heating and other human activities, volatile organic compounds were reduced on a relatively small scale, resulting in an unbalanced reduction between them. This led to a significant increase in atmospheric oxidation capacity in urban areas, resulting in increased ozone pollution. Pei et al. [26] made use of observation data from remote sensing and field measurements and concluded that stable HCHO concentrations in urban areas provided sufficient fuel for the formation of O_3 in the troposphere. HCHO is an important proxy for volatile organic compounds. In addition, during the lockdown, NO in the atmosphere decreased significantly and could not provide stable decomposition for O_3, resulting in increased ozone. The above findings remind us that for China to achieve the goal of new progress in ecological civilization and sustainable improvement of the ecological environment, urban air pollutants with different generation mechanisms should be classified and specifically analyzed, and pollution reduction and emission reduction for various pollutants should be achieved precisely and gradually through scientific and integrated planning.

4.2. Both Intra-City and Inter-City Population Flow Contribute Significantly to Urban Air Pollution

According to the empirical results, for every 1% increase in intra-city population flow, the urban air quality index rises by 0.433% and the concentrations of the main air pollutants increase by 0.593% (PM2.5), 0.516% (PM10), 0.285% (SO_2), 0.273% (CO), 0.474% (NO_2), and 0.050% (O_3). Of these six major urban air pollutants, PM2.5 was the most influenced by intra-city population flow, followed by PM10 and NO_2, which may be related to the fact that intra-city population flow in China is dominated by motor vehicles, as fuel motor vehicle exhaust is the main source of low-level emissions in Chinese cities; PM2.5 and NO_x are the main pollutants in the exhaust of fuel-fired motor vehicles, and PM10 is also associated with motor vehicles.

According to the empirical results, for every 1% increase in inter-city population flow, the urban air quality index increases by 0.201%, and the concentrations of the main air pollutants increase by 0.324% (PM2.5), 0.235% (PM10), 0.127% (SO_2), 0.158% (CO), 0.166% (NO_2), and 0.043% (O_3). Of the six major urban air pollutants, PM2.5 was most affected by inter-city population flow, followed by PM10, and then NO_2 and CO, both of which were equally affected. With the exception of the majority of passenger trains, which are electrically powered and have only a marginal impact on air pollution, aircraft engine emissions and fuel motor vehicle exhaust, both of which contain PM, NOx, and CO, are likely to be the main contributors to this.

The estimated coefficient value of *lnoutcity* for inter-city population flow is overall smaller than that of *lnincity* for intra-city population flow, indicating that the magnitude of the negative impact of intra-city population flow on urban air quality is significantly greater than that of inter-city population flow in terms of urban air quality index indicators and major air pollutant indicators. This finding is enlightening, and implies that urban construction should be well researched and reasonably planned to shorten the commuting distance between work and residential areas, increase public transport facilities, and reduce the need for self-driving trips; at the same time, it should strengthen the construction of living facilities in residential areas, promote the integration of industries and cities, and

reduce the need for long-distance travel within the city. This will improve urban air quality through a combination of measures to reduce the movement of people within the city.

4.3. Proposals for Achieving New Progress in Ecological Civilisation

In order to achieve the goals of new progress in ecological civilization, continuous reduction in total emissions of major pollutants, and continuous improvement of the ecological environment, this paper puts forward the following three policy recommendations. Firstly, further advocate and encourage green travel for the whole society, which is of utmost importance to the improvement of urban air quality. Electric vehicles should continue to be vigorously promoted as an alternative to fuel vehicles, vehicle emission standards should be upgraded, and the public should be encouraged to adopt public transport and shared travel and reduce private passenger travel. Secondly, the precise treatment of air pollutants with complex generation mechanisms, such as ozone, should be strengthened. This paper finds that after a significant reduction in population movement exogenesis, the concentration of a small number of major air pollutants such as ozone increased instead. This suggests that restricting the movement of people, or restricting economic activities such as industrial production, or adopting a "one-size-fits-all" approach to shutting down these air pollutants with complex generation mechanisms is not sufficient to reduce their harmful effects on urban air quality. The treatment and improvement of urban air quality requires further scientific research on the generation mechanisms of various air pollutants at the source, and precise and holistic measures in order to gradually promote pollution reduction and emission reduction. Thirdly, rational planning of urban layout is needed. The empirical results of this paper show that the pollution caused by intra-city population movement is significantly higher than that caused by inter-city population movement. Urban roads should be built to shorten the commuting distance between work and residential areas and to strengthen the construction of rail transport and public transport services; additionally, residential areas should strengthen the construction of living facilities to improve the convenience of residents' lives, so that most of their living and consumption needs can be solved in the vicinity of their homes, reducing the need to travel long distances within the city. For large cities in particular, the construction of new urban areas must be preceded by planning and scientific layout to create new urban areas with "city-industry integration" and planners should strive to realize the "integration of three places" of work, consumption, and residence for residents in the district, so as to avoid becoming a "bedroom community" in the central city, thus decreasing intra-city population flow.

5. Conclusions

The main objective of this paper is to empirically examine the causal impact of population movement on urban air quality and measure the specific magnitude of the effects of intra-city and inter-city population flow on urban air quality. This paper uses the city lockdown policy adopted by Hubei cities in early 2020 in response to the outbreak of the COVID-19 as a quasi-natural experiment with 328 prefecture-level cities in China to firstly identify the causal relationship between population movement and urban air quality, and secondly to measure the specific magnitude of the impact of the two types of population movement on urban air quality based on the distinction between intra-city and inter-city population flow. In the causal identification section, this paper uses data from the 23rd day of the lunar month to the 28th day of the first lunar month in Hubei in 2020 and the rest of Chinese cities in the same period in 2019 to construct a 36-day panel of air quality data for 328 cities, using the same period in the 2019 lunar calendar as a control group to eliminate the "Spring Festival effect". A DID method was used to find a causal effect of reduced population movement on urban air quality improvement. In the impact measurement section, the quantitative impacts of intra and inter-city population flow on urban air quality indices and major air pollutants were estimated using data from 328 prefecture-level cities in China for 29 consecutive days in January and February 2020. The results demonstrate that both intra-city and inter-city population flow have a significant negative impact on

urban air quality. However, the specific impact coefficients differ, with an overall finding that an increase in intra-city population flow leads to a more severe level of air pollution.

This paper focuses on the causal identification and impact measurement of population movement on urban air quality. Future research directions related to this paper may involve clarifying the mechanisms through which population movement affects urban air quality. This would require obtaining more relevant data to support the research.

Author Contributions: Conceptualization, F.H. and Q.W.; methodology, F.H.; software, F.H.; validation, F.H., Q.W. and P.W.; formal analysis, P.W.; data curation, F.H. and P.W.; writing—original draft preparation, F.H.; writing—review and editing, Q.W.; supervision, Q.W.; project administration, Q.W.; funding acquisition, Q.W. All authors have read and agreed to the published version of the manuscript.

Funding: This research was funded by Major project of key research bases on Humanities and Social Sciences of the Ministry of Education, grant number 22JJD790037.

Institutional Review Board Statement: Not applicable.

Informed Consent Statement: Not applicable.

Data Availability Statement: The datasets used and/or analyzed during the current study are available from the corresponding author upon reasonable request.

Acknowledgments: Thanks to Wang Tianru for her advice and help in expressing this article in English.

Conflicts of Interest: The authors declare that they have no conflict of interest.

Appendix A

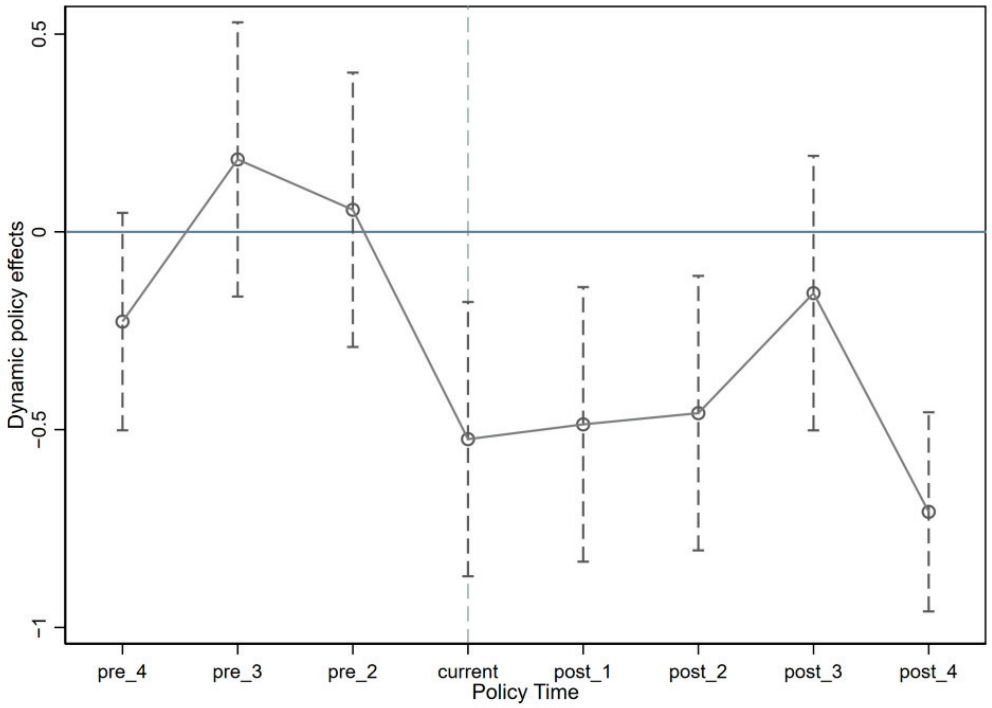

Figure A1. Results of parallel trend hypothesis testing where the explanatory variable is PM2.5. Note: Data for the pre_1 period is not available in the graph as the first period before the policy shock is used as the base group.

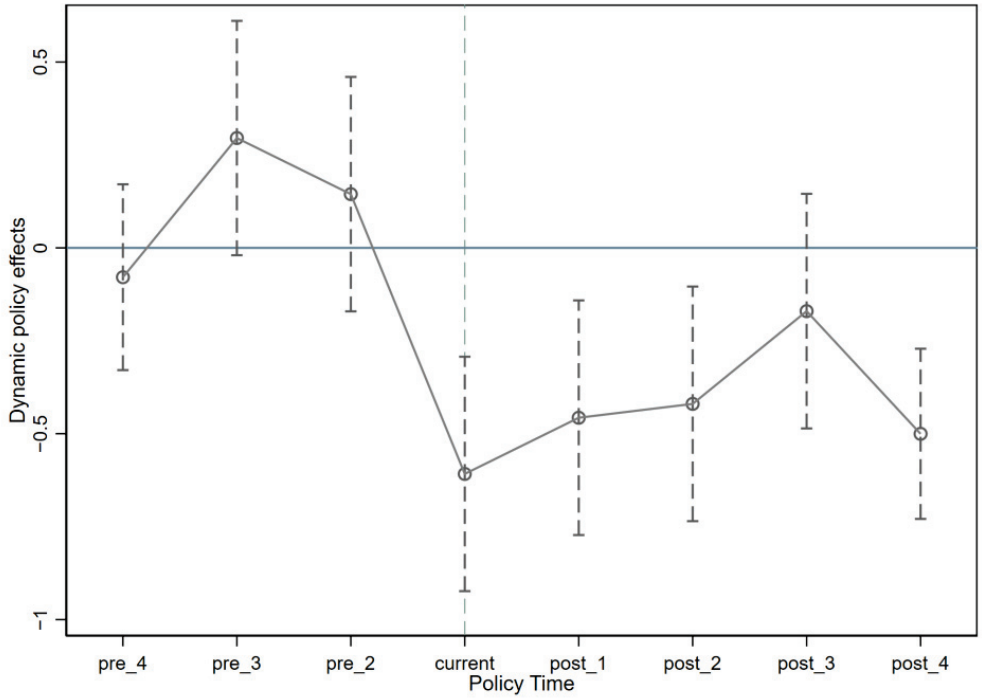

Figure A2. Results of parallel trend hypothesis testing where the explanatory variable is PM10. Note: Data for the pre_1 period is not available in the graph as the first period before the policy shock is used as the base group.

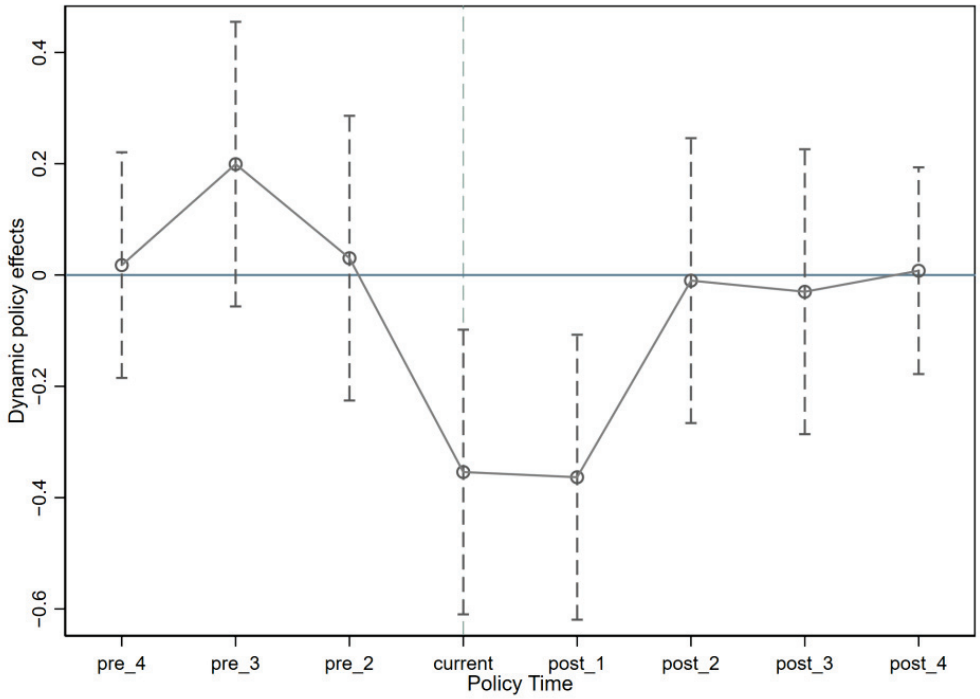

Figure A3. Results of parallel trend hypothesis testing where the explanatory variable is SO_2. Note: Data for the pre_1 period is not available in the graph as the first period before the policy shock is used as the base group.

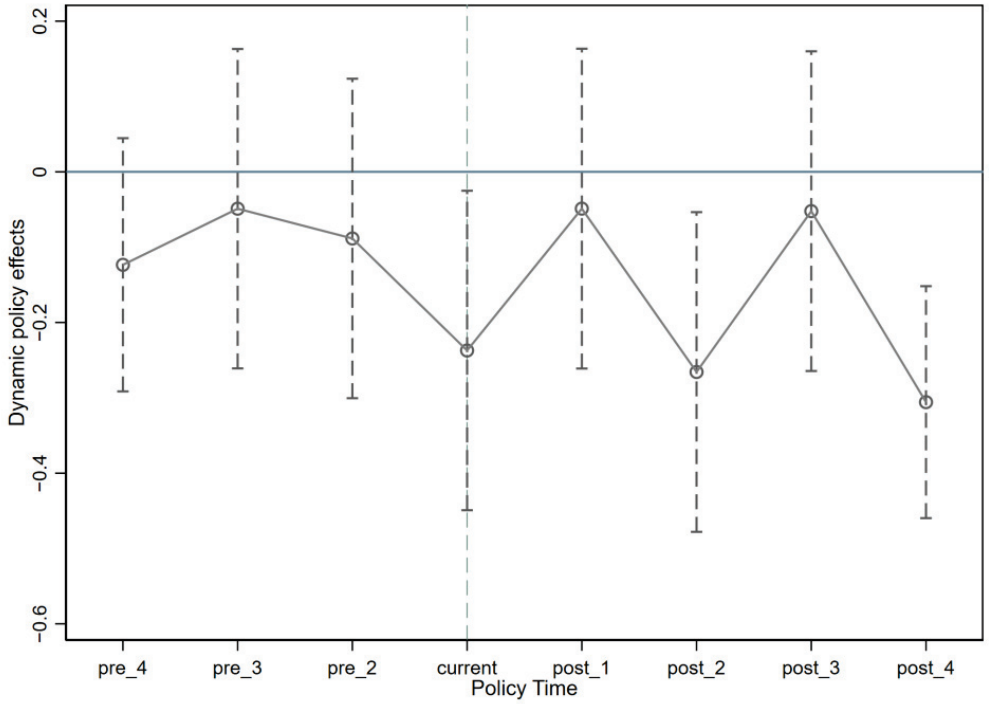

Figure A4. Results of parallel trend hypothesis testing where the explanatory variable is CO. Note: Data for the pre_1 period is not available in the graph as the first period before the policy shock is used as the base group.

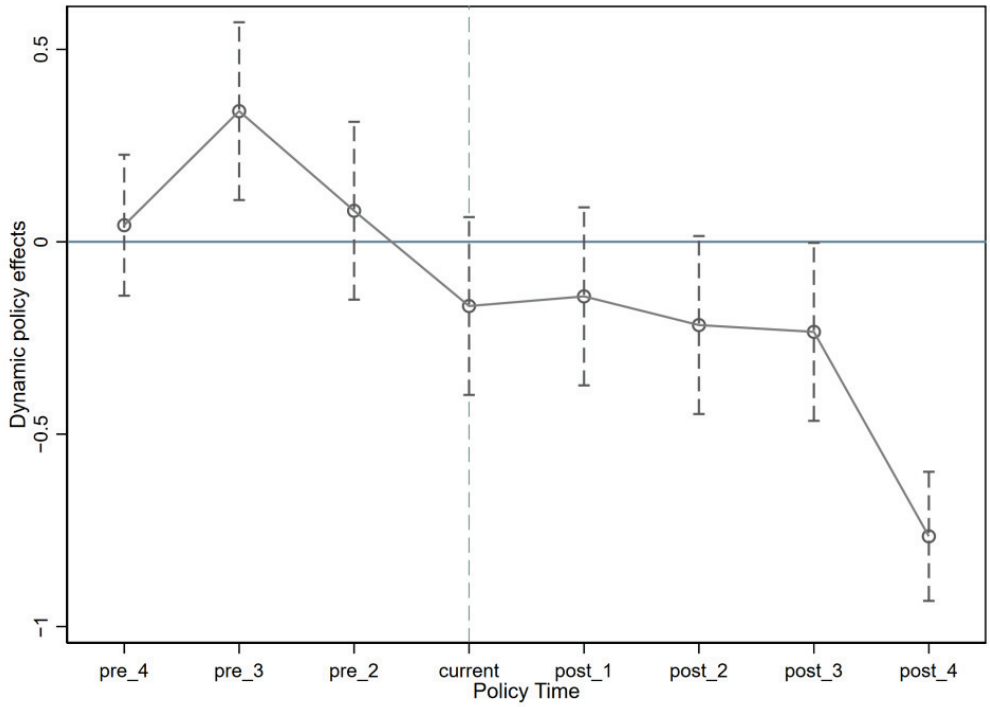

Figure A5. Results of parallel trend hypothesis testing where the explanatory variable is NO_2. Note: Data for the pre_1 period is not available in the graph as the first period before the policy shock is used as the base group.

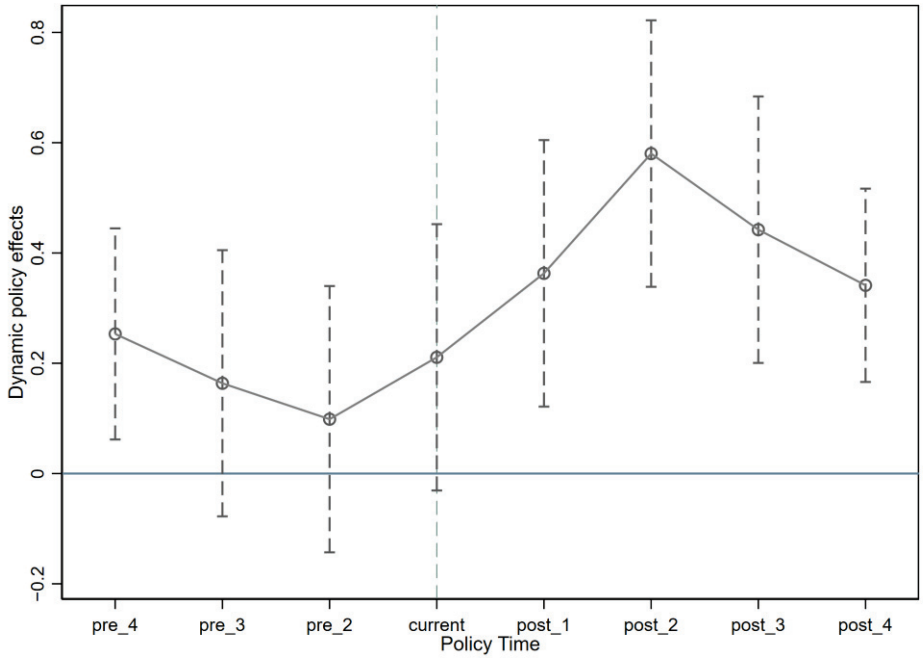

Figure A6. Results of parallel trend hypothesis testing where the explanatory variable is O_3. Note: Data for the pre_1 period is not available in the graph as the first period before the policy shock is used as the base group.

Appendix B

Table A1. A placebo test for causal identification of reduced population movements to improve urban air quality.

	(1) 15 January	(2) 11 January	(3) 8 January
$treat_i * post_t$	1.038	3.626	−2.036
	(2.210)	(2.376)	(3.287)
Lowest temperature	−0.073	−0.056	−0.091
	(0.248)	(0.250)	(0.246)
Highest temperature	2.684 ***	2.675 ***	2.692 ***
	(0.272)	(0.272)	(0.271)
Wind	−13.883 ***	−13.878 ***	−13.898 ***
	(2.445)	(2.443)	(2.440)
Lowest temperature^2	−0.025 ***	−0.025 ***	−0.025 ***
	(0.009)	(0.009)	(0.009)
Highest temperature^2	−0.005	−0.005	−0.005
	(0.010)	(0.010)	(0.010)
Wind^2	1.157 **	1.157 **	1.159 **
	(0.493)	(0.493)	(0.493)
Constant	120.798 ***	121.021 ***	120.573 ***
	(4.904)	(4.937)	(4.958)
Sample size	17,051	17,051	17,051
R-squared	0.526	0.526	0.526
Time FE	YES	YES	YES
Urban FE	YES	YES	YES

Note: Figures in brackets are clustering robustness criteria errors; **, and *** denote significance levels of 5%, and 1%, respectively.

Appendix C

Table A2. Robustness test—replacing the explanatory variables.

	(1)	(2)	(3)	(4)	(5)	(6)	(7)
	lnAQI	***lnPM2.5***	***lnPM10***	***lnSO$_2$***	***lnCO***	***lnNO$_2$***	***lnO$_3$***
$treat_i * post_t$	−0.456 ***	−0.594 ***	−0.523 ***	−0.077 *	−0.183 ***	−0.772 ***	0.144 ***
	(0.042)	(0.049)	(0.045)	(0.042)	(0.042)	(0.043)	(0.039)
Lowest temperature	0.007 ***	0.017 ***	0.009 ***	−0.010 ***	0.000	−0.002	−0.013 ***
	(0.003)	(0.003)	(0.003)	(0.002)	(0.002)	(0.002)	(0.003)
Highest temperature	0.031 ***	0.030 ***	0.038 ***	0.024 ***	0.023 ***	0.026 ***	0.019 ***
	(0.003)	(0.004)	(0.003)	(0.003)	(0.003)	(0.003)	(0.002)
Wind	−0.125 ***	−0.121 ***	−0.180 ***	−0.004	−0.047 **	−0.073 ***	−0.010
	(0.025)	(0.031)	(0.033)	(0.023)	(0.020)	(0.021)	(0.020)
Lowest temperature^2	0.000 ***	0.000 ***	0.001 ***	0.000 **	0.000 **	0.000 ***	−0.000 ***
	(0.000)	(0.000)	(0.000)	(0.000)	(0.000)	(0.000)	(0.000)
Highest temperature^2	0.000	0.001 ***	0.000 *	0.000 *	−0.000 ***	0.000	0.001 ***
	(0.000)	(0.000)	(0.000)	(0.000)	(0.000)	(0.000)	(0.000)
Wind^2	0.011 **	−0.006	0.025 ***	−0.022 ***	−0.013 ***	−0.026 ***	0.004
	(0.005)	(0.006)	(0.007)	(0.005)	(0.004)	(0.004)	(0.004)
Constant	4.506 ***	4.071 ***	4.427 ***	1.884 ***	−0.212 ***	3.848 ***	3.925 ***
	(0.038)	(0.049)	(0.047)	(0.036)	(0.032)	(0.032)	(0.036)
Sample size	11,804	11,804	11,792	11,804	11,804	11,804	11,804
R-squared	0.662	0.711	0.717	0.798	0.611	0.802	0.492
Time FE	YES	YES	YES	YES	YES	YES	YES
Urban FE	YES	YES	YES	YES	YES	YES	YES

Note: Figures in brackets are clustering robustness criteria errors; *, **, and *** denote significance levels of 10%, 5%, and 1%, respectively.

Appendix D

Table A3. Robustness test—multi-period DID model.

	(1)	(2)	(3)	(4)	(5)	(6)	(7)
	lnAQI	***lnPM2.5***	***lnPM10***	***lnSO$_2$***	***lnCO***	***lnNO$_2$***	***lnO$_3$***
D_{it}	−0.448 ***	−0.590 ***	−0.502 ***	−0.067	−0.186 ***	−0.788 ***	0.119 ***
	(0.044)	(0.051)	(0.045)	(0.043)	(0.043)	(0.041)	(0.039)
Lowest temperature	0.007 ***	0.017 ***	0.009 ***	−0.010 ***	0.000	−0.002	−0.013 ***
	(0.003)	(0.003)	(0.003)	(0.002)	(0.002)	(0.002)	(0.003)
Highest temperature	0.031 ***	0.030 ***	0.038 ***	0.024 ***	0.023 ***	0.027 ***	0.019 ***
	(0.003)	(0.004)	(0.003)	(0.003)	(0.003)	(0.003)	(0.002)
Wind	−0.126 ***	−0.123 ***	−0.181 ***	−0.004	−0.048 **	−0.074 ***	−0.009
	(0.025)	(0.031)	(0.032)	(0.023)	(0.020)	(0.021)	(0.020)
Lowest temperature^2	0.000 ***	0.000 ***	0.001 ***	0.000 **	0.000 **	0.000 ***	−0.000 ***
	(0.000)	(0.000)	(0.000)	(0.000)	(0.000)	(0.000)	(0.000)
Highest temperature^2	0.000	0.001 ***	0.000 *	0.000 *	−0.000 ***	0.000	0.001 ***
	(0.000)	(0.000)	(0.000)	(0.000)	(0.000)	(0.000)	(0.000)
Wind^2	0.011 **	−0.006	0.025 ***	−0.022 ***	−0.012 ***	−0.026 ***	0.004
	(0.005)	(0.006)	(0.007)	(0.005)	(0.004)	(0.004)	(0.004)
Constant	4.507 ***	4.071 ***	4.428 ***	1.885 ***	−0.212 ***	3.847 ***	3.923 ***
	(0.038)	(0.049)	(0.047)	(0.036)	(0.032)	(0.032)	(0.036)
Sample size	11,804	11,804	11,792	11,804	11,804	11,804	11,804
R-squared	0.662	0.712	0.717	0.798	0.611	0.803	0.492
Time FE	YES	YES	YES	YES	YES	YES	YES
Urban FE	YES	YES	YES	YES	YES	YES	YES

Note: Figures in brackets are clustering robustness criteria errors; *, **, and *** denote significance levels of 10%, 5%, and 1%, respectively.

References

1. Yuan, Y.; Xu, G.; Chen, X.H.; Jia, J.M. Research on the Interaction Mechanism between Urban Traffic Congestion and Air Pollution-a Big Data Analysis based on DiDi Travel. *J. Manag. Sci.* **2020**, *23*, 54–73.
2. Sun, C.W.; Luo, Y.; Yao, X. Transportation Infrastructure and Urban Air Pollution—Empirical Evidence from China. *Econ. Res.* **2019**, *54*, 136–151.
3. Liang, R.B.; Xi, P.H. Heterogeneous Impact of Rail Transportation on Air Pollution—An Empirical Study based on RDID Method. *China Ind. Econ.* **2016**, *3*, 83–98.
4. Cao, J.; Wang, X.; Zhong, X.H. Has the Traffic Restriction Policy Improved the Air Quality in Beijing? *Econ. Q* **2014**, *13*, 1091–1126.
5. Chester, M.; Horvath, A. High-speed Rail with Emerging Automobiles and Aircraft can Reduce Environmental Impacts in California's future. *Environ. Res. Lett.* **2012**, *7*, 034012.
6. Li, J.M.; Luo, N.S. Has the Opening of High-speed Rail Improved Urban Air Pollution Levels? *Econ. Q* **2020**, *19*, 1335–1354.
7. Xu, W.P.; Jiang, H.; Li, Y.S. A Study on the Differences in Environmental Effects of Population Agglomeration and Economic Agglomeration in China-Analysis based on Provincial Panel Data. *Ecol. Econ.* **2018**, *34*, 123–127.
8. Zhou, S.F.; Zhang, J.J. A Study on the Spatial and Temporal Effects of New Urbanization on Urban Air Pollution in China. *Ind. Technol. Econ.* **2019**, *38*, 66–75.
9. Wang, H.X.; Shi, D.Q. Does New Urbanization Help Alleviate Haze Pollution-Empirical Evidence from Low-carbon City Construction. *J. Shanxi Univ. Financ. Econ.* **2019**, *41*, 15–27.
10. Deng, X.; Zhang, W. Are Large Cities Aggravating Regional Environmental Pollution? *J. Beijing Univ. Technol. (Soc. Sci. Ed.)* **2018**, *20*, 36–44.
11. Guo, S.H.; Gao, M.; Wu, X.P. Economic development, urban expansion and air pollution. *Res. Financ. Econ.* **2017**, *9*, 114–122.
12. Gao, M.; Wu, X.P.; Guo, S.H. Urbanization Process, Environmental Regulation and Air Pollution—An Empirical Analysis based on STIRPAT Model. *Ind. Technol. Econ.* **2016**, *35*, 110–117.
13. Guo, F.; Shi, Q.L. Official Turnover, Collusive Deterrence and Temporary Improvement in Air Quality. *Econ. Res.* **2017**, *52*, 155–168.
14. Huang, R.B.; Zhao, Q.; Wang, L.Y. Natural Resource Asset Separation Audits and Air Pollution Prevention: "Harmony Tournament" or "Environmental Qualification Tournament". *China Ind. Econ.* **2019**, *10*, 23–41.
15. Hu, Y.; Zhang, X.W.; Li, J. Export Trade, Geographical Characteristics and Air Pollution. *China Ind. Econ.* **2019**, *9*, 98–116.
16. Wang, L.; Liu, X.F.; Xiong, Y. Central Environmental Protection Inspectors and Air Pollution Control—An Empirical Analysis based on Micro Panel Data of Prefecture-level Cities. *China Ind. Econ.* **2019**, *10*, 5–22.
17. Shapiro, J.S.; Walker, R. Why is Pollution from US Manufacturing Declining? The Roles of Environmental Regulation, Productivity and Trade. *Am. Econ. Rev.* **2018**, *108*, 3814–3854. [CrossRef]
18. Pandey, A.K.; Singh, S.; Berwal, S.; Kumar, D.; Pandey, P.; Prakash, A.; Lodhi, N.; Maithani, S.; Jain, V.K.; Kumar, K. Spatio—Temporal Variations of Urban Heat Island over Delhi. *Urban Clim.* **2014**, *10*, 119–133.
19. Pandey, A.K.; Rawal, R.S.; Gairola, S.; Bhatt, I.D.; Kumar, R.P.; Priyadarshini, N.; Kumar, A. Protection from Anthropogenic Disturbances Contributed to the Recovery of Vegetation in the Kumaon Himalaya: A Case Study. *Int. J. Geol. Earth Environ. Sci.* **2017**, *7*, 39–50.
20. Sun, W.Z.; Zhang, X.N.; Zheng, S.Q. Air Pollution and Spatial Mobility of Labor Force—A Study based on the Employment Location Selection Behavior of Mobile Population. *Econ. Res.* **2019**, *54*, 102–117.
21. Zhang, H.F.; Lin, X.X.; Liang, R.B.; Lan, J.J. Urban Ecological Civilization Construction and New Generation of Labor Mobility—A New Perspective on Labor Resource Competition. *China Ind. Econ.* **2019**, *4*, 81–97.
22. Xi, P.H.; Liang, R.B. Urban Air Quality and Environmental Migration—An Empirical Study based on Fuzzy Breakpoint Model. *Econ. Sci.* **2015**, *4*, 30–43.
23. Li, M.; Zhang, Y.R. The Migration Effect of Air Pollution—A Study based on the University-city Choice of Incoming Students. *Econ. Res.* **2019**, *54*, 168–182.
24. Menut, L.; Bessagnet, B.; Siour, G.; Mailler, S.; Pennel, R.; Cholakian, A. Impact of Lockdown Measures to Combat COVID-19 on Air Quality over Western Europe. *Sci. Total Environ.* **2020**, *741*, 140426. [PubMed]
25. He, G.J.; Pan, Y.H.; Tanaka, T. The Short-term Impacts of COVID-19 Lockdown on Urban Air Pollution in China. *Nat. Sustain.* **2020**, *3*, 1005–1011. [CrossRef]
26. Pei, Z.P.; Han, G.; Ma, X.; Su, H.; Gong, W. Response of Major Air Pollutants to COVID-19 Lockdowns in China. *Sci. Total Environ.* **2020**, *743*, 140879. [CrossRef] [PubMed]
27. Yang, Z.; Chen, Y.T.; Zhang, P.M. Macroeconomic Shocks, Financial Risk Transmission and Governance Responses under Major Public Emergencies. *Manag. World* **2020**, *36*, 13–35+7.
28. Jiang, H.; Liu, Y. A Comparison of the Economic Effects of Trade Frictions between China and the United States before and after the Outbreak of the New Crown Pneumonia Outbreak. *World Econ. Political Forum* **2021**, *3*, 54–77.
29. Tan, P.H.; Chou, C.; Liang, J.Y.; Charles, C.; Shiu, C.J. Air Pollution "Holiday Effect" Resulting from the Chinese New Year. *Atmos. Environ.* **2009**, *43*, 2114–2124.
30. Almond, D.; Du, X.; Zhang, S. Ambiguous Pollution Response to COVID-19 in China. *NBER Work. Pap.* **2020**. [CrossRef]
31. Fang, H.M.; Wang, L.; Yang, Y. Human Mobility Restrictions and the Spread of the Novel Coronavirus (2019-nCoV) in China. *J. Public Econ.* **2020**, *191*, 104272. [PubMed]

32. Luo, Z.; Zhao, Q.W.; Yan, B. The Impact of Constraint Mechanism and Incentive Mechanism on Long-term Investment of State-owned Enterprises. *China Ind. Econ.* **2015**, *10*, 69–84.
33. Wang, T.; Xue, L.K.; Brimblecombe, P.; Lam, Y.F.; Zhang, L. Ozone Pollution in China: A Review of Concentrations, Meteorological Influences, Chemical Precursors and Effects. *Sci. Total Environ.* **2016**, *575*, 1582–1596. [PubMed]
34. Li, K.; Jacob, D.J.; Liao, H.; Shen, L.; Zhang, Q.; Bates, K.H. Anthropogenic Drivers of 2013–2017 Trends in Summer Surface Ozone in China. *Proc. Natl. Acad. Sci. USA* **2019**, *116*, 422–427. [CrossRef] [PubMed]
35. Lv, Z.; Wang, X.; Deng, F.; Ying, Q.; Archibald, A.T.; Jones, R.L.; Ding, Y.; Cheng, Y.; Fu, M.; Liu, Y.; et al. Significant Reduced Traffic in Beijing Failed to Relieve Haze Pollution during the COVID-19 Lockdown: Implications for Haze Mitigation. *arXiv* **2020**, arXiv:2006.07297.

sustainability

MDPI

Article

Study on Rates of NH_3 Adsorption and Desorption in SCR on Various Engine Operation Conditions

Hyun Jo [1], Ahyun Ko [2], Jinyoung Jang [2] and Ocktaeck Lim [1,*]

[1] Graduate School of Mechanical Engineering, University of Ulsan, Ulsan 44610, Republic of Korea; jhkaist91@naver.com
[2] Korea Institute of Energy Research, Daejeon 34129, Republic of Korea; hydra32@kier.re.kr (A.K.); jy.jang@kier.re.kr (J.J.)
* Correspondence: otlim@ulsan.ac.kr; Tel.: +82-52-259-2852

Abstract: Aging diesel engines on the road require the development of an after-treatment system to meet current emission regulations, and a reduction in NOx (Nitrogen Oxide) is significant. The SCR (Selective Catalytic Reduction) system is the after-treatment system for removing NOx from exhaust gas in diesel engines using NH_3 (Ammonia) gas. However, the mixing and conversion process between NH_3 and NOx in SCR has not been entirely clarified. That process produces NH_3 slip in the catalyst surface; the NH_3 slip will make the after-treatment performance worse. This study informs how the UWS (Urea Water Solution) injection controlling method can minimize the NH_3 slip in the after-treatment system. For this, the NH_3 adsorption and desorption rates are important factors for determining the quantity of UWS injection in the system. The NH_3 adsorption rate and desorption rate in the SCR are not significantly affected by engine speed, i.e., the exhaust gas flow rate. However, as the exhaust gas temperature increased, the adsorption rate and desorption rate of NH_3 in the SCR increased. Through this, the exhaust gas temperature dramatically affects the NH_3 adsorption rate and desorption rate in the SCR. Therefore, if the urea water is injected based on this knowledge that the NH_3 adsorption amount in the SCR decreases as the exhaust gas flow rate increases, NH_3 slip can be suppressed and a high NOx reduction rate can be achieved. Therefore, if the SCR adsorption and desorption mechanisms are analyzed according to the exhaust temperature and the exhaust flow rate in this paper, it can be used as a reference for selecting an appropriate SCR when retrofitting an old diesel engine car.

Keywords: urea-SCR; diesel engine; NH_3 adsorption; NH_3 slip; nitrogen oxides (NOx)

1. Introduction

As environmental regulations on internal combustion engines are strengthened worldwide, technologies to reduce emissions are needed for the future of internal combustion engines. The main harmful exhaust gases of diesel engines are PM (Particle Matter) and NOx. To reduce harmful emissions, various studies are being conducted, ranging in focus from the combustion process to the emission process. Among the methods of after-treatment systems for reducing harmful emissions in exhaust gas, there is the method of oxidizing carbon monoxide (CO) and hydrocarbons through the DOC (Diesel Oxidation Catalyst) and collecting PM through the DPF (Diesel Particle Filter). The DOC and DPF mainly comprise a Pt catalyst and a substrate of cordierite or SiC. However, there are some differences in catalyst composition or substrate characteristics depending on the automobile manufacturer or the after-treatment device. The catalyst oxidizes THC (Total Hydro Carbon) and CO (Carbon Oxide) emissions and regenerates the trapped PM in the DPF. Most of the composition of NOx emitted from diesel engines is NO, but it is converted to NO_2 through DOC and DPF [1,2]. NO_2 would affect the regeneration process of PM in DPF and the performance of SCR [3,4]. To reduce NOx efficiently, controlling

NO_2 conversion in the DOC and DPF is necessary. The LNT (Lean NOx Trap) and SCR are the most representative after-treatment methods for reducing NOx. The NH_3-SCR system is the most widely used in diesel engines due to its high efficiency and wide operating temperature range [5]. Hydrocarbons are alternatives for overcoming the disadvantages of the NH_3-SCR reaction [6,7]; by adding hydrocarbon, the oxygen concentration is increased in the NH_3-SCR system [8]. The chemical properties will assist NH_3 to decrease NOx and increase the generation of H_2O (Water) and CO. In previous studies, the NH_3/NOx ratio, NO_2/NOx ratio, hydrocarbon concentration, NOx conversion efficiency, and HSO (Hydrolysis + SCR + Oxidation catalyst) in the SCR with vanadium and zeolite material were analyzed to judge the possibility of the after-treatment. Experimental studies on the conversion efficiency were used to analyze the performance of NOx reduction, depending on the gas hourly space velocity (GHSV) and the monolith volume for the oxidation catalysts and VHSO (oxidation + HSO catalysts) SCR systems [9–11]. The SCR effectively reduces NOx in a steady-state engine; however, it still has a problem reducing NOx and producing the NH_3 slip in transient-state engines such as vehicles [12–16]. Based on this, the methods for improving Urea-SCR system performance are introduced in this study, in which we control the amount of urea injection into the SCR to improve the performance of the NOx reduction and reduce the NH_3 slip simultaneously via the adsorption and desorption of NH_3 in SCR [17]. When the amount of UWS in the SCR increases, the vapor pressure will decrease; the urea droplet temperature suddenly drops, and this phenomenon leads to low evaporation of urea droplets in the SCR [18]. The hydrolysis phenomenon with various physical models can validate the NH_3 slip quantity in the SCR based on the evaporation quality [19]. The NO and NO_2 ratio, the SCR temperature, and the engine speed conditions can affect the NH_3 slip quantity and the NOx reduction rate [20]. The ratio of NO and NO_2 in the NOx concentration when entering the SCR directly affects the performance of SCR; based on that condition, the commercial after-treatment adds the DOC and DPF in front of the SCR [21]. Since the SCR is greatly affected by the exhaust gas temperature, research was conducted to improve the NOx reduction rate by analyzing the ratio of NO to NO_2 from a low temperature [22]. The temperature of SCR is the main factor of fast chemical reactions in the SCR system to reduce NOx [23]. A study was conducted to develop an optimized injection control strategy where the DOC, DPF, and SCR were installed. To analyze the amount of NH_3 adsorption in SCR, the maximum adsorption amount of NH_3 in SCR for the NOx reduction and the NH_3 slip were separately measured. As a result, the NH_3 slip occurred during the NH_3 adsorption in SCR. Therefore, it was not easy to remove the NH_3 slip altogether without an AOC (Ammonia Oxidation Catalyst) [24,25]. To achieve complete NH_3 slip removal according to various exhaust temperatures and exhaust flow rates, it is necessary to analyze the adsorption amount of NH_3 in the SCR and the adsorption rate and desorption rate.

In this study, we show the performance of the DOC, DPF, and SCR according to reducing harmful emissions such as PM and NOx generated from an aging diesel engine under various engine operating conditions. To achieve this, as mentioned earlier, it is necessary to clarify how the amounts of NH_3 adsorption and desorption in SCR appear under various operating conditions of the engine. In addition, since the NH_3 slip cannot be prevented by any amount of NH_3 adsorption and desorption in SCR, this paper considered strategies to prevent the NH_3 slip by analyzing the adsorption rate and desorption rate of NH_3 in SCR according to engine operating conditions. The DOC and DPF are being developed as a natural regeneration DPF suitable for the retrofit market. The DOC and DPF catalysts used in this study were intermediate developments, consisting of Pt and a promoter with a BPT (Balance Point Temperature) of 285 °C. SCR is a primary material to remove NOx using gaseous NH_3. Observing the NH_3 adsorption and desorption mechanisms is essential in controlling NH_3 slip and optimizing the NOx reduction efficiency. The adsorption and desorption of the NH_3 mechanism in SCR were analyzed according to engine and catalyst conditions.

2. Experimental Setup

Experimental Apparatus

This study used Ssang-yong's in-line 5-cylinder 2696 cc diesel engine. Table 1 shows a detailed description of the engine's specifications. The valve type of the engine is a DOHC (Double OverHead Camshaft). The bore and stroke of each cylinder are 86.2 mm and 92.4 mm, respectively, and the compression ratio is 17.5. The maximum power of the engine is 191 PS at 4000 rpm, and the maximum torque is 410 N·m when the engine speed is at 3000 rpm. The fuel injection system is a common rail, and the environmental regulation that the engine meets is Euro 2. The engine used in the experiment was used only for experimental purposes, and the engine was managed using the manual and reference materials for a vehicle that has the same engine. The reason for using the old version of the engine is that the goal is to research an after-treatment system for the continued use of the old diesel engine. The experiment was carried out under various engine load ranges in which the engine speeds were 1500, 2000, 2500, and 3000 rpm and the exhaust gas temperatures were 250, 300, 350, and 400 °C, respectively. The reason for these conditions is to realize the range of daily driving conditions of a diesel engine.

Table 1. Diesel engine specifications.

No. of Cylinders	5
Valve type	DOHC 20 valve
Strokes	4
Type	Turbo diesel
Rated power P (PS)	186/4000 rpm
Rated torque M (Nm)	418/1600–3000
Experiment engine speed (rpm)	1500, 2000, 2500, 3000
Exhaust gas temperature (°C)	250, 300, 350, 400
Manufacture	2006
Emission standards	Euro 2

An overview of the overall experimental setup is shown in Figure 1. The engine is connected to a dynamometer to control the operating range, and the DOC, DPF, and SCR are installed in the after-treatment system. The specifications for each catalytic unit are given in Table 2. The substrate of the DOC and DPF is cordierite coated with Platinum. The BPT of DOC and DPF is 285 °C, and the cell density of each catalyst is 400 cpsi and 300 cpsi. The diameter is the same at 5.66 inches, and the length is 4 inches for the DOC and 10 inches for the DPF. The DOC and DPF were contained in the same case in this study. The substrate of SCR is cordierite, coated with a Vanadium base. The cell density of the SCR is 400 cpsi, and the diameter and length are 6.77 inches and 10 inches, respectively. The DOC, DPF, and SCR are all sequentially connected in series from the engine, and the experiment is conducted after sufficient time was given for the target exhaust gas temperature to be reached. In this study, AOC is not installed because it is necessary to analyze the amount of NH_3 slip according to the urea water injection strategy. The sampling line of exhaust gas is installed before and after each DOC, DPF, and SCR to analyze the exhaust gas, and a thermocouple is used to measure the temperature. Each tube is connected to HORIBA's MEXA 1400 QL-NX, an exhaust gas analyzer, and NO, NO_2, N_2O, and NH_3 were measured in real time using this equipment. When analyzing the exhaust gas, the sampling line was heated to 150 °C to prevent PM fouling and NH_3 deposition.

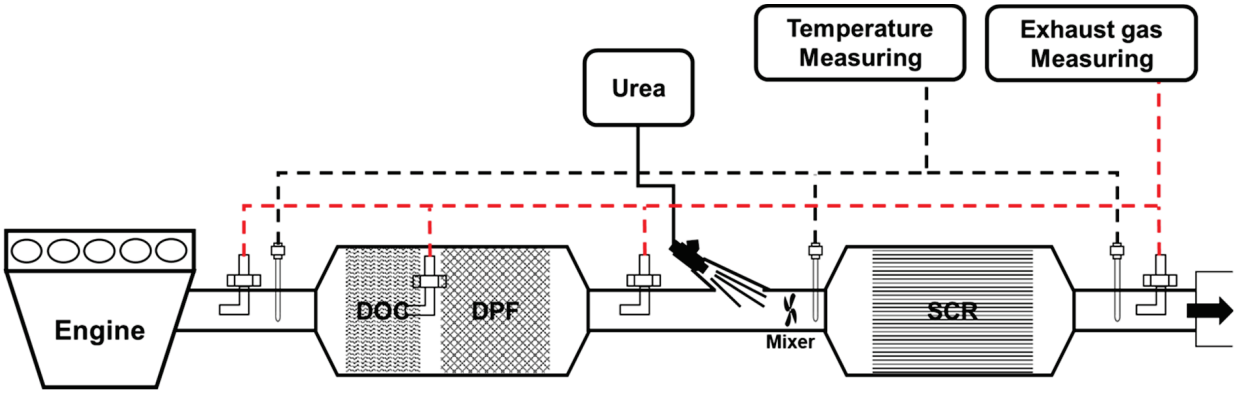

Figure 1. Schematic diagram of experimental equipment.

Table 2. SCR system specifications.

Category	DOC	DPF	SCR
Substrate	Cordierite		
Catalyst	Pt + Promoter/TiO_2		V-W/TiO_2
BPT	285 °C		-
Cell density	400 cpsi	300 cpsi	400 cpsi
Diameter	5.66 inch	5.66 inch	6.77 inch
Length	4 inch	10 inch	10 inch

The urea water is injected between the DOC/DPF and SCR. A mixer is installed at the inlet of the SCR so that the injected urea water is uniformly distributed in the SCR. The injection pressure of urea water is maintained at 5 bar and repeated at a rate of 3.3 Hz.

3. Methods and Analysis

The chemical reaction process of general urea-SCR is as follows. The urea water is first decomposed into NH_3 in two steps. As in Reaction (1), instead, HNCO and NH_3 are produced via the thermolysis of urea water, and NH_3 and CO_2 are produced by isocyanic acid hydrolysis of HNCO in Reaction (2). NH_3 made in this way reacts with nitrogen oxides inside SCR, and the representative responses are called Standard SCR (3), Fast SCR (4), and NO_2 SCR (5).

$$(NH_2)_2CO \rightarrow HNCO + NH_3 \quad (1)$$

$$HNCO + H_2O \rightarrow NH_3 + CO_2 \quad (2)$$

$$4NO + 4NH_3 + O_2 \rightarrow 4N_2 + 6H_2O) \quad (3)$$

$$NO + NO_2 + 2NH_3 \rightarrow 2N_2 + 3H_2O \quad (4)$$

$$6NO_2 + 8NH_3 \rightarrow 7N_2 + 12H_2O \quad (5)$$

Based on this reaction process, the theoretical amount of urea required to reduce NOx emitted was calculated assuming that the ratio of NH_3 to NOx was 1:1. The ratio of NO and NH_3 in the standard SCR reaction and the percentage of NOx and NH_3 in the Fast SCR reaction is 1:1. However, in the NO_2-SCR reaction, the reaction between NO_2 and NH_3 was not 1:1. In general, in NOx emitted from diesel engines, the proportion of NO is higher than that of NO_2, and most of the NO_2 is reduced in the fast SCR reaction. If NO is oxidized through the DOC and DPF, the ratio of NO_2 should be higher than that of NO, but this was not seen in the experimental results. In addition, it did not significantly affect the process of observing the adsorption and slip of NH_3 in the SCR, which is the focus of

this study. Therefore, assuming that the reduction ratio of NH_3 and Nox is 1:1, the injection amount of urea water was calculated as in Equation (6).

$$\dot{M} = \left(N_{in} \times \dot{m} / M_{exh}\right) / \left(d_{urea} / M_{urea} \times 2 \times 10^6\right) \quad (6)$$

As shown in Table 3, the experiment was conducted under 16 different engine operating conditions, respectively, in which the engine speed was 1500, 2000, 2500, and 3000 rpm and the exhaust gas temperature was 250, 300, 350, and 400 °C. After operating the engine and waiting until the fluctuation of emission gas is reduced, the urea-water solution is injected to measure the change in NOx and NH_3 according to the evolution of time when the engine and catalyst conditions are different. The amount of urea-water solution with which NH_3 can react with NOx and create 100 ppm of NH_3 slip was injected. The reason for injecting the excess urea is to check the total amount of NH_3 adsorbed to the SCR by intentionally causing a NH_3 slip and preventing the trend. So, to establish a urea-water-solution injection strategy, we investigated how the amount of NH_3 adsorbed in the SCR appears according to engine and catalyst conditions. Exhaust gas analysis with a single exhaust gas analyzer was performed by controlling valves on the sampling line at different locations. After injecting urea water, sufficient time is required for ammonia to be adsorbed and desorbed in the SCR. Therefore, preliminary experiments were conducted to determine how much time is required for a stable experiment to reduce uncertainty. In this study, a measurement experiment was conducted for 30 min before and after urea water injection to adsorb and desorb the NH_3 in SCR enough.

Table 3. Engine operating conditions under which the experiment was performed.

Category	Engine Operating Conditions
Engine speed [rpm]	1500, 2000, 2500, 3000
Exhaust gas temperature [°C]	250, 300, 350, 400

Figure 2 shows the results of measuring the exhaust gas when the engine speed is 1500 rpm and the exhaust gas temperature is 250 °C according to the above-mentioned method. In the graph, there are fluctuations in the measured value of each exhaust gas. NH_3 and NO fluctuated around 10 ppm and NO_2 fluctuated around 12 ppm. However, it was determined that this fluctuation was negligible and had an insignificant impact on the exhaust gas measurement results, so the error was eliminated by taking sufficient measurement time and analyzing the results by averaging the values. In Phase M_2, after injecting the amount of urea with an excess reduction, NOx decreased and NH_3 slip increased. Phase M_3 shows a tendency of NH_3 slip to reduce and NOx to increase again after the urea water injection stopped. Although the NOx reduction efficiency differs depending on the space velocity and temperature of the exhaust gas depending on the engine conditions, NH_3 slip occurs after a certain period has passed since the NOx reduction was performed in common. The amount of NH_3 adsorbed in the SCR until the NH_3 slip appears through the measured amount of NOx and NH_3 change (M_1), the amount of NH_3 adsorbed after the NH_3 slip (M_2), and the amount of adsorption based on the reduced amount of NOx (M_3) were calculated, respectively.

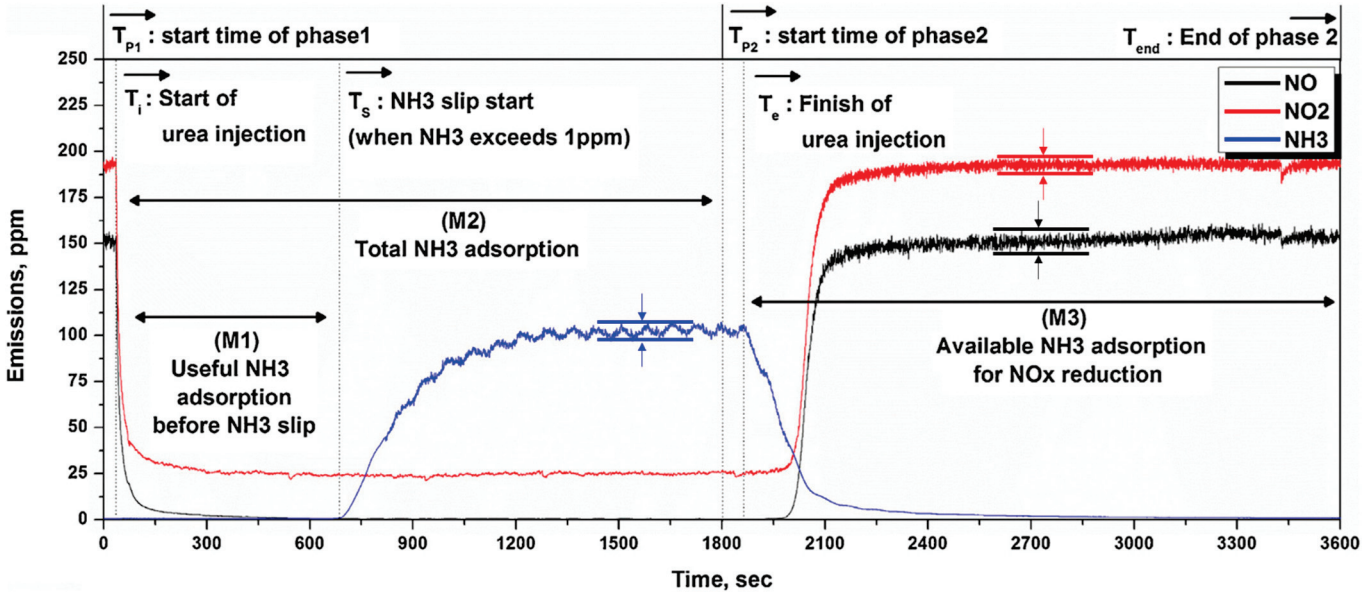

Figure 2. Adsorption and desorption of NH_3 in SCR experiment results and analysis methods (Engine speed: 1500 rpm, Exhaust gas temperature: 250 °C).

To investigate the range that can be controlled so that the NH_3 slip does not appear, the range for measuring the amount of NH_3 adsorbed in the SCR until the NH_3 slip occurs is M_1. The adsorption amount of NH_3 in the period before the occurrence of NH_3 slip is equal to the amount of NH_3 slip during the period in which NH_3 slip appears stably. Therefore, the value obtained by accumulating the amount of NH_3 slip stabilized until the appearance of NH_3 slip for the M_1 period can be regarded as the amount of NH_3 adsorbed on the SCR. Further, assuming that the reaction ratio of NH_3 and NOx is 1:1, NOx appears in the NH_3 slip so it cannot be reduced. Therefore, it is necessary to consider NOx emissions when the NH_3 slip stabilizes and NOx emissions during the transient period. Based on this, the amount of adsorption until the NH_3 slip appears can be calculated by the following formula:

$$M_1 = \int_{t=T_i}^{t=T_s} \left[\{A_{mean} - A_t + (N_{mean} - N_t)\} \times \dot{V}_{exh} \times \rho_{NH3} \right] \quad (7)$$

The standard moment at which the NH_3 slip started to appear was set when NH_3 exceeded 1 ppm—after the appearance of the NH_3 slip, a stabilization time of approximately 1500 to 1800 s passed. Adsorption of NH_3 in the SCR continues even when the NH_3 slip occurs, but the amount of NH_3 that can be adsorbed in the SCR is complete when the NH_3 slip stabilizes. This is because when NH_3 can no longer be adsorbed on the SCR, the further charged NH_3 is discharged as it is. Therefore, the total amount of NH_3 adsorbed in the SCR can be calculated by the following equation, and the calculation range is set to the time when the NH_3 slip stabilizes:

$$M_2 = \int_{t=T_i}^{t=T_{P2}} \left[\{A_{mean} - A_t + (N_{mean} - N_t)\} \times \dot{V}_{exh} \times \rho_{NH3} \right] \quad (8)$$

As mentioned above, the change in NOx emissions after the completion of urea water injection was measured in Phase M_3. When the urea water injection is completed, NOx emissions gradually increase even though ammonia is no longer input. It can be assumed that the conventionally adsorbed NH_3 reacted with NOx if there was no further NH_3 charged in the SCR. Therefore, by integrating the amount of NOx emitted during this period, it is possible to estimate the amount of NH_3 that was conventionally adsorbed on the SCR. However, since this method calculates the amount of NH_3 adsorbed based on

the NOx reduction reaction if the existing NH_3 does not react to the reduction in NOx, it may differ from the result of the amount of NH_3 adsorbed by the M_2 calculation method. Therefore, in the case of M_3, the following equation can be used to estimate the percentage of how much NH_3 adsorbed in the SCR can be used to reduce NOx emissions:

$$M_3 = \int_{t=T_e}^{t=T_{end}} \left\{ (N2_{mean} - N2_t) \cdot \frac{\rho_{NO2}}{M_{NO2}} \right\} \cdot \frac{\dot{V}_{exh}}{1000} \quad (9)$$

4. Results and Discussion

4.1. NH_3 Adsorption in SCR in Different Engine Conditions

Figure 3 shows NO and NO_2 measured after the engine, the DOC, and the DPF. As is generally known, in this experiment, most of the NOx generated during diesel combustion took the form of NO, and the NO increased in proportion to the temperature of the exhaust gas from combustion. When the exhaust gas temperature was approximately 400 °C, the NO was measured to be low due to the activation of the EGR. The EGR was activated when the engine speed and load were medium, and EGR activity stopped when the exhaust gas temperature was above 450 °C to achieve a high engine output. As described above, since the diesel engine used in the experiment satisfies EURO 2, the EGR operating area is relatively narrow compared to the latest machine. After that, looking at the amount of NO and NO_2 through the DOC and DPF, the amount of NO_2 gradually increased due to NO oxidation as the DOC and DPF were activated.

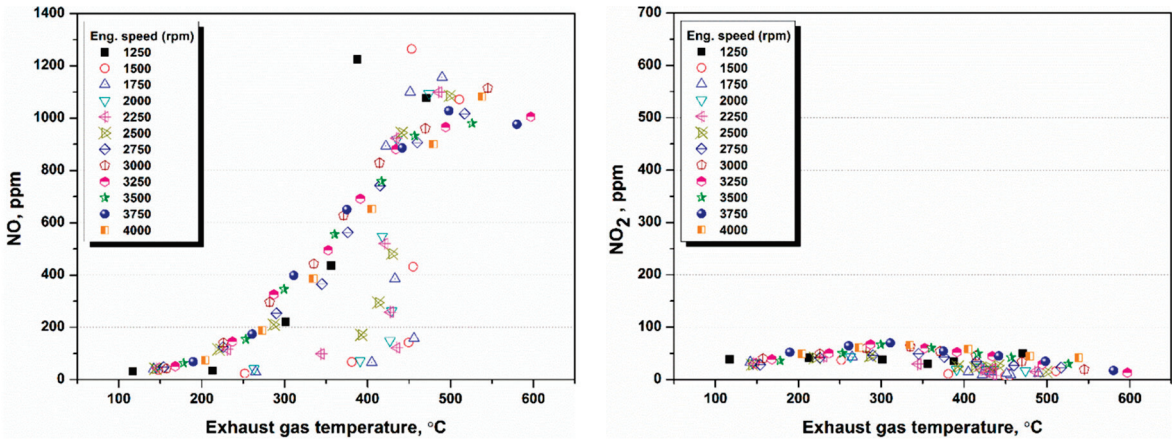

(**a**) After Engine

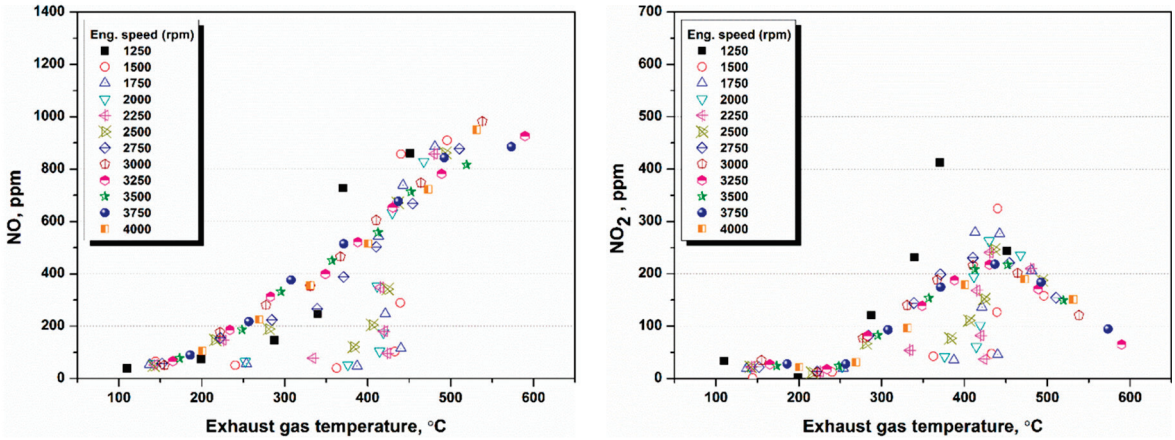

(**b**) After DOC

Figure 3. *Cont.*

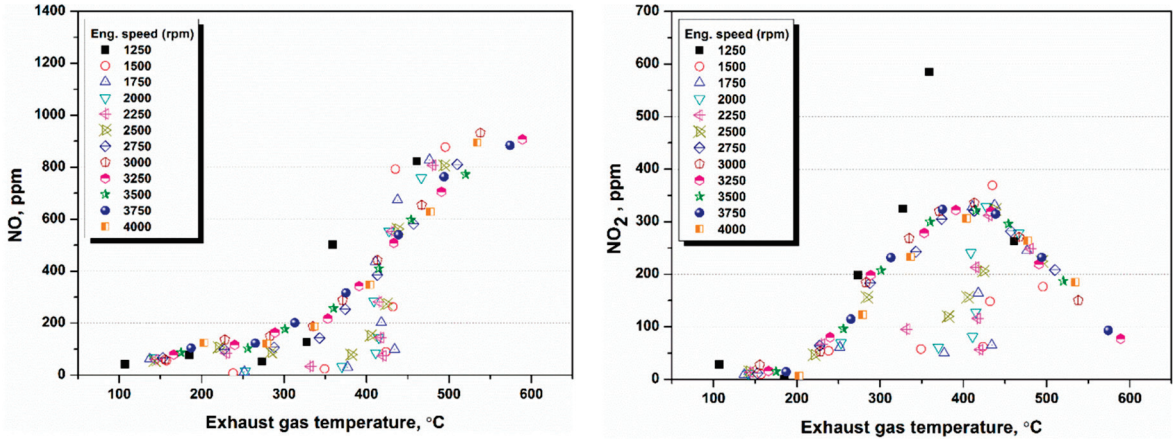

(**c**) After DPF

Figure 3. NO and NO_2 emission characteristics (**a**) after engine, (**b**) after DOC, and (**c**) after DPF.

Figure 4 shows the results of changes in the amount of NO and NO_2 through NO oxidation in the DOC and DPF. When the exhaust gas temperature was below 250 and 200 °C, respectively, NO was hardly oxidized due to the inactivation of the DOC and DPF. Still, as the catalyst started to be activated, NO began to be eroded to NO_2. When the exhaust gas temperature was 450 °C, the oxidation rate of NO was highest in the DOC, and the oxidation rate of NO was highest at 350 °C in the DPF. Through this, the central temperature range of this study was 250 °C to 400 °C, which indicates the temperature at which SCR was activated for the oxidation of NO reached the maximum.

First, the relationship between the reduction efficiency of SCR according to the ratio of NO and NO_2 in NOx was investigated through the experimental results. Figure 5 shows the SCR reduction efficiency according to the NO and NO_2 ratio. Each color represents the engine speed, and the *x*-axis represents the exhaust gas temperature. The solid square results show the NOx reduction ratio of SCR, and the empty square shows the percentage of NO and NO_2 inside the SCR exhaust gas. The right *y*-axis shows the proportion of NO and NO_2, and the left *y*-axis shows the NOx reduction rate. The closer the ratio of NO to NO_2 is to 1:1, the closer to 1, and the larger the percentage of NO, the larger the value. The NOx reduction ratio is more comparable to 1.0 the closer the NOx reduction is to 100%. The solid square results show the NOx reduction ratio of SCR, and the empty square shows the percentage of NO and NO_2 inside the SCR exhaust gas.

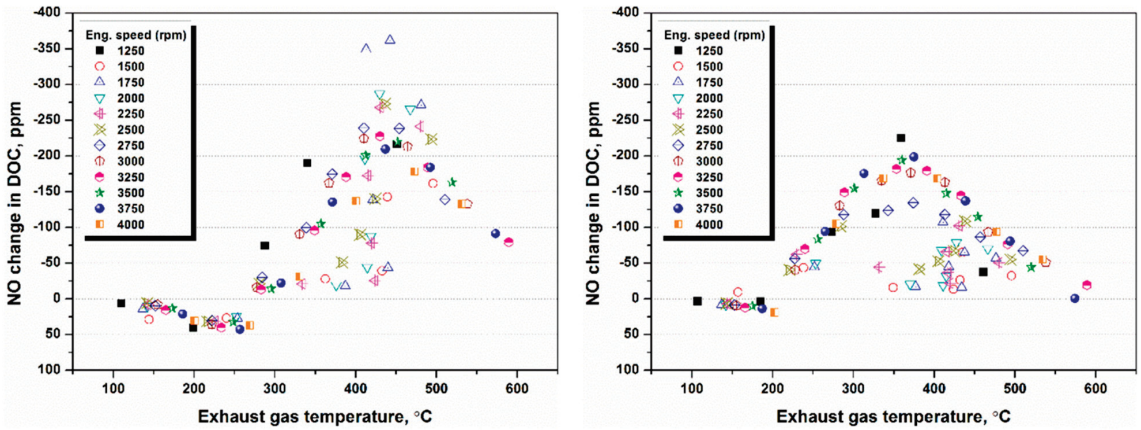

(**a**) NO change in DOC

(**b**) NO_2 change in DOC

Figure 4. *Cont.*

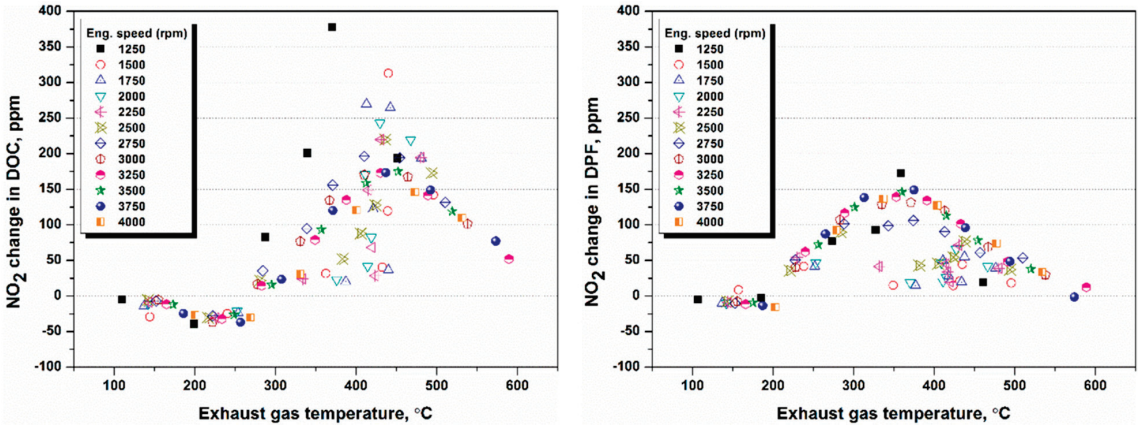

(**c**) NO change in DPF (**d**) NO_2 change in DPF

Figure 4. NO and NO_2 changes in DOC (**a**,**b**) and DPF (**c**,**d**).

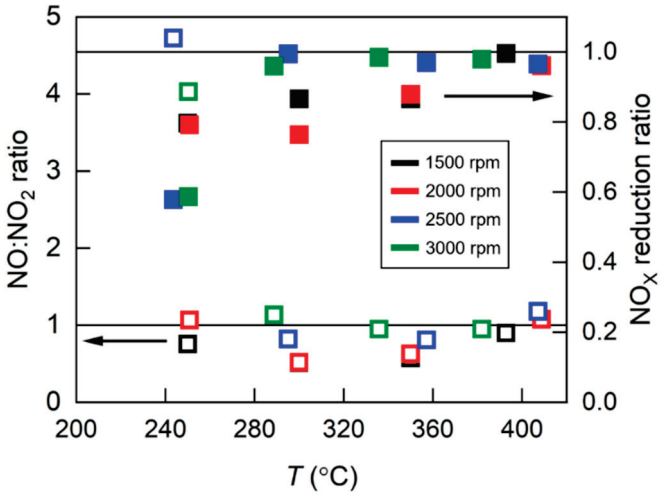

Figure 5. Ratio of NO and NO_2 according to the experimental conditions.

As a result, the ratio of NO and NO_2 in the exhaust gas that passes through the DOC differs depending on the exhaust gas temperature and the engine speed. When the engine cranking speeds were 1500 and 2000 rpm, it was found that NO_2 accounted for a more significant proportion than NO in the range of the exhaust gas temperature in the field of 300 to 350 °C, which lowered the NOx reduction ratio inside the SCR. When the engine speed was 2500 and 3000 rpm, the exhaust gas temperature was slightly 250 °C or less. Still, at this time, the NO ratio was 300 °C or more, significantly higher than NO_2, and the NO to NO_2 ratio was almost 1:1. The NOx reduction ratio inside the SCR was also the lowest when the exhaust gas temperature was approximately 250 °C. Still, the percentage of NO and NO_2 was 1:1, and the reduction efficiency was considerably high. As a result, the exhaust gas was partially oxidized to NO_2 via the shear activation DOC and DPF, and NO and NO_2 in a 1:1 ratio entered the SCR. The highest SCR efficiency was achieved then, and excessive conversion to NO_2 reduced the reduction efficiency. Based on the above NOx reduction ratio, the amount of NH_3 that slipped was predicted from the amount of urea injected, and the NH_3 adsorbed on the SCR was calculated.

Figures 6–8 show the amount of SCR adsorbed on the SCR in different ways through Equations (7)–(9). The adsorption amount at each operating point is displayed, and the average value is displayed on the trend line. As in previous studies, the amount of NH_3 adsorbed on the SCR decreased as the exhaust gas temperature increased. Looking at Figure 6, which shows the amount of NH_3 adsorbed on the SCR until NH_3 slip occurs, the

amount of NH_3 adsorbed is approximately 1.25 to 0.25 g in the exhaust gas temperature range of 250 to 400 °C.

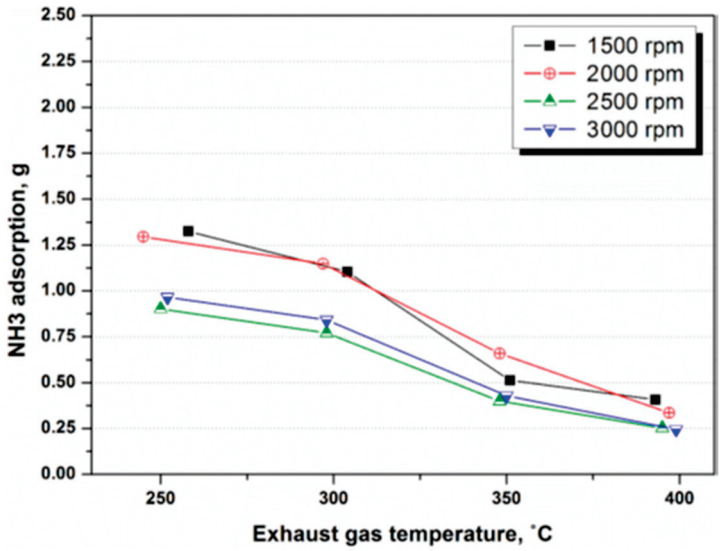

Figure 6. NH_3 storage amount calculated in Phase M_1 according to experimental conditions.

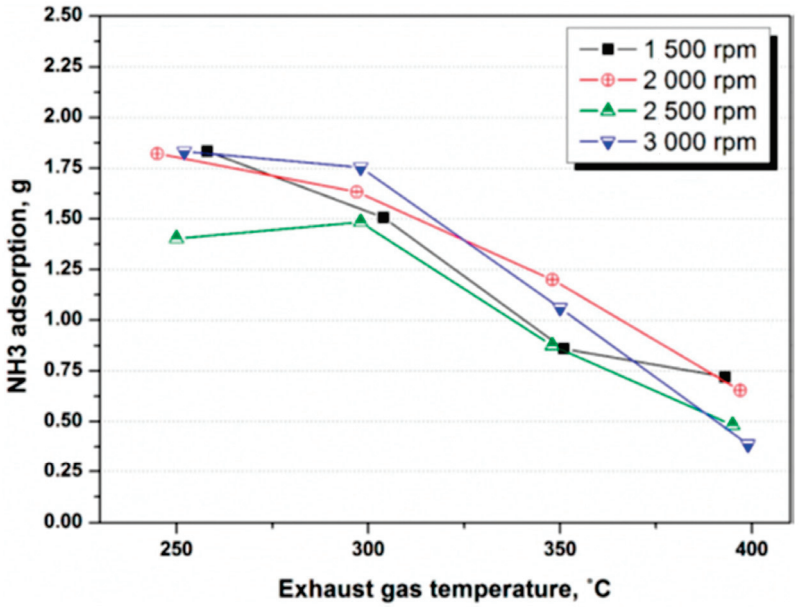

Figure 7. NH_3 storage amount calculated in Phase M_2 according to experimental conditions.

Figures 7 and 8 show the total amount of NH_3 adsorbed on the SCR after the appearance of the NH_3 slip and the total amount of NH_3 adsorbed on the SCR after stopping the urea water injection. From the above results, the total amount of NH_3 adsorbed on the SCR is 1.8 to 0.4 g. Here, the NH_3 adsorption amount substantially utilized for NOx reduction is the result of reversely calculating the NOx amount reduced while desorbing NH_3 adsorbed on the SCR. Therefore, the impact of M_3 can be estimated as the amount of NH_3 adsorbed that can be utilized for actual NOx reduction. It was found that the NH_3 adsorption amount calculated by the M_2 method was slightly higher than the NH_3 adsorption amount calculated by the M_3 method. It can be presumed that this is because NH_3 is adsorbed on the region where the catalyst is not applied and the low-temperature portion, particularly on the outer wall of the SCR.

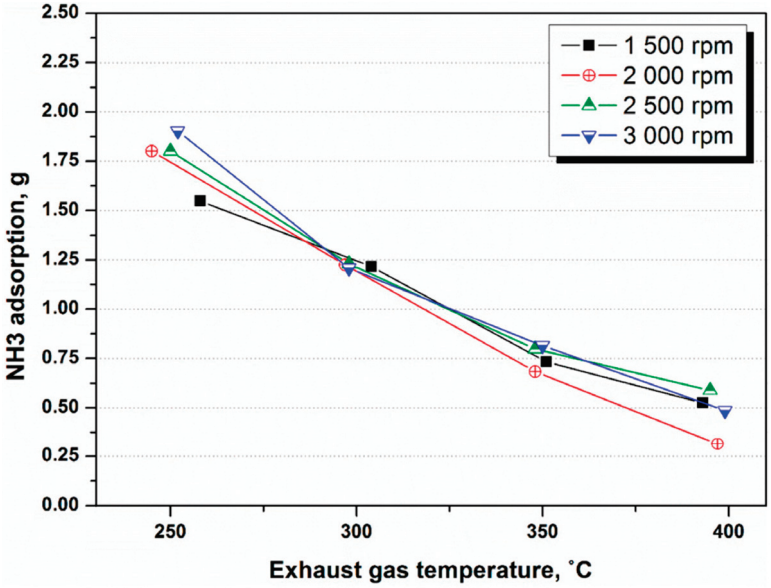

Figure 8. NH_3 storage amount calculated in Phase M_3 according to experimental conditions.

Based on this, the NH_3 adsorption amount used for NOx reduction was regarded as the M_3 result value, and the useless NH_3 adsorption amount was calculated by subtracting the M_3 result value from the M_2 result value. The amount of useless NH_3 adsorption was 0.1 to 0.2 g over the entire temperature range. Figure 9 shows a graph of the proportion of NH_3 adsorption and total adsorption that is unnecessary for NOx reduction. In general, the NH_3 slip reduced the amount of NH_3 adsorbed inside the SCR in the operating region where the exhaust gas temperature was high. In addition, the amount of unnecessary NH_3 adsorption also increased in the active area where the exhaust gas temperature was higher. As a result, the amount of NH_3 adsorbed unnecessarily under the experimental operating conditions was insignificant from 0.1 to 0.2 g. However, the proportion of total NH_3 adsorbed increased to 60% at the highest temperature. As a result, as the exhaust gas temperature increased, the amount of NH_3 adsorption decreased, and the buffer section was reduced, making it challenging to control NH_3 slip.

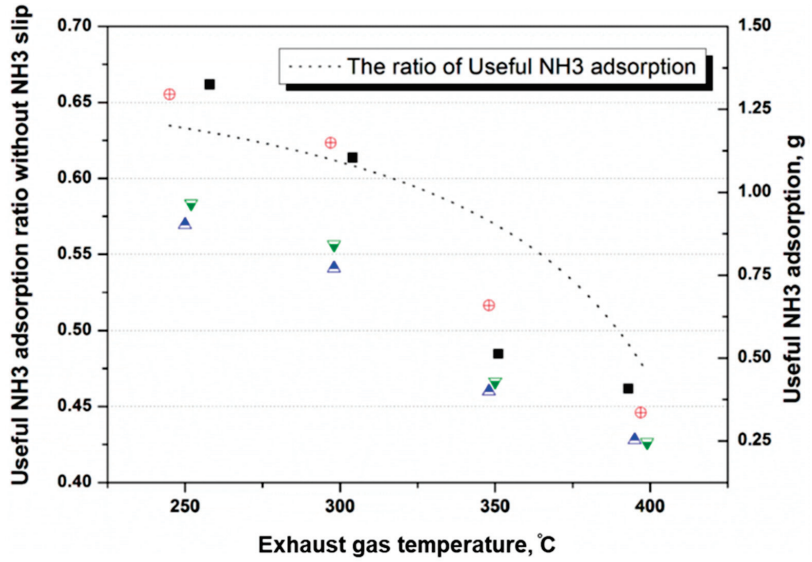

Figure 9. Useful NH_3 adsorption amount and ratio used for actual NOx reduction according to exhaust gas temperature.

4.2. NH_3 Adsorption and Desorption Rate in SCR in Different Engine Conditions

The amount of NH_3 adsorbed in the SCR varies depending on the engine's operating conditions. Therefore, if not only the adsorption amount but also the adsorption rate and the desorption rate are not considered, an acceptable urea water injection strategy for controlling the NH_3 slip can be established. Figure 10 shows how the NH_3 adsorption and desorption rates were calculated.

$$\dot{m}_{ammonia,\ adsorb} = \partial m_{NH3,adsorb}/\partial t \tag{10}$$

$$\dot{m}_{ammonia,desorp} = \partial m_{NH3,desorp}/\partial t \tag{11}$$

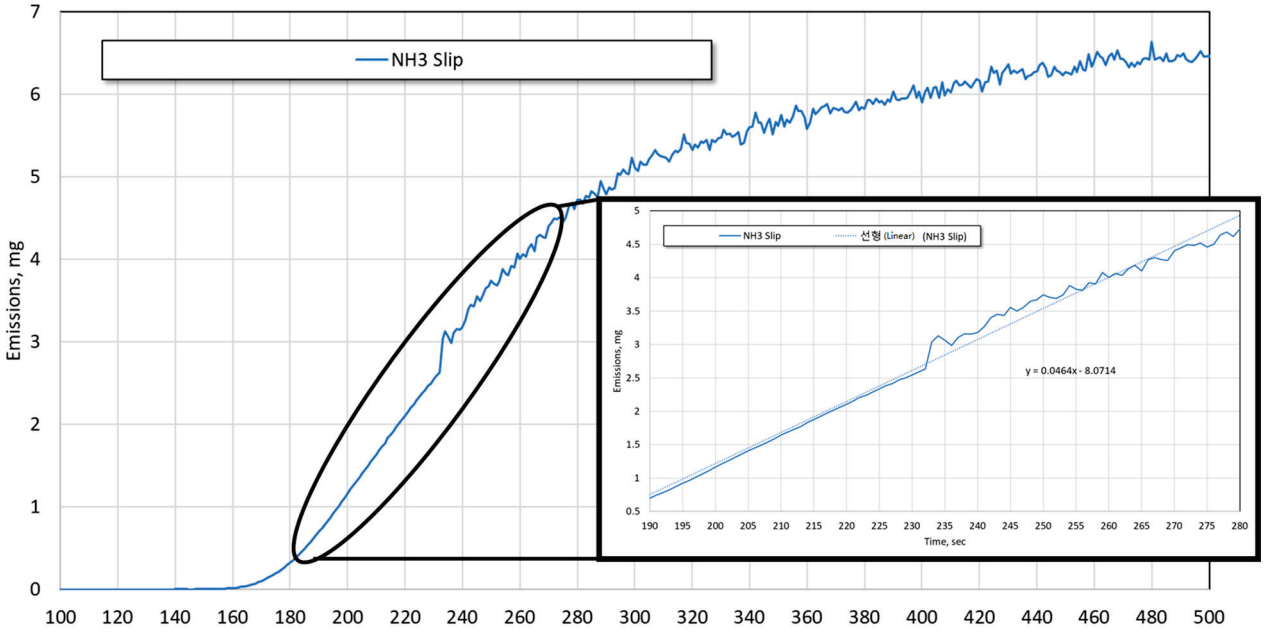

Figure 10. Calculation of the NH_3 adsorption rate and desorption rate (at 3000 rpm and 300 °C).

Figure 11 shows the results calculated according to Equations (9) and (10) for the NH_3 adsorption and desorption rates inside the SCR under experimental operating conditions. Graph (a) shows the NH_3 adsorption rate in the SCR depending on the operating conditions and graph (b) shows the NH_3 desorption rate in the SCR. Looking at the adsorption rate, the adsorption rate appeared relatively fast at an engine cranking speed of 2000 rpm and temperatures of 300 to 350 °C. The proportion of NO_2 in NOx discharged in this range is high, the NOx reduction efficiency is relatively low, and a large amount of NH_3 slip occurs, so the adsorption rate of SCR seems to appear rapidly. Therefore, this result alone does not clearly show the relationship between the NH_3 adsorption rate and the desorption rate depending on the operating conditions. The total amount of NH_3 adsorbed in the SCR changes depending on the operating conditions, and the NH_3 slip also changes. Therefore, the results of calculating and comparing the adsorption and desorption rates of NH_3 in consideration of the NH_3 storage amount are shown in Figure 12.

The results in Figure 12 show that the engine cranking speed does not significantly affect the adsorption and desorption rates of NH_3 in the SCR. However, it turned out to be substantially affected by the exhaust gas temperature. This supports the idea that the total occlusion of NH_3 decreases as the exhaust gas temperature rises so that the rate at which NH_3 is adsorbed inside the SCR and the desorption rate increase. In addition, as the temperature of the exhaust gas rises, it affects the internal temperature distribution of the entire SCR, and it can be expected that the degree of catalytic activation will also be affected. For this reason, in later studies, it is necessary to analyze the NH_3 adsorption and desorption rates depending on the temperature distribution inside the SCR and the

degree of activation. Based on these results, if a urea water injection strategy is established through experiments on the relationship between the temperature distribution inside the SCR and the engine's operating conditions, NH_3 slip can be reduced while maximizing the NOx reduction efficiency.

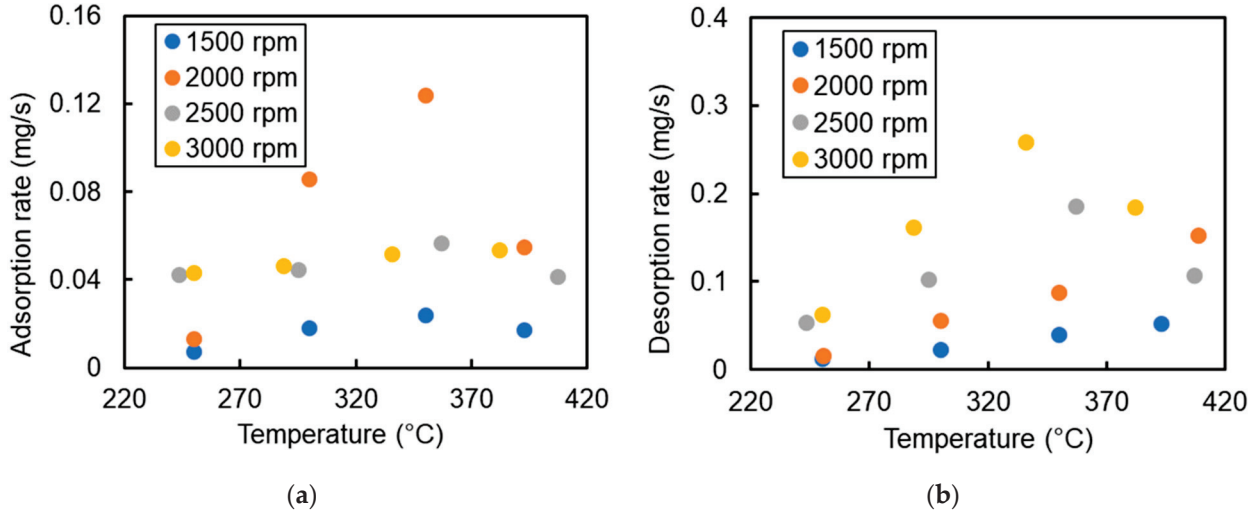

(**a**) (**b**)

Figure 11. Adsorption (**a**) and desorption (**b**) rates of NH_3 in SCR in various conditions.

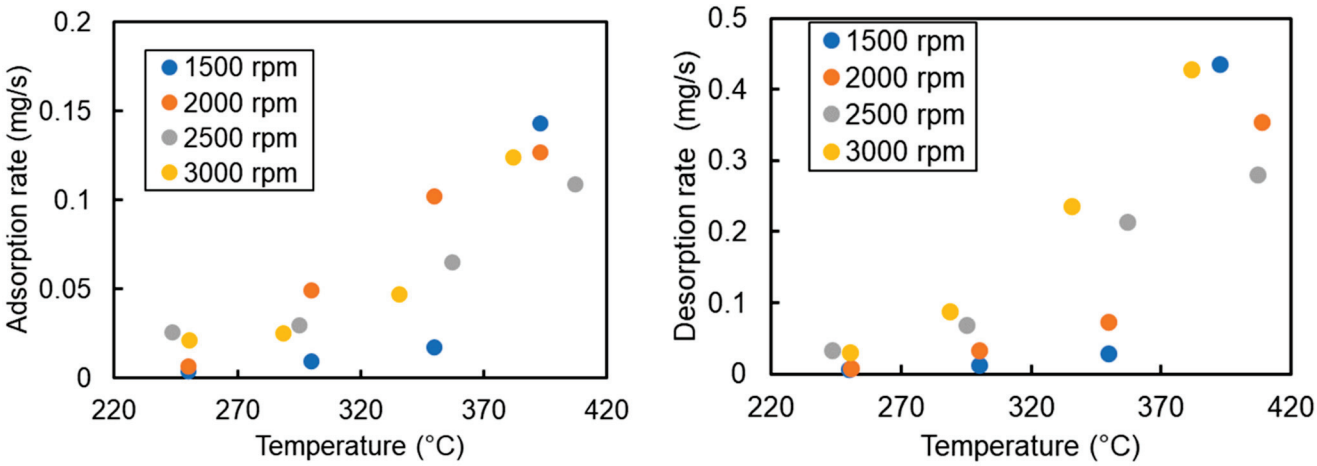

(**a**) (**b**)

Figure 12. Relative values of adsorption (**a**) and desorption (**b**) rates of NH_3 in SCR in various conditions.

5. Conclusions

The adsorption and desorption mechanism of NH_3 in SCR is one of the key factors to prevent NH_3 slip while improving the NOx reduction performance. In particular, the control strategy is more complicated in the real-time operation method, in which the temperature of the exhaust gas changes in real time. In this study, we considered improving the NOx reduction efficiency and preventing the NH_3 slip by analyzing the adsorption rate and desorption rate of NH_3 in SCR under various engine operating conditions.

The amount of NH_3 adsorbed inside the SCR under the engine operating conditions of this experiment was 0.4 to 1.8 g. The amount of NH_3 adsorbed inside the SCR decreased as the exhaust gas temperature increased. Among the NH_3 adsorbed inside the SCR, the amount of NH_3 not utilized to reduce NOx was approximately 0.1 g to 0.2 g. This ranged from 65% to 94% of the solubility, and similarly, the higher the exhaust gas temperature, the lower the availability. Further, the range of the amount of NH_3 adsorbed until just before

the appearance of NH_3 slip is 0.25 g to 1.25 g, and the availability calculated based on this is 47% to 63%.

In real-time operation conditions, analyzing the adsorption rate and desorption rate of NH_3 in SCR and the total adsorption amount of NH_3 in SCR is necessary. As a result, the adsorption rate and desorption rate of NH_3 in SCR were not significantly affected by the engine rotation speed. However, it was shown that the adsorption rate and desorption rate increase as the exhaust gas temperature rises. This is expected to increase the adsorption rate and desorption rate as the total amount of NH_3 adsorbed in the SCR decreases. In addition, although not analyzed in this study, it is necessary to examine the adsorption mechanism by comparing the temperature distribution inside the SCR with the exhaust gas temperature and the degree of activation. As a result, the decrease in the amount of NH_3 adsorbed inside the SCR at a high exhaust gas temperature suggests that NH_3 slip control is difficult when the engine is under high-load transient conditions. However, the urea water injection strategy is established by grasping the temperature of the exhaust gas and the temperature change inside the SCR according to the engine's operating conditions. In that case, the urea water consumption efficiency can be improved while reducing the NH_3 slip.

As exhaust emission regulations for diesel engines are becoming stricter worldwide, it is unavoidable that aging diesel engine vehicles be retrofitted with aftertreatment devices such as SCR. In this paper, the mechanism of ammonia adsorption in the SCR is dependent on the exhaust temperature and exhaust flow rate. Therefore, if the SCR adsorption and desorption mechanisms are analyzed according to the exhaust temperature and exhaust flow rate of each old diesel engine in this paper, it can be used as a reference for selecting an appropriate SCR when retrofitting an old diesel engine vehicle.

Author Contributions: Conceptualization, H.J.; methodology, H.J.; validation, H.J.; formal analysis, H.J.; investigation, H.J., J.J., A.K. and O.L.; resources, H.J., J.J., A.K. and O.L.; data curation, H.J., J.J., A.K. and O.L.; writing—original draft preparation, H.J.; writing—review and editing, O.L.; visualization, H.J., J.J., A.K. and O.L.; supervision, J.J., A.K. and O.L.; project administration, J.J., A.K. and O.L.; funding acquisition, J.J., A.K. and O.L. All authors have read and agreed to the published version of the manuscript.

Funding: This research is financially supported by the Global Top Environmental Technology Development Project of the Korea Environmental Industry and Technology Institute (RE202001110, Development and Demonstration of simultaneous PM and NO*x* reduction system of military vehicles and RE2016001420002; Development of the PM·NO*x* purifying system and the core technology; Shipbuilding and Offshore Industry Core Technology Development Business by the Ministry of Trade, Industry, and Energy (MOTIE, Republic of Korea) [Development of Low Print Point Alternative Fuel Injection System for Small and Medium Vessel Engines for Ships Hazardous Emission Reduce]. (20013146).

Institutional Review Board Statement: Not applicable.

Informed Consent Statement: Not applicable.

Data Availability Statement: Not applicable.

Acknowledgments: This work was supported by a research program in the Department of Mechanical Engineering (Generation Fuel and Smart Power Train Laboratory), University of Ulsan, Republic of Korea. This research is financially supported by the Global Top Environmental Technology Development Project of the Korea Environmental Industry and Technology Institute (RE202001110, Development and Demonstration of simultaneous PM and NO*x* reduction system of military vehicles and RE2016001420002; Development of the PM·NO*x* purifying system and the core technology; Shipbuilding and Offshore Industry Core Technology Development Business by the Ministry of Trade, Industry, and Energy (MOTIE, Republic of Korea) [Development of Low Print Point Alternative Fuel Injection System for Small and Medium Vessel Engines for Ships Hazardous Emission Reduce]. (20013146). This research is financially supported by the individual basic research project by the National Research Foundation of Korea (NRF-2021R1F1A1048238, Reliability Improvement of Ammonia- Diesel Dual-Fuel Combustion Model regarding Optimized Combustion Strategy for

Improved Combustion Efficiency and Emission Characteristics). This results was supported by 'Regional Innovation Strategy (RIS)' through the National Research Foundation of Korea(NRF) funded by the Ministry of Education(MOE)(2021RIS-003).

Conflicts of Interest: The authors declare no conflict of interest.

Nomenclature

DOC	Diesel Oxidation Catalyst
DPF	Diesel Particulate Filter
UWS	Urea Water Solution
SCR	Selective Catalyst Reduction
NH_3	Ammonia
H_2O	Water
NO_x	Nitrogen Oxide
N_2	Nitrogen
O_2	Oxygen
CO	Carbon Oxide
THC	Total Hydro Carbon
PM	Particle Matter
BPT	Balance Point Temperature
LNT	Lean NOx Trap
DOHC	Double OverHead Camshaft
AOC	Ammonia Oxidation Catalyst

References

1. Liang, Y.; Ding, X.; Dai, J.; Zhao, M.; Zhong, L.; Wang, J.; Chen, Y. Active oxygen-promoted NO catalytic on monolithic Pt-based diesel oxidation catalyst modified with Ce. *Catal. Today* **2019**, *327*, 64–72. [CrossRef]
2. Salman, A.; Enger, B.; Auvray, X.; Lødeng, R.; Menon, M.; Waller, D.; Rønning, M. Catalytic oxidation of NO to NO_2 for nitric acid production over a Pt/Al_2O_3 catalyst. *Appl. Catal. A Gen.* **2018**, *564*, 142–146. [CrossRef]
3. Tighe, C.; Twigg, M.; Hayhurst, A.; Dennis, J. The kinetics of oxidation of Diesel soots by NO_2. *Combust. Flame* **2012**, *159*, 77–90. [CrossRef]
4. Jiao, P.; Li, Z.; Shen, B.; Zhang, W.; Kong, X.; Jiang, R. Research of DPF regeneration with NOx-PM coupled chemical reaction. *Appl. Therm. Eng.* **2017**, *110*, 737–745. [CrossRef]
5. Radojevic, M. Reduction of nitrogen oxides in flue gases. *Environ. Pollut.* **1998**, *102*, 685–689. [CrossRef]
6. Iwamoto, M.; Yahiro, H.; Tanda, K. Catalytic decomposition of nitrogen-monoxide over copper ionexchanged zeolites. *Stud. Surf. Sci. Catal.* **1989**, *44*, 219–226.
7. Shirahama, N.; Mochida, I.; Korai, Y.; Choi, K.; Enjoji, T.; Shimohara, T.; Yasutake, A. Reaction of NO with urea supported on activated carbons. *Appl. Catal. B Environ.* **2005**, *57*, 237–245. [CrossRef]
8. Traa, Y.; Burger, B.; Weitkamp, J. Zeolite-based materials for the selective catalytic reduction of NOx with hydrocarbons. *Microporous Mesoporous Mater.* **1999**, *30*, 3–41. [CrossRef]
9. Dumesic, J.; Topsøe, N.; Topsøe, H.; Chen, Y.; Slabiak, T. Kinetics of Selective Catalytic Reduction of Nitric Oxide by Ammonia over Vanadia/Titania. *J. Catal.* **1996**, *163*, 409–417. [CrossRef]
10. Madia, G. Measures to Enhance the NOx Conversion in Urea-SCR Systems for Automotive Applications. , ETH Zurich, Zurich Switzerland. Doctoral Dissertation, ETH Zurich, Zurich, Switzerland.
11. Gieshoff, J.; Schäfer-Sindlinger, A.; Spurk, P.; van den Tillaart, J.; Garr, G. *Improved SCR Systems for Heavy Duty Applications*; SAE Technical Paper 2000-01-0189; SAE International: Warrendale, PA, USA, 2000.
12. Liu, Y.; Liu, Z.; Mnichowicz, B.; Harinath, A.; Li, H.; Bahrami, B. Chemical deactivation of commercial vanadium SCR catalysts in diesel emission control application. *Chem. Eng. J.* **2016**, *287*, 680–690. [CrossRef]
13. Colombo, M.; Nova, I.; Tronconi, E. A comparative study of the NH3-SCR reactions over a Cu-zeolite and a Fe-zeolite catalyst. *Catal. Today* **2010**, *151*, 223–230. [CrossRef]
14. Lü, L.; Wang, L. Model-based optimization of parameters for a diesel engine SCR system. *Int. J. Automot. Technol.* **2013**, *14*, 13–18. [CrossRef]
15. Fu, M.; Ge, Y.; Wang, X.; Tan, J.; Yu, L.; Liang, B. NOx emissions from Euro IV busses with SCR systems associated with urban, suburban and freeway driving patterns. *Sci. Total Environ.* **2013**, *452–453*, 222–226. [CrossRef]
16. Willems, F.; Cloudt, R.; van den Eijnden, E.; van Genderen, M.; Verbeek, R.; de Jager, B.; Boomsma, W.; den Heuvel, I. *Is Closed-Loop SCR Control Required to Meet Future Emission Targets?* SAE Technical Paper 2007-01-1574; SAE International: Warrendale, PA, USA, 2007.

17. Bonfils, A.; Creff, Y.; Lepreux, O.; Petit, N. Closed-Loop Control of a SCR System Using a NOx Sensor Cross-Sensitive to NH_3. *IFAC Proc. Vol.* **2012**, *45*, 738–743.
18. Song, Q.; Zhu, G. *Model-Based Closed-Loop Control of Urea SCR Exhaust Aftertreatment System for Diesel Engine*; SAE Technical Paper 2002-01-0287; SAE International: Warrendale, PA, USA, 2002.
19. Ham, Y.; Park, S. A Study of NH_3 Adsorption/Desorption Characteristics and Model Based Control in the Urea-SCR System. *Trans. KSAE* **2016**, *24*, 302–309. [CrossRef]
20. Schär, C.; Onder, C.; Geering, H. Modeling and control of an SCR system. *IFAC Proc. Vol.* **2004**, *37*, 355–360. [CrossRef]
21. Wang, T.; Baek, S.; Jung, M.; Yeo, G. A Study of NH_3 Adsorption/Desorption Characteristics in the Monolithic NH_3-SCR Reactor. *Trans. KSAE* **2006**, *14*, 125–132.
22. Chen, P.; Wang, J. Nonlinear and adaptive control of NO/NO_2 ratio for improving SCR system performance. *J. Frankl. Inst.* **2013**, *350*, 1992–2012. [CrossRef]
23. Mok, Y.; Yoon, E.; Dors, M.; Mizeraczyk, J. Optimum NO2/NOx ratio for efficient Selective Catalytic Reduction. *Acta Phys. Slovaca* **2005**, *55*, 467–478.
24. Ko, A.; Woo, Y.; Jang, J.; Jung, J.; Pyo, Y.; Jo, H.; Lim, O.; Lee, Y. Availability of NH3 adsorption in vanadium-based SCR for reducing NOx emission and NH3 slip. *J. Ind. Eng. Chem.* **2019**, *78*, 433–439. [CrossRef]
25. Ko, A.; Woo, Y.; Jang, J.; Jung, J.; Pyo, Y.; Jo, H.; Lim, O.; Lee, Y. Complementary effects between NO oxidation of DPF and NO_2 decomposition of SCR in light-duty diesel engine. *J. Ind. Eng. Chem.* **2019**, *80*, 160–170. [CrossRef]

MDPI AG
Grosspeteranlage 5
4052 Basel
Switzerland
Tel.: +41 61 683 77 34

Sustainability Editorial Office
E-mail: sustainability@mdpi.com
www.mdpi.com/journal/sustainability

Academic Open
Access Publishing

mdpi.com

ISBN 978-3-7258-5896-5